



2016

# FIELD, GEOCHRONOLOGIC, AND GEOCHEMICAL CONSTRAINTS ON LATE PRECAMBRIAN TO EARLY PALEOZOIC TERRANE ACCRETION IN THE SOUTHERN APPALACHIAN BLUE RIDGE PROVINCE

Emma A. Larkin

*University of Kentucky*, [emma.larkin@uky.edu](mailto:emma.larkin@uky.edu)

Digital Object Identifier: <http://dx.doi.org/10.13023/ETD.2016.311>

**[Click here to let us know how access to this document benefits you.](#)**

---

## Recommended Citation

Larkin, Emma A., "FIELD, GEOCHRONOLOGIC, AND GEOCHEMICAL CONSTRAINTS ON LATE PRECAMBRIAN TO EARLY PALEOZOIC TERRANE ACCRETION IN THE SOUTHERN APPALACHIAN BLUE RIDGE PROVINCE" (2016). *Theses and Dissertations--Earth and Environmental Sciences*. 39.  
[https://uknowledge.uky.edu/ees\\_etds/39](https://uknowledge.uky.edu/ees_etds/39)

This Master's Thesis is brought to you for free and open access by the Earth and Environmental Sciences at UKnowledge. It has been accepted for inclusion in Theses and Dissertations--Earth and Environmental Sciences by an authorized administrator of UKnowledge. For more information, please contact [UKnowledge@lsv.uky.edu](mailto:UKnowledge@lsv.uky.edu).

**STUDENT AGREEMENT:**

I represent that my thesis or dissertation and abstract are my original work. Proper attribution has been given to all outside sources. I understand that I am solely responsible for obtaining any needed copyright permissions. I have obtained needed written permission statement(s) from the owner(s) of each third-party copyrighted matter to be included in my work, allowing electronic distribution (if such use is not permitted by the fair use doctrine) which will be submitted to UKnowledge as Additional File.

I hereby grant to The University of Kentucky and its agents the irrevocable, non-exclusive, and royalty-free license to archive and make accessible my work in whole or in part in all forms of media, now or hereafter known. I agree that the document mentioned above may be made available immediately for worldwide access unless an embargo applies.

I retain all other ownership rights to the copyright of my work. I also retain the right to use in future works (such as articles or books) all or part of my work. I understand that I am free to register the copyright to my work.

**REVIEW, APPROVAL AND ACCEPTANCE**

The document mentioned above has been reviewed and accepted by the student's advisor, on behalf of the advisory committee, and by the Director of Graduate Studies (DGS), on behalf of the program; we verify that this is the final, approved version of the student's thesis including all changes required by the advisory committee. The undersigned agree to abide by the statements above.

Emma A. Larkin, Student

Dr. David P. Moecher, Major Professor

Dr. Edward W. Woolery, Director of Graduate Studies

---

FIELD, GEOCHRONOLOGIC, AND GEOCHEMICAL CONSTRAINTS ON LATE  
PRECAMBRIAN TO EARLY PALEOZOIC TERRANE ACCRETION IN THE  
SOUTHERN APPALACHIAN BLUE RIDGE PROVINCE

---

THESIS

---

A thesis submitted in partial fulfillment of the  
requirements for the degree of Master of Science in the  
College of Arts and Sciences  
at the University of Kentucky

By

Emma Anne Larkin

Lexington, Kentucky

Director: Dr. David P. Moecher, Professor of Geology

Lexington, Kentucky

2016

Copyright © Emma Anne Larkin 2016

## ABSTRACT OF THESIS

### FIELD, GEOCHRONOLOGIC, AND GEOCHEMICAL CONSTRAINTS ON LATE PRECAMBRIAN TO EARLY PALEOZOIC TERRANE ACCRETION IN THE SOUTHERN APPALACHIAN BLUE RIDGE PROVINCE

Xenolith-bearing orthogneiss of Amazonian affinity discovered in the Dellwood quadrangle in the Blue Ridge basement complex represents the oldest crustal component of the southern Appalachians (1.33 – 1.37 Ga: Quinn, 2012). New U-Pb zircon ages for migmatitic paragneiss of the Cartoogechaye terrane exposed in the Dellwood quadrangle reveal two unique detrital zircon age signatures that indicate either a local eastern Laurentian margin source or an exotic source. Detailed mapping, whole rock geochemistry, and U-Pb zircon geochronology were conducted to determine whether this exotic crustal component extends farther south into the Hazelwood 7.5" quadrangle. Lithological similarities exist between paragneisses in the Dellwood quadrangle and those in the Hazelwood quadrangle. However, the increase in proportion of leucosome and polyphase folding prevent direct correlation of lithologies between the areas. Whole rock major element compositions overlap the composition of basement orthogneisses. Zircon ages of six paragneiss samples reveal multiple detrital zircon age modes that are dominated by two Grenville modes at ~1050 and 1150 Ma. Minor zircon populations exist at ~450 – 480, 700 – 900, and 1300 – 1500 Ma. Age distributions and compositional trends are evidence that the protolith of the paragneiss in the Hazelwood quadrangle was Neoproterozoic rift sediments with a dominant Laurentian margin source.

**KEYWORDS:** Blue Ridge Province, Grenville Basement, Hazelwood Quadrangle, Cartoogechaye Terrane, Detrital Zircon Geochronology

---

Emma A. Larkin

---

July 26, 2016

---

FIELD, GEOCHRONOLOGIC, AND GEOCHEMICAL CONSTRAINTS ON LATE  
PRECAMBRIAN TO EARLY PALEOZOIC TERRANE ACCRETION IN THE  
SOUTHERN APPALACHIAN BLUE RIDGE PROVINCE

By

Emma Anne Larkin

David P. Moecher

---

Director of Thesis

Edward W. Woolery

---

Director of Graduate Studies

July 26, 2016

---

## ACKNOWLEDGMENTS

Foremost, I would like to thank my advisor Dr. David Moecher. I have benefited enormously from his scientific guidance, support, and patience. His enthusiasm for geologic mapping and Appalachian geology allowed for the successful completion of this thesis. Under his direction, I have I grown as a scientist. I thank my other thesis committee members, Dr. J. Ryan Thigpen and Dr. Kent Ratajeski, for their reviews and suggestions. I also extend my thanks to the rest of the EES department for continued support.

Without funding from USGS EDMAP Grant G14AC00113, my fieldwork and lab analysis would not have been possible. Additionally, the Ferm and the Brown-McFarlan Funds, provided by the Earth and Environmental Science department helped me with travel costs to conduct my research and present at a conference. I appreciate all the help from the Arizona Laserchron Center with my zircon geochronology. I would also like to thank Jason Backus at the Kentucky Geological Survey for helping me run my XRF analysis.

Additionally, I would like to thank my mom, dad, and sister for their support and care. I am also grateful for my partner in crime, Bobby, for his constant encouragement and maintaining good spirits. Finally, I would like to thank my friends for their help with proof-reading, motivation, and much needed comedic relief.

## TABLE OF CONTENTS

Acknowledgments.....	iii
List of Figures .....	v
List of Files .....	ix
Chapter I. Introduction.....	1
Geologic Setting .....	6
Purpose of Study.....	11
Chapter II. Analytical Methods.....	12
Geologic Mapping .....	12
U-Pb Zircon Geochronology .....	14
Whole Rock Geochemistry: X-ray Fluorescence .....	19
Chapter III. Field Observations and Petrographic Descriptions .....	20
General Lithostratigraphy .....	20
Structure.....	39
Metamorphism .....	45
Chapter IV. Results of U-Pb Zircon Geochronology.....	45
Orthogneiss .....	46
Paragneiss .....	48
Discussion.....	60
Chapter V. Results of Geochemistry .....	65
Discussion.....	66
Chapter VI. Conclusions.....	71
Appendices.....	80
References.....	122
VITA.....	127

## LIST OF FIGURES

Figure 1.1: Simplified geologic map of the southern Appalachians (after Moecher et al. 2011; modified from Rankin et al., 1990).....	3
Figure 1.2: Probability density plots from Dellwood quadrangle biotite gneiss (modified from Quinn, 2012).....	4
Figure 1.3: Terra-Wasserburg plot of sample DEL10-7-b (modified from Quinn, 2012)..	5
Figure 1.4: Timeline of crust-forming events in the southern Appalachians .....	10
Figure 2.1: Simplified geologic map of the north half of the Hazelwood 7.5” quadrangle with sample locations.....	13
Figure 2.2: Age plots from standard FC-1 .....	18
Figure 3.1: Geologic map of the Hazelwood 7.5” quadrangle, western North Carolina..	24
Figure 3.2: Photograph of hand sample of biotite gneiss sample H15-002 .....	26
Figure 3.3: Photomicrograph of biotite gneiss sample H15-002 .....	26
Figure 3.4: Photograph of hand sample of augen gneiss sample H15-001.....	27
Figure 3.5: Photomicrograph of augen gneiss sample H15-001.....	27
Figure 3.6: Photomicrograph in polarized light of augen gneiss sample H15-001 .....	28
Figure 3.7: Photograph of a hand sample of Copperhill metapsammite.....	28
Figure 3.8: Photomicrograph of Copperhill metapsammite sample H15-008.....	29
Figure 3.9: Photograph of hand sample of Copperhill biotite-muscovite schist sample H15-007 .....	29
Figure 3.10: Photomicrograph of Copperhill biotite-muscovite schist sample H14-008 .	30
Figure 3.11: Figure 3.11: Photomicrograph of Copperhill biotite-muscovite schist sample H14-006 .....	30
Figure 3.12: Photomicrograph of Copperhill biotite-muscovite schist sample H15-007 .	31



Figure 3.13: Photomicrograph of biotite-muscovite schist sample H14-006 .....	31
Figure 3.14: Photograph of hand sample of Copperhill schist sample H15-009 .....	32
Figure 3.15: Photograph of hand sample of Cartoogechaye biotite gneiss sample DEL14-2 .....	32
Figure 3.16: Photograph of Cartoogechaye biotite gneiss sample H15-003 .....	33
Figure 3.17: Photomicrograph of Cartoogechaye biotite gneiss sample DEL14-2 .....	33
Figure 3.18: Photograph of hand sample of Cartoogechaye migmatitic biotite gneiss sample H14-003 .....	34
Figure 3.19: Photograph of hand sample of Cartoogechaye migmatitic biotite gneiss sample H14-009 .....	34
Figure 3.20: Photograph of hand sample of Cartoogechaye migmatitic biotite gneiss sample H14-004 .....	35
Figure 3.21: Photomicrograph in polarized light of Cartoogechaye migmatitic biotite gneiss sample H15-004 .....	36
Figure 3.22: Photograph of hand sample of Cartoogechaye migmatitic hornblende-biotite gneiss sample H14-011 .....	36
Figure 3.23 Photomicrograph of amphibolite pod in Cartoogechaye hornblende-biotite gneiss sample H14-011: .....	37
Figure 3.24 Photomicrograph of leucosome in Cartoogechaye hornblende-biotite gneiss: .....	37
Figure 3.25: Photograph of hand sample of Otto gneissic metapsammite .....	38
Figure 3.26: Photograph of hand sample of Otto biotite schist sample H14-001 .....	38
Figure 3.27: Photomicrograph of Otto biotite schist sample H14-001 .....	39

Figure 3.28: F1 isoclinal folds in amphibolite pod surrounded by vertical S2 foliation ..	40
Figure 3.29: Vertical S2 foliation in migmatitic biotite gneiss.....	41
Figure 3.30: Open F3 folding deforming subvertical S2 foliation and F1 isoclinal fold refolded by F2 isoclinal fold refolded by closed F3 fold.....	42
Figure 3.31: Photomicrograph in polarized light of protomylonite sample H14-017 .....	43
Figure 3.32: Photograph of D4 drag folds .....	43
Figure 3.33: Photograph of D4 veins and inclusion of migmatitic biotite gneiss in D4 pegmatite.....	44
Figure 4.1: Cathodoluminescence and back scatter electron images of grains 1-3 from H14-020 .....	47
Figure 4.2: Concordia diagram from sample H14-020 zircon data .....	48
Figure 4.3: Cathodoluminescence images of representative sections of zircon mounts...	52
Figure 4.4: Results of LA-ICP-MS of zircon from sample DEL14-1 .....	53
Figure 4.5: Results of LA-ICP-MS of zircon from sample H14-011 .....	54
Figure 4.6: Mean ‘best’ age plot of data with ages under 500 Ma and greater than 90% concordance from sample from sample H14-011 .....	55
Figure 4.7: Results of LA-ICP-MS of zircon from sample H15-003 .....	56
Figure 4.8: Results of LA-ICP-MS of zircon from sample H15-004 .....	57
Figure 4.9: Results of LA-ICP-MS of zircon from sample H14-007 .....	58
Figure 4.10: Results of LA-ICP-MS of zircon from sample H14-002 .....	59
Figure 4.11: Mean ‘best’ age plot of data with ages under 500 Ma and greater than 90% concordance from sample from sample H14-002 .....	60

Figure 4.12: Figure 4.12: Probability density plots for all samples analyzed with LA-ICP-MS.....	63
Figure 4.13: Probability density plots for H14-011 showing the variation in modes with concordance .....	64
Figure 5.1: Harker variation diagrams for select samples in the study area .....	68
Figure 5.2: AFM diagram of select samples in the study area .....	69
Figure 5.3: AFM diagram of geochemistry data from this study compared with geochemistry data from Chakraborty (2010), Loughry (2010), and Quinn (2012).....	70
Figure 6.1: Probability density plots for all samples analyzed with LA-ICP-MS with zircon producing events .....	75
Figure 6.2: Probability density curves from this study compared to the Grenville detrital signature and exotic detrital signature from Quinn, 2012.....	76
Figure 6.3: Probability density curves from this study compared to the Ocoee Supergroup from Chakraborty, 2010.....	77
Figure 6.4: Tera-Wasserburg showing apparent linear trend of discordance .....	78
.....	79
Figure 6.5: Tera-Wasserburg showing zircon analyses from the Wading Branch Formation.....	79

## LIST OF FILES

File 1: Geologic\_Map\_Hazelwood\_7.5-minute\_Quadrangle.tiff, 162 MB

## CHAPTER I. INTRODUCTION

Laurentia, like all the major cratons, was assembled from Archean granite gneiss and greenstone terranes, Paleoproterozoic mobile belts that stitched together the Archean terranes, and late Proterozoic to Phanerozoic orogens/terranes that added varying amounts of new or recycled crust to the Laurentian margin (Hoffman, 1999; Whitmeyer and Karlstrom, 2007). The ultimate origin and timing of the assembly of all the crustal components comprising the major cratons is a fundamental question regarding evolution of Earth's lithosphere. Previous interpretations have suggested that eastern Laurentian crustal assembly involved episodic accretion of tectonostratigraphic terranes, including many considered exotic, from the Mesoproterozoic to the end of the Paleozoic (Sinha et al., 1996; Loewy et al., 2003; Tohver et al., 2004; Fisher et al., 2010). However, many questions remain to be resolved regarding eastern Laurentian margin evolution, with respect to understanding crustal terranes that composed the Blue Ridge basement in the southern Appalachian orogen. Multiple periods of deformation and high-grade metamorphism have led to overprinting and pose a challenge for unraveling crustal evolution in the southern Appalachian Blue Ridge. Despite these complexities, integration of rigorous geologic mapping, petrology, geochemistry, and geochronology can be used to place constraints on the origin of crustal terranes and their assembly history.

The southern Appalachians are comprised of multiple tectonostratigraphic terranes that comprise a large composite thrust sheet (Figure 1.1; Hatcher et al., 2005; Thigpen et al., 2005). The terrane divisions include the western Blue Ridge, central Blue Ridge, eastern Blue Ridge, and the Mars Hill, Inner Piedmont, and Cat Square terranes

(Hatcher, 2005). This thesis will focus on the examining the provenance of the central Blue Ridge, specifically the Cartoogechaye terrane.

The Cartoogechaye terrane is an enigmatic package of lithologies that includes highly deformed and intensively metamorphosed sedimentary and igneous rocks within the central Blue Ridge. New U-Pb zircon age data from Quinn (2012) indicate that there are at least two unique detrital zircon age signatures of paragneisses within the Cartoogechaye, including suites that are both typical and atypical of Grenville rocks with Laurentian provenance (Figure 1.2). The atypical age spectra are similar to the Carvers Gap paragneiss in the Mars Hill terrane, which is interpreted to be derived from rocks of Amazonian crustal affinity (Aleinkoff, 2013). The Cartoogechaye terrane geochemical signatures (whole rock Sm-Nd, and feldspar Pb systematics) and U-Pb zircon ages of some of the basement orthogneisses are similar to the southwestern Amazon craton in Brazil (Figure 1.3; Quinn, 2012). The complexity and heterogeneous nature of the detritus that contributed to the formation of the Cartoogechaye terrane requires further investigation of the extent of exotic metasedimentary units in order to produce a meaningful tectonic model of Proterozoic terrane amalgamation.

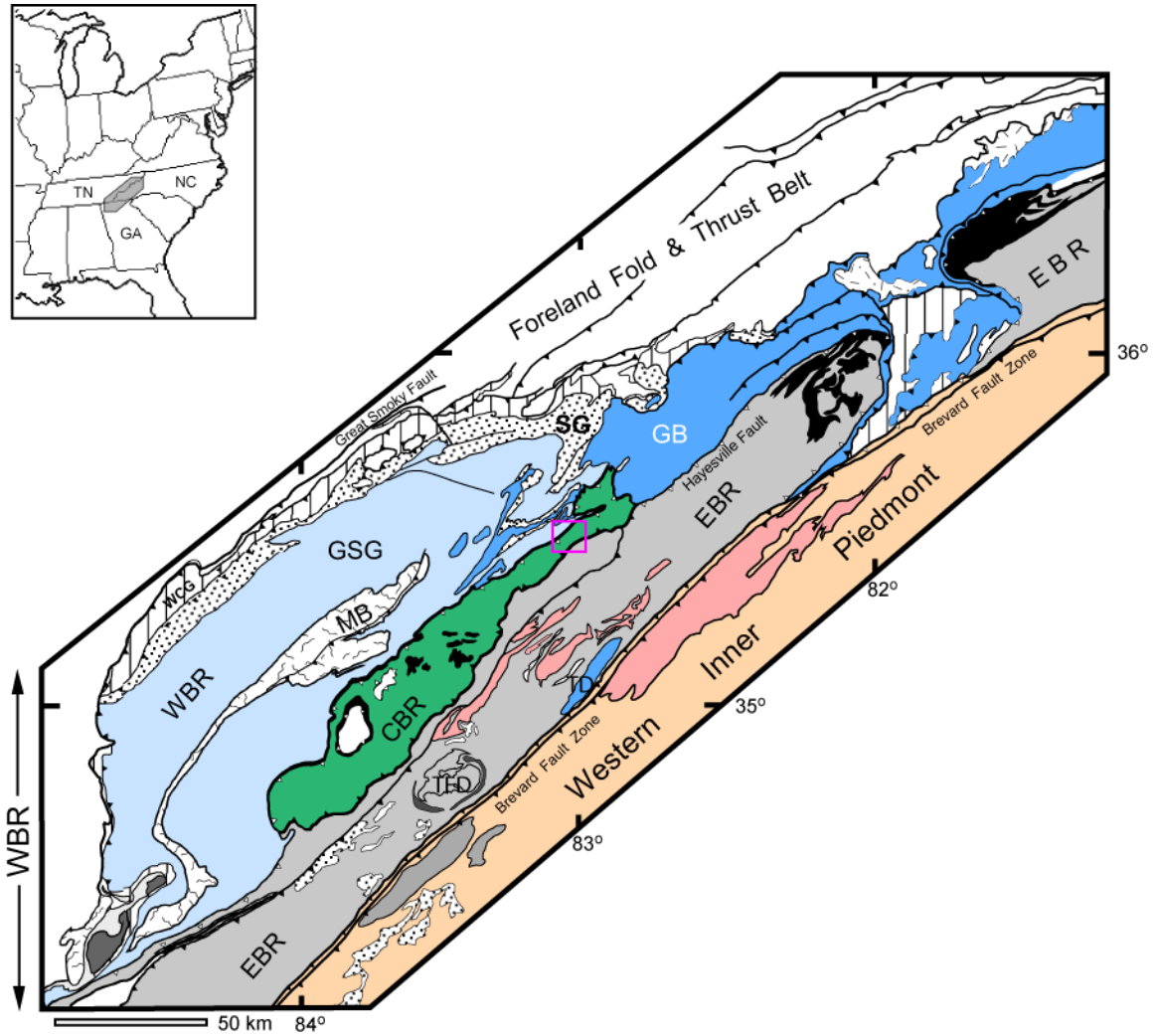


Figure 1.1: Generalized geologic map of the southern Appalachians, showing major terranes, plutonic rocks, and faults (after Moecher et al., 2011, modified from Rankin et al., 1990). Pink rectangle outlines the study area. WBR- western Blue Ridge; CBR- central Blue Ridge; EBR-eastern Blue Ridge; GB-Grenville Basement orthogneiss; GSG and GS- Great Smoky Group and Snowbird Group metasediments; MB- Murphy Belt; TD- Toxaway dome; TFD- Tallulah Falls dome; WCG-Walden Creek Group; white-Paleozoic strata; black- mafic and ultramafic metamorphic rocks, pink-Paleozoic granites.

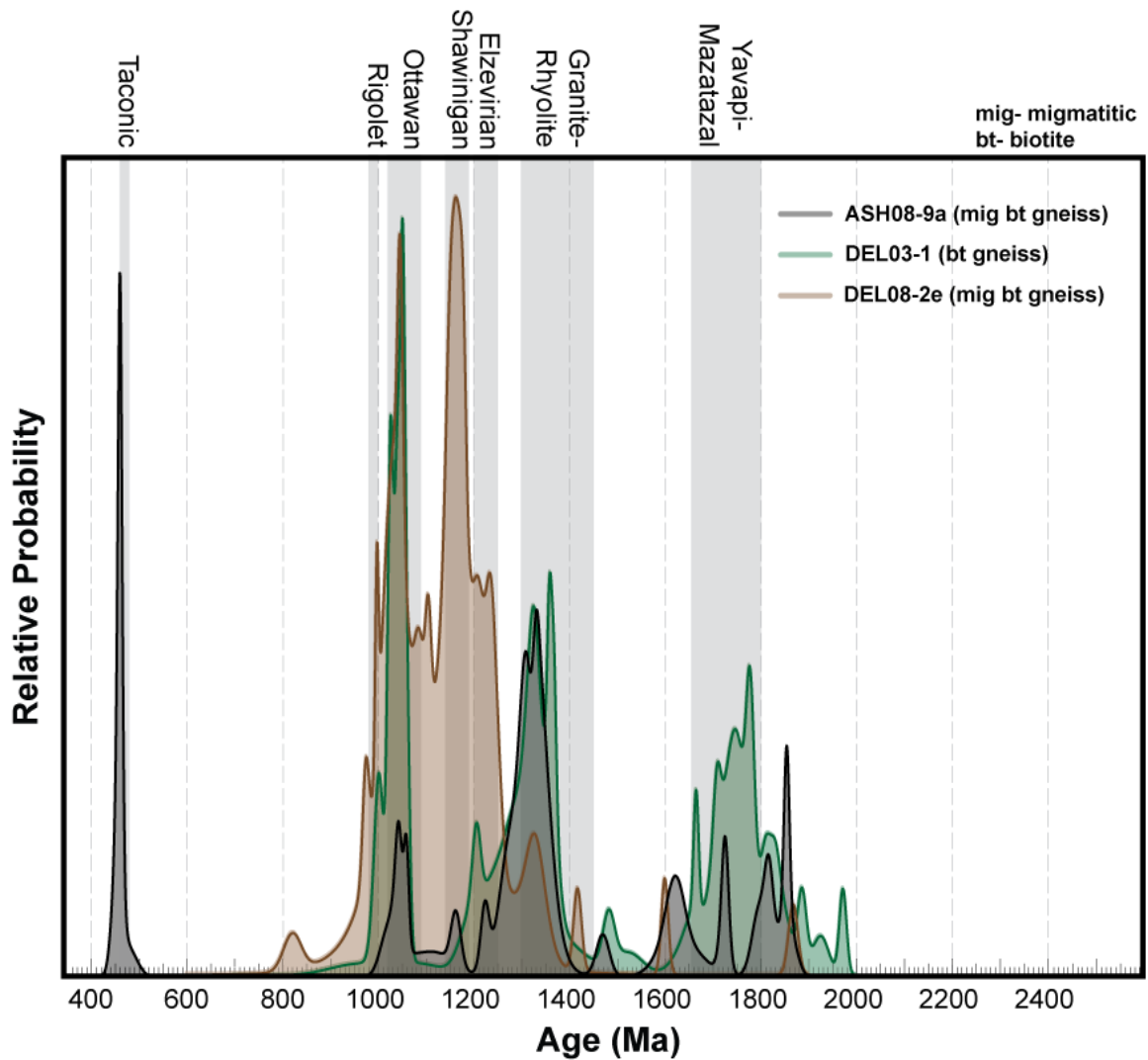


Figure 1.2: Probability density plots of zircon from three biotite gneiss samples from the Dellwood 7.5° quadrangle (data from Quinn, 2012). Sample DEL08-2e (brown) has an age spectrum that exemplifies a Grenville zircon signature. Samples ASH08-9a (gray) and DEL03-1 (green) have age spectra that are atypical of Grenville sourced rocks suggesting an exotic or mixed protolith. A Grenville zircon signature will typically have age modes that represent the orogenic phases of the Grenville orogeny, in particular, the Shawinigan (ca. 1150 Ma) and Ottawa (ca. 1050 Ma) phases. An exotic zircon signature is characterized by an abundance of Paleoproterozoic grains and a lack of at least one of the two main Grenville age modes. An age mode between 450 and 480 Ma is not indicative of either a Grenville or exotic protolith as it correlates with the Taconic orogeny. Gray shaded bars represent crust forming events. Timing of Paleoproterozoic orogenesis from Whitmeyer and Karlstrom, 2007. Timing of Mesoproterozoic orogenesis from Rivers, 2008; Hynes and Rivers, 2010. Timing of Paleozoic orogenesis from Hatcher, 2005; Moecher et al., 2011.



DEL10-7-b

data-point error ellipses are 68.3% conf.

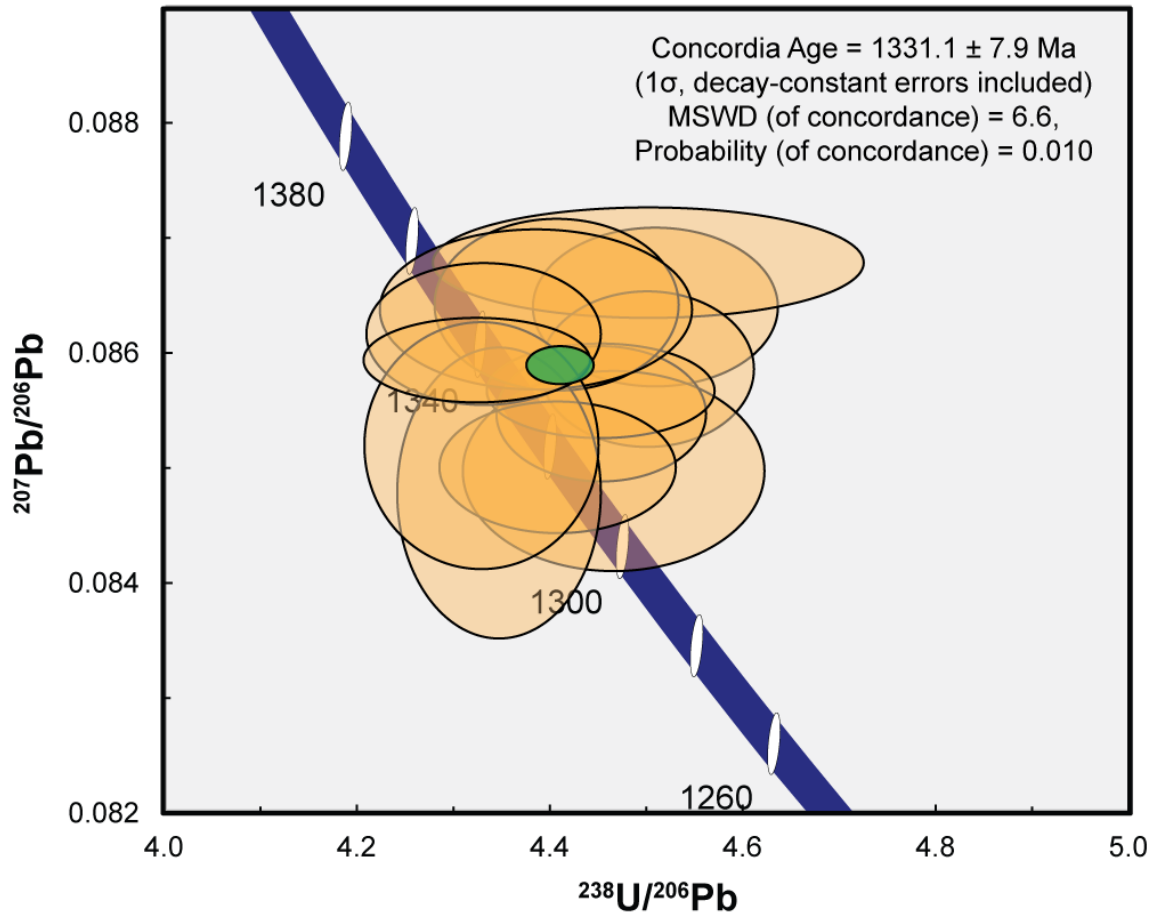


Figure 1.3: Tera-Wasserburg plot modified from Quinn, 2012 of U-Pb isotopic data for zircon from a hornblende orthogneiss sample collected in the Dellwood 7.5" quadrangle. A magmatic age of ~1330 indicates a crust forming event occurred prior to the Grenville orogeny. Feldspar Pb isotope data for this sample are most consistent with an Amazonian crustal affinity.

## **Geologic Setting**

The Blue Ridge terrane is a continuous northeast trending belt that extends from south-central Pennsylvania to northern Georgia. It experienced multiple compressional and extensional events from the Mesoproterozoic to the Permian (Figure 1.4). The earliest event, the Grenville Orogeny, involved diachronous collision of the eastern margin of Laurentia with Amazonia from 1090-980 Ma to produce the supercontinent Rodinia (Tohver et al., 2006; Rivers et al., 2008). The main stages of the Grenville orogeny include the Elzevirian, Shawinigan, Ottawan, and Rigolet (McLelland et al., 1996; Rivers, 2008; Figure 1.4). The Grenville orogeny produced large volumes of clastic sediments that were derived from the mountain chain and transported away from the orogen by a pan-continental river system (Rainbird et al., 2012).

Rifting and breakup of Rodinia occurred in two distinct pulses at 765-680 Ma and 620-550 Ma, with formation of intracratonic (Ocoee) and continental margin rift basins that formed the incipient Iapetus Ocean (Rankin et al., 1997; Tollo, 2004). Rifting was followed by development of a passive margin drift phase from the late Neoproterozoic to Lower Ordovician (Tollo, 2004). The drift phase was followed by a reversal in plate motion, leading to subduction of Iapetan oceanic crust and formation of the Taconic volcanic arc. Hatcher (2005) suggested that during the early stages of the Taconic orogeny, oceanic and arc assemblages were obducted onto the Laurentian margin and the central Blue Ridge was transported along the Haysville thrust fault into juxtaposition with the western Blue Ridge. However, Massey and Moecher (2005) suggest there is a lack of structural evidence to support the interpretation of a thrust contact between these two

terrane. Taconic orogenesis lasted from 480-450 Ma, with peak metamorphism at ca. 450-460 Ma (Moecher et al., 2004, 2011; Miller et al., 2006; Corrie and Kohn 2007).

Collision of the Laurentian margin with the Carolina superterrane between ca. 390-350 Ma resulted in the Neocadian orogeny, which is primarily recorded in metamorphic zircon rim ages in migmatites and metaplutonic rocks of the eastern Blue Ridge, Inner Piedmont and Cat Square terranes (Bream et al., 2004; Hatcher, 2005; Merschat, 2009). However, within the western and central Blue Ridge terranes evidence of the Neocadian orogeny is generally not observed.

The final collisional event, the Alleghanian orogeny, led to the present day configuration of the Appalachians and involved the collision of the Laurentian margin with the African plate at 325-265 Ma. This orogeny resulted in development of a foreland basin and fold-thrust belt during emplacement of the Appalachian hinterland along the Great Smoky thrust (Hatcher et al., 1989). In the Blue Ridge, evidence of the Alleghanian orogen includes retrograde greenschist facies metamorphism and localized retrograde ductile shear zones (Hatcher et al, 2005; Kunk et al., 2006).

### ***Western Blue Ridge***

The western Blue Ridge (WBR) is comprised of Neoproterozoic-Cambrian sedimentary rocks deposited in normal fault-bounded rift basins unconformably above Mesoproterozoic Grenvillian continental crust (King et al., 1958; Hadley and Goldsmith, 1963; Rankin, 1975). WBR Grenville basement paragneiss consists of migmatitic biotite gneiss and orthogneisses that consist predominately of granitoid gneiss and augen gneiss (Southworth, et al. 2005, 2012). Other lithologies include hornblende-biotite gneiss, amphibolite, dunites and websterites, and isolated bodies of calc-silicate granofels. The

Neoproterozoic Ocoee Supergroup (OSG), which consists of a >10 km thick sequence of immature feldspathic metaclastic rocks, unconformably overlies the Grenville basement. The OSG is subdivided into the Snowbird, Great Smoky, and the Walden Creek Groups (King et al., 1958; Hadley and Goldsmith, 1963). The Cambrian Chilhowee Group, which stratigraphically overlies the OSG, consists of a dominantly passive margin clastic sequence that includes quartzite, shale, and siltstone. (Hatcher et al., 2005).

### ***Central Blue Ridge***

The central Blue Ridge (CBR) is a ductile fault bounded terrane separated from the adjacent terranes by the Hayesville fault to the northwest and the Soque River fault to the southeast. The CBR is divided into several sub-terranes that have been interpreted to represent a crystalline thrust stack located between the western and eastern Blue Ridge. The terrane divisions, from structurally highest to lowest, include the Cartoogechaye terrane, Cowrock, and Dahlenega gold belt (Hatcher, 2005).

The Cartoogechaye terrane is dominated by migmatitic biotite paragneiss (and orthogneiss?) with lesser amphibolite, dunite, and peridotite (Hadley and Nelson, 1971; Merschat, 2009). The biotite gneiss and amphibolite are interpreted to have been deposited as deepwater sedimentary and volcanic rocks on the distal Laurentian margin. The amphibolite, dunite, and peridotite are interpreted to be remnants of ophiolites (Hatcher, 2005). From U-Pb zircon dating of Cartoogechaye orthogneiss and mafic xenoliths, Quinn (2012) identified magmatic pulses at ca. 1130, 1180, and 1330 Ma. Merschat et al. (2010) present preliminary U-Pb zircon age data that imply the presence of Grenville basement orthogneiss (Trimont Ridge complex) in the Cartoogechaye terrane. The

amount of Grenville basement present in the Cartoogechaye is uncertain and remains to be tested.

The Cowrock terrane, the southernmost terrane, is exposed primarily in Georgia and subdivided into three formations: the Persimmon Creek Gneiss, Coleman River Formation, and Ridgepole Mountain Formation (Hatcher, 1979). Biotite schist and quartzite of the Ridgepole Mountain Formation overlay metasandstone and pelitic schist of the Coleman River Formation. The Persimmon Creek Gneiss, a ~468 Ma tonalitic pluton, intrudes into the Coleman River Formation (Hatcher, 1979; McDowell et al., 2002; Merschat, 2009).

The Dahlonega gold belt is exposed in a continuous northeast trending belt as well as in the Great Balsams Window (Figure 1.3). The Otto Formation of the Dahlonega gold belt, which is exposed in the Great Balsams window, consists of a siliciclastic sequence of immature metaclastic rocks interpreted as deepwater sedimentary deposits that are lithologically similar to and potentially temporally equivalent with the Copperhill Formation (Great Smoky Group) to the northwest. Merschat (2009) recognized an interlayered mafic component, which the study used to separate the Otto and Copperhill formations.

### ***Eastern Blue Ridge***

The eastern Blue Ridge, the structurally highest fault bounded Blue Ridge terrane, is comprised of the Neoproterozoic to Cambrian Ashe-Tallulah Falls Formation, Paleozoic plutons, and few Mesoproterozoic basement massifs (Hatcher et al., 2005). The Ashe-Tallulah Falls Formation, which consists of primarily metagraywacke, amphibolite, and mica schist, is interpreted as Laurentian affinity metaclastic rocks deposited

nonconformably on Grenvillian and oceanic crust (Bream, 2003; Bream et al. 2004; Hatcher et al., 2004). Paleozoic magmas intruded the Ashe-Tallalah Falls Formation in three phases during the Ordovician, Devonian, and Mississippian (Miller et al., 2006). Mesoproterozoic basement is exposed in the Tallulah Falls and Toxaway dome (Hatcher et al., 2004). The eastern Blue Ridge is not exposed in the study area, however, it has been suggested that the Cartoogechaye terrane contains rocks from the Tallulah Falls Formation (Hatcher, et al., 2003).

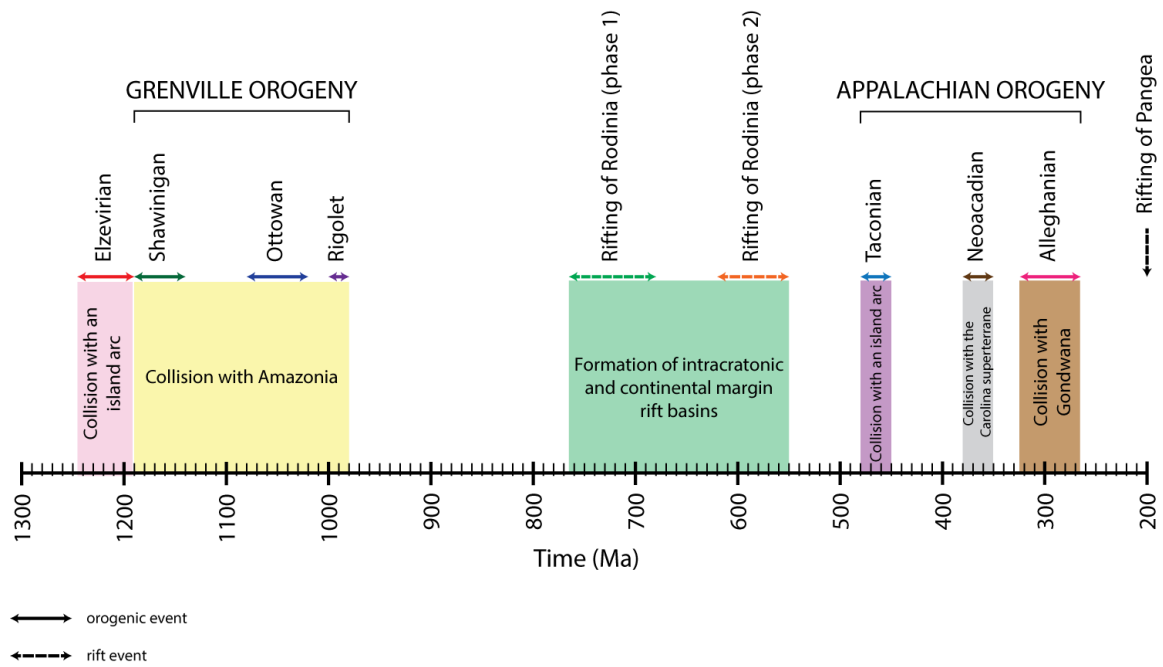


Figure 1.4: Timeline of crust-forming events in the southern Appalachians. Timing of Mesoproterozoic orogenesis from Rivers, 2008; Hynes and Rivers, 2010. Timing of Neoproterozoic rifting from Tollo, 2004. Timing of Paleozoic and Mesozoic orogenesis and rifting from Hatcher, 2005; Moecher et al., 2011.

## **Purpose of Study**

Recent work by a number of other studies in the Dellwood (Chakraborty, 2010; Loughry, 2010; Anderson, 2011; Quinn, 2012) and Waynesville (Mersch, 2009) 7.5-minute quadrangles has refined the stratigraphic, geochronologic, and geochemical/isotopic signatures of western and central Blue Ridge units. The purpose of this study is to use these latter characteristics for comparison and correlation in the Hazelwood quadrangle, immediately south of the Dellwood quadrangle, in order to further test models of terrane accretion in the southern Blue Ridge. Previous geologic mapping of the Hazelwood study area was by Edelman (unpublished mapping) and Montes (1997). However, no previously published maps of the north half Hazelwood quadrangle were produced at a 1:24000 scale, therefore, the first task was to conduct bedrock mapping of the north half of the Hazelwood quadrangle (Plate 1) in order to test whether the lithologies exposed in the Dellwood quadrangle (immediately north of the Hazelwood quadrangle) extend farther south. Sampling of map units and geochemical analysis will permit assessment of unit provenance and evaluation of suspected Mesoproterozoic bedrock recycling. The second major task, zircon U-Pb geochronology, will permit further assessment of an igneous vs. sedimentary protolith for the migmatitic gneisses that dominate the bedrock in the study area. If the protolith is determined to be sedimentary, then the detrital zircon age distributions will provide constraints on provenance – either a Laurentian or an exotic (Amazonian: Loewy et al., 2003; Tohver et al., 2010) source.

## CHAPTER II. ANALYTICAL METHODS

### Geologic Mapping

Detailed 1:24,000-scale geologic mapping of the north half of the Hazelwood 7.5-minute quadrangle was conducted over a six month field season during the summer and winter of 2014. Outcrop locations were determined using Trimble Outdoors GPS software and a Holux GPS receiver coupled with a Dell Axim PDA running ArcPad<sup>®</sup>. Station numbers were assigned to each outcrop location to relate the field data and observations to the locations recorded via GPS. Thirty-five samples were collected and prepared for petrographic, geochronological, and geochemical analysis (Figure 2.1). When possible, samples were spatially oriented. A digital geologic map was created using ESRI Arcmap<sup>®</sup> and Adobe Illustrator<sup>®</sup>. The 2013 topographic base map was produced by the USGS.



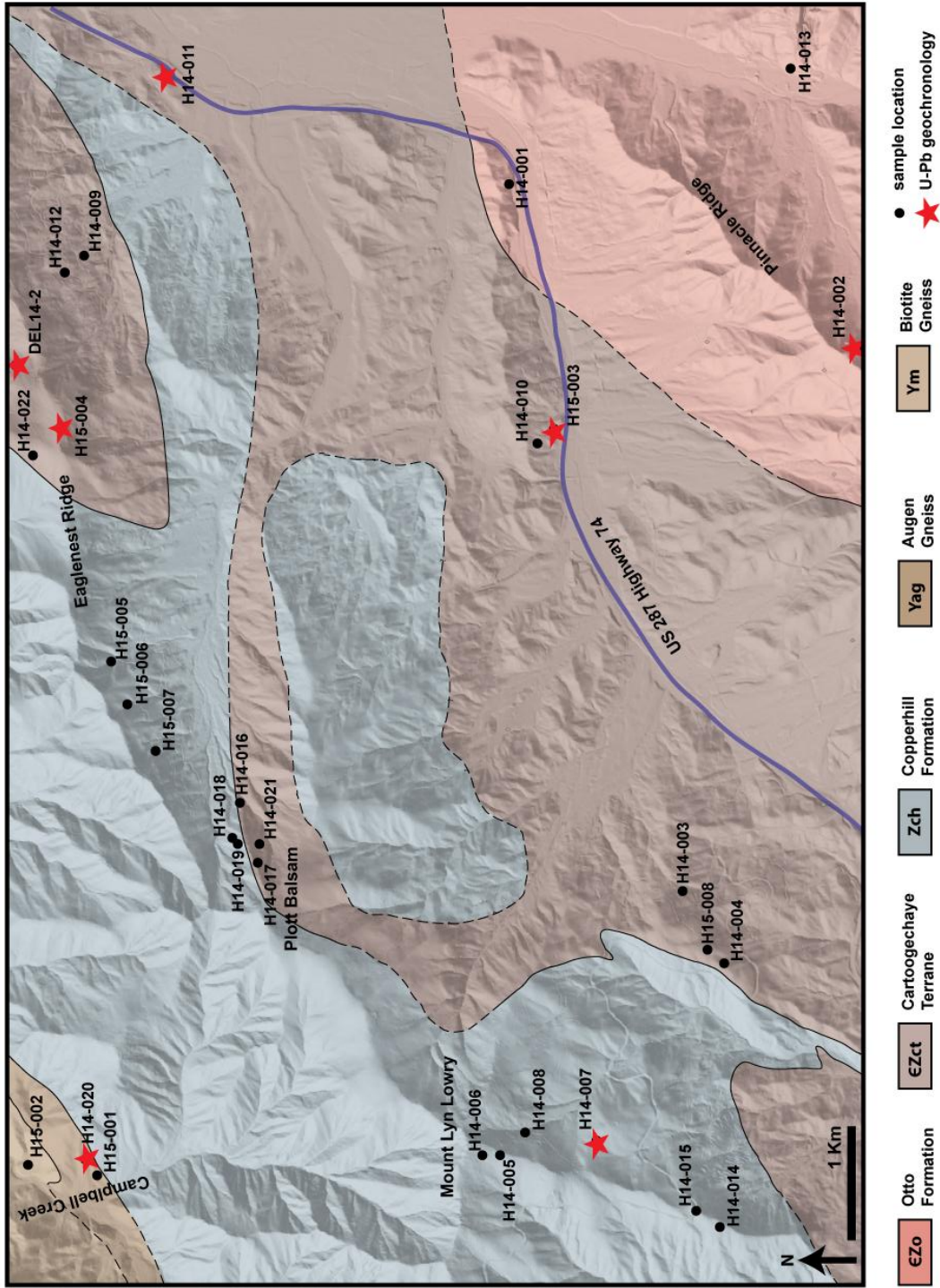


Figure 2.1: Simplified geologic map of the north half of the Hazelwood 7.5' quadrangle with sample locations. Red stars indicate samples collected for U-Pb zircon geochronology

## **U-Pb Zircon Geochronology**

U-Pb zircon geochronology was carried out by laser ablation-inductively coupled plasma-mass spectrometry (LA-ICP-MS) and secondary ion mass spectrometry (SIMS). Six paragneiss samples and one orthogneiss sample were selected as representative samples for analysis. The paragneiss samples were analyzed at the Arizona Laserchron Center on a Thermo Element2 multi-collector ICPMS. The orthogneiss sample was analyzed at the University of California Los Angeles (UCLA) on a CAMECA 1270 secondary ion microprobe.

Samples were prepared at the University of Kentucky. Approximately 1 kg of sample was crushed into gravel-sized fragments using a jaw crusher and then milled into a fine-grain sand using an iron disc mill. Between each sample, the equipment was cleaned with a vacuum, compressed air, and isopropyl alcohol. The samples were wet sieved using 250, 125, and 53  $\mu\text{m}$  disposable plastic mesh. New mesh was used for each sample to avoid cross-contamination. The 125-250 and 53-125  $\mu\text{m}$  aliquots were ultrasonically rinsed and dried in an oven. Heavy minerals were separated using acetylene tetrabromide (specific gravity = 2.96) and methylene iodide (SG = 3.32). Magnetic minerals were removed using a ceramic block magnet and a Frantz Isodynamic Magnetic Separator Model LB-1. Mineral separates were collected for 0.25, 0.5, and 1.0 Amp. Samples with remaining apatite were separated with a third heavy liquid separation of methylene iodide. Remaining pyrite was handpicked from each sample.

After sufficient zircons were separated (< ~10% impurities), detrital grains were mounted for LA-ICP-MS and the magmatic grains were mounted for SIMS. The zircons from the paragneiss samples were analyzed as detrital grains (i.e., large n) as the protolith

for many paragneisses are uncertain due to the high proportion of zircons related to migmatite formation in these samples. For these samples, a glass mounting tube from the Arizona Laserchron Center was attached to a ceramic tile with 2 inch wide 3M<sup>®</sup> double sided tape. A single sample was poured into the mounting tube and rotated to distribute the grains. Excess zircons were removed by holding the tile upside down over weighting paper. Standard grains from the Arizona Laserchron Center were mounted using forceps around the sample based on a diagram from the lab. The zircons from orthogneiss were analyzed as magmatic zircons. For this sample, grains were handpicked and placed on a ceramic tile with 2 inch wide 3M<sup>®</sup> double sided tape. For all samples, a 1 inch plastic mounting ring was placed around the zircons. An epoxy mount was created by combining 5 parts Buehler Epo-Thin<sup>®</sup> epoxy resin with 2 parts Buehler Epo-Thin<sup>®</sup> epoxy hardener. The resin and hardener were slowly mixed for 5 minutes and then placed in a Branson 2210 ultrasonic cleaner for 2 minutes. The epoxy mixture was poured into the mounting ring over the grains and left undisturbed to set for 24 hours. The mounts were removed from the plates and polished to expose the grain cores using 1200 grit sandpaper followed by 2000 grit sandpaper. The mount was polished with a 0.3 $\mu$ m alumina powder polish to remove scratches. The mount was then ultrasonically washed to remove excess polish.

For all paragneiss samples, backscatter electron (BSE) and cathodoluminescence (CL) images were collected at the University of Kentucky on the CAMECA sx50 electron probe microanalyzer. For the orthogneiss sample, BSE and CL images were collected at UCLA. BSE and CL images were used to identify internal zoning, metamorphic overgrowths, inherited cores, inclusions, and fractures in the zircon grains.

This information was used to guide spot locations for analysis and to interpret the meaning of the U-Pb age data.

Detrital zircons were analyzed at the Arizona Laserchron Center. Operating conditions of the LA-ICP-MS described by Gehrels et al. (2008) were used. Zircon standards Sri Lanka (~563 Ma), FC-1 (~1099 Ma), and R33 (~419 Ma) were analyzed every five grains. The standard grains define a probability density function with a normal distribution (Figure 2.2b). A single analysis has an analytical error (Figure 2.2a) associated with it that is related to the standard deviation of the mean of the six isotopic ratios measured for each spot. However, additional uncertainties, that combine to define the age population, can create outliers; therefore, the date for a single grain analyzed is merely an estimate of the true age of the population of grains which means multiple dates are required to determine a geologically meaningful age (Pullen et al., 2014).

Approximately 300 grains were analyzed for each sample. CL images, collected before analysis, were used to locate the cores of the grains. For each analysis, zircons were ablated with a Photon Machines Analyte G2 excimer laser equipped with a HelEx ablation cell using a spot diameter of 20  $\mu\text{m}$ . The ablated material was transported in helium to the Element2 ICP-MS. The process involved 5 seconds of measuring peaks with a non-firing laser to collect background intensities followed by 10 seconds of measuring peaks with the laser firing. A 20 second delay between each sample was set to purge the system of ablated material and save the analysis file. Raw U-Th-Pb data reduction to calculate concentrations, isotope ratios, and ages for the unknowns was performed at the University of Arizona with a Python decoding routine and an excel

spreadsheet (E2agecalc). All Concordia, Tera-Wasserburg, weighted mean, and relative probability plots were created using Isoplot 3.60 (Ludwig, 2008).

For the orthogneiss sample (H14-020), the mount was coated with approximately 100Å of Au. Operating conditions of the SIMS are similar to those described by Hietpas et al. (2011). Zircon grains of standard AS3 (~1099 Ma: Paces and Miller, 1993) were analyzed to make a calibration curve for comparison with unknown analyses. The analyses were carried out using a primary O<sup>-2</sup> ion beam with a spot diameter of 15 µm. The sample chamber was flooded with oxygen to increase secondary ionization of Pb<sup>+1</sup>. Each analysis consisted of 6 cycles yielding a run time of 6 min per analysis. Raw U-Th-Pb data reduction was performed using Isoplot (Ludwig, 1999).

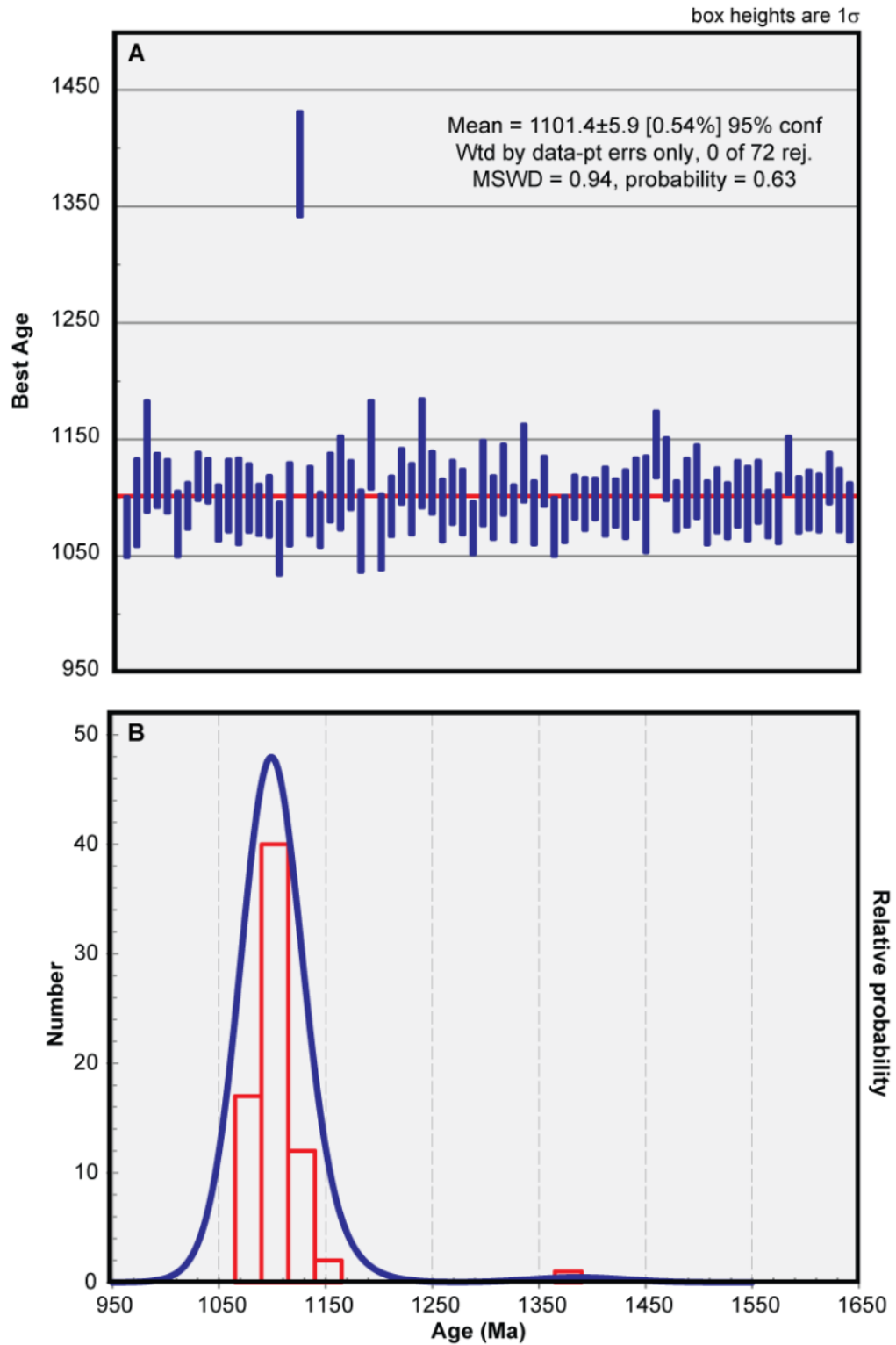


Figure 2.2: Age plots from standard FC-1. (A) Mean 'best age' plot. (B) Probability density plot. All analyses are by LA-ICP-MS. A single outlier at ~1385 Ma demonstrates analysis of an older zircon core. Therefore, when interpreting results of sample age spectra it is necessary to have more than one zircon age to define a significant population. The accepted age of FC-1 is  $1099 \pm 1$  Ma (Paces and Miller, 1993).

## **Whole Rock Geochemistry: X-ray Fluorescence**

Whole rock analysis of major, minor, and trace elements was carried out by X-ray fluorescence spectrometry (XRF). Ten representative gneiss samples were prepared and analyzed at the Kentucky Geologic Survey. Samples were washed and weathered surfaces were removed with a wire brush. Approximately 1 kg of sample was crushed into gravel-sized fragments using a jaw crusher. A portion of the sample was powdered using a 3-puck shatterbox with tungsten carbide steel grinding pucks to produce approximately 50 ml of fine powder. The jaw crusher and shatterbox chambers were cleaned between each sample with a vacuum, compressed air, and isopropyl.

Low dilution lithium tetraborate fused discs were prepared at the Kentucky Geologic Survey X-ray analytical lab. A mixture of  $4.000 \pm 0.001$  g of sample and  $8.000 \pm 0.001$  g of Fluxite<sup>®</sup> (90 Li<sub>2</sub>Br<sub>4</sub>O<sub>7</sub>: 10 LiF) was placed in a platinum crucible and two drops of 5.8 M LiBr were added. Fused discs were made using a Katanax K1 Prime electric fluxer with a maximum temperature of 1080°C. The fused discs were analyzed on a 4-kW Bruker S4 Pioneer wavelength dispersive X-ray fluorescence spectrometer. The elemental concentrations of the unknown samples were calculated using Spectra Plus<sup>®</sup>, which compares the X-ray intensities for each element with the intensities of standards. The standards used were from the USGS (DNC-1, BIR-1, W2a, BCR-2, BHVO-1, BHVO-2, AVG-2, G-2, STM-1, GSP-1), Irish Geologic Association (OU-3, OU-4, AMH-1, YG-1, KPT-1), Canadian Certified References Materials Project (MRG-1, SY-2, S-3), South African Reference Materials SARM 4, SARM 50), Centre de Recherches Pétrographiques et Géochimiques (BE-N) and Chinese National Standard (GBW 07105). Concentrations calculated by Spectrum Plus<sup>®</sup> for vanadium, uranium, thorium, and

gallium were anomalous and omitted from this study. One possible explanation for anomalous data is that elemental concentrations for these elements are too low for accurate analysis.

## **CHAPTER III. FIELD OBSERVATIONS AND PETROGRAPHIC DESCRIPTIONS**

### **General Lithostratigraphy**

#### ***Western Blue Ridge***

The western Blue Ridge in the Hazelwood quadrangle (Figure 3.1) consists of Grenville basement augen orthogneiss and variably migmatitic biotite paragneiss in contact with pelitic schist and metapsammite of the Copperhill Formation (Great Smoky Group). The Copperhill Formation is the dominant unit in the northwestern portion of the study area. Augen orthogneiss and migmatitic biotite paragneiss are only observed as the nose of the Campbell Creek anticline in the northwestern corner of the quadrangle. The augen orthogneiss mapped in Hazelwood quadrangle is spatially continuous with a band of the same unit in the basement complex of the Dellwood quadrangle (Hadley and Goldsmith, 1963).

Biotite gneiss (Ym) is light-gray to medium-gray, fine- to medium-grained, inequigranular to equigranular, and foliated (Figures 3.2-3.3). It consists of quartz, plagioclase, potassium feldspar, biotite, and muscovite. Augen orthogneiss (Yag) is light-gray to medium-gray, medium- to coarse-grained with megacrysts (augen) of microcline, inequigranular, massive to well-foliated, protomylonitic (Figure 3.4), and consists of quartz, microcline, plagioclase, biotite, epidote, and muscovite (Figure 3.5). Augen are comprised of potassium feldspar aggregates and are commonly wrapped by



biotite (Figure 3.6). The augen gneiss is exposed within the core of the Campbell Creek anticline.

The Copperhill Formation (Zch) consists of metapsammite to gneissic metapsammite and biotite-muscovite schist. Metapsammite is tan to light-gray, fine- to medium-grained, non-foliated to foliated, inequigranular to equigranular (Figure 3.7), and consists of quartz, plagioclase, biotite, muscovite, and garnet (Figure 3.8) and is commonly interlayered with pelitic schist with layer thickness ranging from 1 cm to 2 m. Biotite-muscovite schist is light-gray to dark-gray, rusty weathering, medium- to coarse-grained; well foliated, lepidoblastic, porphyroblastic (Figure 3.9), and consists of muscovite, biotite, quartz, plagioclase, KyS garnet, kyanite or sillimanite, and staurolite (Figures 3.10-3.13).

### ***Central Blue Ridge***

The central Blue Ridge in the Hazelwood quadrangle contains two distinct lithologies: Cartoogechaye gneiss and Otto Formation metaclastic rocks of the Dahlonaga Gold Belt (Bream and Hatcher, 2002; Hatcher, 2005). The Cartoogechaye gneiss is exposed as a northeast trending belt extending across the entire map area. The Otto Formation is exposed in the southeastern corner of the map area (Figure 3.1). Lithologic similarities are common between the Otto formation and the psammitic meBimbers of the Copperhill Formation, however, correlation of the units in the southeastern portion to the Otto Formation is based on previous work to the southwest by Montes (1997) and to the east by Merschhat (2009), both of which recognized amphibolite bodies enclosed by hornblende gneiss in the Otto Formation along strike, and thus distinguishing the Otto Formation from the Copperhill Formation.

The Cartoogechaye terrane gneiss (Czct) is a heterogeneous assemblage of dominantly migmatitic biotite gneiss and hornblende-biotite gneiss, with lesser amphibolite. Migmatitic biotite gneiss, which is the dominant unit in the study area, is medium- to dark-gray, medium- to coarse-grained, well-foliated (layered, with leucosomes), inequigranular, and locally porphyroblastic. It consists of quartz, plagioclase, biotite, potassium feldspar, muscovite, epidote, and garnet porphyroblasts (Figures 3.14-3.21). Hornblende-biotite gneiss, which occurs as lenses in biotite gneiss, is a medium- to dark-gray, medium- to coarse-grained, foliated, inequigranular, and locally porphyroblastic unit. It consists of quartz, plagioclase, biotite, hornblende and garnet (Figure 3.24). Amphibolite is common, and occurs as as cm to m scale boudins, lenses, and layers in migmatitic biotite gneiss (Figure 3.22). Amphibolite is dark-gray, medium- to coarse-grained, and inequigranular and consists of plagioclase, hornblende, and garnet (Figure 3.23). The degree and style of migmatization is variable, but is the most conspicuous and characteristic aspect of Cartoogechaye rocks. Stromatic and schlieren migmatite structures are common throughout the Cartoogechaye terrane. Agmatite structures, which involve leucosome and migmatitic biotite gneiss folded around lenses and blocks of amphibolite and biotite gneiss, are only observed in outcrops with amphibolite present.

The Otto Formation of the Dahlonga gold belt (CZo) consists primarily of gneissic metapsammite and biotite schist. Gneissic metapsammite is tan to medium-gray, fine- to medium-grained, equigranular, foliated, and locally migmatitic (Figure 3.25). Unit mineralogy consists of quartz, plagioclase, muscovite, biotite, potassium feldspar, and garnet. Gneissic metapsammite is commonly interlayered with pelitic schist

and metasiltstone with layer thickness ranging from 1 cm to 2 m. Biotite schist is dark-gray, orange-yellow weathering, fine- to medium-grained, lepidoblastic, and porphyroblastic (Figure 3.26). It contains quartz, biotite, muscovite, garnet, and sillimanite (Figure 3.27).

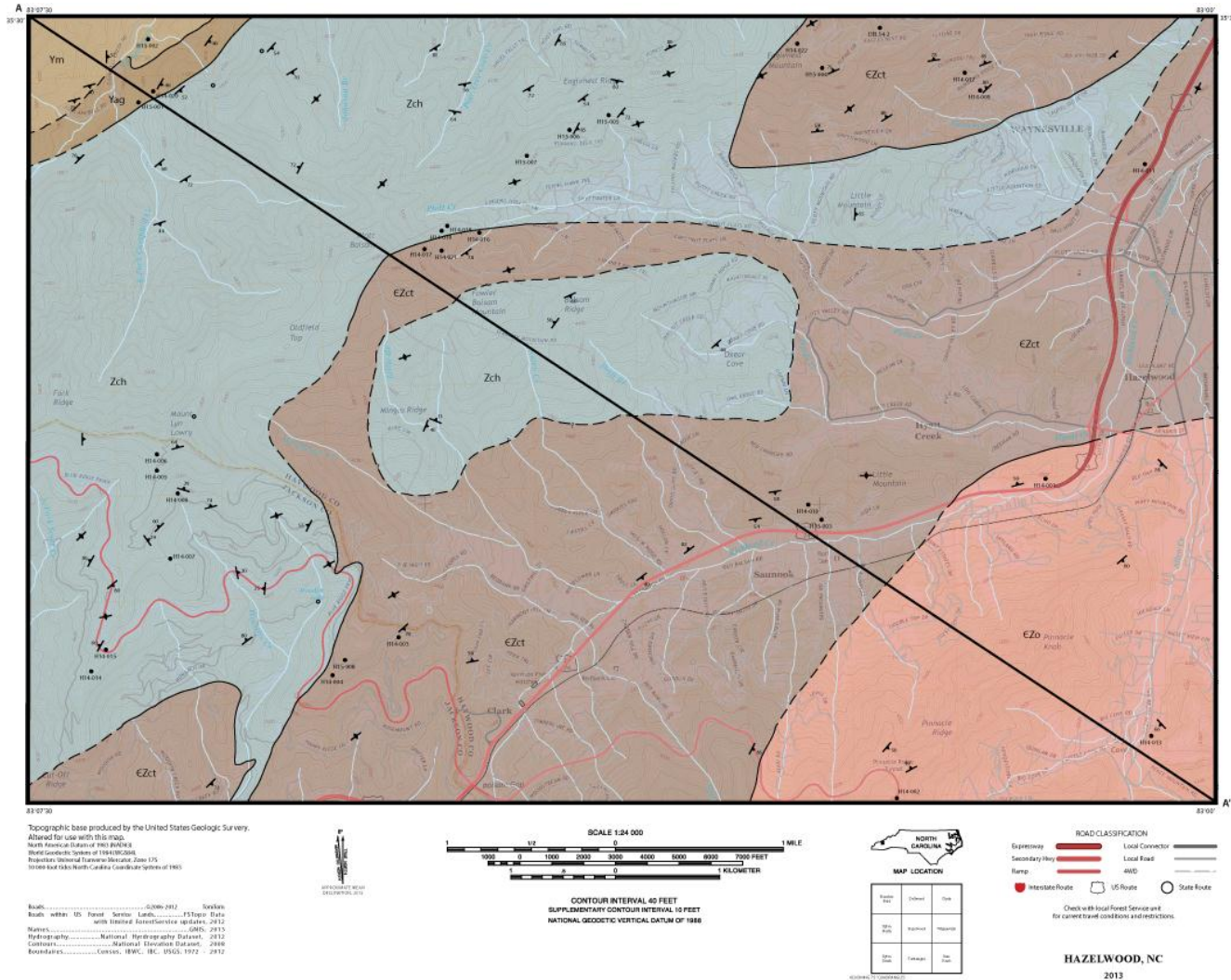
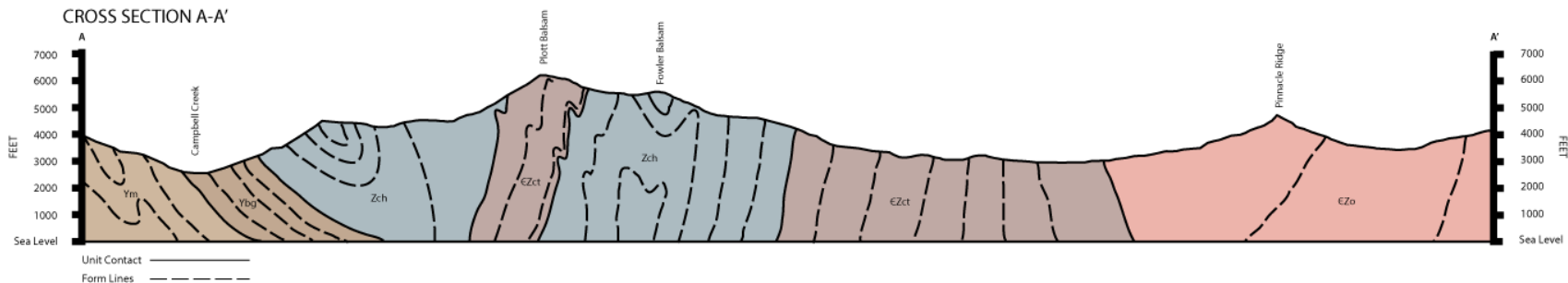


Figure 3.1: Geologic map of the Hazelwood 7.5'' quadrangle, western North Carolina. Ym: migmatitic biotite gneiss; Yag: augen gneiss; Zch: Copperhill Formation; EZct: Cartoagechaye terrane; EZo: Otto Formation. A high resolution version of this map is available in file 1.



**MAP UNITS**

- EZo** **Otto Formation**
- EZct** **Cartoogechaye terrane**
- Zch** **Copperhill Formation**
- Yag** **Augen gneiss**
- Ym** **Migmatitic biotite gneiss**

**EXPLANATION OF MAP SYMBOLS**

**CONTACTS**

- Contact—Identity and existence certain, location accurate
- Contact—Identity and existence certain, location inferred
- Contact—Identity or existence questionable, location inferred

**PLANAR FEATURES**

- Inclined metamorphic or tectonic foliation—Showing strike and dip
- Vertical metamorphic or tectonic foliation—Showing strike

**LINEAR FEATURES**

- Inclined generic (origin or type not known or not specified) lineation or linear structure—Showing bearing and plunge

**OTHER FEATURES**

- Sample locality—Showing sample number

Figure 3.1: Continued. Cross-section and explanation for the geologic map of the Hazelwood 7.5" quadrangle.

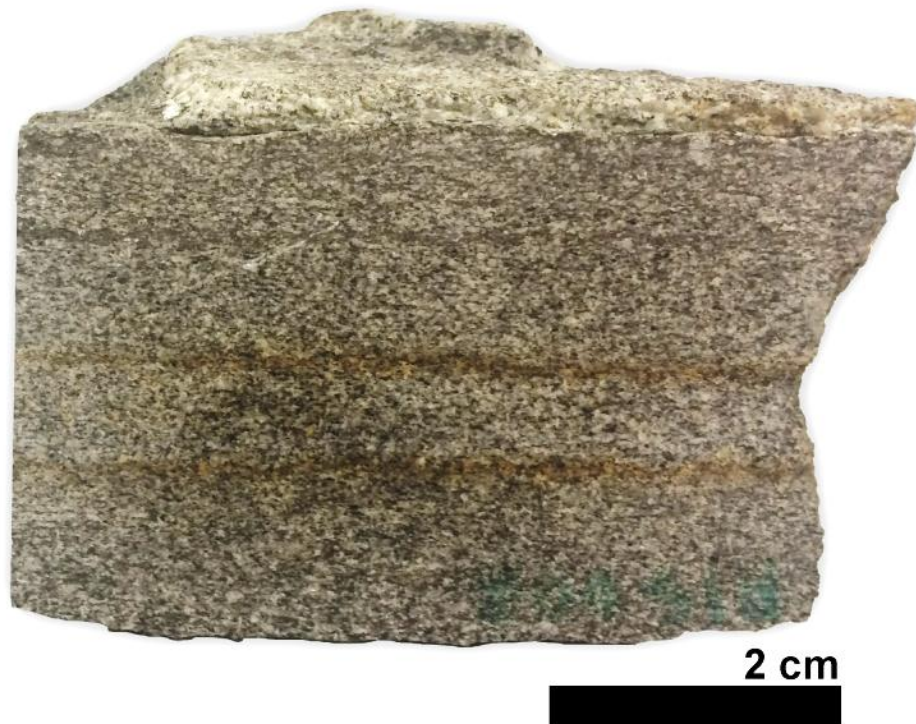


Figure 3.2: Photograph of hand sample of biotite gneiss sample H15-002. Collected in the rim of the Campbell Creek anticline.

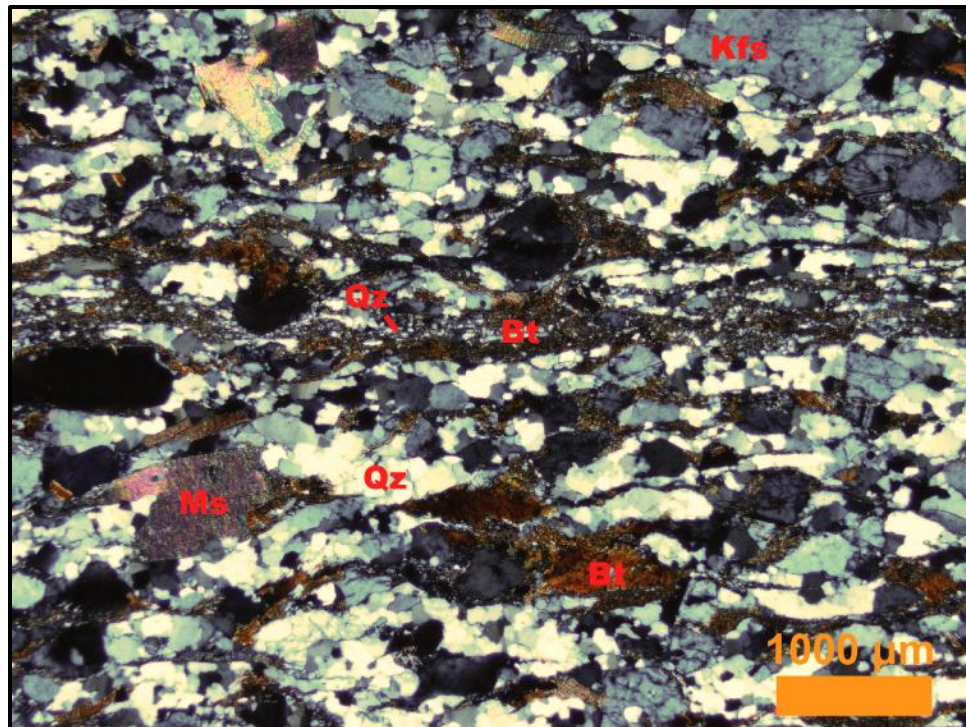


Figure 3.3: Photomicrograph in polarized light of biotite gneiss sample H15-002. Fine-grained biotite and recrystallized quartz define the dominant foliation.



Figure 3.4: Photograph of hand sample of augen gneiss sample H15-001 collected in the core of the Campbell Creek anticline.

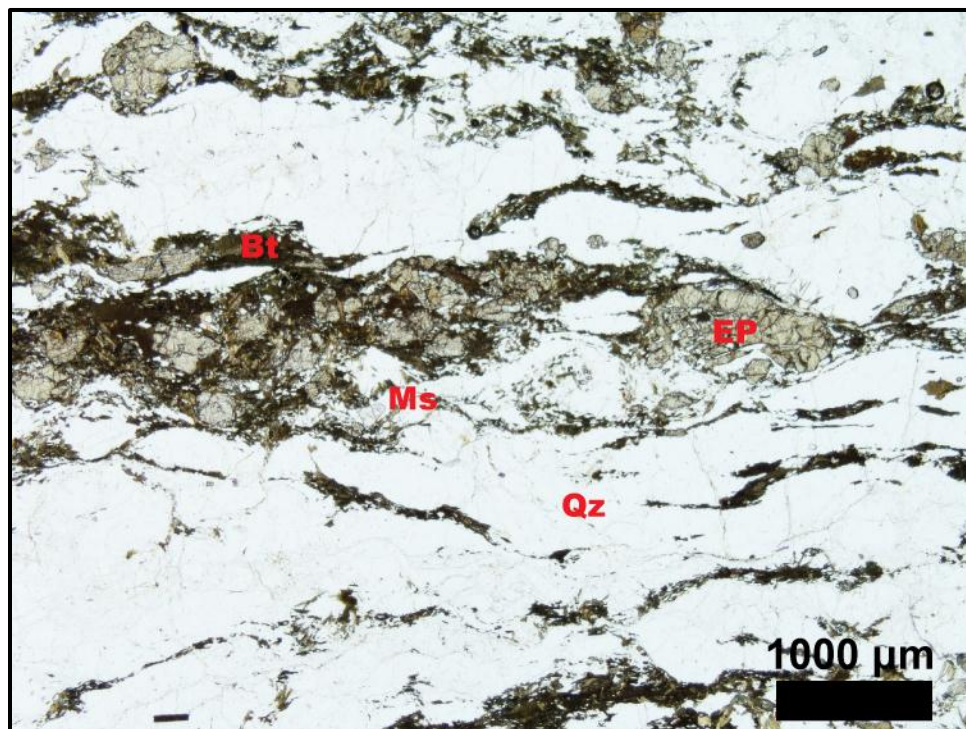


Figure 3.5: Photomicrograph of augen gneiss sample H15-001 annotated to show mineral assemblage and foliation defined by recrystallized biotite, epidote, and quartz.

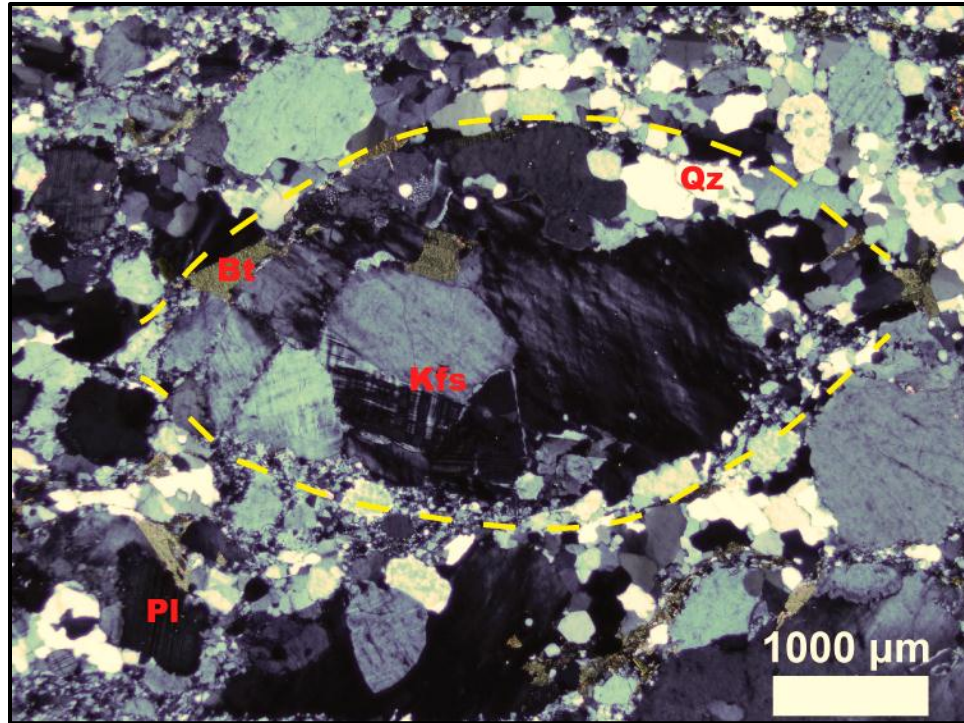


Figure 3.6: Photomicrograph (crossed polar) of augen gneiss sample H15-001 showing biotite grains wrapping around relict Kfs phenocryst recrystallized to porphyroblast (augen: yellow line).



Figure 3.7: Photograph of a hand sample of Copperhill metapsammite. Photograph taken at the location of sample H14-007.



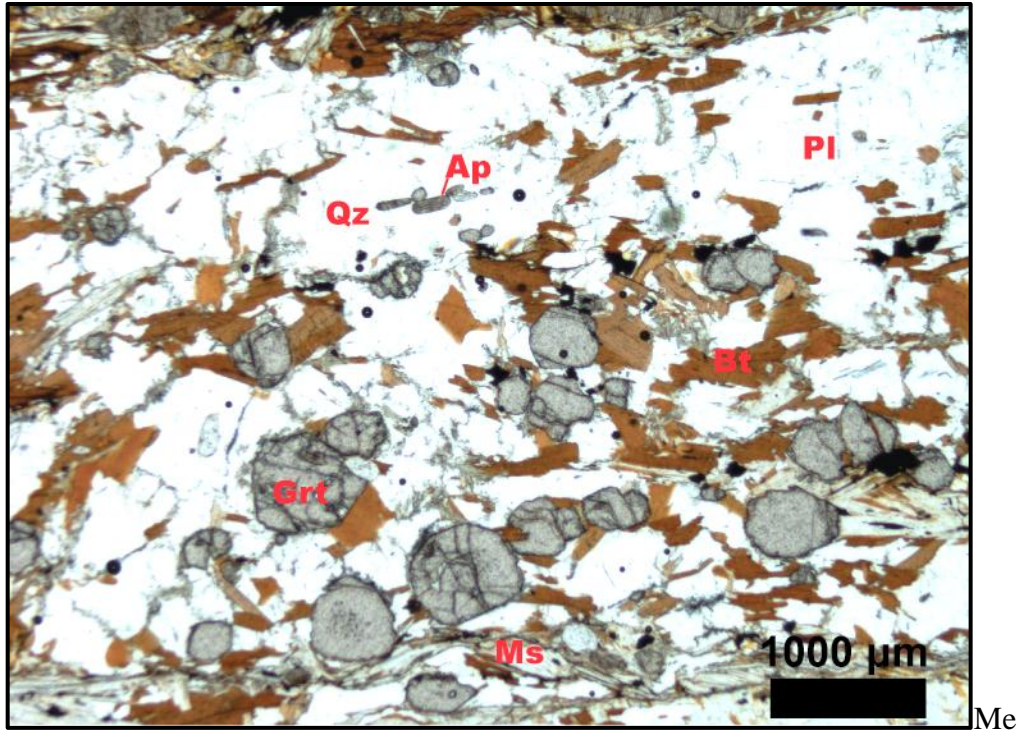


Figure 3.8: Photomicrograph of Copperhill metapsammite sample H15-008 annotated to show mineral assemblage.



Figure 3.9: Photograph of hand sample of Copperhill biotite-muscovite schist sample H15-007 containing a deformed leucosome parallel to the foliation. Parallelism of cm-scale kyanite porphyroblasts, biotite and muscovite defines the dominant fabric.

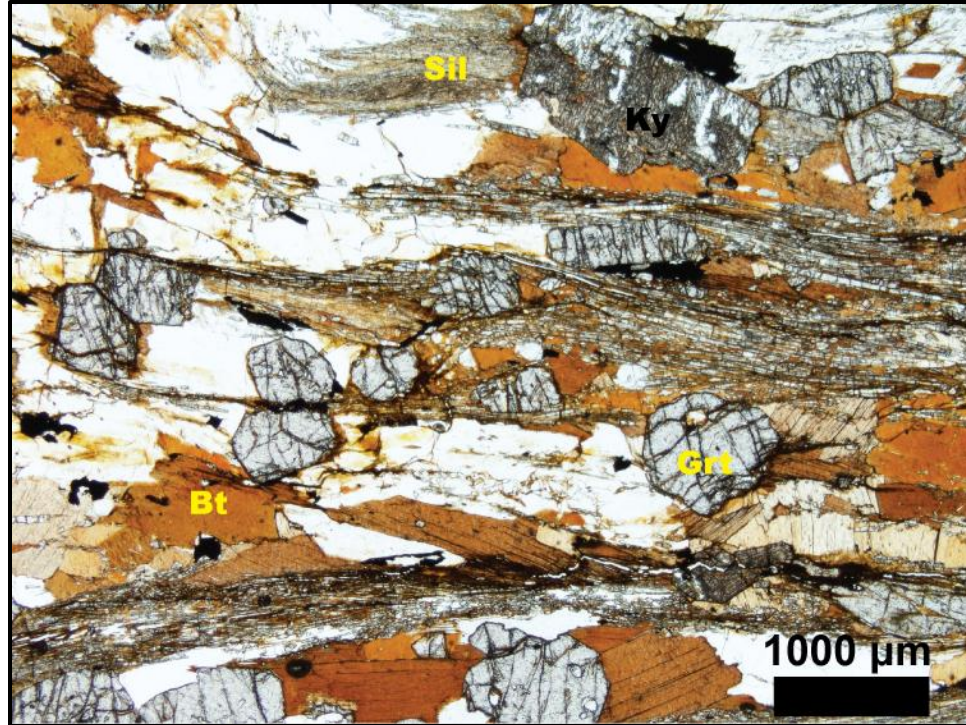


Figure 3.10: Photomicrograph of Copperhill biotite-muscovite schist sample H14-008 annotated to show mineral assemblage. Fibrous sillimanite is crystallizing at the grain boundary of kyanite and is interlayered with muscovite.

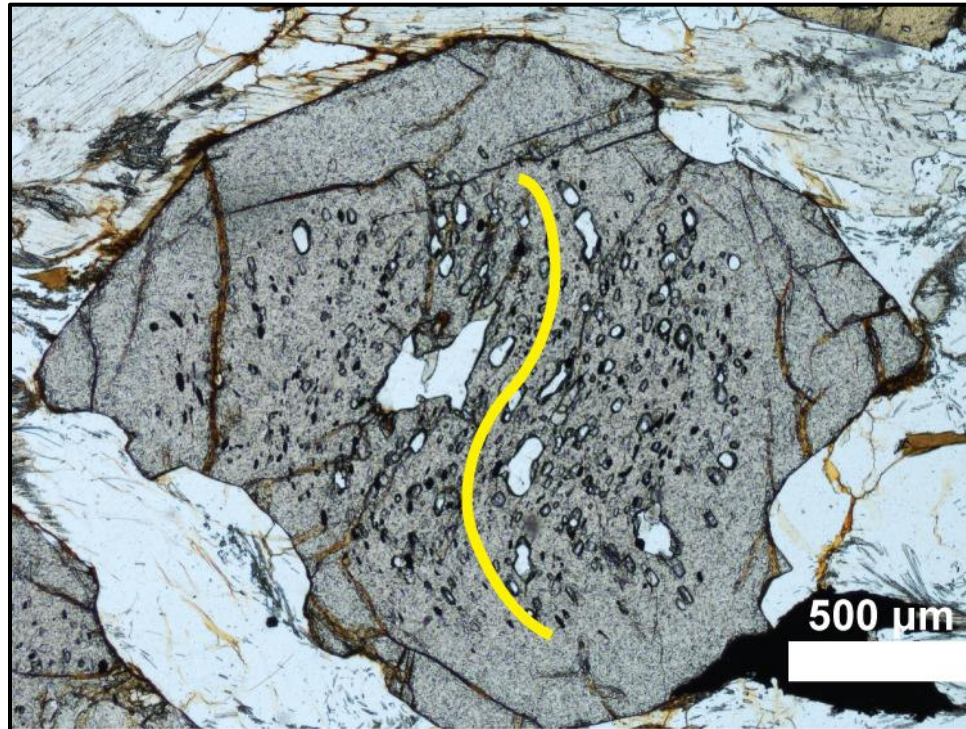


Figure 3.11: Photomicrograph of sigmoidal inclusion trail in subhedral, partly resorbed garnet from Copperhill biotite-muscovite schist sample H14-006.

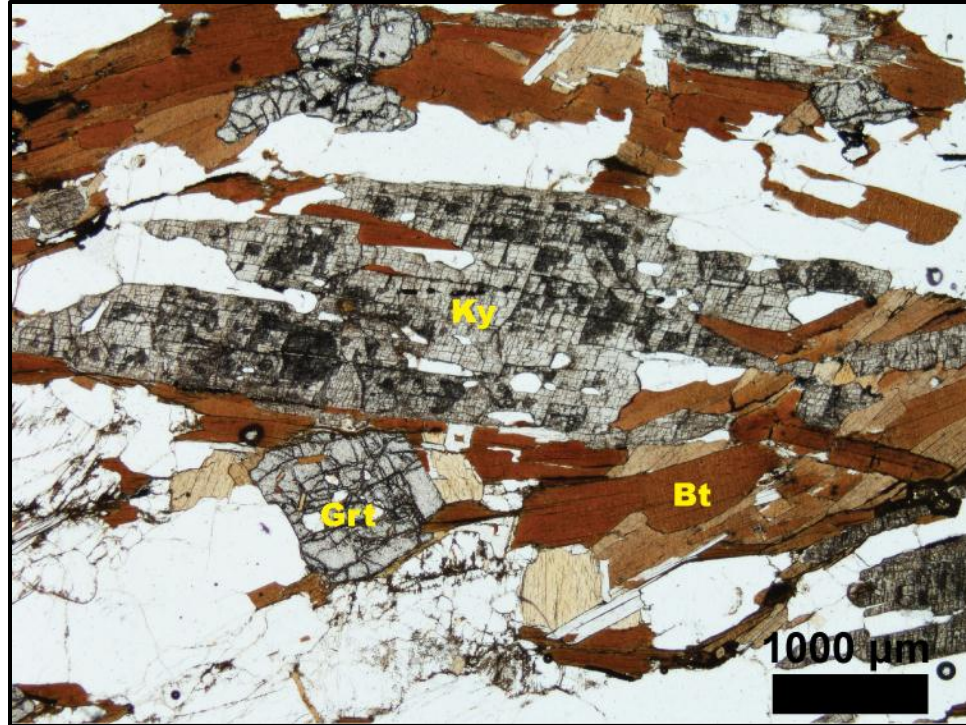


Figure 3.12: Photomicrograph of poikioblastic kyanite and garnet in Copperhill biotite-muscovite schist sample H15-007. Abundant pleochroic halos surround zircon inclusions in kyanite and biotite.

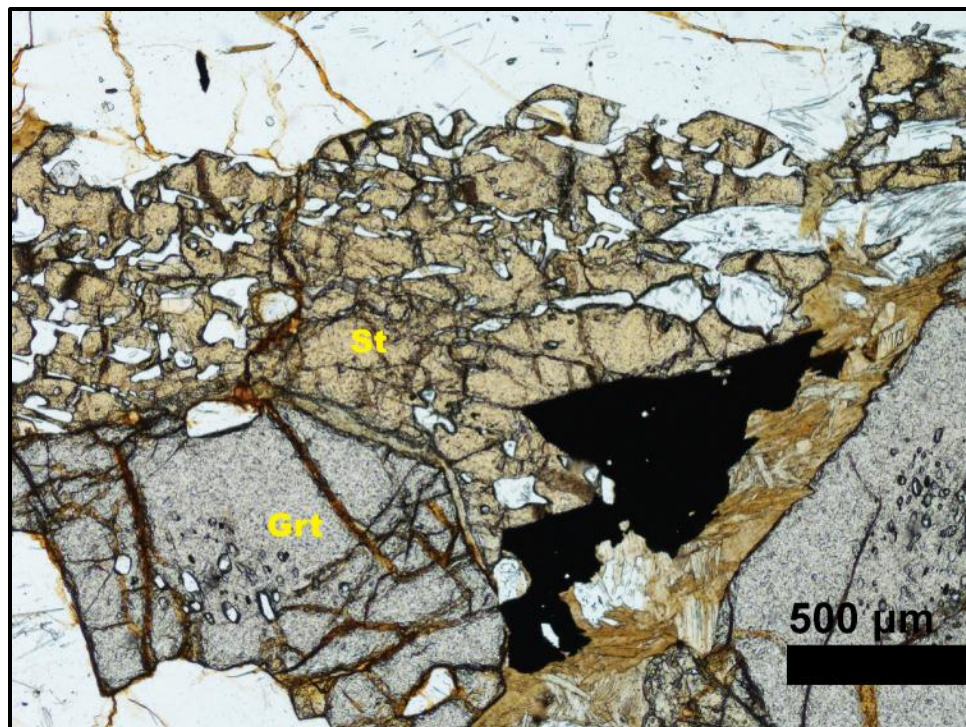


Figure 3.13: Photomicrograph of poikioblastic staurolite and garnet in biotite-muscovite schist sample H14-006. Intergrowth of sillimanite + biotite is crystalizing around the rim of the garnet. Staurolite partly envelops garnet.



Figure 3.14: Photograph of hand sample of Copperhill schist sample H15-009 showing retrograde muscovite pseudomorphs replacing kyanite.



Figure 3.15: Photograph of hand sample of Cartoogechaye biotite gneiss sample DEL14-2. Sample collected at the same location as DEL14-1.



Figure 3.16: Photograph of Cartoogechaye biotite gneiss sample H15-003.



Figure 3.17: Photomicrograph of Cartoogechaye biotite gneiss sample DEL14-2 annotated to show mineral assemblage. Biotite and muscovite define the weak and folded foliation.



**3 cm**

Figure 3.18: Photograph of hand sample of Cartoogechaye migmatitic biotite gneiss sample H14-003. Stromatic layering is continuous and folded.



**3 cm**

Figure 3.19: Photograph of hand sample of Cartoogechaye migmatitic biotite gneiss sample H14-009. Stromatic layering is irregularly folded with many folds appearing intrafolial.



Figure 3.20: Photograph of hand sample of Cartoogechaye migmatitic biotite gneiss sample H15-004. Stromatic layering is continuous and not folded at the scale of the hand sample.

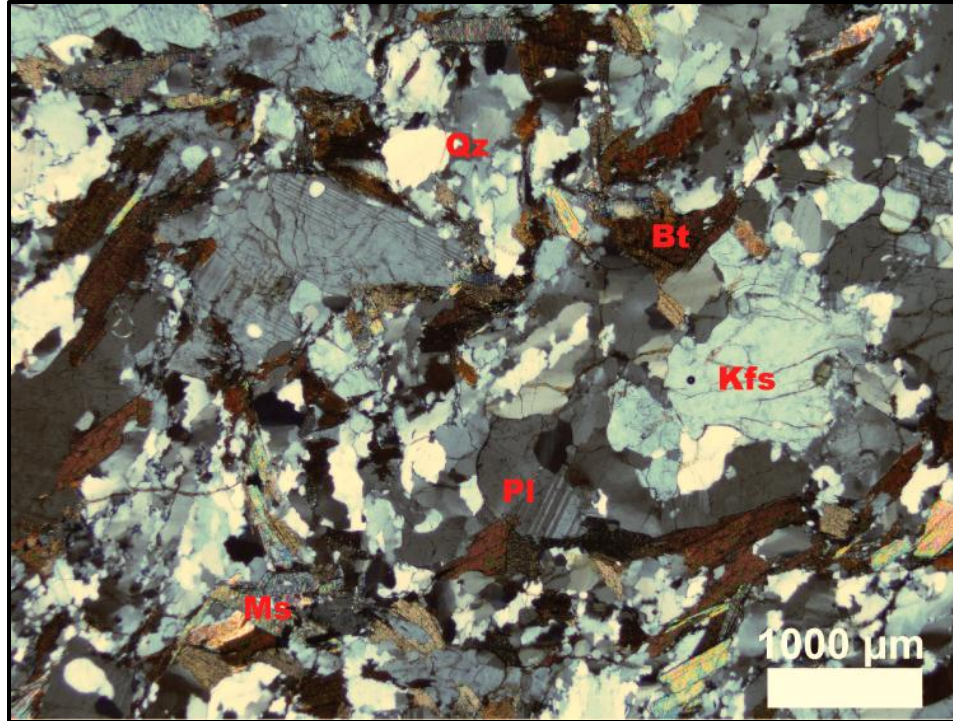


Figure 3.21: Photomicrograph in polarized light of Cartoogechaye migmatitic biotite gneiss sample H15-004 annotated to show mineral assemblage.



Figure 3.22: Photograph of hand sample of Cartoogechaye migmatitic hornblende-biotite gneiss sample H14-011. Migmatite structure is agmatitic with angular fragments of melanosome and garnet-rich amphibolite pods surrounded by feldspar leucosome.



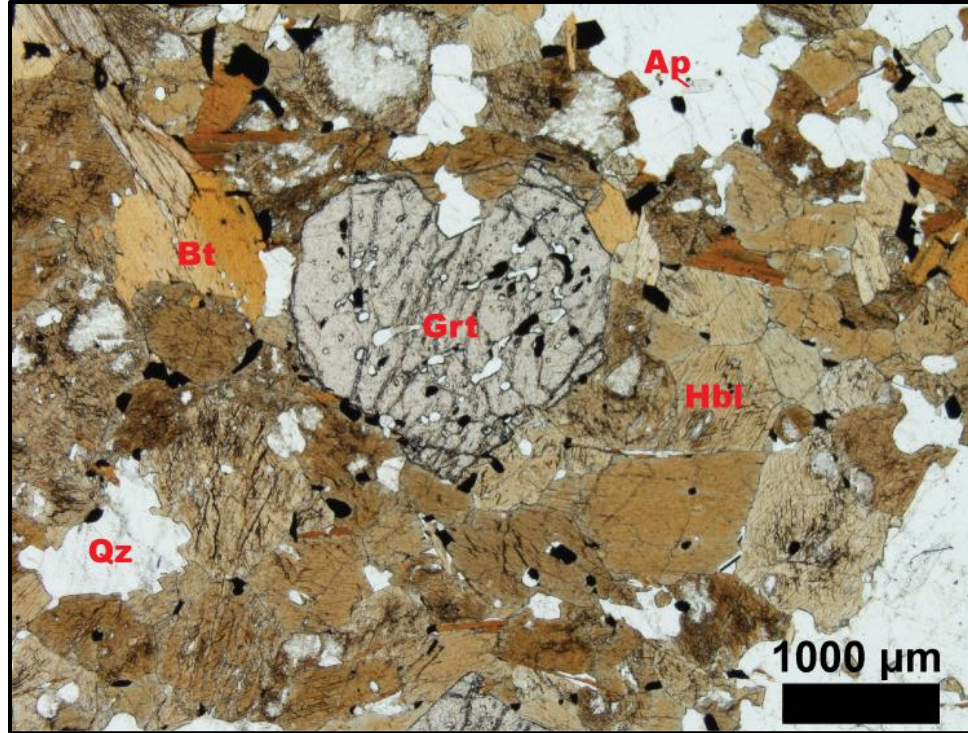


Figure 3.23: Photomicrograph of amphibolite pod in Cartoogechaye hornblende-biotite gneiss sample H14-011. Subhedral hornblende and biotite grains surround poikloblastic garnet.

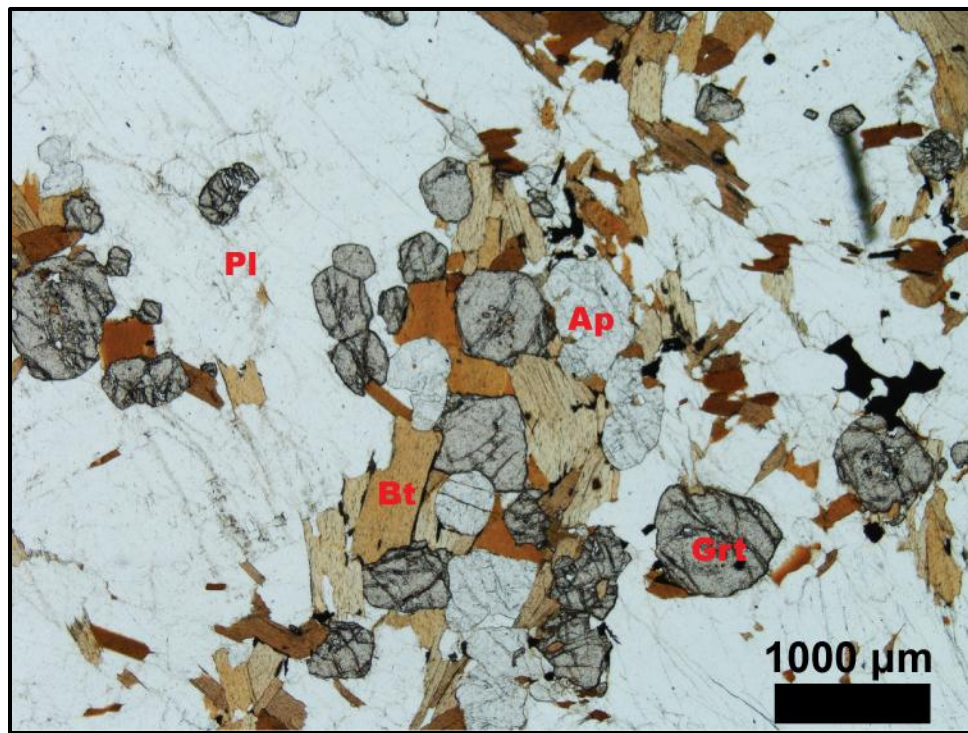


Figure 3.24: Photomicrograph of leucosome in Cartoogechaye hornblende-biotite gneiss sample H14-011. Biotite, garnet and apatite are surrounded by a plagioclase matrix.



Figure 3.25: Photograph of hand sample of Otto gneissic metapsammite. Sample collected at the same location as sample H14-002. Although primarily a metapsammite, the bulk composition was appropriate for generating leucosomes.



Figure 3.26: Photograph of hand sample of Otto biotite schist sample H14-001.

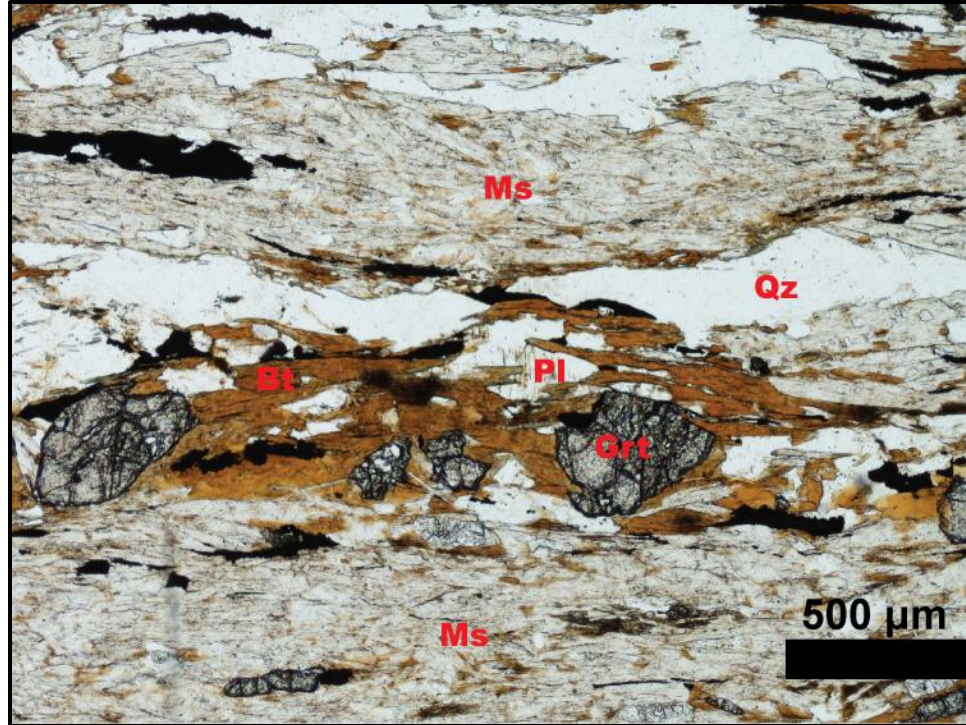


Figure 3.27: Photomicrograph of Otto biotite schist sample H14-001 annotated to show mineral assemblage. Layers of aligned muscovite and biotite define the dominant fabric.

## Structure

The rocks in the Hazelwood quadrangle experienced at least four periods of Paleozoic deformation. The oldest period of deformation ( $D_1$ ) is recognized by relict bed parallel foliation/schistosity ( $S_1$ ) and isoclinal folds ( $F_1$ ) preserved in amphibolite boudins (Figure 3.28).  $S_1$  foliation is interpreted to be bed-parallel, based on evidence of  $S_0$  from compositional layering in metapsammite observed to the east of the quadrangle.

The second period of deformation ( $D_2$ ) is recognized by a penetrative foliation ( $S_2$ ) that bounds intrafolial isoclinal folds ( $F_2$ ).  $S_2$  is the dominant foliation in the study area and overprints  $S_1$ . In thin section,  $S_2$  is defined by parallelism of muscovite, biotite, elongate quartz grains, and kyanite.  $S_2$  foliation strikes NE and is steeply dipping to subvertical (Figure 3.29).

The third period of deformation ( $D_3$ ) is recognized by open to isoclinal flexural flow folds ( $F_3$ ) and the development of an axial plane cleavage (Figure 3.30).  $F_3$  fold axes predominantly trend northeast.  $S_3$  is defined by folded/kinked muscovite and dynamic recrystallization of quartz (Figure 3.31). Evidence of  $S_3$  is limited to thin section observation.

The last period of deformation ( $D_4$ ) is recognized by high angle brittle faults, localized shear zones, and drag folds ( $F_4$ ) (Figure 3.32). Quartz veins and pegmatite intrusions are commonly observed in fault zones (Figure 3.33).

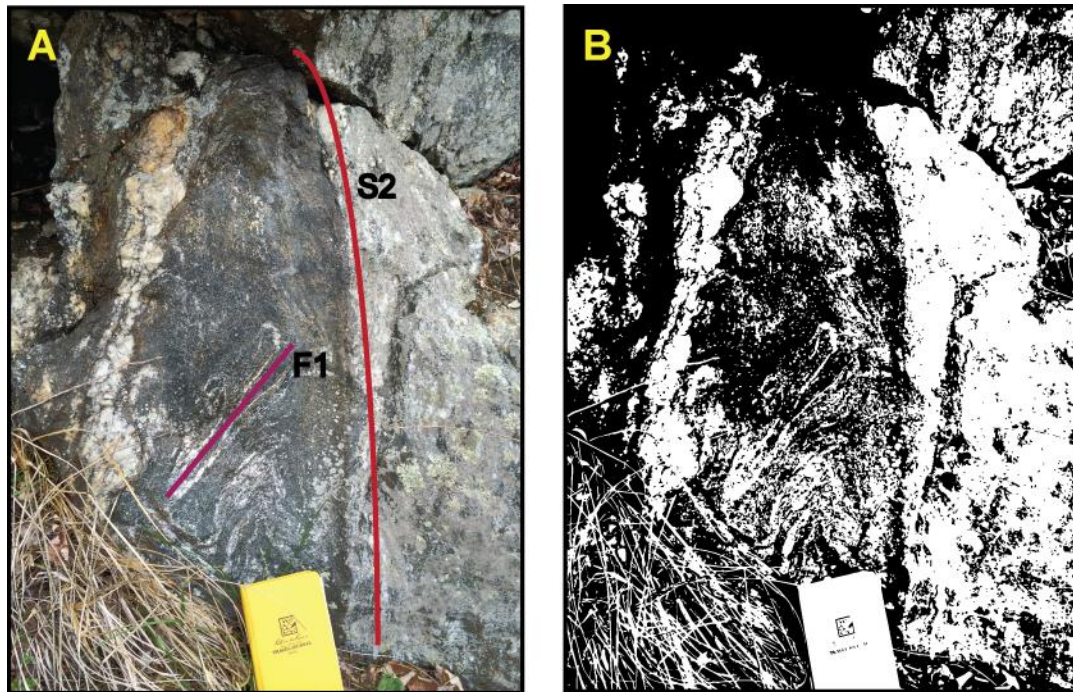


Figure 3.28:  $F_1$  isoclinal folds in amphibolite pod surrounded by vertical  $S_2$  foliation. (a) Photograph taken at Mount Lyn Lowry overlook on the Blue Ridge parkway. (b) Black and white image trace of photograph A.

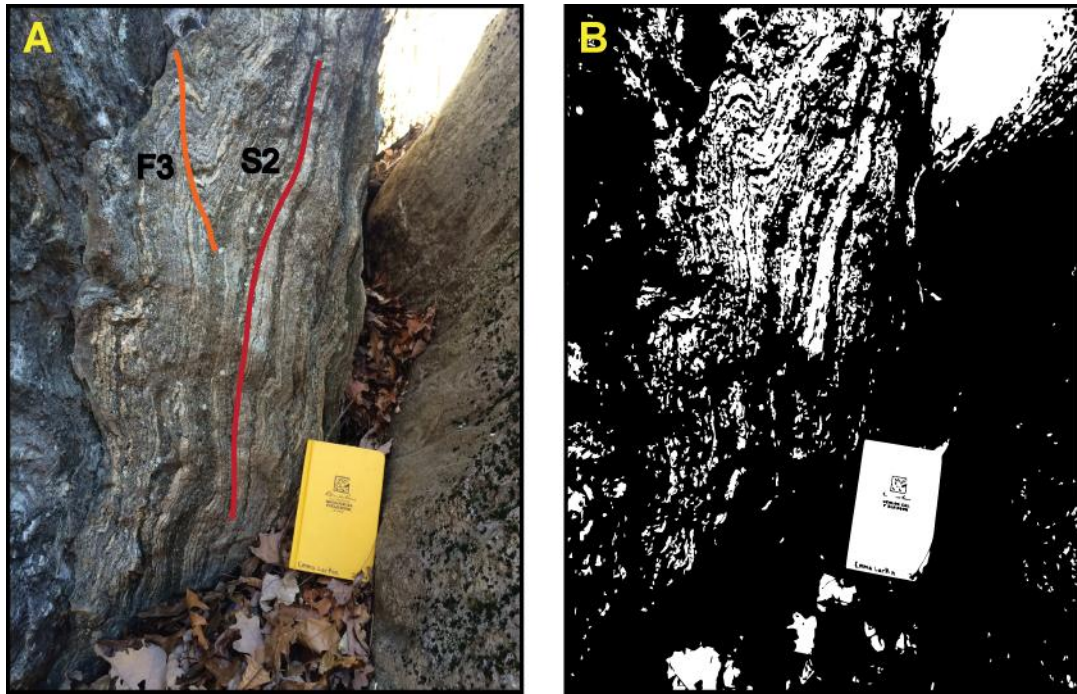


Figure 3.29: Vertical S2 foliation in migmatitic biotite gneiss. (a) Photograph taken on Rocky Knob Road. (b) Black and white image trace of photograph A.

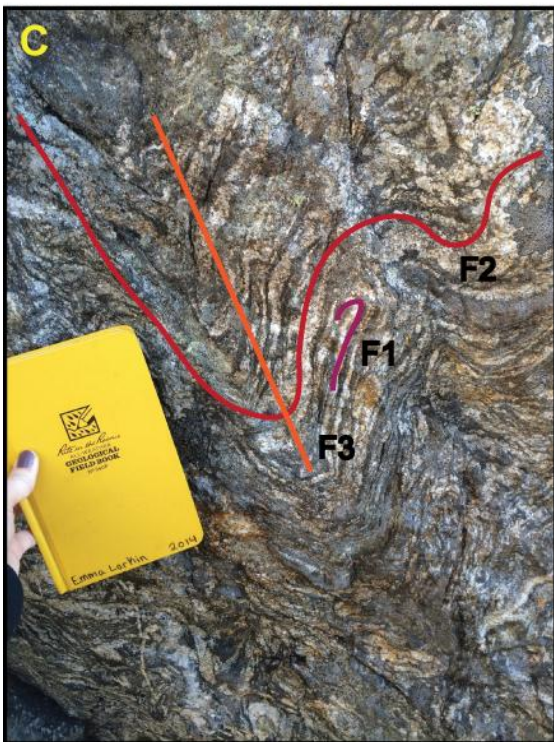


Figure 3.30: (a). Open F3 folding deforming subvertical S2 foliation. Photograph taken near the peak of Plott Balsam Mt. (b) Black and white image trace of photograph A. (c) F1 isoclinal fold refolded by F2 isoclinal fold refolded by closed F3 fold. Photograph taken at end of Eagle Ridge Drive. (d) Black and white image trace of photograph C.

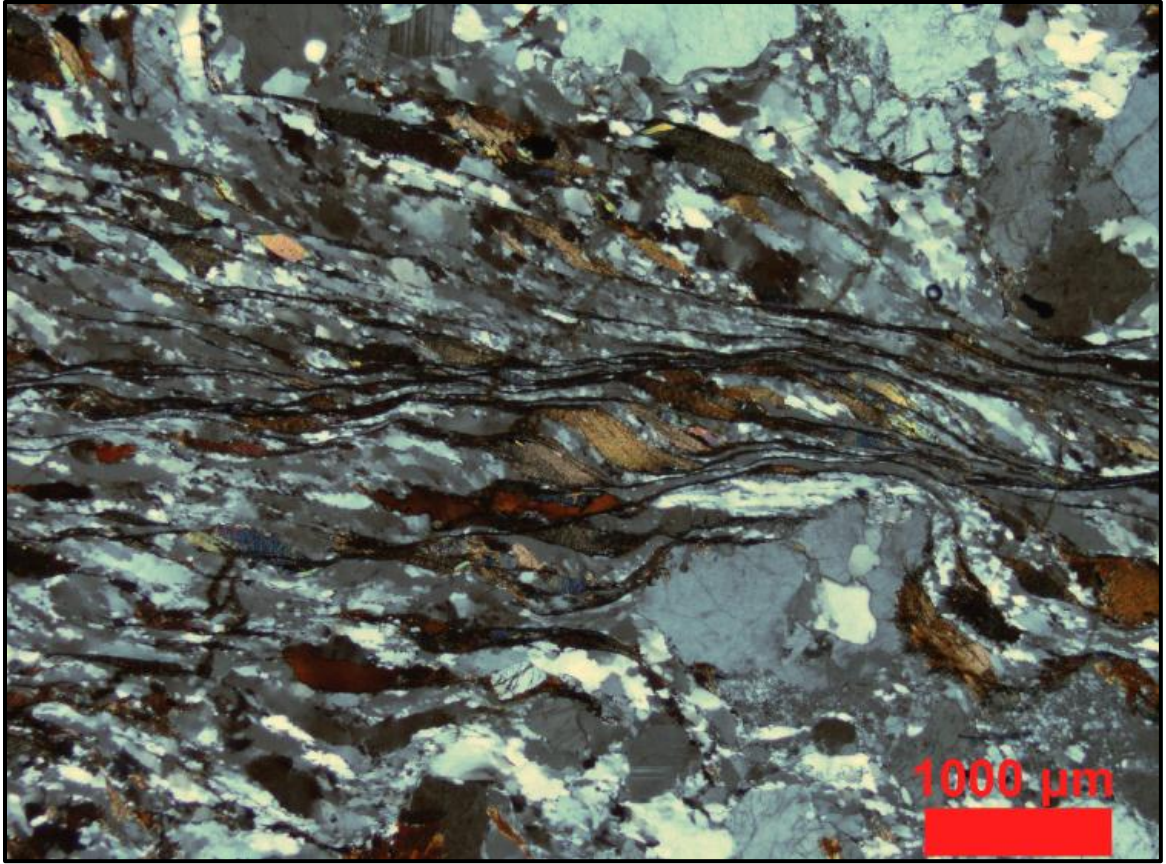


Figure 3.31: Photomicrograph of protomylonite sample H14-017. Dynamically recrystallized quartz and mica fish produce a shear band cleavage (S-C fabric).

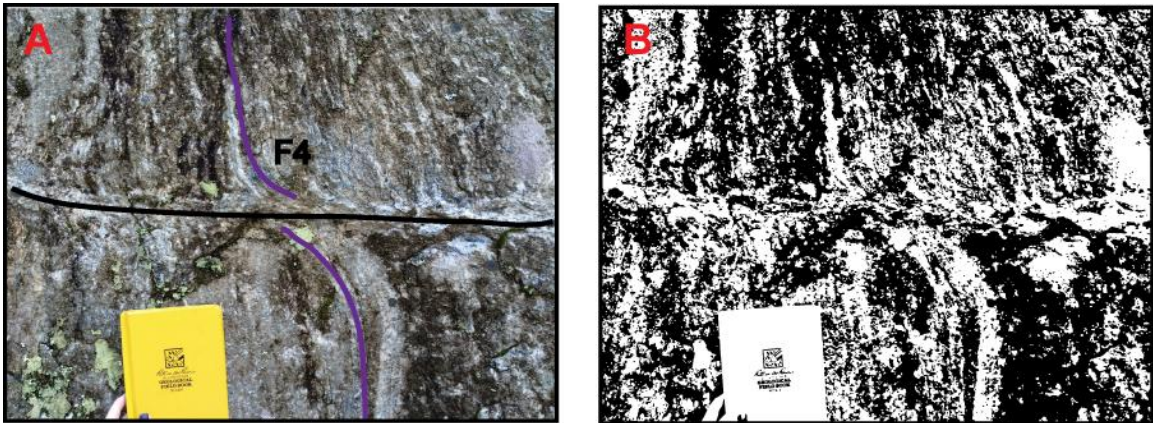


Figure 3.32: (a) Photograph of D4 drag folds. Photograph taken on OlliTrail. (b) Black and white image trace of photograph A.



Figure 3.33: (a) Photograph of D4 veins. Photograph taken at sample location H14-011. (b) Black and white image trace of photograph A. (c) Inclusion of migmatitic biotite gneiss in D4 pegmatite. Photograph taken on Turkey Trail. (d) Black and white image trace of photograph C.



## **Metamorphism**

Metamorphism in the Hazelwood quadrangle ranges from amphibolite to upper amphibolite facies (kyanite to sillimanite grade) and increases from the northwest to the southeast, as evidenced by kyanite porphyroblasts, fibrous mats of sillimanite replacing kyanite in the pelitic rocks (Figure 3.10), and increased proportion of leucosome in gneiss. The rocks in the western Blue Ridge reached amphibolite facies whereas the rocks in the Central Blue Ridge reached upper amphibolite facies. Peak metamorphism occurred during the Taconic orogeny (Moecher et al., 2004) and Alleghanian retrograde metamorphism is indicated in the western and central Blue Ridge by replacement of garnet with biotite and chlorite as well as sericitization of kyanite (Figure 3.14).

## **CHAPTER IV. RESULTS OF U-PB ZIRCON GEOCHRONOLOGY**

Apparent cores of zircons separated from Cartoogechaye terrane (DEL14-1, H14-011, H15-003, and H15-004), Otto Formation (H14-002), and Copperhill Formation (H14-007) paragneiss were analyzed at the University of Arizona LaserChron Center on the Thermo Element2 multi-collector inductively coupled plasma-mass spectrometer. These analyses were used to identify zircon age populations that could correspond to several potential events, including: (1) the magmatic or metamorphic ages of source rocks, if the zircon grains are detrital or (2) timing of metamorphism/migmatization of the paragneiss if the zircon formed in a leucosome during high grade metamorphism. Additionally, if the grain is detrital, its age would serve as a constraint on the maximum age of deposition of the sedimentary protolith. Cores of magmatic zircon from an orthogneiss sample (H14-020) were analyzed at the University of California Los Angeles on the CAMECA 1270 ion microprobe to determine the age of crystallization of the

igneous protolith. A description of analytical procedures can be found in Chapter II. Geochronologic data are compiled in Appendices B-H. The “best ages” were determined from  $^{206}\text{Pb}/^{238}\text{U}$  ages for grains less than 900 Ma and  $^{206}\text{Pb}/^{207}\text{Pb}$  ages for grains greater than 900 Ma. This is because  $^{206}\text{Pb}/^{238}\text{U}$  ages are more precise for younger systems and  $^{206}\text{Pb}/^{207}\text{Pb}$  ages are more precise for older systems (Gehrels, 2008). Discordance is common among the zircons analyzed by LA-ICP-MS. This could be due to lead loss during prolonged heating, or lead loss during zircon recrystallization during high grade metamorphism. Apparent discordance could also result from laser spots falling on an age boundary. Probability density plots are based on zircons that are greater than 90% concordant. The implications of discordance for interpretation of ages are discussed later.

### **Orthogneiss**

Orthogneiss sample H14-020 was collected from an outcrop of Augen gneiss in the core of the Campbell anticline (Figure 2.1). Zircons from this sample are subhedral with strong to weak oscillatory zoned cores and unzoned rims that range from 1-30  $\mu\text{m}$  in thickness (Figure 4.1). Many zircons have fractures, inclusions, and metamict cores, which were intentionally avoided during selection of analysis spots. Nine cores of zircons from this sample were analyzed, which yielded ages that range from 1087 to 1232 Ma. A concordant age of  $1147 \pm 8$  Ma is the proposed age of the magmatic cores, which is interpreted to represent the crystallization age of the protolith of the orthogneiss (Figure 4.2).

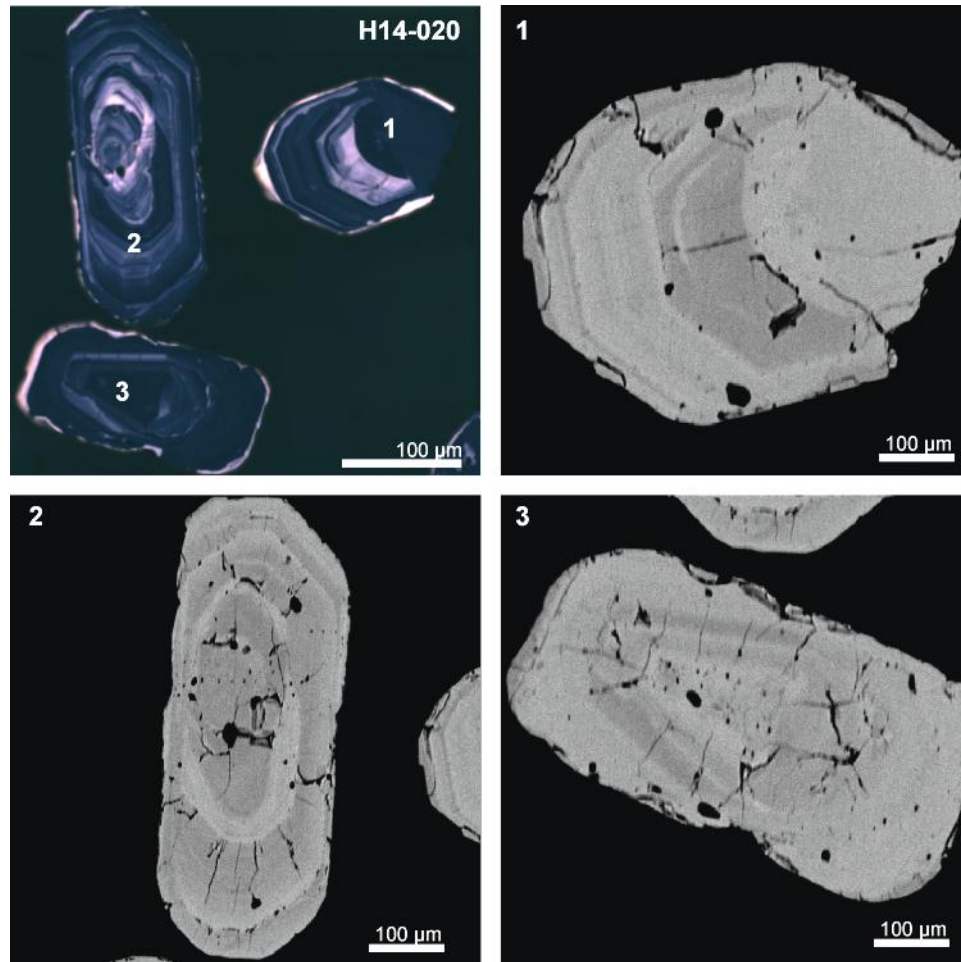


Figure 4.1: Cathodoluminescence (upper left) and back scatter electron images of grains 1-3 from H14-020 showing oscillatory (magmatic) zoning and distribution of inclusions. Grain 2 contains a xenocrystic core.

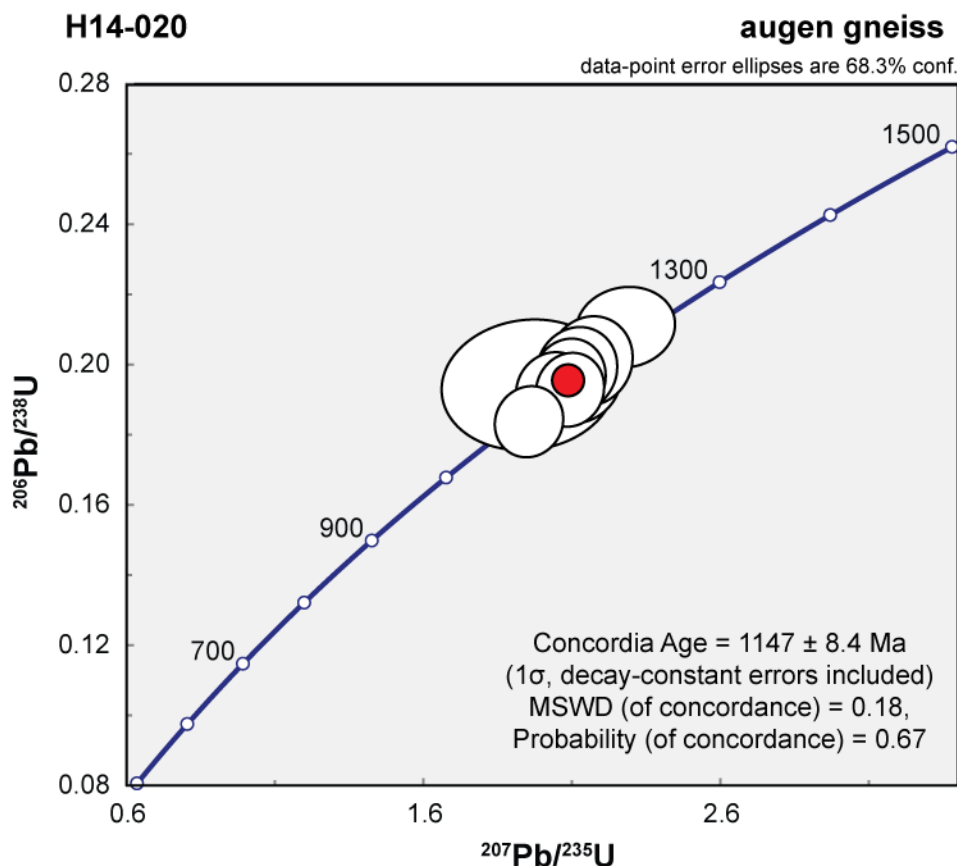


Figure 4.2: Concordia diagram from sample H14-020 zircon data. Analyses are by SIMS.

### Paragneiss

Paragneiss samples were collected from representative outcrops within the Cartoogechaye terrane, Otto Formation, and Copperhill Formation for detrital zircon geochronology. Highly variable and complex zonation patterns are common in all of the samples. These zircons are primarily subhedral to anhedral, with oscillatory and/or sector zoned and unzoned cores. Few zircons cores contain metamict structures. Weakly zoned to unzoned rims that range from ~5-20  $\mu\text{m}$  in thickness are common and consistent with metamorphic growth. BSE and Cl images (Figure 4.3) were used to avoid analysis of overlapping zones, metamict cores, and metamorphic rims.

***DEL14-1 (Cartoogechaye biotite gneiss):***

Cores of 308 zircons were analyzed in a sample of migmatitic biotite gneiss collected from the north side of Eaglesnest Ridge (Figure 2.1). 287 analyses are greater than 90% concordant. Concordant zircon ages range from approximately 995 Ma to 1688 Ma with two dominant Mesoproterozoic age populations at 1030 Ma and 1150-1200 Ma (Figure 4.4). Minor age populations include the Mesoproterozoic (1420 and 1510 Ma); Paleoproterozoic ( $1688 \pm 21$  Ma), single grain; and Neoproterozoic ( $724 \text{ Ma} \pm 9 \text{ Ma}$ ), single grain.

***H14-011 (Cartoogechaye migmatitic hornblende biotite gneiss):***

Cores of 314 zircons were analyzed in a sample of migmatitic hornblende biotite gneiss collected along US 287 Highway 74 (Figure 2.1). This sample had the lowest proportion of concordant grains with only 174 analyses being greater than 90% concordant. Concordant zircon ages range from approximately 442 Ma to 1734 Ma, with five distinct age populations (Figure 4.5) including: (1) Mesoproterozoic grains with age modes at 1025 Ma and 1150 Ma; (2) Mesoproterozoic grains with ages between approximately 1350 Ma and 1450 Ma; (3) Paleoproterozoic grains between approximately 1620 Ma and 1735 Ma are present; (4) Neoproterozoic grains between approximately 730 Ma and 875 Ma; (5) Paleozoic grains with a weighted mean age of  $465 \pm 2$  Ma that comprise approximately 20% of this sample (Figure 4.6).

***H15-003 (Cartoogechaye migmatitic biotite gneiss):***

Cores of 300 zircons were analyzed in a sample of migmatitic biotite gneiss collected south of sample H14-011 along US Highway 74 (Figure 2.1). 258 analyses are greater than 90% concordant. Concordant zircon ages range from approximately 450 Ma

to 1252 Ma with two distinct age populations (Figure 4.7). The majority (~ 90%) of the zircons are Mesoproterozoic, with a peak at 1180 Ma. Although sample H15-003 contains zircons at ~1000 Ma, it is the only sample analyzed that does not exhibit the two distinct Mesoproterozoic age modes typical of Grenville zircons. In addition, it is the only Cartoogechaye gneiss sample that does not have Paleoproterozoic zircons. Paleozoic metamorphic zircons with peaks at 480 and 460 Ma make up approximately 10% of this sample and are consistent with Taconic orogenesis. Many of the grains define a linear trend on the Tera-Wasserburg diagram between ca. 1150 and ca. 450 Ma (Figure 4.7).

***H15-004 (Cartoogechaye migmatitic felsic gneiss):***

Cores of 291 zircons were analyzed in a sample of migmatitic felsic gneiss collected on the peak of Eaglenest Mountain (Figure 2.1). 236 analyses are greater than 90% concordant and concordant zircon ages range from 457 Ma to 2077 Ma (Figure 4.8). Mesoproterozoic grains make up 90% of the sample, with age modes at 1040 Ma and 1100 Ma. Mesoproterozoic zircons ranging from approximately 1300-1580 Ma are also present and three Paleoproterozoic grains were analyzed at  $1644 \pm 18$  Ma,  $2076 \pm 14$  Ma, and  $2077 \pm 20$  Ma. Neoproterozoic zircons define an age population with a peak at 680 Ma. Paleozoic zircon age populations are shown at 540 Ma and between 460 Ma and 480 Ma; this is the only sample in which zircons with greater than 90% concordance have ages at ~540 Ma.

***H14-007 (Copperhill Formation metapsammite)***

Apparent cores of 286 detrital zircons were analyzed in a sample of metapsammite collected on the south side of Mount Lyn Lowry (Figure 2.1) and 241 analyses were greater than 90% concordant. Ages range from 763 Ma to 1846 Ma (Figure

4.9), with the most abundant ages being Mesoproterozoic (1060 Ma, 1170 Ma, and 1440 Ma). Paleoproterozoic age populations have peaks at 1650 Ma, 1730 Ma, and 1840 Ma and a single Neoproterozoic age ( $763 \pm 12$  Ma) was also present. No Paleozoic metamorphic grains were recognized.

***H14-002 (Otto Formation gneissic metapsammite)***

Apparent cores of 251 detrital zircons were analyzed in a sample of metapsammite collected on Pinnacle Ridge (Cove Field Ridge overlook on the Blue Ridge parkway) (Figure 2.1) and 174 analyses are greater than 90% concordant. Concordant zircon ages range from approximately 434 Ma to 2519 Ma (Figure 4.10), with greater than 90% being Mesoproterozoic with age populations at 1020 Ma, 1150 Ma, and 1320 Ma. Minor age populations include a single Archean zircon ( $2519 \pm 18$  Ma), which represents the oldest age revealed in the study and two Neoproterozoic ages ( $\sim 850$  Ma). Paleozoic zircons with a weighted mean age of  $454 \pm 10$  Ma make up approximately 20% of this sample (Figure 4.11).

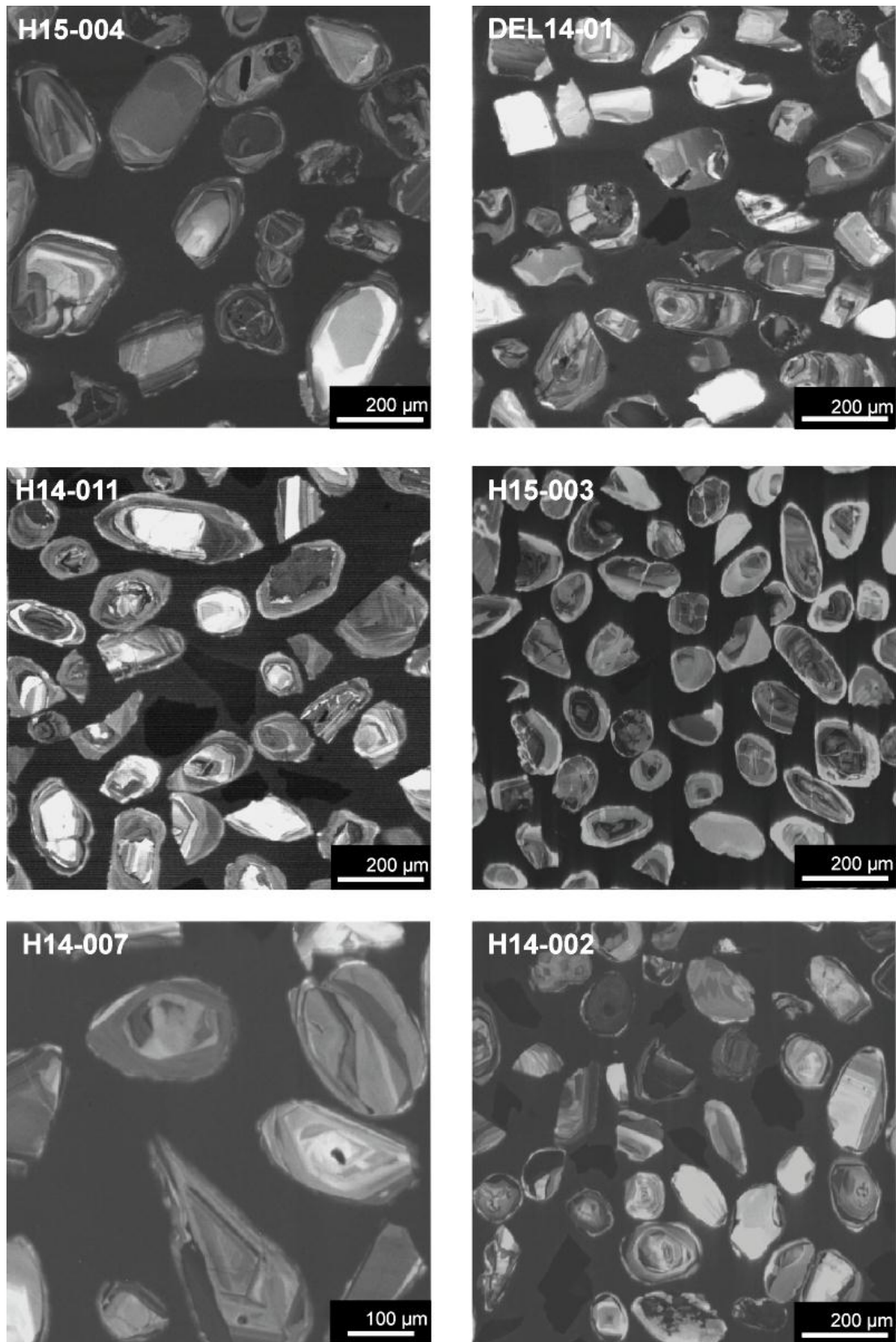


Figure 4.3: Cathodoluminescence images of representative sections of zircon mounts.



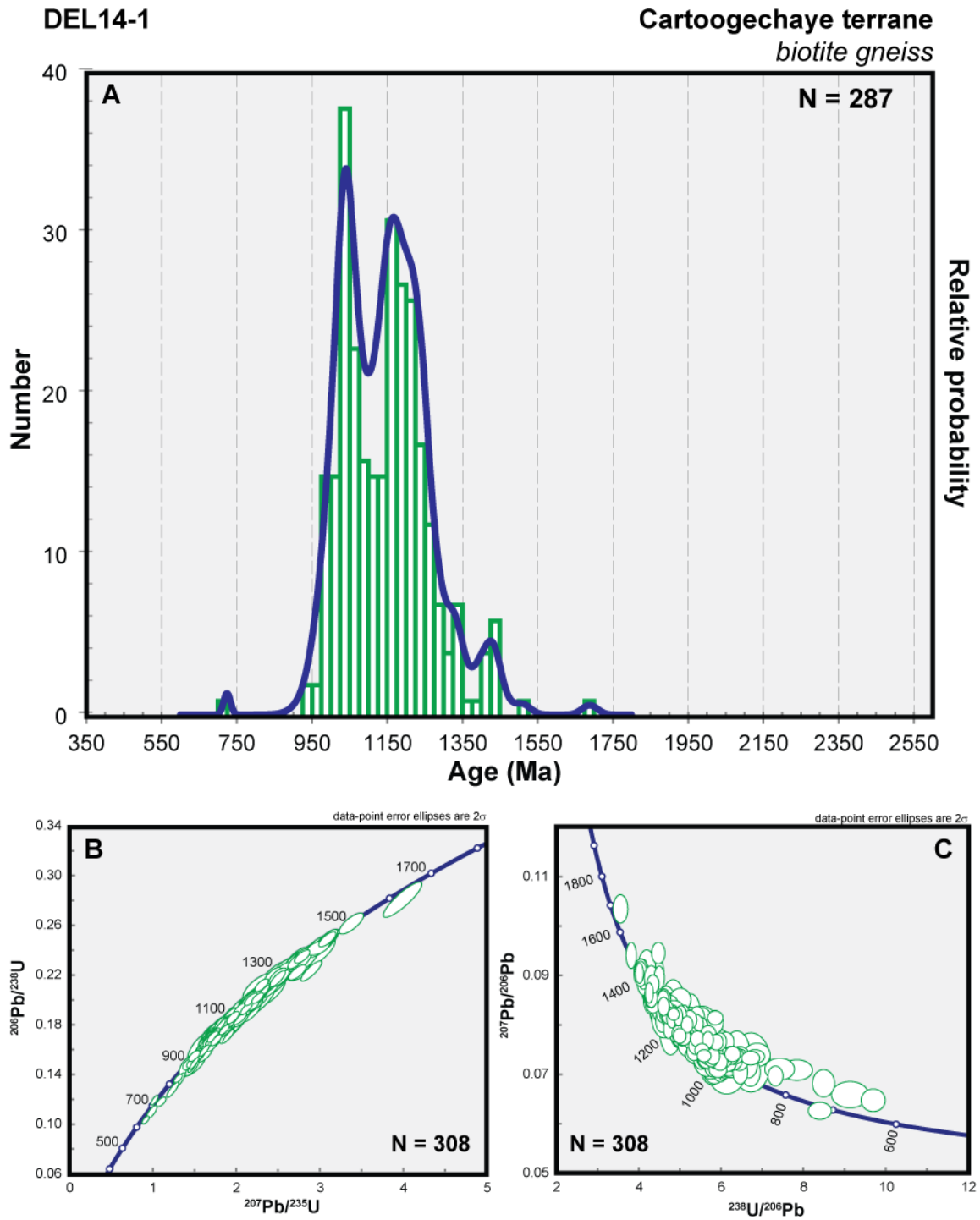


Figure 4.4: Results of LA-ICP-MS of zircon from sample DEL14-1. (a) Probability density plot of data with greater than 90% concordance. (b) Concordia diagram of all data. (c) Tera-Wasserburg diagram of all data.

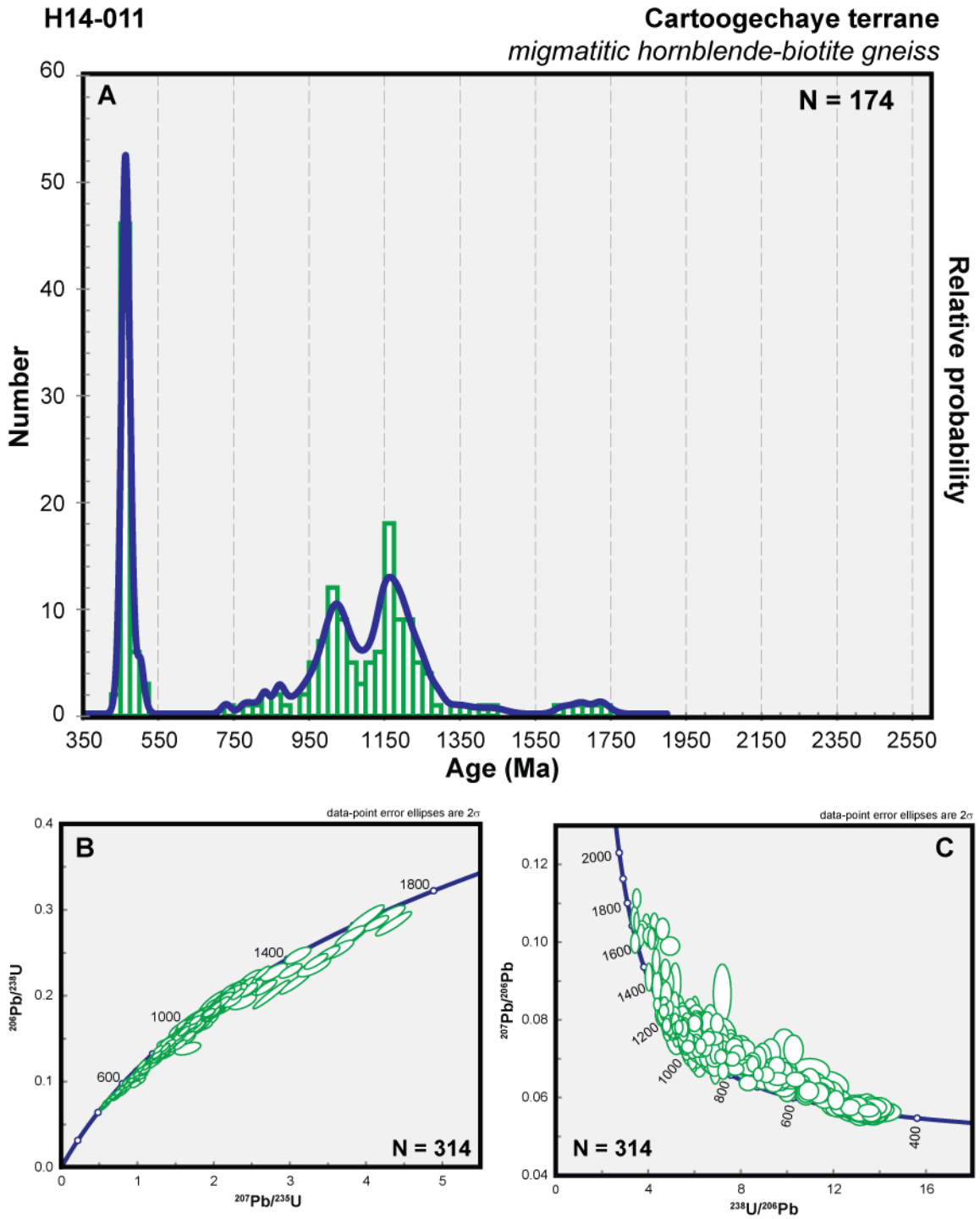


Figure 4.5: Results of LA-ICP-MS of zircon from sample H14-011. (a) Probability density plot of data with greater than 90% concordance. (b) Concordia diagram of all data. (c) Tera-Wasserburg diagram of all data.

H14-011

**Cartoogechaye terrane**  
*migmatitic hornblende-biotite gneiss*  
data-point error symbols are  $1\sigma$

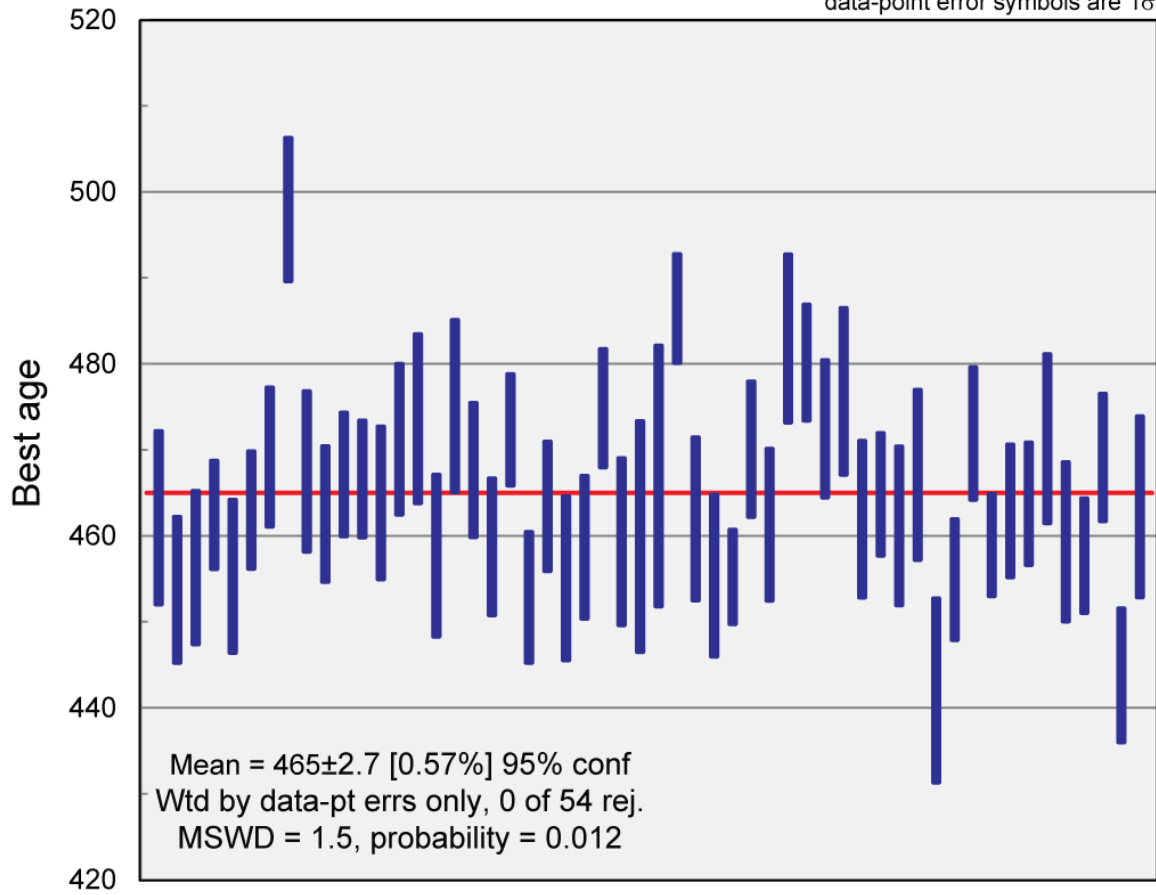


Figure 4.6: Mean 'best' age plot of data with ages under 500 Ma and greater than 90% concordance from sample H14-011. The mean 'best' age of  $465 \pm 3$  is the proposed age of Taconic metamorphism for the sample. It should be noted that this calculation of the mean age of metamorphism may be producing an apparent older age due to the presence of a shoulder off of the dominant Taconic peak seen in figure 4.5.

H15-003

Cartoogechaye terrane  
*biotite gneiss*

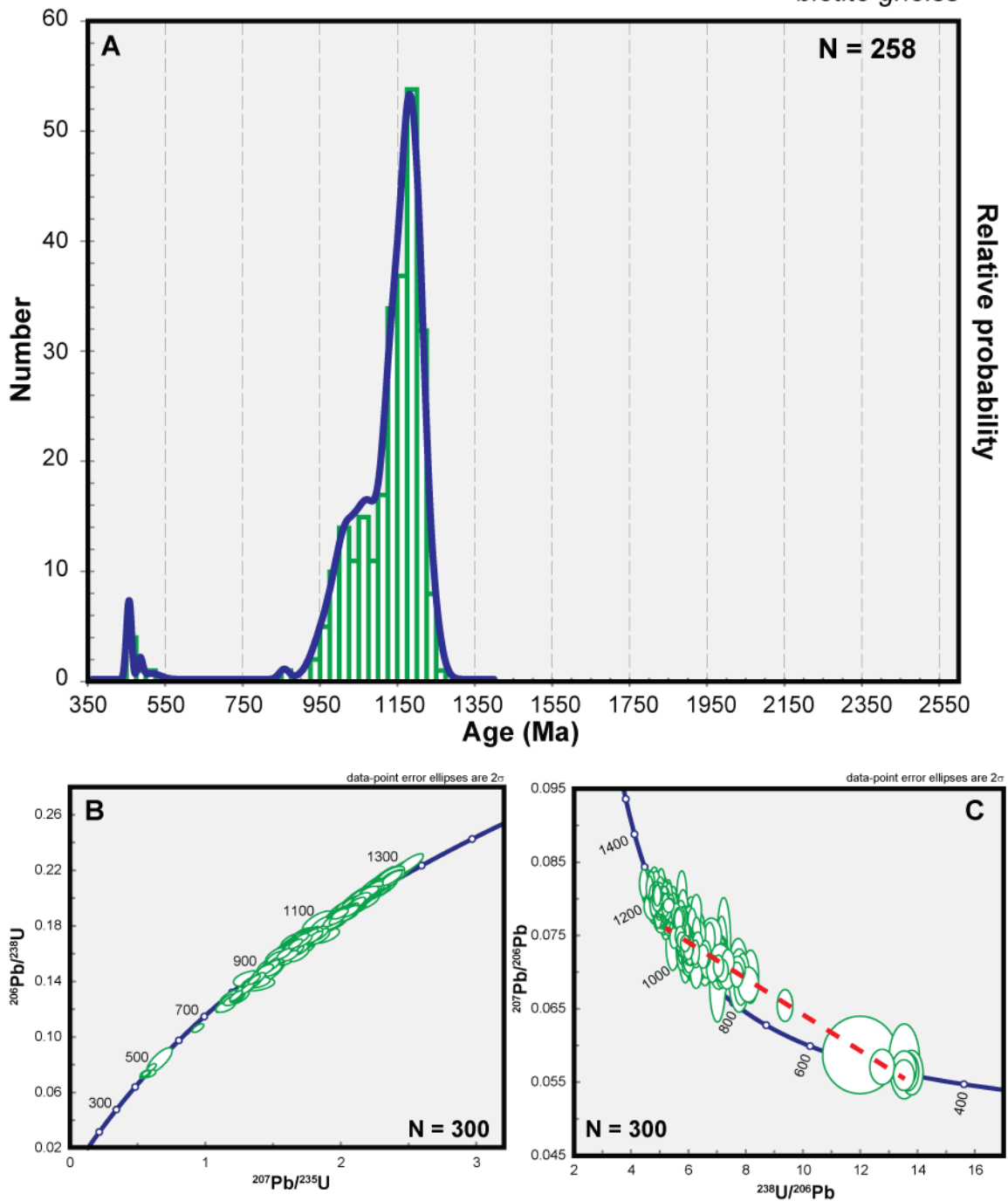


Figure 4.7: Results of LA-ICP-MS of zircon from sample H15-003. (a) Probability density plot of data with greater than 90% concordance. (b) Concordia diagram of all data. (c) Tera-Wasserburg diagram of all data. Red dashed line shows apparent linear trend between ca. 1150 and ca. 450 Ma.

H15-004

Cartoogechaye terrane  
*migmatitic felsic gneiss*

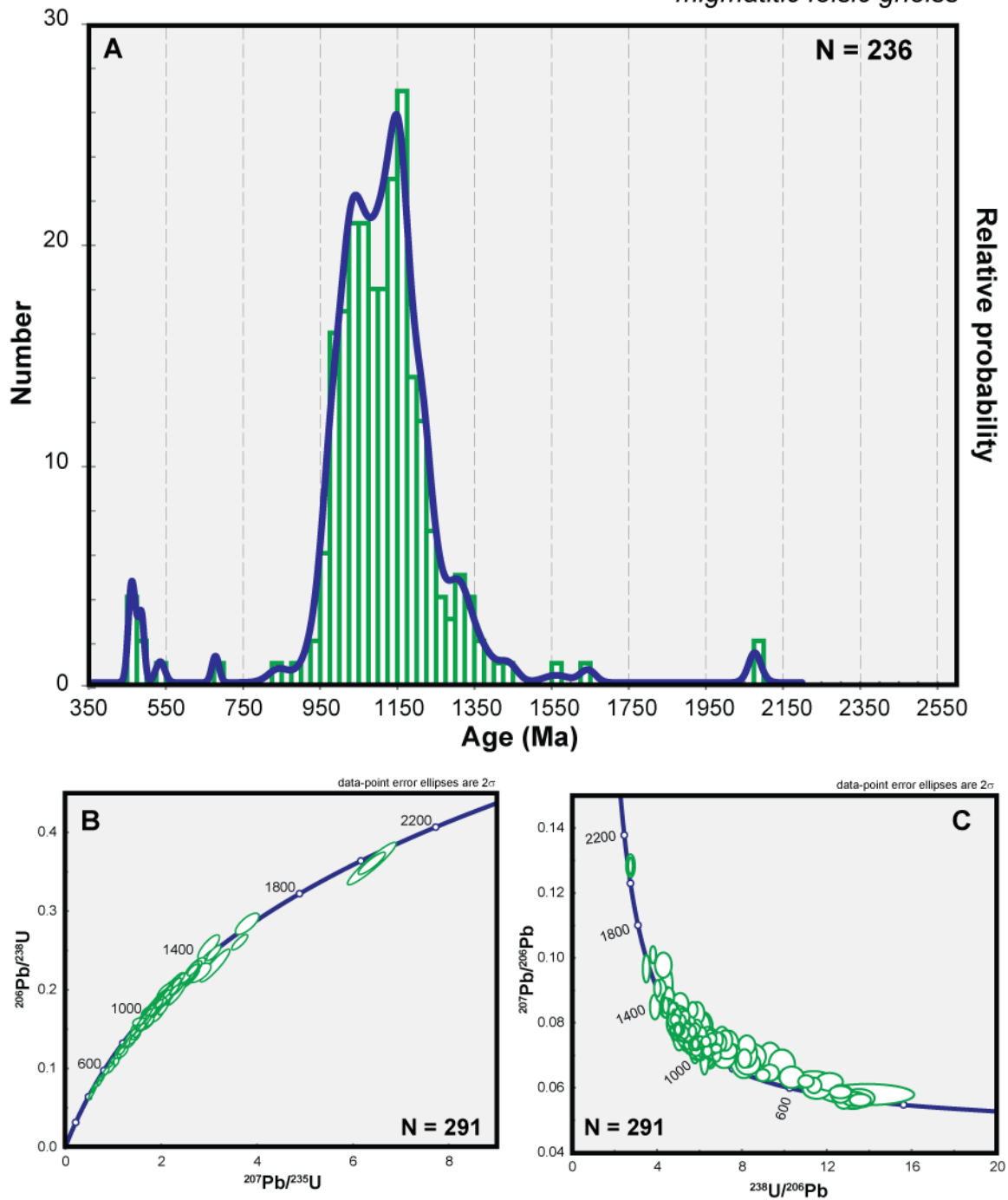


Figure 4.8: Results of LA-ICP-MS of zircon from sample H15-004. (a) Probability density plot of data with greater than 90% concordance. (b) Concordia diagram of all data. (c) Tera-Wasserburg diagram of all data.

H14-007

Copperhill Formation  
*metapsammite*

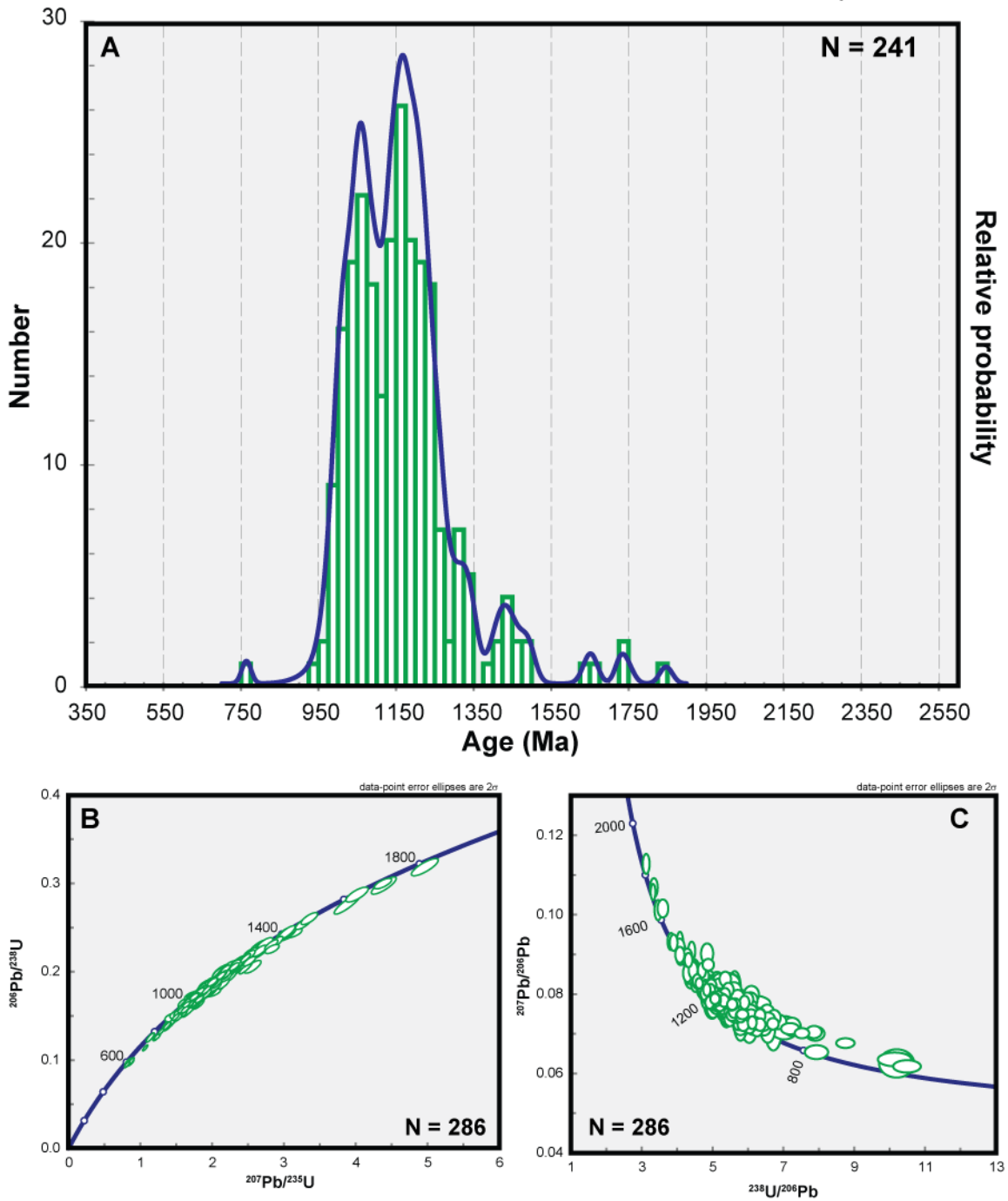


Figure 4.9: Results of LA-ICP-MS of zircon from sample H14-007. (a) Probability density plot of data with greater than 90% concordance. (b) Concordia diagram of all data. (c) Tera-Wasserburg diagram of all data.

H14-002

Otto Formation  
metapsammite

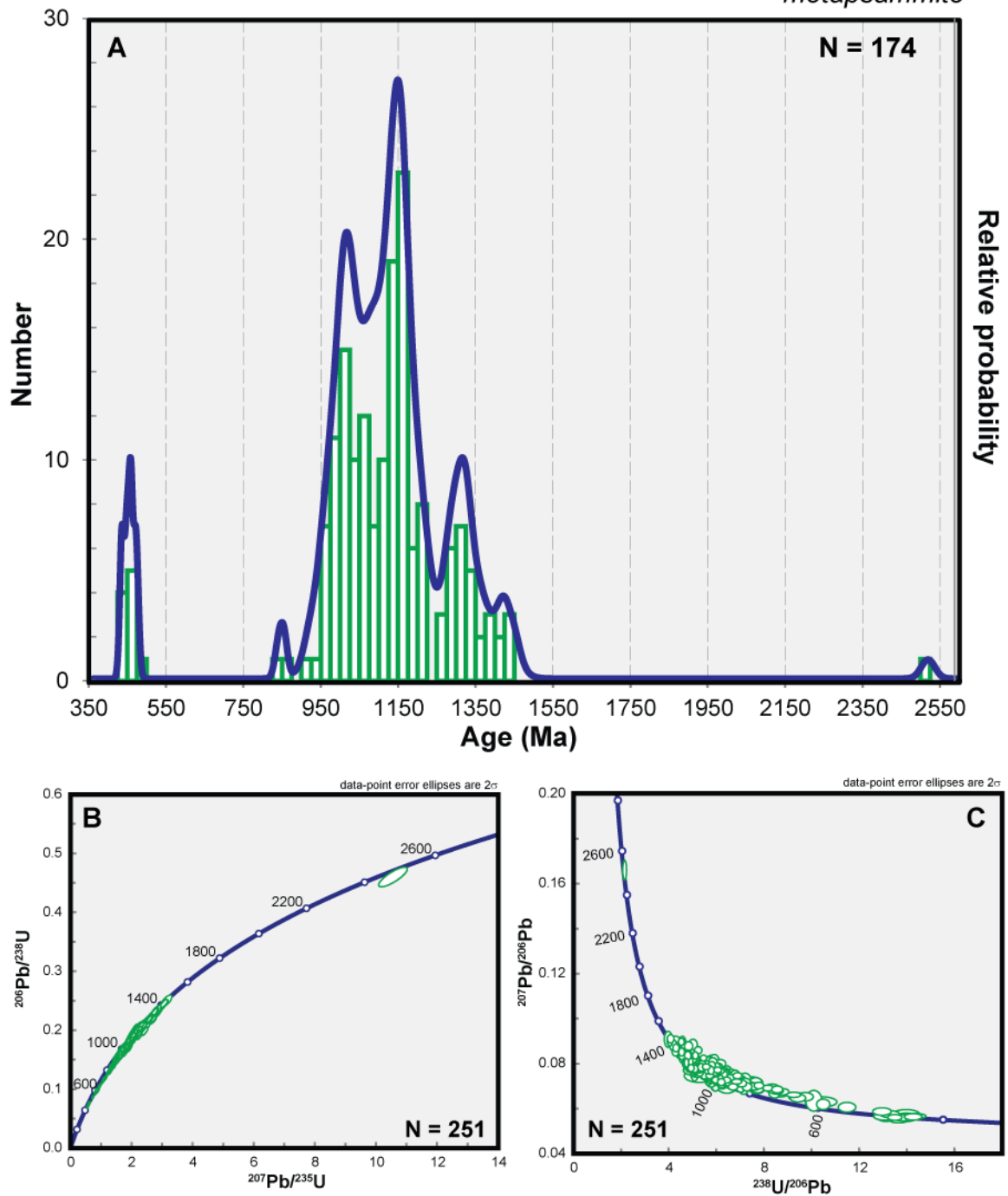


Figure 4.10: Results of LA-ICP-MS of zircon from sample H14-002. (a) Probability density plot of data with greater than 90% concordance. (b) Concordia diagram of all data. (c) Tera-Wasserburg diagram of all data.

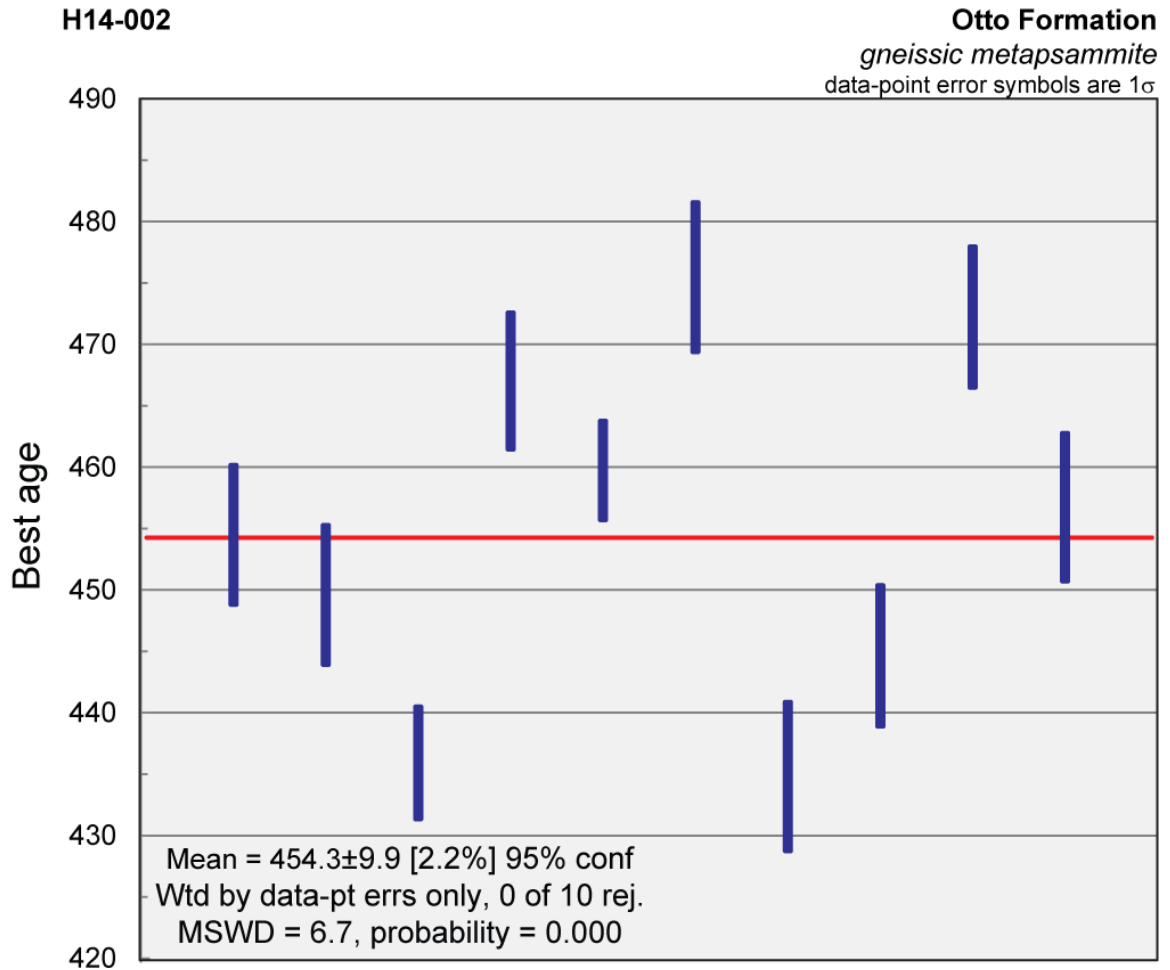


Figure 4.11: Mean ‘best’ age plot of data with ages under 500 Ma and greater than 90% concordance from sample from sample H14-002. The mean ‘best’ age of  $454 \pm 10$  is the proposed age of Taconic metamorphism for the sample.

## Discussion

The basement lithologies include a Grenville orthogneiss (H14-020) that is ca. 1150 Ma in age. This unit correlates with the augen gneiss of Hadley and Goldsmith (1963) in the Dellwood quad, and is the same age as an augen gneiss that occurs in the center of the Dellwood quad (Quinn, 2012). No other occurrence of augen gneiss was observed in the study area, which may suggest that this occurrence is the southeasternmost extent of Grenville basement in the region. However, biotite gneiss sample H15-003 is dominated by a single age mode at ca. 1150 Ma, with minor age



modes at ca. 1050 and 450 Ma. This could indicate that the biotite gneiss could be a 1150 Ma orthogneiss that experienced Grenville (Ottowan) and Taconic metamorphism to produce the younger generations of zircon.

U-Pb detrital zircon geochronology for the Cartoogechaye, Copperhill, and Otto samples (DEL-14-1, H14-002, H14-007, H14-011, and H15-004) yield age spectra that are dominated by two Mesoproterozoic age modes at ca. 1050 and 1150 Ma, corresponding to Grenville magmatism and metamorphism (Figure 4.12). Zircon ages in the range 1200-1500 are less common but, along with the 1050 and 1150 age modes, are most similar to detrital zircon age spectra for the Ocoee Supergroup (e.g. Chakraborty, 2010). This supports the interpretation that the protoliths of the gneisses were clastic sedimentary rocks, and the dominant sediment source was local Laurentian Mesoproterozoic basement. Paleoproterozoic grains are rare, but are present in all of the samples, with the exception of sample H14-002 and H15-003. Archean grains were only present in sample H14-002 (Otto Formation). The grains older than 1500 Ma are interpreted to be inherited cores. Neoproterozoic grains ranging between 700 and 900 Ma are present in all of the paragneiss samples and are interpreted to represent the youngest magmatic ages. The youngest detrital zircon age obtained suggests deposition occurred in the Neoproterozoic at 700 and 750 Ma. This is consistent with deposition in a Laurentian margin rift basin. An early Cambrian age of ~545 Ma is present in sample H15-004. Although this age mode is not common in the southern Appalachians, it is recognized as the final rift-related age in the northern Appalachians (Cawood, 2001).

All of the samples underwent Taconic metamorphism ca. ~450 Ma, however, only four samples include this population. This is likely due to the variable degree of

migmatitization, increased grade of metamorphism to the southeast, and the dependence of zircon solubility on bulk composition. Sample H14-011 is the most migmatitic sample analyzed, has the largest population of Taconic zircons, and has the highest proportion of discordant grains. In this sample, 140 grains were discordant, out of the 314 analyzed grains, and over half yielded ages less than 800 Ma. The variations in this discordant age mode are illustrated in Figure 4.13, where an apparent Neoproterozoic age population decreases with an increasing limit of concordance. The effect of the Taconic is evident in all samples through zircon discordance along a line through 450 Ma, which is best illustrated on Tera-Wasserburg diagrams (Figure 4.7). For several samples, the discordant ages spread out along a line between the oldest zircon ages and ca. 450 Ma. This trend is consistent with Pb loss at ca. 450 Ma during upper amphibolite facies regional metamorphism ( $T \sim 700 - 750 \text{ }^{\circ}\text{C}$ ). Although the closure  $T$  for Pb diffusion in zircon is higher (ca.  $900 \text{ }^{\circ}\text{C}$ : Cherniak and Watson, 2001), some Pb loss could have occurred along fractures, inclusion boundaries, and cracks.

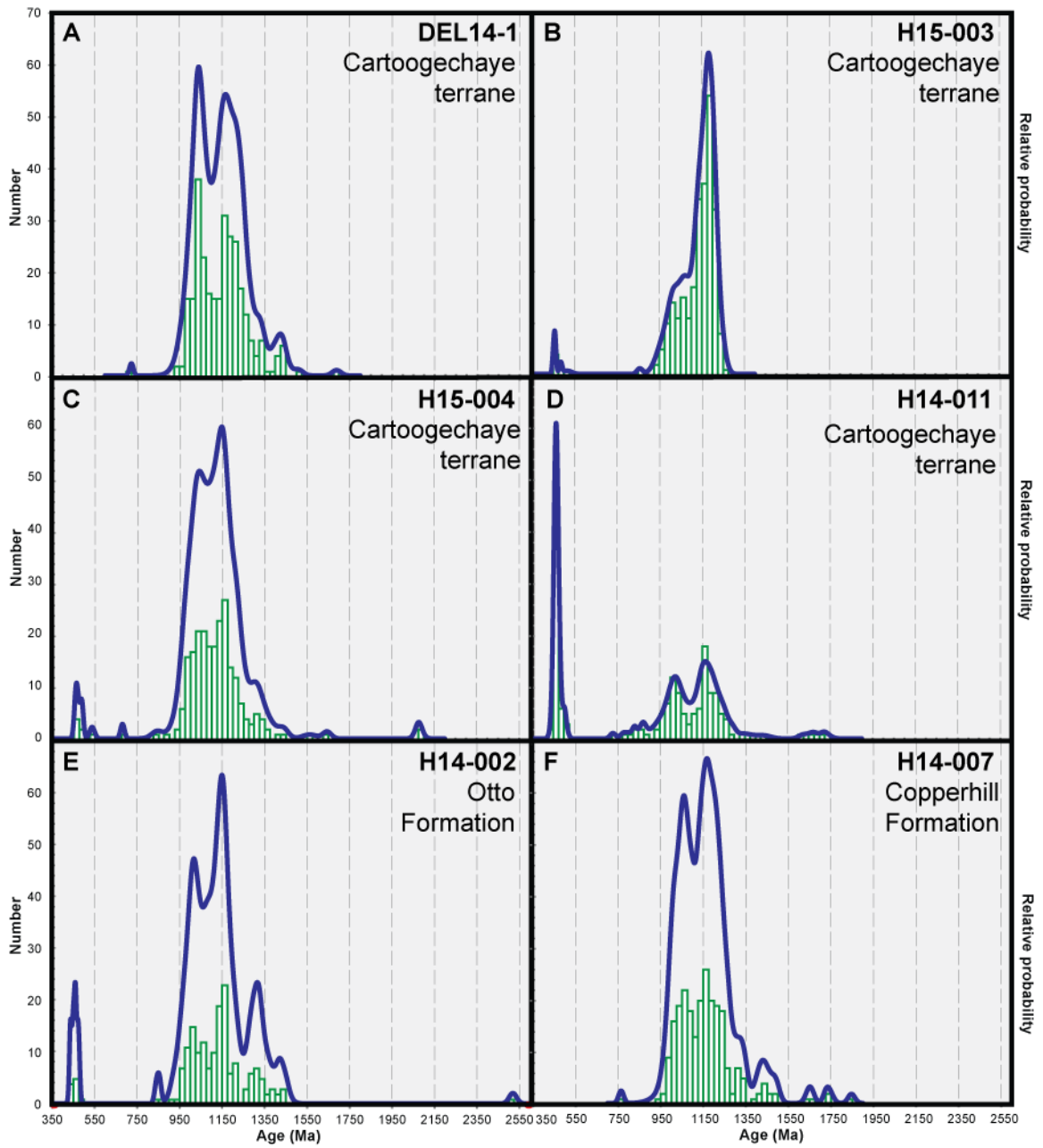


Figure 4.12: Probability density plots for all samples analyzed with LA-ICP-MS.

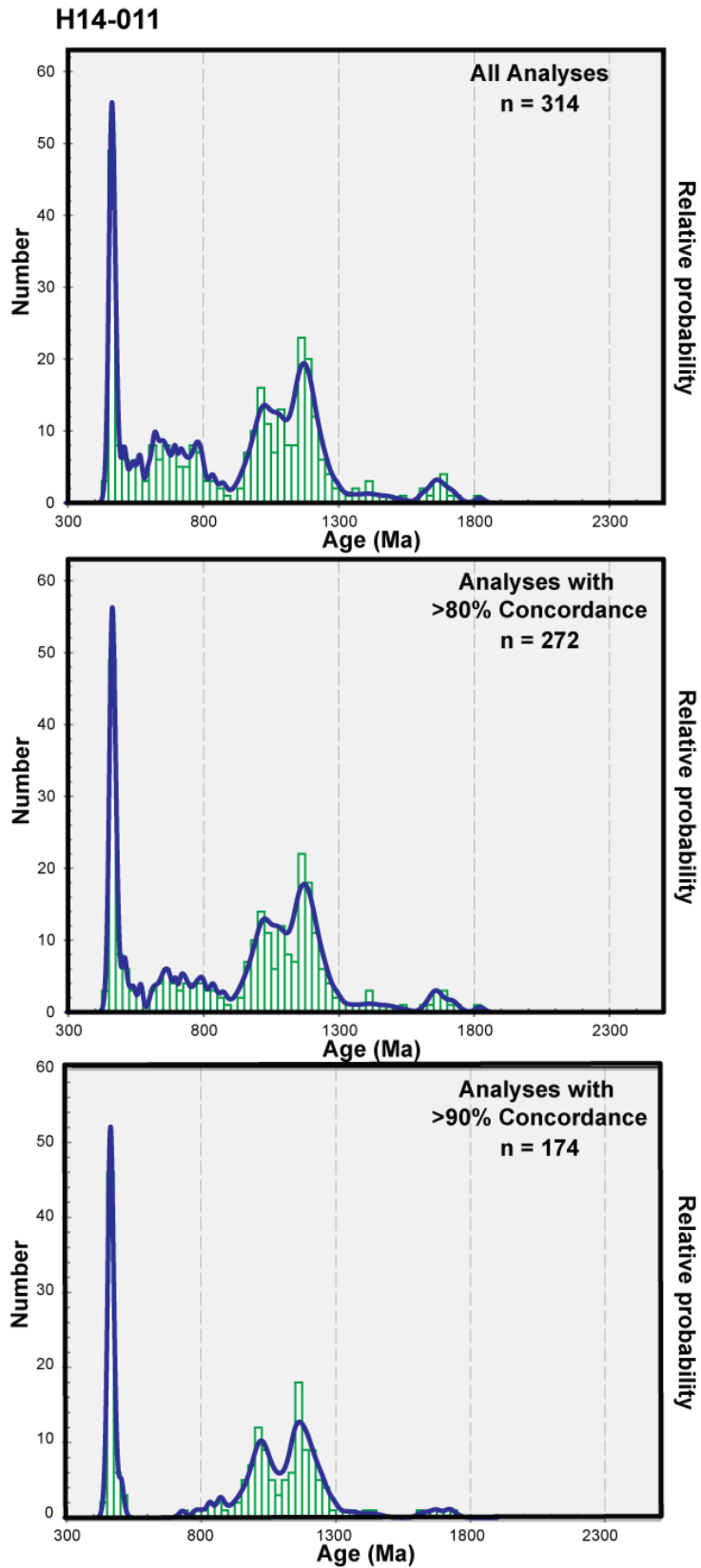


Figure 4.13: Probability density plots for H14-011 showing the variation in modes with concordance. The most abundant population of discordant ages range from ~500-800 Ma.

## CHAPTER V. RESULTS OF GEOCHEMISTRY

Whole rock major and trace element X-ray fluorescence (XRF) spectrometry was carried out on ten representative samples of migmatitic biotite paragneiss (DEL14-1, H14-009, H14-017, H14-021, and H15-004), migmatitic hornblende biotite paragneiss (H14-003 and H14-011), migmatitic felsic paragneiss (H15-004), augen orthogneiss (H14-020), and metapsammite (H14-007). These analyses were used to identify geochemical trends that are associated with the provenance of the paragneiss and to compare to geochemical data from previous studies (Loughry, 2010; Chakraborty, 2010; Quinn, 2012). A description of the analytical procedures can be found in Chapter II. Geochemical data are compiled in Appendix A.

The elemental compositions of these high grade gneisses reflect the heterogeneous nature of the rocks exposed in the Hazelwood quadrangle. The analyzed samples have concentrations of SiO<sub>2</sub> that range from 57 to 76 wt. %. Harker diagrams of major element oxides vs. SiO<sub>2</sub> show that in most samples potassium increases whereas aluminum, calcium, iron, magnesium, manganese, titanium, and phosphorus decrease with increasing silica content (Figure 5.1). No compositional relationship is noticeable between sodium and silica. On an AFM diagram, the samples define a calc-alkaline trend (Figure 5.2).

In order to evaluate the effect of weathering on the source rocks of the gneisses, the Chemical Index of Alteration (CIA) and the Plagioclase Index of Alteration (PIA) were calculated (Appendix A). These indices integrate bulk major element compositions into a single value that can be used to compare to a model value of a fresh, unweathered source rock (Price and Velbel, 2003). The CIA is used as a measure of the alteration of feldspars to clay and therefore based on the proportions of aluminum, calcium, sodium,

and potassium (Nesbitt and Young, 1982; Fedo et al., 1995). The CIA is calculated using molecular proportions and the equation:  $CIA = [Al_2O_3 / (Al_2O_3 + CaO^* + Na_2O + K_2O)] \times 100$ , where  $CaO^*$  is the amount incorporated into the silicate fraction of the rock (Nesbitt and Young, 1982). The CIA value for unaltered basalt should be between 30 and 45 whereas unaltered granites and granodiorites have CIA values that range between 45 and 55 (Nesbitt and Young, 1982). The CIA values for the gneisses in this study range from 58 to 68.

The PIA is used as an alternative to the CIA and was developed as a measure of plagioclase weathering to clays or to potassium feldspar (Fedo et al., 1995). It is based on the molecular proportions of aluminum, potassium, calcium, and sodium and is calculated through the equation:  $PIA = [(Al_2O_3 - K_2O) / (Al_2O_3 + CaO^* + Na_2O - K_2O)] \times 100$ , where  $CaO^*$  is the amount incorporated into the silicate fraction of the rock (Fedo, 1995). The value of a fresh, unaltered rock should be 50 whereas a weathered rock will have values close to 100. The PIA calculated for the gneisses in this study range from 60 to 76.

## **Discussion**

Paragneiss derived from first cycle volcanic and plutonic sediments typically have similar geochemical signatures to the source rocks (McLennan et. al., 1993). Loughry (2010) and Chakraborty (2010) analyzed the whole rock geochemistry of various basement rocks in the eastern Great Smoky Mountains and known sedimentary rocks derived from Grenville basement rocks (Ocoee Supergroup). The majority of the granitic metaplutonic rocks and Grenville affinity metasedimentary rocks exhibit a calc-alkaline trend, whereas most amphibolite is tholeiitic. An AFM diagram (Figure 5.3) comparing

data from this study to past data indicates that the geochemical signature of the paragneiss is consistent with that of Grenville basement rocks. This supports the interpretation that the gneisses in Hazelwood quadrangle are metamorphosed equivalents of immature, feldspathic, first cycle sediments derived from weathering of Grenville basement rocks. However, a whole rock geochemical signature of the exotic basement and related detritus (identified in Quinn, 2012) has yet to be determined conclusively, and therefore sediment input from an exotic source cannot be dismissed.

The indices of alteration (CIA and PIA) have values that suggest little alteration of the source rock of the paragneisses and of the basement orthogneiss. Chakraborty (2010) conducted a detailed geochemical study of the Ocoee Supergroup sedimentary rocks and established that, for the Ocoee rocks, the CIA values range from 50 to 72 and the PIA values range from 64 to 68. Additionally, the Grenville basement orthogneisses have CIA values that ranged from 51 to 64 and PIA values that ranged from 51 to 70 (Chakraborty, 2010). The similarity of the Grenville basement and the Ocoee Supergroup sedimentary rocks suggest that the sedimentary rocks are first cycle clastic sediments derived from the Grenville basement. The samples analyzed in this study have CIA values that range from 58 to 68 and PIA values that range from 60 to 76 (Appendix A), which further support the interpretation that the highly metamorphosed sedimentary rocks that make up the Cartoogechaye terrane are derived from a local Laurentian margin source.

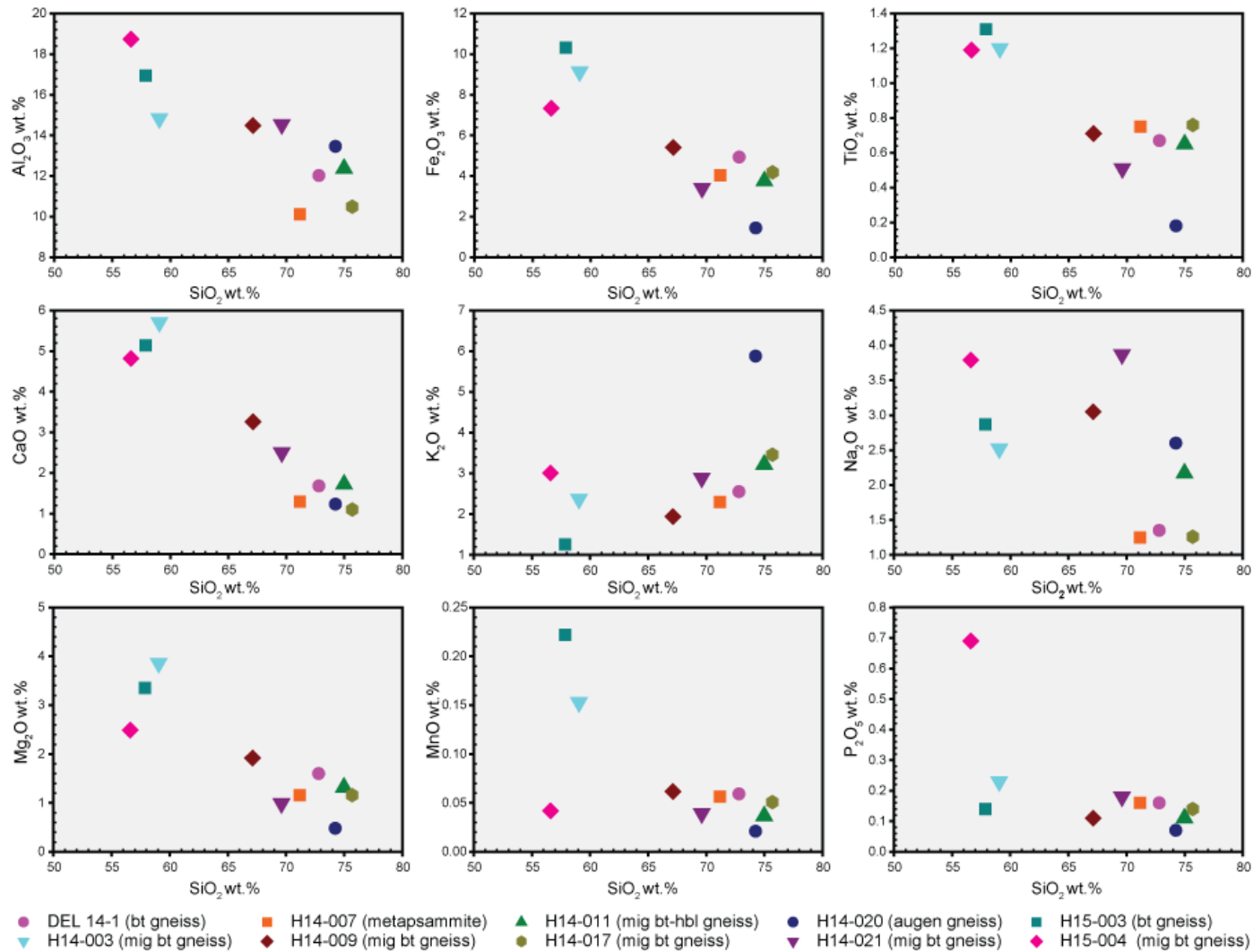


Figure 5.1: Harker variation diagrams for select samples in the study area. Cartoogechaye terrane: DEL14-1, H14-003, H14-009, H14-011, H14-017, H14-021, H15-003, and H15-004; Copperhill Formation: H14-007; and Augen gneiss: H14-020.



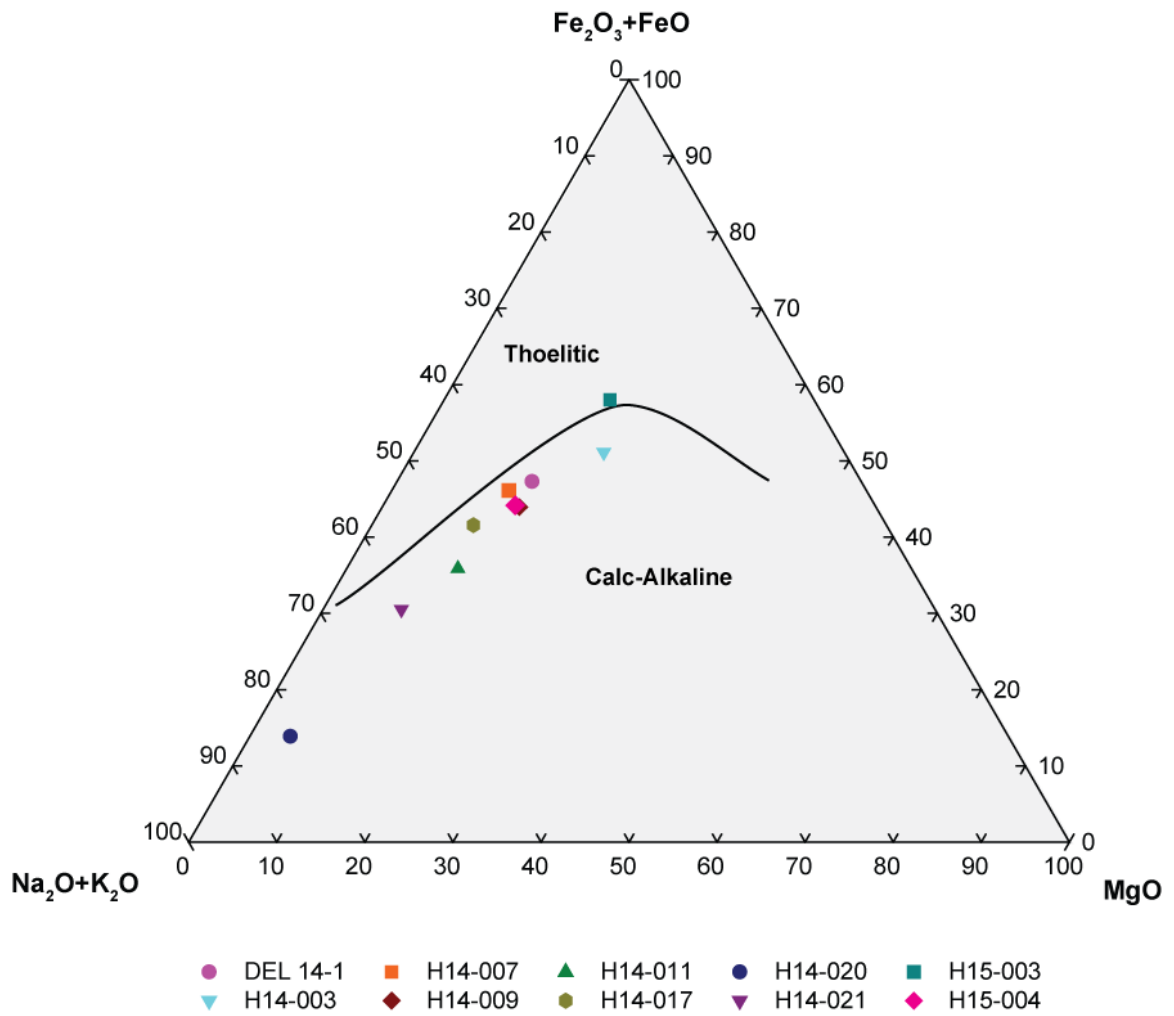


Figure 5.2: AFM diagram of select samples in the study area. Cartoogechaye terrane: DEL14-1, H14-003, H14-009, H14-011, H14-017, H14-021, H15-003, and H15-004; Copperhill Formation: H14-007; and Augen gneiss: H14-020.

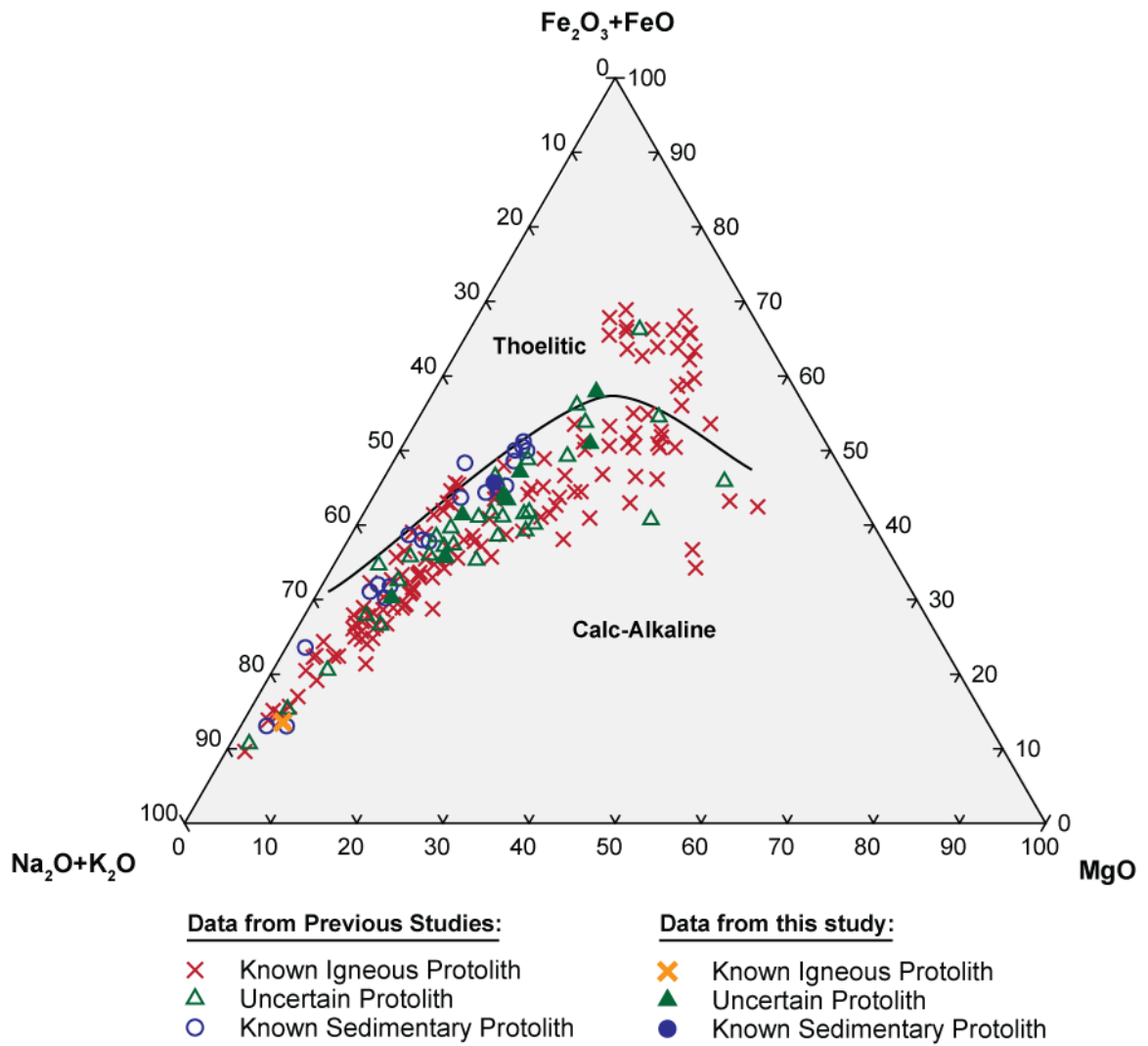


Figure 5.3: AFM diagram of geochemistry data from this study compared with geochemistry data from Chakraborty (2010), Loughry (2010), and Quinn (2012).

## CHAPTER VI. CONCLUSIONS

Highly deformed and intensively metamorphosed sedimentary and igneous rocks from the Cartoogechaye terrane, Ocoee Supergroup, and the Dahlenega gold belt were examined using field observations, U-Pb geochronology, and whole rock geochemistry to determine potential sources for the metasedimentary units. Derivation from a local eastern Laurentian margin basement source is a well-established interpretation for the provenance of the Ocoee Supergroup (Hadley and Goldsmith, 1963; Chakraborty, 2010). Quinn (2012) identified two unique detrital zircon age signatures for the Cartoogechaye terrane; one which suggests a dominantly local Grenville source, similar to the Ocoee Supergroup, and another which is atypical of rocks with a Laurentian provenance. This thesis provides new data that give insight on the extent of the exotic signature within the Cartoogechaye terrane.

The northern half of the Hazelwood quadrangle is underlain primarily by migmatitic paragneisses of the Cartoogechaye terrane. Lithologically and geochemically, the gneisses are similar to the migmatitic biotite gneiss and migmatitic hornblende gneiss that are recognized to the north in the Dellwood quadrangle and are widespread within the basement complex of the eastern Great Smoky Mountains (Hadley and Goldsmith, 1963; Quinn, 2012). The biotite paragneiss from the Dellwood quadrangle appears to grade southward into a more deformed, leucosome-rich variety. However, the increased degree of migmatization and polyphase folding prevents direct correlation of the two lithologies. These complexities also inhibit the direct identification of the protolith as either igneous or sedimentary.

The Cartoogechaye migmatitic biotite gneiss has whole rock major element compositions that follow a calc-alkaline trend, which overlaps with the trend defined by

the basement orthogneisses from the Dellwood area (Loughry, 2010; Quinn, 2012). This similarity could imply the protolith being: (1) igneous or (2) immature, first-cycle sediments with the composition of the source rock. Mafic garnet amphibolite pods and lenses entrained in the biotite gneiss must have a basaltic origin. Zircons extracted from four samples of biotite gneiss have variable morphologies. Samples DEL14-01, H14-011, H15-003, and H15-004 contain zircons with nonsymmetrical angular cores and zircons with rounded cores with variable amounts of fractures. Both euhedral and anhedral rims are present. The heterogeneity of the zircons is consistent with the interpretation that the biotite gneiss has a sedimentary protolith. U-Pb zircon data from all biotite gneiss samples reveal multiple age modes. The dominant and most common age modes, present in all but H15-003, are at ca. 1050 and 1150 Ma that corresponds, respectively, to the Ottowan and Shawinigan phases of the Grenville orogeny (Figure 6.1). These age spectra are consistent with a sedimentary protolith, because a plutonic protolith should exhibit a single age mode. Although older and younger zircons are present in these samples, the dominance of the two Grenville age modes indicate an eastern Laurentian margin provenance. H15-003 is dominated by a single age mode at ca. 1150 Ma, however, grains with ages of 1050 are present. This suggests that biotite gneiss sample H15-003 could be either a meta-igneous rock that produced a new generation of zircon during 1150 Ma metamorphism or a meta-sedimentary rock produced from a single detrital source.

The Copperhill and Otto Formations have bulk compositions (pelite and psammite) and textural relationships that suggest a sedimentary origin, which is consistent with numerous previous studies of the Ocoee Supergroup (Hadley and Goldsmith, 1968; Chakraborty, 2012; Kelly, 2014). Therefore the zircons extracted from

the leucosome-poor (psammitic) units are the most likely to be detrital grains. The morphology of the zircons from the Copperhill and Ocoee samples supports a detrital interpretation with subangular and rounded cores that are enclosed in subhedral to anhedral rims. U-Pb zircon data reveal multiple age modes that confirm a sedimentary origin for these units. The zircon age distributions are very similar to Ocoee Supergroup units (Snowbird, Great Smoky, Walden Creek Groups: Chakraborty et al., 2012; Kelly 2014) in exhibiting the characteristic Grenville age doublet in addition to 1250 to 1350 Ma grains. These ages support the interpretation of an eastern Laurentian margin source.

None of the samples exhibit detrital zircon age spectra that are as non-Grenvillian as the two biotite paragneiss samples analyzed by Quinn (2012), from the Dellwood quadrangle (Figure 6.2b). Five of the six samples analyzed have age spectra that correlate well to the detrital age spectra of the Grenville affinity rocks identified by Quinn (2012) (Figure 6.2a). Additionally, the Cartoogechaye terrane biotite gneisses have age spectra that are similar to the Ocoee Supergroup detrital spectrum identified by Chakraborty (2010) (Figure 6.3). These U-Pb zircon age similarities along with field and geochemical observations support the model that the biotite gneiss represents Neoproterozoic Laurentian margin rift sediments that were derived primarily from local Mesoproterozoic Grenville basement. In addition, the similar age spectra of the Cartoogechaye terrane gneisses and the Otto Formation metapsammite to the Ocoee Supergroup may indicate that the central Blue Ridge is a contemporaneous, distal equivalent of the western Blue Ridge. Age distributions also support the middle Ordovician (Taconian) being the time of regional metamorphism and migmatization.

Discordance of zircon ages is common in all of the paragneiss samples analyzed and is an indicator of the complex tectonic history of the grains. The discordance of the grains makes provenance interpretations particularly challenging and it is important to determine the mechanism of discordance. Discordance can occur when the individual analysis spot of a zircon overlaps multiple age domains or when there is a disturbance in the U-Pb system (Gehrels, 2014). In the samples of paragneiss, lead loss appears to follow a linear trend between ca. 1150 and 450 Ma (Figure 6.4). The unmetamorphosed lithologies from the Ocoee Supergroup, which are interpreted as having the same provenance as the samples in this study, have relatively concordant zircon ages (Chakraborty, 2010; Figure 6.5). This suggests that lead loss in the samples may be caused by Taconic regional metamorphism.

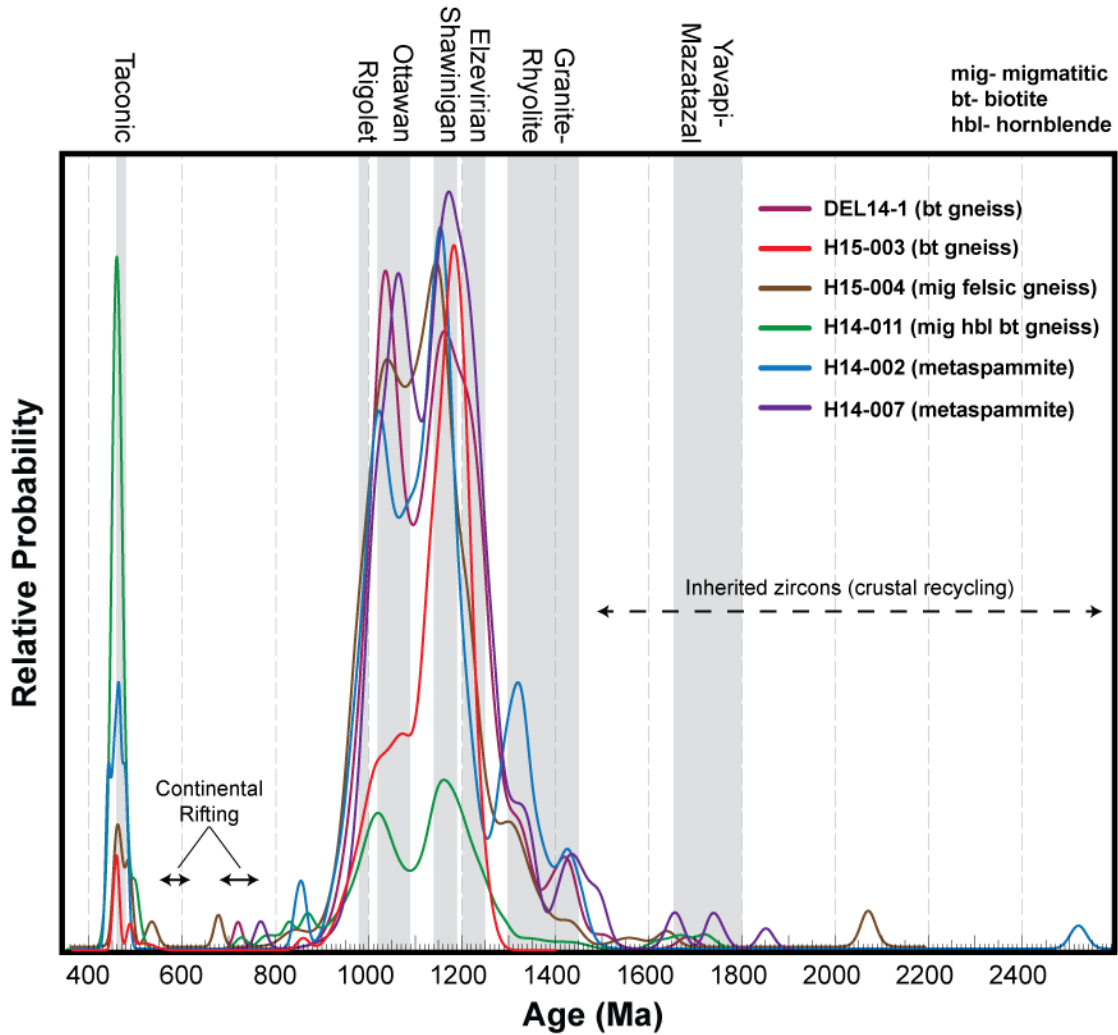


Figure 6.1: Probability density plots for all samples analyzed with LA-ICP-MS. Shaded bars represent zircon-producing orogenic events in the southern Appalachians. Solid arrows represent zircon producing rift events. Dashed arrow represents ages proposed to be a result of inheritance during crustal recycling. Gray shaded bars represent crust forming events. Timing of Paleoproterozoic orogenesis from Whitmeyer and Karlstrom, 2007. Timing of Mesoproterozoic orogenesis from Rivers, 2008; Hynes and Rivers, 2010. Timing of Neoproterozoic rifting from Tollo, 2004. Timing of Paleozoic orogenesis from Hatcher, 2005; Moecher et al., 2011.

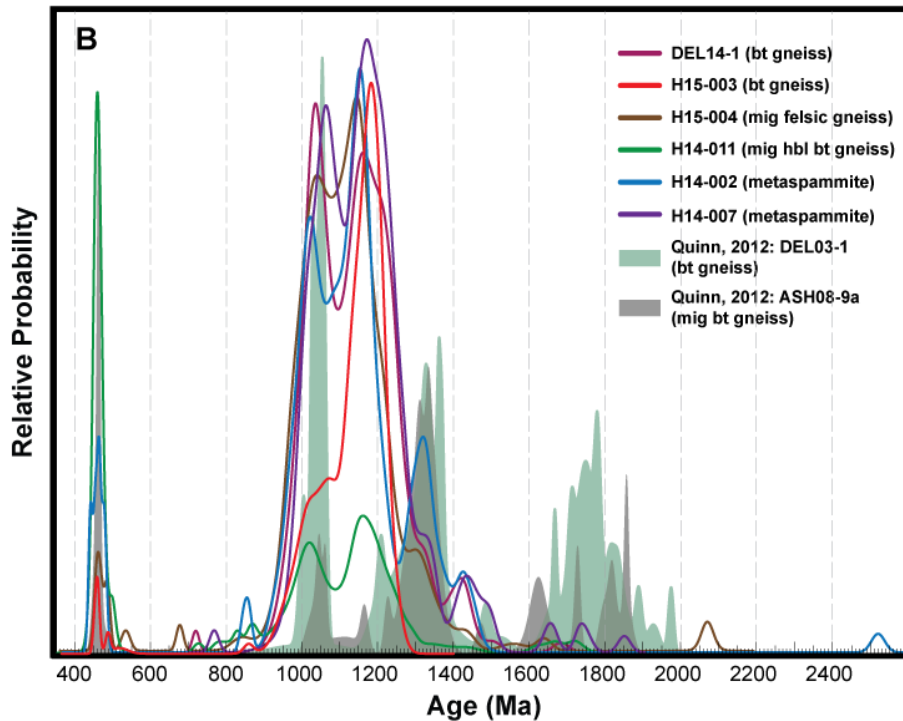
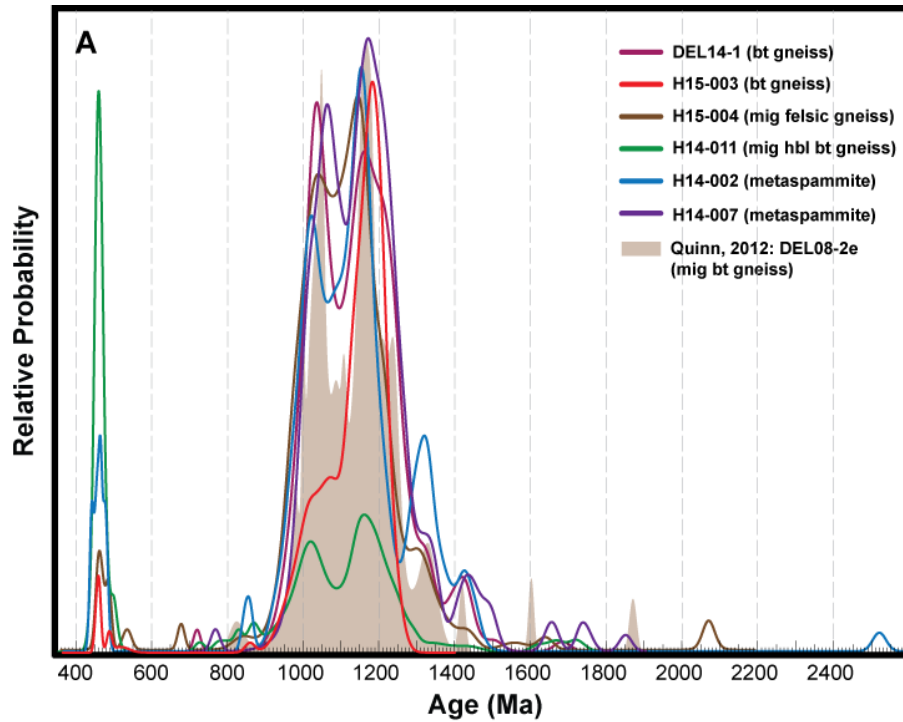


Figure 6.2: Probability density curves from this study (solid lines) compared to the Grenville detrital signature (top, shaded brown) and exotic detrital signature (bottom, shaded gray and green) from Quinn, 2012. Notice samples from this study have age spectra that are more similar to the Grenville detrital signature than the exotic detrital signatures. All samples with the exception of H15-003 differ from the Grenville signature due to ages younger than 800 Ma. Sample H15-003 differs from the Grenville signature due to the lack of a significant age population around ~1000 Ma



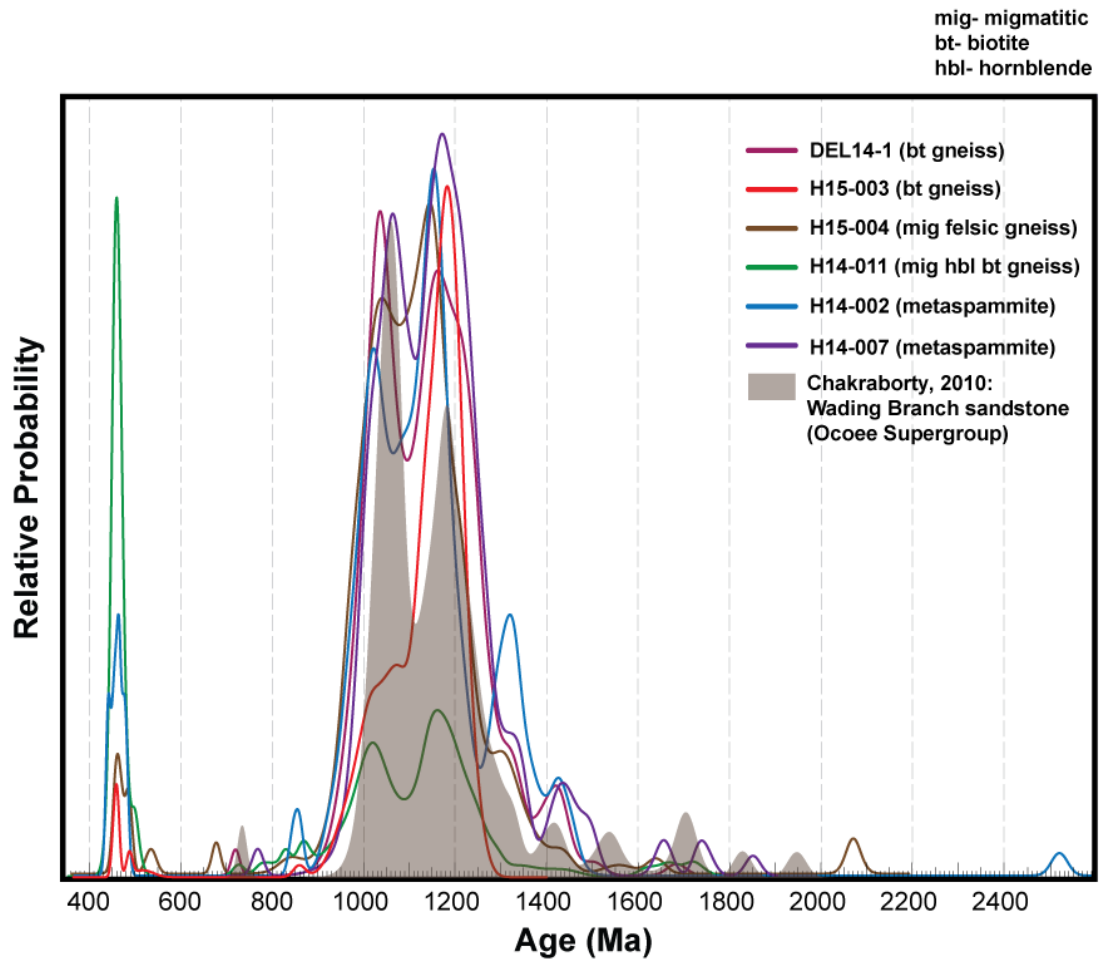


Figure 6.3: Probability density curves from this study (solid lines) compared to the detrital signature of the Wading Branch Ocoee Supergroup (shaded gray) from Chakraborty, 2010.

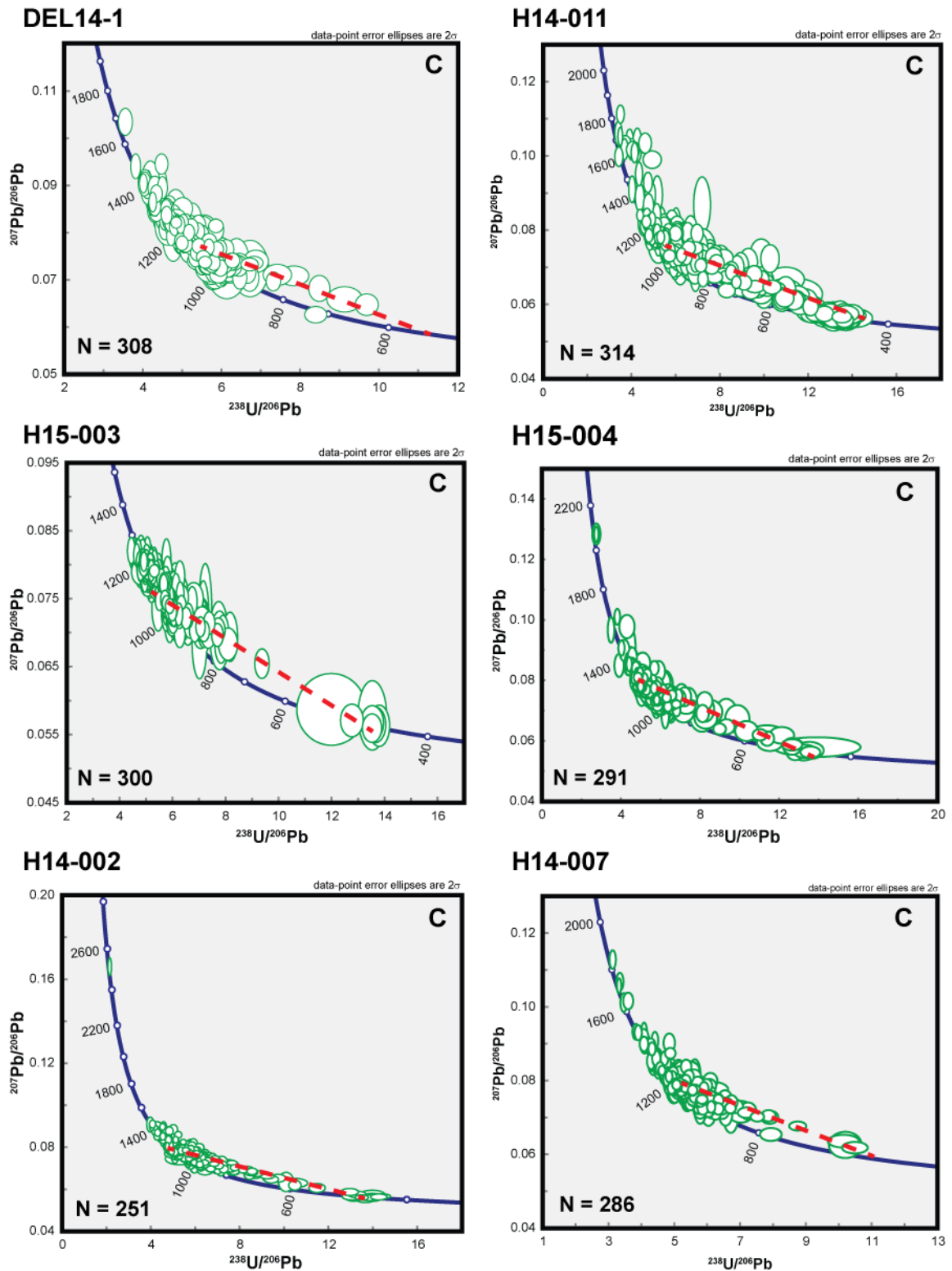


Figure 6.4: Tera-Wasserburg showing apparent linear trends of discordance in six samples of paragneiss analyzed in this study.

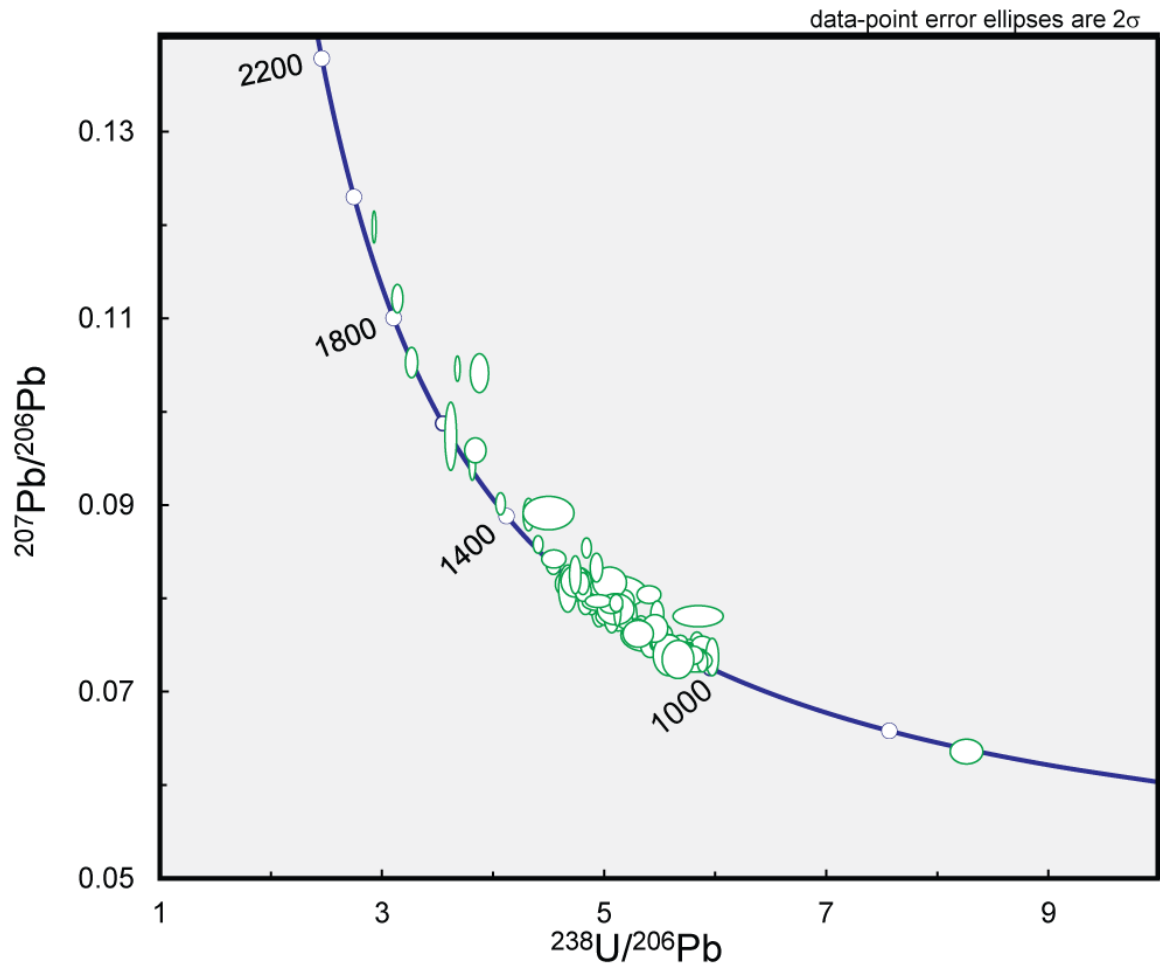


Figure 6.5: Tera-Wasserburg showing zircon analyses from the Wading Branch Formation of the Ocoee Supergroup from Chakraborty, 2010.

## APPENDICES

Appendix A: Whole Rock X-Ray Fluorescence Spectrometric Analysis

Major-Minor

Sample Map Unit	DEL14-1† Ezct	H14-003 Ezct	H14-007† Zch	H14-009 Ezct	H14-011† Ezct	H14-017 Ezct	H14-020† Ym	H14-021 Zch	H15-003† Ezct	H15-004† Ezct
SiO2 (wt. %)	72.81	59.05	78.04	67.13	74.98	75.68	74.24	69.61	57.86	56.6
TiO2 (wt. %)	0.67	1.2	0.70	0.71	0.65	0.76	0.18	0.51	1.31	1.19
Al2O3 (wt. %)	12.02	14.83	10.15	14.49	12.37	10.49	13.46	14.54	16.94	18.74
Fe2O3 (wt. %)	4.93	9.14	4.01	5.41	3.75	4.18	1.44	3.4	10.33	7.34
MgO (wt. %)	1.6	3.86	1.14	1.92	1.32	1.16	0.48	0.99	3.35	2.49
CaO (wt. %)	1.68	5.71	1.27	3.26	1.72	1.1	1.23	2.5	5.14	4.82
Na2O (wt. %)	1.35	2.52	1.27	3.05	2.17	1.26	2.6	3.87	2.87	3.79
K2O (wt. %)	2.55	2.37	2.33	1.94	3.22	3.46	5.88	2.89	1.26	3.01
P2O5 (wt. %)	0.16	0.23	0.15	0.11	0.11	0.14	0.07	0.18	0.14	0.69
MnO (wt. %)	0.06	0.15	0.06	0.06	0.04	0.05	0.02	0.04	0.22	0.04
LOI	0.89	1.75	1.10	0.76	0.69	1.10	0.67	0.74	0.90	0.68
ClA	68.30	58.32	67.58	63.72	63.50	64.32	58.09	61.09	64.63	61.73
PIA	75.76	60.22	75.48	66.54	70.17	74.87	66.43	64.65	66.19	64.63
<b>Total</b>	<b>98.72</b>	<b>100.81</b>	<b>100.22</b>	<b>98.85</b>	<b>101.02</b>	<b>99.38</b>	<b>100.27</b>	<b>99.27</b>	<b>100.32</b>	<b>99.39</b>

Trace

Sample Map Unit	DEL14-1† Ezct	H14-003 Ezct	H14-007† Zch	H14-009 Ezct	H14-011† Ezct	H14-017 Ezct	H14-020† Ym	H14-021 Zch	H15-003† Ezct	H15-004† Ezct
Pb (PPM)	13	10	13	12	17	15	19	12	7	12
Cu (PPM)	13	14	12	12	7	<2	37	17	116	11
Co (PPM)	13	33	7	19	11	7	<2	5	28	15
Ni (PPM)	30	55	24	40	20	23	9	17	47	18
Cr (PPM)	266	197	236	160	128	283	64	117	201	72
Ce (PPM)	119	85	89	82	80	101	39	194	82	225
V (PPM)*	37	64	34	49	48	39	<5	17	60	79
La (PPM)	27	31	47	24	20	13	8	90	26	92
Ba (PPM)	839	706	598	821	994	938	1433	791	457	802
Nb (PPM)	24	15	17	11	10	17	8	30	15	9
Zr (PPM)	474	223	449	275	430	465	139	365	265	456
Y (PPM)	46	38	39	36	33	35	33	49	52	41
Sr (PPM)	212	410	169	548	298	220	581	556	230	717
Rb (PPM)	78	52	84	52	82	95	115	84	33	83
U (PPM)*	3	<2	3	2	3	3	3	3	<2	2
Th (PPM)*	19	12	13	20	16	19	11	43	11	26
Ga (PPM)*	18	19	18	19	17	16	16	20	19	25
Zn (PPM)	97	106	103	74	73	82	32	41	137	137

\*Calculated  
† Dated samples  
PPM V = 33.9733 + 3.91727\*Intensity  
PPM U = -5.26919 + 1.02804\*Intensity  
PPM Th = 18.3981 + 91.7536\*Intensity  
PPM Ga = 10.5428 + 86.4394\*Intensity

Appendix B: LA-ICPMS U-Pb Zircon Geochronology

Analysis	U (ppm)	206Pb/204Pb	U/Th	206Pb*/207Pb*	Isotope ratios				Apparent ages (Ma)				Best age (Ma)	± (Ma)	Conc (%)				
					± (%)	207Pb*/235U*	± (%)	206Pb*/238U*	± (%)	error corr.	206Pb*/238U*	± (Ma)				207Pb*/235U	± (Ma)	206Pb*/207Pb*	± (Ma)
H14-002 27May2015-Spot 2	505	71582	2.0	12.7244	1.3	1.9060	1.8	0.1759	1.3	0.72	1044.5	12.4	1083.2	12.0	1161.8	24.8	1161.8	24.8	89.9
H14-002 27May2015-Spot 3	440	132639	1.3	11.6609	1.0	2.6853	1.7	0.2271	1.3	0.80	1319.3	15.8	1324.4	12.2	1332.7	19.1	1332.7	19.1	99.0
H14-002 27May2015-Spot 4	88	68488	2.2	13.1080	1.1	1.9484	1.7	0.1852	1.3	0.77	1095.3	13.4	1097.9	11.5	1103.0	21.7	1103.0	21.7	99.3
H14-002 27May2015-Spot 5	1515	131049	27.3	12.3715	1.0	1.8974	1.6	0.1703	1.3	0.80	1013.5	12.1	1080.2	10.7	1217.3	18.9	1217.3	18.9	83.3
H14-002 27May2015-Spot 7	1133	53329	6.7	14.4460	0.8	1.1659	1.5	0.1222	1.3	0.87	743.0	9.3	784.7	8.3	905.4	15.5	743.0	9.3	82.1
H14-002 27May2015-Spot 8	336	117668	2.4	11.0837	1.0	3.0563	1.5	0.2457	1.1	0.74	1416.2	14.4	1421.8	11.7	1430.2	19.7	1430.2	19.7	99.0
H14-002 27May2015-Spot 9	321	102799	3.8	13.6228	1.1	1.6946	1.5	0.1674	1.0	0.69	997.9	9.6	1006.5	9.7	1025.2	22.2	1025.2	22.2	97.3
H14-002 27May2015-Spot 10	346	58433	3.1	13.5937	1.1	1.7105	1.5	0.1686	1.1	0.71	1004.6	10.1	1012.5	9.8	1029.5	21.8	1029.5	21.8	97.6
H14-002 27May2015-Spot 11	1381	264343	2.3	12.7674	0.9	1.9493	1.6	0.1805	1.4	0.84	1069.7	13.5	1098.2	10.9	1155.1	17.4	1155.1	17.4	92.6
H14-002 27May2015-Spot 12	461	120803	2.5	11.2880	1.1	2.4221	1.8	0.1983	1.5	0.81	1166.2	15.8	1249.2	13.2	1395.3	20.9	1395.3	20.9	83.6
H14-002 27May2015-Spot 13	1964	8293851	53.9	13.0041	0.7	1.7173	1.4	0.1620	1.2	0.85	967.7	10.8	1015.0	9.0	1118.6	14.6	1118.6	14.6	86.5
H14-002 27May2015-Spot 14	192	123980	2.7	12.6134	1.0	2.1228	1.9	0.1942	1.6	0.84	1144.1	16.6	1156.2	13.0	1179.2	20.4	1179.2	20.4	97.0
H14-002 27May2015-Spot 15	484	204043	3.4	12.7573	1.1	2.1214	1.6	0.1963	1.1	0.71	1155.3	12.0	1155.8	11.0	1156.7	22.1	1156.7	22.1	99.9
H14-002 27May2015-Spot 16	844	116595	8.4	12.6182	0.9	1.8741	1.4	0.1715	1.1	0.76	1020.4	10.0	1072.0	9.3	1178.4	18.1	1178.4	18.1	86.6
H14-002 27May2015-Spot 17	870	111592	5.0	13.8079	1.2	1.5430	2.2	0.1545	1.8	0.82	926.2	15.4	947.7	13.3	997.8	24.9	997.8	24.9	92.8
H14-002 27May2015-Spot 18	283	123584	2.5	13.6294	0.8	1.5673	1.6	0.1549	1.3	0.84	928.5	11.4	957.3	9.7	1024.2	17.0	1024.2	17.0	90.7
H14-002 27May2015-Spot 20	192	55727	3.8	13.6986	1.6	1.3928	2.1	0.1384	1.4	0.66	835.5	10.9	885.9	12.4	1013.9	32.0	1013.9	32.0	82.4
H14-002 27May2015-Spot 21	315	86982	2.3	12.7580	0.9	2.0512	1.7	0.1898	1.5	0.84	1120.3	15.1	1132.7	11.9	1156.6	18.5	1156.6	18.5	96.9
H14-002 27May2015-Spot 22	371	161265	14.9	13.4197	1.0	1.5403	1.7	0.1499	1.3	0.78	900.5	11.0	946.6	10.3	1055.5	21.0	1055.5	21.0	85.3
H14-002 27May2015-Spot 23	271	170880	2.5	11.7885	1.0	2.5876	1.7	0.2212	1.4	0.81	1288.4	16.4	1297.1	12.8	1311.6	19.9	1311.6	19.9	96.2
H14-002 27May2015-Spot 24	2153	3092542	2.7	14.5752	0.9	1.1021	1.4	0.1165	1.1	0.77	710.4	7.4	754.4	7.6	887.0	19.0	710.4	7.4	80.1
H14-002 27May2015-Spot 25	429	153438	3.2	11.8465	1.1	2.3557	1.8	0.2024	1.5	0.79	1188.2	15.8	1229.3	13.1	1302.1	21.6	1302.1	21.6	91.3
H14-002 27May2015-Spot 27	1206	490860	3.1	13.1007	0.8	1.6762	1.5	0.1679	1.2	0.84	1000.6	11.4	1033.5	9.6	1103.8	16.1	1103.8	16.1	90.7
H14-002 27May2015-Spot 28	117	129216	9.9	11.9695	1.2	2.4404	1.8	0.2119	1.3	0.74	1238.7	14.9	1254.6	12.8	1282.0	23.1	1282.0	23.1	96.6
H14-002 27May2015-Spot 29	346	137716	9.8	12.7776	0.9	1.8011	1.8	0.1689	1.6	0.86	995.1	14.6	1045.9	12.0	1153.5	18.5	1153.5	18.5	86.3
H14-002 27May2015-Spot 30	675	195176	4.0	13.1185	0.9	1.9752	1.5	0.1679	1.2	0.79	1110.2	12.3	1107.1	10.3	1101.0	18.7	1101.0	18.7	100.8
H14-002 27May2015-Spot 31	272	166362	3.4	13.7125	0.9	1.6858	1.6	0.1677	1.3	0.81	999.2	12.0	1003.2	10.2	1011.9	18.8	1011.9	18.8	96.7
H14-002 27May2015-Spot 32	427	83649	2.1	12.6565	1.0	1.8418	1.8	0.1691	1.5	0.84	1006.9	14.4	1060.5	12.0	1172.4	19.4	1172.4	19.4	85.9
H14-002 27May2015-Spot 33	111	29029	1.9	12.9430	1.6	2.0853	2.2	0.1957	1.5	0.67	1152.4	15.7	1144.0	15.2	1128.0	32.8	1128.0	32.8	102.2
H14-002 27May2015-Spot 34	185	217539	3.1	12.3090	1.3	1.9198	2.2	0.1714	1.7	0.79	1019.8	16.0	1088.0	14.4	1227.3	26.2	1227.3	26.2	83.1
H14-002 27May2015-Spot 35	918	1748692	3.8	14.5607	1.0	1.2202	1.6	0.1289	1.3	0.80	781.3	9.4	809.9	8.9	889.1	19.9	781.3	9.4	87.9
H14-002 27May2015-Spot 36	685	50467	21.6	17.0039	1.2	0.6245	1.7	0.0770	1.2	0.73	478.3	5.7	482.6	6.6	560.1	25.3	478.3	5.7	85.4
H14-002 27May2015-Spot 39	368	331330	3.8	12.6153	1.1	2.2612	1.9	0.2069	1.6	0.84	1212.2	17.9	1200.3	13.6	1178.9	20.8	1178.9	20.8	102.8
H14-002 27May2015-Spot 40	356	54800	4.1	11.2654	1.6	2.6624	2.1	0.2175	1.4	0.65	1268.8	15.6	1318.1	15.5	1399.1	30.8	1399.1	30.8	90.7
H14-002 27May2015-Spot 41	602	176483	2.4	13.2743	0.8	1.6455	1.4	0.1584	1.2	0.81	998.0	10.1	987.8	9.0	1077.4	16.7	1077.4	16.7	88.0
H14-002 27May2015-Spot 42	613	167622	4.0	12.9135	0.9	1.9836	1.6	0.1858	1.3	0.83	1086.4	13.4	1109.9	10.8	1132.5	17.6	1132.5	17.6	97.0
H14-002 27May2015-Spot 43	146	61988	2.4	12.7808	1.3	2.1019	1.9	0.1948	1.4	0.74	1147.5	15.1	1149.4	13.4	1153.0	26.0	1153.0	26.0	91.5
H14-002 27May2015-Spot 44	697	224157	2.4	13.1975	1.0	1.7413	1.6	0.1667	1.2	0.77	993.8	11.4	1023.9	10.4	1089.0	20.7	1089.0	20.7	99.3
H14-002 27May2015-Spot 45	429	217547	1.5	12.8615	1.1	2.0556	1.4	0.1918	0.9	0.66	1130.9	9.6	1134.2	9.6	1140.5	21.1	1140.5	21.1	99.2
H14-002 27May2015-Spot 46	792	70438	4.1	12.7438	0.9	2.0076	1.4	0.1856	1.1	0.76	1097.3	10.8	1118.1	9.6	1158.8	18.3	1158.8	18.3	94.7
H14-002 27May2015-Spot 47	161	76272	2.0	12.4693	1.5	2.1641	2.0	0.1957	1.3	0.63	1152.3	13.2	1169.6	13.7	1201.8	30.2	1201.8	30.2	95.9
H14-002 27May2015-Spot 48	823	80696	3.5	13.6360	0.9	1.6283	1.5	0.1610	1.2	0.80	962.5	10.8	981.2	9.5	1023.2	18.4	1023.2	18.4	94.1
H14-002 27May2015-Spot 49	517	43953	3.2	18.0035	1.3	0.5593	1.9	0.0730	1.3	0.70	454.4	5.8	451.1	6.8	434.2	29.9	454.4	29.9	104.7
H14-002 27May2015-Spot 50	312	53711	3.0	12.5518	1.0	2.825	1.6	0.2078	1.3	0.80	1217.0	14.4	1206.9	11.4	1188.8	19.2	1188.8	19.2	102.4
H14-002 27May2015-Spot 51	45	37635	2.6	12.7618	1.4	2.1258	2.0	0.1968	1.4	0.71	1157.9	15.2	1157.2	14.0	1156.0	28.5	1156.0	28.5	100.2
H14-002 27May2015-Spot 52	1023	164572	3.2	14.0247	0.9	1.858	1.5	0.1410	1.2	0.81	850.1	9.4	882.9	8.6	966.1	17.6	966.1	17.6	88.0
H14-002 27May2015-Spot 53	216	244208	3.3	13.9917	1.2	1.5775	1.8	0.1601	1.3	0.74	957.2	11.9	961.4	11.2	970.9	24.8	970.9	24.8	98.6
H14-002 27May2015-Spot 54	163	89180	1.8	13.3100	1.0	1.8774	1.5	0.1812	1.1	0.73	1073.7	11.0	1073.2	10.1	1072.0	21.0	1072.0	21.0	100.2

Appendix B: LA-ICPMS U-Pb Zircon Geochronology (continued)

Hf14-002		Isotope ratios										Apparent ages (Ma)									
U (ppm)	Analysis	U/Pb	206Pb*/207Pb*	± (%)	207Pb*/235U*	± (%)	206Pb*/238U	± (%)	error corr.	206Pb*/238U*	± (Ma)	207Pb*/235U	± (Ma)	206Pb*/207Pb*	± (Ma)	Best age (Ma)	± (Ma)	Conc (%)			
																			206Pb	204Pb	206Pb
134	H14-002 27May2015-Spot 55	67257	2.3	12.8891	1.5	1.9448	2.1	0.1818	1.5	0.72	1076.8	14.9	1086.7	14.1	1136.3	29.0	1136.3	29.0	94.8		
83	H14-002 27May2015-Spot 56	86716	1.8	12.4722	1.6	2.1835	2.7	0.1975	2.2	0.80	1161.9	22.9	1175.8	18.8	1201.4	32.0	1201.4	32.0	96.7		
846	H14-002 27May2015-Spot 57	150940	5.2	14.4594	1.1	1.1402	1.7	0.1196	1.5	0.81	728.1	10.2	772.6	10.0	903.6	22.5	728.1	10.2	80.6		
211	H14-002 27May2015-Spot 58	103850	2.1	13.5893	1.4	1.7733	2.0	0.1748	1.4	0.69	1038.4	13.0	1035.7	12.8	1030.2	29.0	1030.2	29.0	100.8		
394	H14-002 27May2015-Spot 59	191867	2.3	11.7169	0.8	2.6654	1.9	0.2265	1.7	0.90	1316.1	20.2	1318.9	13.9	1323.4	15.7	1323.4	15.7	99.5		
202	H14-002 27May2015-Spot 60	89286	2.2	13.3805	1.1	1.8400	1.8	0.1786	1.4	0.78	1059.1	13.4	1059.9	11.6	1061.4	22.5	1061.4	22.5	99.8		
408	H14-002 27May2015-Spot 61	113999	2.2	13.6889	1.1	1.6238	1.3	0.1612	0.8	0.60	963.5	7.2	979.5	8.4	1015.4	21.7	1015.4	21.7	94.9		
189	H14-002 27May2015-Spot 64	941796	1.7	12.2361	1.2	1.8967	1.8	0.1683	1.3	0.72	1002.8	11.8	1079.9	11.7	1238.9	23.8	1238.9	23.8	80.9		
488	H14-002 27May2015-Spot 65	55127	7.0	13.8155	1.1	1.6184	1.6	0.1622	1.1	0.72	968.8	10.1	977.4	9.8	996.7	22.2	996.7	22.2	97.2		
808	H14-002 27May2015-Spot 66	131773	4.7	14.2969	1.0	1.2651	1.5	0.1312	1.2	0.78	794.6	9.0	830.2	8.8	926.8	19.8	794.6	9.0	85.7		
257	H14-002 27May2015-Spot 67	118105	3.9	12.6553	1.1	2.0865	1.6	0.1915	1.2	0.72	1129.5	12.0	1144.4	11.1	1172.6	22.1	1172.6	22.1	96.3		
209	H14-002 27May2015-Spot 68	214722	2.2	13.8206	1.3	1.6111	1.8	0.1615	1.2	0.68	985.0	11.1	974.5	11.4	996.0	27.1	996.0	27.1	96.9		
716	H14-002 27May2015-Spot 69	109209	2.9	13.5513	1.1	1.6942	1.8	0.1665	1.4	0.79	992.9	13.1	1006.4	11.5	1035.8	22.4	1035.8	22.4	95.9		
97	H14-002 27May2015-Spot 72	118139	2.1	13.4058	1.1	1.6757	2.2	0.1629	1.3	0.59	973.0	11.7	999.4	13.8	1057.6	35.2	1057.6	35.2	92.0		
273	H14-002 27May2015-Spot 73	84229	2.2	13.0580	0.9	1.6580	1.6	0.1570	1.4	0.85	940.2	12.2	982.6	10.4	1110.3	17.5	1110.3	17.5	84.7		
1796	H14-002 27May2015-Spot 74	232921	4.7	12.8997	1.0	1.7258	1.8	0.1814	1.5	0.83	964.8	13.5	1018.2	11.6	1134.8	19.8	1134.8	19.8	85.0		
325	H14-002 27May2015-Spot 75	112857	3.9	12.7854	1.5	1.9571	3.1	0.1615	2.7	0.85	1075.0	26.3	1100.9	20.5	1152.3	29.8	1152.3	29.8	93.3		
567	H14-002 27May2015-Spot 76	100712	4.7	14.0893	1.0	1.3852	2.0	0.1415	1.7	0.86	853.4	13.8	882.7	11.9	956.7	21.1	956.7	21.1	89.2		
267	H14-002 27May2015-Spot 77	85921	2.8	11.8849	1.1	2.4196	1.8	0.2086	1.5	0.79	1221.1	16.2	1248.4	13.3	1296.8	22.1	1296.8	22.1	94.2		
207	H14-002 27May2015-Spot 78	157431	1.2	12.5079	1.1	2.1861	1.8	0.1983	1.4	0.78	1166.3	15.3	1176.6	12.7	1195.7	22.3	1195.7	22.3	97.5		
871	H14-002 27May2015-Spot 79	56558	2.7	12.9479	0.7	1.7511	1.3	0.1644	1.1	0.84	981.4	9.7	1027.6	8.2	1127.2	13.8	1127.2	13.8	87.1		
387	H14-002 27May2015-Spot 80	156353	1.1	12.7560	1.0	2.1614	1.7	0.2000	1.4	0.82	1175.1	15.2	1168.7	12.0	1156.9	19.8	1156.9	19.8	101.6		
143	H14-002 27May2015-Spot 81	48604	1.9	12.7677	1.4	2.1103	2.0	0.1954	1.4	0.69	853.0	14.3	1152.2	13.6	1155.1	28.3	1155.1	28.3	99.6		
126	H14-002 27May2015-Spot 82	78174	3.1	13.9148	1.6	1.4019	2.1	0.1415	1.4	0.65	853.0	11.0	889.8	12.6	982.2	33.0	982.2	33.0	86.9		
2162	H14-002 27May2015-Spot 83	863689	62.7	12.7445	1.0	1.7954	1.6	0.1660	1.2	0.76	989.8	10.9	1043.8	10.1	1158.7	19.8	1158.7	19.8	85.4		
36	H14-002 27May2015-Spot 84	40403	1.5	12.7005	3.3	2.1246	3.7	0.1957	1.7	0.75	1152.2	17.5	1156.8	25.5	1165.5	65.5	1165.5	65.5	98.9		
364	H14-002 27May2015-Spot 86	85377	1.8	11.8807	1.0	2.3971	1.6	0.2066	1.2	0.79	1210.4	13.6	1241.7	11.2	1296.5	18.6	1296.5	18.6	93.4		
974	H14-002 27May2015-Spot 87	517527	22.7	14.1313	0.9	1.3313	1.8	0.1364	1.6	0.87	824.5	12.2	859.4	10.5	950.6	18.3	824.5	12.2	86.7		
315	H14-002 27May2015-Spot 91	106391	2.2	12.7903	1.0	2.0619	1.8	0.1913	1.5	0.81	1128.3	15.0	1136.3	12.2	1151.5	20.8	1151.5	20.8	98.0		
99	H14-002 27May2015-Spot 92	39353	4.5	12.6983	1.5	2.1318	2.1	0.1963	1.5	0.70	1155.6	15.6	1159.2	14.6	1165.9	30.0	1165.9	30.0	99.1		
444	H14-002 27May2015-Spot 93	227763	1.8	12.8440	1.0	2.0088	1.4	0.1871	1.0	0.72	1105.8	10.4	1118.5	9.6	1143.2	19.4	1143.2	19.4	96.7		
779	H14-002 27May2015-Spot 96	145606	5.2	17.8454	1.0	0.5681	1.6	0.0722	1.3	0.79	449.6	5.5	450.3	5.8	453.9	21.8	449.6	5.5	99.1		
217	H14-002 27May2015-Spot 98	112298	1.4	13.3934	1.6	1.9364	5.2	0.1881	4.9	0.95	1111.1	50.1	1093.8	34.5	1059.5	31.7	1059.5	31.7	104.9		
157	H14-002 27May2015-Spot 99	59931	5.0	16.1229	1.5	0.8130	1.9	0.0951	1.1	0.58	585.5	6.1	604.1	8.6	674.9	33.0	585.5	6.1	86.7		
574	H14-002 27May2015-Spot 100	119354	4.5	15.4378	1.1	0.9446	1.8	0.1058	1.4	0.79	648.1	8.7	675.3	8.7	767.1	22.7	648.1	8.7	84.5		
29	H14-002 27May2015-Spot 101	38728	2.9	11.0000	1.6	3.1345	2.3	0.2501	1.6	0.71	1438.8	20.8	1441.2	17.5	1444.7	30.3	1444.7	30.3	99.6		
371	H14-002 27May2015-Spot 102	171999	3.6	12.3554	0.9	2.3207	1.6	0.2080	1.3	0.81	1217.9	14.4	1218.6	11.3	1219.9	18.4	1219.9	18.4	99.8		
499	H14-002 27May2015-Spot 104	128607	4.2	13.3089	1.0	1.7035	1.8	0.1644	1.5	0.82	981.4	13.4	1009.8	11.5	1072.2	20.6	1072.2	20.6	91.5		
220	H14-002 27May2015-Spot 105	185984	6.3	13.2429	0.8	1.7812	2.1	0.1711	2.0	0.93	1018.1	18.5	1038.6	13.7	1082.2	15.5	1082.2	15.5	94.1		
661	H14-002 27May2015-Spot 106	206067	6.1	13.3733	1.1	1.6671	1.7	0.1617	1.3	0.75	966.2	11.4	996.1	10.7	1062.5	22.3	1062.5	22.3	90.9		
704	H14-002 27May2015-Spot 107	269272	2.2	12.4883	0.9	1.6163	1.7	0.1613	1.4	0.84	963.9	12.8	1038.4	11.0	1198.8	18.0	1198.8	18.0	80.4		
334	H14-002 27May2015-Spot 108	249741	2.6	14.3350	0.8	1.4309	1.5	0.1488	1.2	0.82	894.1	10.0	901.9	8.8	921.3	17.2	921.3	17.2	97.0		
530	H14-002 27May2015-Spot 109	211388	9.6	13.7661	0.9	1.5307	2.1	0.1528	1.9	0.91	916.8	16.1	942.8	12.8	1004.0	17.6	1004.0	17.6	91.3		
349	H14-002 27May2015-Spot 111	110133	9.0	15.8530	1.5	0.8341	3.0	0.0959	2.6	0.87	590.4	14.7	615.9	13.8	710.9	31.3	590.4	14.7	83.0		
1852	H14-002 27May2015-Spot 112	365033	8.0	13.2738	1.1	1.6199	1.5	0.1560	1.0	0.68	934.2	8.8	978.0	9.4	1077.5	22.1	1077.5	22.1	86.7		
484	H14-002 27May2015-Spot 113	964661	2.4	11.3871	0.9	2.4942	1.7	0.2060	1.5	0.84	1207.4	16.0	1270.4	12.6	1378.5	18.1	1378.5	18.1	87.6		
382	H14-002 27May2015-Spot 115	109037	3.0	13.3138	1.1	1.6601	1.8	0.1603	1.4	0.80	958.4	12.8	993.4	11.4	1071.5	21.8	1071.5	21.8	89.5		
48	H14-002 27May2015-Spot 117	38325	2.0	14.1140	2.2	1.5094	3.7	0.2509	2.9	0.79	926.2	25.1	934.2	22.5	953.2	46.0	953.2	46.0	87.2		
101	H14-002 27May2015-Spot 118	50524	1.8	13.6747	1.9	1.7364	2.6	0.1722	1.8	0.67	1024.3	16.6	1022.1	16.7	1017.5	38.9	1017.5	38.9	100.7		

Appendix B: LA-ICPMS U-Pb Zircon Geochronology (continued)

Analysis	U (ppm)	206Pb/204Pb	U/Th	206Pb*/207Pb*	± (%)	Isotope ratios				Apparent ages (Ma)						Conc (%)			
						207Pb*/235U*	± (%)	206Pb*/238U	± (%)	error corr.	206Pb*/238U*	± (Ma)	207Pb*/235U	± (Ma)	206Pb*/207Pb*		± (Ma)	Best age (Ma)	± (Ma)
						1.7	1.8848	2.3	0.1765	1.4	0.64	1047.7	14.0	1075.8	15.0		1133.1	34.8	1133.1
H14-002 27May2015-Spot 119	72	37304	3.4	12.9088	1.7	1.8848	2.3	0.1765	1.4	0.64	1047.7	14.0	1075.8	15.0	1133.1	34.8	1133.1	34.8	92.5
H14-002 27May2015-Spot 121	541	264012	11.4	17.3356	1.4	0.5682	2.1	0.0714	1.6	0.76	444.8	7.0	456.8	7.9	517.8	30.5	444.8	30.5	85.9
H14-002 27May2015-Spot 122	241	172037	3.2	11.9592	1.0	2.3103	1.9	0.2004	1.6	0.85	1177.4	17.7	1215.5	13.7	1263.7	19.9	1263.7	19.9	91.7
H14-002 27May2015-Spot 123	194	184658	3.1	14.3342	1.4	1.3646	1.8	0.1419	1.1	0.62	855.2	8.9	873.8	10.5	921.4	28.8	855.2	28.8	92.8
H14-002 27May2015-Spot 124	175	82497	1.4	12.4136	1.2	2.3409	1.8	0.2108	1.3	0.75	1232.8	15.1	1224.8	12.8	1210.7	23.4	1210.7	23.4	101.8
H14-002 27May2015-Spot 125	202	228253	3.2	13.1193	1.1	1.7915	1.7	0.1705	1.3	0.75	1014.7	11.8	1042.4	10.9	1100.9	22.4	1100.9	22.4	92.2
H14-002 27May2015-Spot 126	273	87198	6.9	13.8125	1.1	1.6468	1.7	0.1650	1.3	0.77	984.4	12.3	988.3	11.0	997.1	22.6	997.1	22.6	98.7
H14-002 27May2015-Spot 128	62	35049	1.8	15.7229	2.9	0.8667	3.2	0.0988	1.4	0.42	607.5	7.9	633.8	15.3	728.4	62.3	607.5	62.3	83.4
H14-002 27May2015-Spot 130	390	89239	2.1	11.9470	0.8	2.2431	1.3	0.1944	1.0	0.78	1144.9	10.2	1194.6	8.8	1285.6	15.4	1285.6	15.4	89.1
H14-002 27May2015-Spot 131	148	43758	3.6	11.7068	1.4	2.6520	1.8	0.2252	1.2	0.65	1309.1	13.8	1315.2	13.3	1325.1	26.5	1325.1	26.5	98.8
H14-002 27May2015-Spot 140	276	151962	10.9	14.0632	1.4	1.4071	2.6	0.1435	2.2	0.84	864.5	17.7	891.9	15.3	960.5	28.2	960.5	28.2	90.0
H14-002 27May2015-Spot 141	1251	63072	26.1	17.3383	1.1	0.5977	1.7	0.0752	1.3	0.76	467.1	5.7	475.7	6.3	517.4	23.8	467.1	23.8	90.3
H14-002 27May2015-Spot 142	560	67273	4.4	13.8491	1.0	1.5991	1.9	0.1606	1.6	0.84	960.2	13.9	969.9	11.6	991.8	20.5	991.8	20.5	96.8
H14-002 27May2015-Spot 143	873	74647	3.2	13.2791	1.0	1.5232	1.4	0.1467	1.0	0.71	882.5	8.4	939.8	8.8	1076.7	20.4	1076.7	20.4	82.0
H14-002 27May2015-Spot 144	97	61981	2.9	11.6673	1.2	2.6819	1.8	0.2289	1.3	0.72	1318.5	15.0	1323.5	13.0	1331.6	23.5	1331.6	23.5	96.0
H14-002 27May2015-Spot 145	1362	220417	28.4	13.3851	0.8	1.4897	1.4	0.1446	1.1	0.83	870.7	9.2	926.2	8.3	1067.7	15.3	1067.7	15.3	82.1
H14-002 27May2015-Spot 146	249	98794	7.8	12.9550	1.2	1.9017	1.9	0.1787	1.4	0.75	1059.8	14.0	1081.7	12.6	1126.1	24.8	1126.1	24.8	94.1
H14-002 27May2015-Spot 147	441	165355	4.2	13.3480	1.0	1.5647	1.8	0.1515	1.5	0.83	909.1	12.9	956.3	11.4	1066.6	20.6	1066.6	20.6	85.2
H14-002 27May2015-Spot 149	191	119471	9.6	13.9295	1.3	1.4028	2.0	0.1417	1.5	0.74	854.4	11.9	890.1	11.9	980.0	27.3	980.0	27.3	87.2
H14-002 27May2015-Spot 150	412	178946	4.2	13.4729	1.4	1.7200	2.0	0.1681	1.5	0.74	1001.4	14.0	1016.0	13.0	1047.6	27.4	1047.6	27.4	95.6
H14-002 27May2015-Spot 151	200	183571	8.2	13.3051	1.2	1.8780	1.8	0.1812	1.4	0.76	1073.6	13.6	1073.3	11.9	1072.8	23.4	1072.8	23.4	100.1
H14-002 27May2015-Spot 152	185	122009	2.8	12.0656	1.5	2.2919	2.0	0.2006	1.3	0.65	1178.3	13.8	1209.8	13.9	1266.4	29.0	1266.4	29.0	93.0
H14-002 27May2015-Spot 153	394	52942	4.4	13.6517	1.1	1.6365	1.8	0.1620	1.4	0.80	968.1	12.9	984.4	11.3	1020.9	21.5	1020.9	21.5	94.8
H14-002 27May2015-Spot 154	136	108522	1.6	13.2377	1.3	1.8368	2.3	0.1763	1.9	0.82	1047.0	18.6	1058.7	15.4	1082.9	26.5	1082.9	26.5	96.7
H14-002 27May2015-Spot 157	411	187517	1.8	13.2204	1.1	1.5678	1.7	0.1503	1.3	0.77	902.8	10.8	957.6	10.4	1085.6	21.3	1085.6	21.3	83.2
H14-002 27May2015-Spot 158	42	47439	1.8	13.7983	2.6	1.6720	3.0	0.1673	1.6	0.52	997.3	14.7	997.9	19.3	999.2	52.7	999.2	52.7	99.8
H14-002 27May2015-Spot 159	168	62481	1.9	12.9408	1.1	2.0370	1.7	0.1912	1.3	0.77	1127.8	13.3	1127.9	11.4	1128.3	21.3	1128.3	21.3	100.0
H14-002 27May2015-Spot 160	196	54526	1.7	13.4341	1.6	1.6823	2.0	0.1639	1.2	0.58	978.5	10.5	1001.8	12.6	1053.4	32.5	1053.4	32.5	92.9
H14-002 27May2015-Spot 161	1485	211684	5.2	14.2126	0.8	1.2417	1.4	0.1280	1.1	0.78	776.4	7.7	819.7	7.6	938.9	17.4	776.4	17.4	82.7
H14-002 27May2015-Spot 162	1525	185046	15.3	13.9846	0.9	1.4703	1.8	0.1491	1.5	0.87	896.1	12.9	918.3	10.7	971.9	17.4	971.9	17.4	92.2
H14-002 27May2015-Spot 164	101	98639	4.7	13.6646	1.7	1.6490	2.3	0.1634	1.6	0.69	975.8	14.3	989.2	14.5	1019.0	33.7	1019.0	33.7	95.8
H14-002 27May2015-Spot 166	1169	653033	2.1	11.1344	0.7	2.7188	1.3	0.2196	1.1	0.84	1279.5	13.1	1333.6	10.0	1421.5	14.2	1421.5	14.2	90.0
H14-002 27May2015-Spot 168	151	87366	2.1	12.4655	1.7	1.9237	2.0	0.1739	1.1	0.55	1033.7	10.7	1089.4	13.7	1202.4	33.8	1202.4	33.8	86.0
H14-002 27May2015-Spot 169	148	37546	1.9	12.9772	0.9	1.8306	1.3	0.1723	0.9	0.70	1024.7	8.7	1056.5	8.6	1122.7	18.5	1122.7	18.5	91.3
H14-002 27May2015-Spot 170	374	53175	2.0	12.4251	1.0	2.3261	1.3	0.2096	0.8	0.61	1226.8	8.6	1220.3	9.0	1208.9	19.6	1208.9	19.6	101.5
H14-002 27May2015-Spot 171	979	60824	2.9	13.0358	1.1	1.8016	1.6	0.1703	1.1	0.72	1014.0	10.6	1046.1	10.3	1113.7	22.1	1113.7	22.1	91.0
H14-002 27May2015-Spot 172	80	76447	1.1	13.3818	1.3	1.7190	1.7	0.1668	1.2	0.68	994.6	11.0	1015.6	11.2	1061.2	25.5	1061.2	25.5	93.7
H14-002 27May2015-Spot 173	590	212515	7.4	13.4349	0.9	1.6169	1.7	0.1533	1.4	0.85	943.1	12.5	976.8	10.6	1053.3	18.1	1053.3	18.1	89.5
H14-002 27May2015-Spot 174	306	113028	4.1	13.1461	1.0	1.6373	1.8	0.1561	1.5	0.83	935.1	13.2	984.7	11.5	1096.8	20.1	1096.8	20.1	85.3
H14-002 27May2015-Spot 175	343	103805	3.6	13.3991	1.2	1.6202	1.8	0.1574	1.3	0.75	942.6	11.5	978.1	11.0	1058.6	23.3	1058.6	23.3	89.0
H14-002 27May2015-Spot 176	98	54852	1.9	12.6940	1.4	1.9556	1.9	0.1800	1.3	0.68	1067.2	12.5	1100.4	13.6	1166.5	27.5	1166.5	27.5	91.5
H14-002 27May2015-Spot 177	119	96097	1.2	13.5162	1.7	1.5775	2.2	0.1546	1.4	0.64	926.9	12.1	961.4	13.6	1041.0	34.2	1041.0	34.2	89.0
H14-002 27May2015-Spot 179	150	96902	3.5	11.3238	1.1	2.8937	1.8	0.2377	1.5	0.79	1374.5	18.0	1380.3	13.9	1389.2	21.5	1389.2	21.5	98.9
H14-002 27May2015-Spot 180	1289	57313	20.6	14.3373	1.0	1.3158	1.6	0.1368	1.1	0.74	826.7	8.9	852.7	8.9	921.0	21.5	826.7	21.5	89.8
H14-002 27May2015-Spot 181	363	81386	4.4	13.8896	1.0	1.5509	1.8	0.1562	1.5	0.83	928.7	9.7	952.3	8.3	1007.2	15.2	1007.2	15.2	92.2
H14-002 27May2015-Spot 182	909	110584	20.6	13.7440	0.7	1.5546	1.3	0.1550	1.1	0.83	928.7	9.7	952.3	8.3	1007.2	15.2	1007.2	15.2	92.2
H14-002 27May2015-Spot 183	181	132386	3.1	12.7683	1.0	2.0372	2.2	0.1886	2.0	0.90	1114.1	20.3	1128.0	18.2	1155.0	19.2	1155.0	19.2	96.5
H14-002 27May2015-Spot 184	56	48597	2.3	12.5149	1.6	2.2394	2.6	0.2033	2.1	0.80	1192.8	22.5	1193.5	18.2	1194.6	31.0	1194.6	31.0	99.8
H14-002 27May2015-Spot 185	501	73659	2.9	11.4897	0.8	2.7711	1.5	0.2309	1.3	0.85	1339.3	15.4	1347.8	11.2	1361.2	15.4	1361.2	15.4	96.4



Appendix B: LA-ICPMS U-Pb Zircon Geochronology (continued)

Analysis		Isotope ratios											Apparent ages (Ma)					Conc (%)	
		U (ppm)	206Pb 204Pb	U/Th	206Pb* 207Pb*	± (%)	207Pb* 235U*	± (%)	206Pb* 238U	± (%)	error corr.	206Pb* 238U*	± (Ma)	207Pb* 235U	± (Ma)	206Pb* 207Pb*	± (Ma)		Best age (Ma)
H14-002 27May2015-Spot 188	104	97020	1.6	11.7576	1.3	2.5976	1.7	0.2215	1.1	0.64	1289.8	12.8	1300.0	12.5	1316.7	25.2	1316.7	25.2	98.0
H14-002 27May2015-Spot 189	885	331656	7.1	15.3145	1.1	0.9527	2.0	0.1058	1.7	0.83	648.4	10.2	679.5	9.9	783.9	23.6	648.4	10.2	82.7
H14-002 27May2015-Spot 191	174	64356	3.6	11.3673	1.5	2.7155	2.7	0.2239	2.2	0.83	1302.3	25.9	1332.7	19.7	1381.8	28.7	1381.8	28.7	94.2
H14-002 27May2015-Spot 192	229	101091	2.4	14.1294	1.1	1.4885	1.9	0.1505	1.5	0.81	903.7	12.8	917.5	11.3	950.9	22.7	950.9	22.7	95.0
H14-002 27May2015-Spot 193	1390	62678	36.5	16.4769	1.4	0.7266	1.9	0.0968	1.3	0.67	536.8	6.7	554.6	8.3	628.3	31.0	536.8	6.7	85.4
H14-002 27May2015-Spot 194	362	55358	1.3	11.9613	0.9	2.3910	1.5	0.2074	1.2	0.78	1215.1	13.0	1239.9	10.8	1283.3	18.5	1283.3	18.5	94.7
H14-002 27May2015-Spot 195	924	99374	3.1	12.8919	0.8	1.8328	1.6	0.1714	1.4	0.87	1019.7	13.5	1057.3	10.8	1135.8	16.1	1135.8	16.1	89.8
H14-002 27May2015-Spot 196	464	72972	6.2	13.9523	1.5	1.3262	3.2	0.1342	2.9	0.89	811.8	21.8	857.2	18.6	976.7	29.9	811.8	21.8	83.1
H14-002 27May2015-Spot 197	1277	95027	31.4	17.7930	0.9	0.5728	1.3	0.0739	0.9	0.70	459.7	4.0	459.8	4.8	460.3	20.6	459.7	4.0	99.9
H14-002 27May2015-Spot 198	668	255729	1.2	12.7076	0.7	1.9379	1.4	0.1786	1.2	0.87	1059.4	11.6	1094.3	9.1	1164.4	13.2	1164.4	13.2	91.0
H14-002 27May2015-Spot 199	766	62582	14.0	17.6475	1.2	0.5981	1.8	0.0765	1.3	0.74	475.5	6.1	476.0	6.8	478.5	26.5	475.5	6.1	99.4
H14-002 27May2015-Spot 200	781	53418	11.9	13.9115	0.9	1.5998	1.3	0.1604	1.0	0.76	959.0	9.1	966.2	8.4	982.7	17.7	982.7	17.7	97.6
H14-002 27May2015-Spot 201	433	78596	5.1	12.5605	0.8	2.0238	1.5	0.1444	1.3	0.83	1090.8	12.8	1123.5	10.4	1187.5	16.7	1187.5	16.7	91.9
H14-002 27May2015-Spot 204	477	213626	12.8	13.5666	0.9	1.4690	1.8	0.1045	1.5	0.86	870.3	12.6	917.7	10.8	1033.5	18.6	1033.5	18.6	84.2
H14-002 27May2015-Spot 207	477	213626	12.8	13.5666	0.9	1.4690	1.8	0.1045	1.5	0.86	870.3	12.6	917.7	10.8	1033.5	18.6	1033.5	18.6	84.2
H14-002 27May2015-Spot 208	134	43817	2.8	12.8223	1.2	2.1075	1.5	0.1960	1.0	0.65	1153.7	10.6	1151.3	10.6	1146.6	23.1	1146.6	23.1	100.6
H14-002 27May2015-Spot 222	213	228607	1.8	12.3462	0.7	0.9844	1.5	0.2037	1.1	0.73	1195.0	11.8	1204.4	10.5	1221.4	20.1	1221.4	20.1	97.8
H14-002 27May2015-Spot 223	1796	68883	11.0	15.1003	0.7	0.9844	1.5	0.2037	1.1	0.73	1195.0	11.8	1204.4	10.5	1221.4	20.1	1221.4	20.1	97.8
H14-002 27May2015-Spot 224	258	75020	2.9	12.7321	0.9	2.0463	1.8	0.1890	1.5	0.86	1115.7	15.4	1131.1	12.0	1160.6	18.0	1160.6	18.0	96.1
H14-002 27May2015-Spot 225	243	81151	3.1	12.9590	0.9	1.8789	1.3	0.1766	1.0	0.74	1048.3	9.6	1073.7	8.9	1125.5	18.1	1125.5	18.1	93.1
H14-002 27May2015-Spot 227	1180	434088	4.7	12.8293	1.1	1.8326	1.7	0.1705	1.4	0.79	1015.0	13.0	1057.2	11.4	1145.5	21.1	1145.5	21.1	88.6
H14-002 27May2015-Spot 228	398	236787	2.7	11.7169	1.0	2.6250	1.7	0.2231	1.3	0.80	1298.1	15.8	1307.7	12.3	1323.4	19.2	1323.4	19.2	96.1
H14-002 27May2015-Spot 229	531	100140	9.1	13.0618	1.0	1.7274	1.6	0.1636	1.2	0.76	977.0	10.9	1018.8	10.2	1109.7	20.4	1109.7	20.4	88.0
H14-002 27May2015-Spot 230	348	79132	3.8	15.3030	1.2	0.9236	1.9	0.1025	1.4	0.78	664.3	8.6	664.3	9.0	785.5	24.4	629.1	8.6	80.1
H14-002 27May2015-Spot 232	146	70017	3.5	11.4578	1.1	2.7668	1.9	0.2299	1.5	0.80	1334.1	18.3	1346.6	14.2	1366.6	22.0	1366.6	22.0	97.6
H14-002 27May2015-Spot 233	360	93151	2.3	12.4597	1.2	2.1794	1.7	0.1969	1.2	0.72	1158.9	13.1	1174.5	12.0	1203.3	23.6	1203.3	23.6	96.3
H14-002 27May2015-Spot 234	414	133778	3.8	13.6035	0.9	1.5382	1.5	0.1518	1.1	0.77	910.8	9.6	945.8	9.0	1028.0	18.9	1028.0	18.9	88.6
H14-002 27May2015-Spot 237	249	66216	2.8	13.0958	1.0	1.7724	1.6	0.1683	1.3	0.80	1003.0	11.9	1035.4	10.4	1104.5	19.2	1104.5	19.2	90.8
H14-002 27May2015-Spot 238	124	65441	8.5	12.4794	1.6	2.1270	2.8	0.1924	2.3	0.82	1134.5	24.4	1157.6	19.7	1201.2	31.9	1201.2	31.9	94.4
H14-002 27May2015-Spot 239	60	45953	1.7	12.4592	1.5	1.9316	2.0	0.1745	1.4	0.70	1037.1	13.5	1092.1	13.6	1203.4	28.7	1203.4	28.7	86.2
H14-002 27May2015-Spot 240	591	235443	3.1	13.9575	0.9	1.5024	1.6	0.1521	1.3	0.80	912.6	10.8	931.3	9.7	975.9	19.3	975.9	19.3	93.5
H14-002 27May2015-Spot 242	813	202522	6.8	13.8601	0.7	1.4465	1.4	0.1454	1.3	0.89	875.2	10.4	908.4	8.6	990.2	13.3	990.2	13.3	88.4
H14-002 27May2015-Spot 243	413	82401	3.1	12.7990	0.8	2.1712	1.4	0.2015	1.1	0.80	1183.6	11.8	1171.9	9.5	1150.2	16.5	1150.2	16.5	102.9
H14-002 27May2015-Spot 244	2988	141434	25.9	17.6244	0.9	0.5458	1.7	0.0898	1.4	0.85	434.8	6.0	442.2	6.0	481.4	19.7	434.8	6.0	90.3
H14-002 27May2015-Spot 245	689	74195	4.9	13.5761	0.9	1.6810	1.7	0.1655	1.4	0.82	987.4	12.6	1001.4	10.6	1032.1	19.1	1032.1	19.1	95.7
H14-002 27May2015-Spot 247	263	76544	1.7	12.9434	1.1	1.8026	1.6	0.1692	1.1	0.70	1007.8	10.4	1046.4	10.4	1127.9	22.5	1127.9	22.5	89.3
H14-002 27May2015-Spot 249	379	152079	3.7	12.7433	1.0	2.0969	1.6	0.1938	1.3	0.80	1141.9	13.5	1147.8	11.1	1158.8	19.2	1158.8	19.2	98.5
H14-002 27May2015-Spot 250	1026	92782	4.5	13.6352	1.1	1.5609	2.0	0.1544	1.6	0.83	925.4	14.1	954.8	12.3	1023.3	22.6	1023.3	22.6	90.4
H14-002 27May2015-Spot 252	475	175249	1.6	11.7291	0.9	2.1757	1.4	0.2191	1.1	0.79	1277.2	12.7	1293.8	10.2	1321.4	16.5	1321.4	16.5	96.7
H14-002 27May2015-Spot 253	78	81419	3.3	12.6691	1.4	2.2293	1.9	0.2048	1.3	0.69	1201.3	14.3	1190.3	13.2	1170.4	27.0	1170.4	27.0	102.6
H14-002 27May2015-Spot 254	1038	616530	4.8	13.5298	0.9	1.6407	1.9	0.1610	1.7	0.88	962.3	14.8	986.0	11.9	1039.0	18.4	1039.0	18.4	92.6
H14-002 27May2015-Spot 259	766	107660	2.8	13.2826	1.0	1.6306	1.6	0.1764	1.3	0.77	1047.3	12.2	1056.7	10.7	1076.2	20.7	1076.2	20.7	97.3
H14-002 27May2015-Spot 260	638	137437	2.4	13.6395	1.0	1.6506	1.5	0.1633	1.2	0.76	974.9	10.5	989.8	9.7	1022.8	20.2	1022.8	20.2	95.3
H14-002 27May2015-Spot 263	190	71939	16.7	13.5753	1.3	1.6913	1.8	0.1665	1.3	0.71	992.9	11.5	1005.2	11.3	1032.2	25.3	1032.2	25.3	96.2
H14-002 27May2015-Spot 264	428	202277	6.7	17.7729	1.4	0.5540	1.9	0.0714	1.3	0.69	444.6	5.6	447.6	6.8	462.9	30.4	444.6	5.6	96.1
H14-002 27May2015-Spot 265	320	50879	5.0	12.1048	1.3	2.4191	2.5	0.2124	2.1	0.85	1241.5	23.9	1248.3	17.9	1260.1	25.7	1260.1	25.7	98.5
H14-002 27May2015-Spot 267	1358	585213	11.2	12.9925	1.1	1.6442	1.7	0.1549	1.3	0.74	928.6	10.9	987.3	10.7	1120.4	22.7	1120.4	22.7	82.9
H14-002 27May2015-Spot 268	276	148320	3.6	13.4637	1.1	1.7757	1.7	0.1734	1.3	0.77	1030.8	12.7	1036.6	11.2	1048.9	22.0	1048.9	22.0	98.3
H14-002 27May2015-Spot 269	295	105200	1.9	14.5906	1.1	1.2220	1.9	0.1293	1.5	0.82	783.9	11.3	810.7	10.4	884.9	21.9	783.9	11.3	88.6
H14-002 27May2015-Spot 270	154	149460	4.4	12.8816	1.0	2.0216	1.7	0.1889	1.4	0.79	1115.3	13.9	1122.8	11.6	1137.4	20.7	1137.4	20.7	96.1

Appendix B: LA-ICPMS U-Pb Zircon Geochronology (continued)

Analysis	U (ppm)	206Pb/204Pb	U/Th	206Pb*/207Pb*	Isotope ratios				Apparent ages (Ma)				Best age (Ma)	± (Ma)	Conc (%)				
					± (%)	207Pb*/235U*	± (%)	206Pb*/238U	error corr.	206Pb*/238U*	± (Ma)	207Pb*/235U				± (Ma)	206Pb*/207Pb*	± (Ma)	
																			206Pb*/207Pb*
H14-002 27May2015-Spot 272	243	145670	3.4	11.6086	1.0	2.7359	1.6	0.2303	1.2	0.77	1336.3	14.7	1338.3	11.7	1341.4	19.4	1341.4	19.4	98.6
H14-002 27May2015-Spot 273	1313	186124	7.7	13.1818	0.8	1.7594	1.7	0.1682	1.5	0.87	1002.2	13.5	1030.6	10.9	1091.4	16.8	1091.4	16.8	91.8
H14-002 27May2015-Spot 274	385	119836	8.7	13.6901	1.0	1.6393	1.0	0.1628	1.2	0.77	972.1	10.4	985.4	9.4	1015.2	19.4	1015.2	19.4	95.8
H14-002 27May2015-Spot 275	252	135008	3.3	14.8851	1.5	1.0826	1.9	0.1180	1.2	0.63	718.8	8.1	749.8	10.0	843.4	30.6	718.8	8.1	85.2
H14-002 27May2015-Spot 277	352	220286	5.6	13.7585	1.0	1.5838	1.7	0.1580	1.4	0.81	945.9	12.3	963.8	10.6	1005.1	20.1	1005.1	20.1	94.1
H14-002 27May2015-Spot 278	611	164206	2.7	14.9126	1.1	1.0620	2.0	0.1149	1.7	0.84	700.9	11.3	734.8	10.6	839.5	22.7	700.9	11.3	83.5
H14-002 27May2015-Spot 279	57	27004	1.5	13.9305	2.2	1.6517	2.6	0.1669	1.4	0.53	984.9	12.6	990.2	16.4	979.8	44.8	979.8	44.8	101.5
H14-002 27May2015-Spot 280	1426	154176	9.1	13.9071	1.1	1.2913	1.8	0.1302	1.4	0.79	789.3	10.4	841.9	10.2	983.3	22.4	789.3	10.4	80.3
H14-002 27May2015-Spot 282	228	70661	3.1	14.2020	1.3	1.4267	2.1	0.1470	1.7	0.80	883.9	14.0	900.2	12.6	940.4	25.8	940.4	25.8	94.0
H14-002 27May2015-Spot 283	140	46190	2.0	14.3507	1.6	1.2572	2.2	0.1309	1.4	0.65	792.7	10.6	826.7	12.3	919.0	33.8	792.7	10.6	86.3
H14-002 27May2015-Spot 287	615	75797	2.1	13.2123	1.0	1.7363	1.0	0.1664	1.5	0.84	982.2	13.9	1022.1	11.6	1086.8	19.6	1086.8	19.6	91.3
H14-002 27May2015-Spot 289	84	37179	4.0	14.0577	1.3	1.5636	1.9	0.1594	1.3	0.71	953.6	11.8	955.9	11.7	961.3	27.3	961.3	27.3	99.2
H14-002 27May2015-Spot 290	386	71904	3.2	13.3170	1.0	1.8741	1.9	0.1810	1.7	0.87	1072.0	16.7	1072.0	12.9	1071.0	19.4	1071.0	19.4	100.1
H14-002 27May2015-Spot 292	115	54890	1.6	14.3870	1.8	1.3361	2.2	0.1394	1.2	0.56	841.4	9.6	861.5	12.7	913.8	37.3	841.4	9.6	92.1
H14-002 27May2015-Spot 293	602	84658	1.8	12.7771	0.8	2.0324	1.7	0.1883	1.5	0.87	1112.4	15.0	1126.4	11.5	1153.6	16.7	1153.6	16.7	96.4
H14-002 27May2015-Spot 294	125	96813	2.4	12.7260	1.8	1.9064	2.4	0.1760	1.6	0.68	1044.8	15.7	1083.3	15.9	1161.5	34.7	1161.5	34.7	90.0
H14-002 27May2015-Spot 295	1091	498368	3.4	13.2836	0.9	1.6486	1.8	0.1588	1.5	0.86	950.2	13.6	989.0	11.4	1076.0	18.7	1076.0	18.7	88.3
H14-002 27May2015-Spot 297	210	213991	1.9	12.8534	1.3	1.8611	1.9	0.1735	1.4	0.73	1031.3	13.3	1067.4	12.6	1141.8	26.0	1141.8	26.0	90.3
H14-002 27May2015-Spot 299	84	27549	2.1	13.6568	1.5	1.7717	1.9	0.1755	1.2	0.62	1042.3	11.5	1035.2	12.6	1020.1	30.9	1020.1	30.9	102.2
H14-002 27May2015-Spot 304	166	83993	1.1	13.0436	1.5	2.0246	1.9	0.1915	1.3	0.64	1129.7	13.0	1123.8	13.2	1112.5	29.8	1112.5	29.8	101.5
H14-002 27May2015-Spot 300	127	172098	1.9	6.0194	1.1	10.5454	1.8	0.4604	1.5	0.81	2441.2	30.1	2483.9	16.9	2519.0	17.8	2519.0	17.8	96.9
H14-002 27May2015-Spot 302	317	83611	4.0	13.8575	1.3	1.5635	1.9	0.1571	1.5	0.76	940.9	12.8	955.9	12.0	990.6	25.7	990.6	25.7	95.0
H14-002 27May2015-Spot 303	608	334553	2.0	12.5957	1.0	1.9522	1.6	0.1783	1.2	0.78	1057.9	12.0	1089.2	10.7	1182.0	19.7	1182.0	19.7	89.5
H14-002 27May2015-Spot 308	209	55365	1.1	13.0289	1.0	2.0243	1.6	0.1913	1.3	0.81	1128.4	13.8	1123.7	11.2	1114.7	19.2	1114.7	19.2	101.2
H14-002 27May2015-Spot 309	406	616941	1.9	12.8845	0.9	1.8698	1.4	0.1747	1.0	0.73	1038.1	9.6	1070.5	9.1	1137.0	18.8	1137.0	18.8	91.3
H14-002 27May2015-Spot 314	286	64261	2.5	13.0171	1.0	2.0359	1.8	0.1922	1.5	0.82	1133.3	15.7	1127.6	12.5	1176.6	20.7	1176.6	20.7	101.5
H14-002 27May2015-Spot 315	225	158320	3.3	10.9696	0.8	3.0637	1.6	0.2437	1.4	0.86	1406.1	17.7	1423.7	12.5	1450.0	16.1	1450.0	16.1	97.0
H14-002 27May2015-Spot 317	763	163319	31.7	12.7115	0.9	1.7877	1.7	0.1648	1.4	0.84	983.5	13.2	1041.0	11.1	1163.8	18.1	1163.8	18.1	84.5
H14-002 27May2015-Spot 318	474	177496	15.4	13.4195	0.9	1.8453	1.8	0.1796	1.5	0.86	1064.8	14.9	1061.8	11.7	1055.6	18.3	1055.6	18.3	100.9
H14-002 27May2015-Spot 319	725	219954	12.7	17.6431	1.6	0.5940	2.1	0.0760	1.3	0.61	472.2	5.7	473.4	7.8	472.2	5.7	472.2	5.7	96.6
H14-002 27May2015-Spot 320	2186	1337333	8.1	13.7273	0.8	1.6664	1.5	0.1659	1.3	0.85	989.5	11.8	995.8	9.5	1009.7	15.9	1009.7	15.9	96.0
H14-002 27May2015-Spot 322	304	60689	2.9	11.9136	1.0	2.5283	1.6	0.2185	1.2	0.77	1273.7	14.4	1280.2	11.7	1291.1	19.9	1291.1	19.9	98.7
H14-002 27May2015-Spot 323	802	172427	2.1	12.1060	0.6	2.0758	1.2	0.1823	1.0	0.85	1079.3	10.1	1140.9	8.2	1259.9	12.2	1259.9	12.2	85.7
H14-002 27May2015-Spot 325	310	143569	2.7	12.8594	0.9	2.0950	1.4	0.1954	1.1	0.76	1147.2	11.3	1147.2	9.7	1140.8	18.0	1140.8	18.0	100.8
H14-002 27May2015-Spot 327	1316	489936	23.3	17.7157	0.9	0.5715	1.6	0.0734	1.4	0.84	456.8	6.0	459.0	6.0	470.0	19.8	456.8	6.0	97.2
H14-002 27May2015-Spot 328	83	140820	3.4	12.8724	1.8	1.9936	2.9	0.1861	2.3	0.78	1100.3	22.8	1113.3	19.6	1138.9	36.4	1138.9	36.4	96.6
H14-002 27May2015-Spot 329	2721	2203911	7.7	14.7069	0.9	1.0971	1.6	0.1170	1.4	0.85	713.4	9.5	752.0	8.7	868.4	17.8	713.4	9.5	82.2
H14-002 27May2015-Spot 330	177	70840	2.5	12.9609	1.2	2.1064	3.5	0.1980	3.3	0.94	1164.6	35.1	1150.9	24.1	1125.2	23.6	1125.2	23.6	103.5

Appendix C: LA-ICPMS U-Pb Zircon Geochronology

Analysis	U (ppm)	206Pb/204Pb	U/Th	206Pb*/207Pb*	± (%)	Isotope ratios						Apparent ages (Ma)						Conc (%)	
						207Pb*/235U*	± (%)	206Pb*/238U*	± (%)	207Pb*/235U*	± (Ma)	206Pb*/207Pb*	± (Ma)	Best age (Ma)	± (Ma)				
						1.0	1.9763	1.6	0.1861	1.1	1.8017	1.7	0.1760	1.3	0.79	1102.2	12.8		1107.4
H14-007_27May2015-Spot 1	1009	93695	3.6	12.9842	1.0	1.9763	1.6	0.1861	1.3	0.79	1102.2	12.8	1107.4	10.8	1121.6	19.7	1121.6	19.7	98.1
H14-007_27May2015-Spot 2	448	51389	13.0	13.4705	1.1	1.8017	1.7	0.1760	1.4	0.79	1045.2	13.2	1046.1	11.3	1047.9	21.4	1047.9	21.4	99.7
H14-007_27May2015-Spot 3	382	23965	1.4	13.8000	1.0	1.6456	1.6	0.1647	1.2	0.77	982.9	11.3	987.9	10.2	999.0	21.0	999.0	21.0	98.4
H14-007_27May2015-Spot 4	346	130684	1.5	13.3608	1.0	1.8863	1.6	0.1828	1.3	0.81	1082.2	11.3	1076.3	10.8	1064.4	19.2	1064.4	19.2	101.7
H14-007_27May2015-Spot 5	151	50667	3.4	11.0513	1.1	3.0499	1.7	0.2445	1.2	0.73	1409.8	15.4	1420.2	12.8	1435.8	21.9	1435.8	21.9	98.2
H14-007_27May2015-Spot 6	74	63130	3.2	12.9549	1.7	2.1181	2.3	0.1990	1.5	0.67	1170.0	16.3	1154.7	15.6	1126.1	33.3	1126.1	33.3	103.9
H14-007_27May2015-Spot 7	294	187908	1.1	13.4837	1.3	1.8112	1.8	0.1771	1.2	0.67	1051.2	11.4	1049.5	11.5	1045.9	26.4	1045.9	26.4	100.5
H14-007_27May2015-Spot 8	51	87419	3.6	12.9814	2.1	1.9847	2.6	0.1869	1.4	0.56	1104.4	14.6	1110.3	17.4	1122.1	42.7	1122.1	42.7	98.4
H14-007_27May2015-Spot 10	52	36224	1.9	12.2547	1.3	2.3765	2.0	0.2112	1.5	0.74	1235.3	16.3	1235.5	14.1	1236.0	26.3	1236.0	26.3	99.9
H14-007_27May2015-Spot 11	1067	56497	6.4	13.4259	0.8	1.6852	1.6	0.1641	1.4	0.87	979.5	12.4	1003.0	10.0	1054.6	15.9	1054.6	15.9	92.9
H14-007_27May2015-Spot 12	318	142916	3.4	12.9523	1.2	2.0608	2.2	0.1936	1.9	0.85	1140.8	19.9	1135.9	15.3	1126.5	23.8	1126.5	23.8	101.3
H14-007_27May2015-Spot 13	378	116973	3.9	12.9847	1.0	2.0233	1.6	0.1905	1.2	0.81	1124.3	12.1	1123.4	10.7	1121.6	20.8	1121.6	20.8	100.2
H14-007_27May2015-Spot 14	386	193510	5.8	12.1963	0.9	2.2712	1.5	0.2009	1.2	0.81	1180.2	13.3	1203.4	10.8	1245.3	17.8	1245.3	17.8	94.8
H14-007_27May2015-Spot 15	347	85466	2.6	13.5591	1.0	1.7250	1.7	0.1696	1.4	0.81	1010.1	13.2	1017.9	11.2	1034.6	20.6	1034.6	20.6	97.6
H14-007_27May2015-Spot 16	119	70126	1.5	13.4096	1.5	1.8846	1.9	0.1833	1.2	0.63	1084.9	11.7	1075.7	12.4	1057.0	29.2	1057.0	29.2	102.6
H14-007_27May2015-Spot 17	794	234432	6.1	13.3989	0.9	1.6188	1.3	0.1573	1.0	0.73	941.8	8.4	977.5	8.3	1058.7	18.1	1058.7	18.1	89.0
H14-007_27May2015-Spot 18	175	147208	7.3	12.8601	1.3	2.0067	2.0	0.1872	1.5	0.76	1106.0	15.7	1117.8	13.7	1140.8	26.1	1140.8	26.1	97.0
H14-007_27May2015-Spot 19	1049	241111	6.5	14.0171	0.8	1.3653	1.7	0.1388	1.5	0.87	837.9	11.6	874.2	9.9	967.2	16.7	967.2	16.7	86.6
H14-007_27May2015-Spot 20	235	352515	2.3	12.4470	1.2	2.1246	1.7	0.1918	1.2	0.71	1131.1	12.6	1156.8	11.9	1205.4	24.1	1205.4	24.1	93.8
H14-007_27May2015-Spot 22	862	176070	4.9	12.3141	0.9	1.9938	1.8	0.1781	1.5	0.85	1056.4	14.8	1113.4	12.1	1226.5	18.5	1226.5	18.5	86.1
H14-007_27May2015-Spot 23	284	229954	5.8	12.0390	1.1	2.0871	2.4	0.1822	2.1	0.88	1079.2	20.5	1144.6	16.1	1270.7	21.9	1270.7	21.9	84.9
H14-007_27May2015-Spot 24	65	62206	0.9	12.2798	1.3	2.3656	1.9	0.2107	1.4	0.73	1232.4	16.0	1232.3	13.9	1232.0	26.1	1232.0	26.1	100.7
H14-007_27May2015-Spot 25	76	43542	2.3	13.1716	1.6	1.7377	2.2	0.1729	1.4	0.66	1028.0	13.5	1022.6	13.9	1011.1	33.0	1011.1	33.0	101.7
H14-007_27May2015-Spot 26	600	474274	1.5	12.8040	1.0	1.9867	1.7	0.1845	1.4	0.80	1091.5	13.9	1111.0	11.7	1149.4	20.5	1149.4	20.5	95.0
H14-007_27May2015-Spot 27	1775	69696	3.7	13.3181	0.8	1.6439	1.6	0.1588	1.3	0.85	950.0	11.7	987.2	9.9	1070.8	16.8	1070.8	16.8	88.7
H14-007_27May2015-Spot 29	212	174609	2.5	12.2154	0.9	2.3912	1.5	0.2118	1.2	0.81	1238.6	13.3	1240.0	10.5	1242.2	17.0	1242.2	17.0	99.7
H14-007_27May2015-Spot 30	366	199629	5.1	13.9461	0.9	1.6317	1.4	0.1650	1.0	0.75	984.7	9.4	982.5	8.6	977.6	18.3	977.6	18.3	100.7
H14-007_27May2015-Spot 32	252	62864	1.0	13.7318	1.1	1.7458	1.5	0.1739	1.1	0.72	1033.4	10.4	1025.6	9.8	1009.0	21.4	1009.0	21.4	102.4
H14-007_27May2015-Spot 33	279	54871	1.6	10.7486	0.9	3.2768	1.5	0.2554	1.2	0.79	1466.5	15.2	1475.6	11.4	1488.6	17.1	1488.6	17.1	98.5
H14-007_27May2015-Spot 34	126	87067	2.0	12.5921	1.4	2.2024	1.9	0.2011	1.3	0.67	1181.4	14.1	1181.8	13.5	1182.5	28.2	1182.5	28.2	99.9
H14-007_27May2015-Spot 35	545	118929	2.6	12.4816	0.9	1.9515	1.9	0.1767	1.6	0.87	1048.7	15.9	1099.0	12.7	1199.9	18.6	1199.9	18.6	87.4
H14-007_27May2015-Spot 36	82	52878	7.7	11.8492	1.5	2.5814	2.2	0.2218	1.6	0.73	1291.6	19.1	1295.4	16.3	1301.6	29.5	1301.6	29.5	99.2
H14-007_27May2015-Spot 37	172	504301	1.0	13.2657	1.2	1.7607	1.9	0.1694	1.4	0.75	1008.8	13.2	1031.1	12.1	1078.7	24.7	1078.7	24.7	93.5
H14-007_27May2015-Spot 38	411	87008	1.8	12.6025	1.1	2.1609	1.7	0.1975	1.2	0.74	1161.9	13.1	1168.6	11.5	1180.9	21.9	1180.9	21.9	98.4
H14-007_27May2015-Spot 39	150	63425	2.6	12.4117	1.2	2.1982	1.7	0.1979	1.2	0.70	1163.9	12.5	1180.5	11.7	1210.9	23.5	1210.9	23.5	96.1
H14-007_27May2015-Spot 40	283	193837	2.2	13.2953	1.2	1.8945	1.8	0.1827	1.3	0.75	1081.6	13.1	1079.2	11.7	1074.3	23.5	1074.3	23.5	100.7
H14-007_27May2015-Spot 41	418	125497	8.8	13.4133	0.9	1.8432	1.6	0.1793	1.3	0.83	1063.2	12.8	1061.0	10.3	1056.5	17.3	1056.5	17.3	100.6
H14-007_27May2015-Spot 42	69	51818	3.1	12.1535	2.1	1.9944	2.4	0.1772	1.2	0.50	1051.9	11.8	1113.6	16.5	1236.2	41.4	1236.2	41.4	85.1
H14-007_27May2015-Spot 43	795	95686	6.3	13.1302	1.0	1.8819	1.6	0.1792	1.3	0.79	1062.6	12.4	1074.7	10.7	1099.3	19.9	1099.3	19.9	96.7
H14-007_27May2015-Spot 44	64	59127	1.6	12.3346	1.6	2.3373	2.0	0.2091	1.2	0.61	1224.0	13.5	1223.7	14.1	1223.2	30.9	1223.2	30.9	100.1
H14-007_27May2015-Spot 45	356	128341	3.2	12.6196	0.8	2.1107	1.4	0.1933	1.1	0.81	1138.6	11.4	1152.3	9.4	1178.2	15.8	1178.2	15.8	96.6
H14-007_27May2015-Spot 46	1787	1317617	16.4	12.5242	0.9	2.1355	1.8	0.1940	1.5	0.86	1142.9	16.1	1160.4	12.4	1193.2	18.1	1193.2	18.1	95.8
H14-007_27May2015-Spot 47	173	161979	2.1	12.5259	1.2	2.1277	1.6	0.1933	1.2	0.71	1139.2	12.2	1157.8	11.3	1192.9	22.7	1192.9	22.7	95.5
H14-007_27May2015-Spot 48	302	135701	3.1	13.4206	0.9	1.8237	1.4	0.1775	1.0	0.74	1053.4	9.9	1054.0	9.0	1055.4	18.8	1055.4	18.8	99.8
H14-007_27May2015-Spot 50	77	34245	2.7	12.3989	1.4	2.2192	1.9	0.1996	1.3	0.69	1173.0	14.2	1187.1	13.4	1213.0	27.2	1213.0	27.2	96.7
H14-007_27May2015-Spot 51	523	191649	2.6	12.6394	0.7	1.9085	1.9	0.1749	1.7	0.92	1039.3	16.5	1084.0	12.5	1175.1	14.8	1175.1	14.8	88.4

Appendix C: LA-ICPMS U-Pb Zircon Geochronology (continued)

Analysis	U (ppm)	206Pb/204Pb	U/Th	206Pb*/207Pb*	± (%)	Isotope ratios				Apparent ages (Ma)				Best age (Ma)	± (Ma)	Conc (%)			
						206Pb*/238U	± (%)	error corr.	206Pb*/238U*	± (Ma)	207Pb*/235U	± (Ma)	206Pb*/207Pb*				± (Ma)		
H14-007_27May2015-Spot 52	3830	135330	46.1	15.7234	1.1	0.8634	2.2	0.0985	1.9	0.87	605.4	11.0	632.0	10.4	728.4	23.5	605.4	11.0	83.1
H14-007_27May2015-Spot 53	401	68214	2.0	12.7269	1.0	2.0667	1.5	0.1908	1.1	0.73	1125.7	11.0	10667	10.0	1161.4	20.0	1161.4	20.0	96.9
H14-007_27May2015-Spot 54	174	90996	1.6	11.7131	1.1	2.7326	1.6	0.2321	1.2	0.74	1345.7	14.4	1337.4	12.0	1324.0	21.2	1324.0	21.2	101.6
H14-007_27May2015-Spot 55	504	106680	2.5	12.5073	1.4	1.9816	1.8	0.1798	1.2	0.65	1065.6	11.7	1109.3	12.5	1195.8	27.8	1195.8	27.8	89.1
H14-007_27May2015-Spot 56	412	120471	8.8	12.4854	1.0	2.0233	1.7	0.1832	1.4	0.81	1084.5	13.5	1123.4	11.4	1199.3	19.5	1199.3	19.5	90.4
H14-007_27May2015-Spot 57	169	56102	1.4	14.0020	1.1	1.5717	1.6	0.1596	1.2	0.71	954.6	10.2	959.1	10.0	969.4	23.1	969.4	23.1	98.5
H14-007_27May2015-Spot 58	170	57687	1.4	12.0155	0.9	2.5062	1.5	0.2184	1.1	0.79	1273.4	13.3	1273.8	10.6	1274.5	17.5	1274.5	17.5	99.9
H14-007_27May2015-Spot 59	261	80763	3.0	12.2414	1.1	2.1824	1.5	0.1938	1.0	0.68	1141.7	10.9	1175.4	10.6	1238.1	21.9	1238.1	21.9	92.2
H14-007_27May2015-Spot 60	930	99354	2.1	13.3025	1.2	1.8471	1.9	0.1782	1.5	0.79	1057.2	14.4	1062.4	12.3	1073.2	23.1	1073.2	23.1	98.5
H14-007_27May2015-Spot 61	130	67820	3.0	11.5814	1.2	2.6626	1.7	0.2236	1.2	0.73	1301.1	14.7	1318.1	12.7	1345.9	22.8	1345.9	22.8	96.7
H14-007_27May2015-Spot 62	57	139677	1.9	12.4892	1.4	2.5690	2.0	0.2055	1.4	0.70	1204.9	15.5	1202.7	14.2	1198.7	28.4	1198.7	28.4	100.5
H14-007_27May2015-Spot 63	80	63886	2.1	12.3134	1.5	2.3056	2.0	0.2055	1.4	0.67	1207.0	15.0	1214.0	14.4	1226.6	29.6	1226.6	29.6	98.4
H14-007_27May2015-Spot 64	113	101160	1.4	11.6077	1.3	2.7062	1.7	0.2278	1.2	0.66	1323.1	13.9	1330.1	13.0	1341.5	25.3	1341.5	25.3	98.6
H14-007_27May2015-Spot 65	1371	200520	2.4	12.5006	0.8	2.0560	1.4	0.1864	1.1	0.80	1101.9	11.1	1134.3	9.4	1196.9	16.2	1196.9	16.2	92.1
H14-007_27May2015-Spot 66	260	108613	1.0	13.6949	0.8	1.6870	1.4	0.1676	1.1	0.79	998.6	10.1	1003.6	8.8	1014.5	17.1	1014.5	17.1	98.4
H14-007_27May2015-Spot 67	1146	64068	9.8	14.1835	0.9	1.2336	1.4	0.1269	1.1	0.78	770.2	8.1	816.0	8.1	943.1	18.5	770.2	8.1	81.7
H14-007_27May2015-Spot 68	842	116255	2.0	13.4715	0.7	1.7094	1.6	0.1670	1.4	0.89	995.6	13.2	1012.0	10.3	1047.8	14.7	1047.8	14.7	95.0
H14-007_27May2015-Spot 69	1291	133462	7.4	13.4830	1.1	1.5146	1.5	0.1481	1.1	0.73	890.4	9.3	936.3	9.4	1046.0	21.3	1046.0	21.3	85.1
H14-007_27May2015-Spot 70	598	205049	2.4	12.8418	1.1	2.0938	1.6	0.1950	1.2	0.72	1148.5	12.3	1146.8	11.2	1143.6	22.5	1143.6	22.5	100.4
H14-007_27May2015-Spot 71	139	170218	1.5	12.1157	1.7	2.3247	2.7	0.2043	2.1	0.78	1198.2	23.3	1219.8	19.3	1258.3	33.3	1258.3	33.3	95.2
H14-007_27May2015-Spot 72	104	66534	1.6	13.4494	1.3	1.7920	1.7	0.1748	1.2	0.66	1038.5	11.0	1042.6	11.4	1051.1	26.4	1051.1	26.4	98.8
H14-007_27May2015-Spot 73	370	236766	2.0	11.6222	0.9	2.5172	1.4	0.2122	1.0	0.74	1240.4	11.3	1277.0	9.8	1339.1	17.4	1339.1	17.4	92.6
H14-007_27May2015-Spot 74	701	384545	3.7	12.5851	0.9	1.9146	1.5	0.1748	1.3	0.83	1038.3	12.2	1086.2	10.2	1183.6	17.0	1183.6	17.0	87.7
H14-007_27May2015-Spot 75	56	44661	2.6	13.0086	1.6	2.0033	2.0	0.1890	1.2	0.61	1116.0	12.5	1116.6	13.6	1117.9	31.8	1117.9	31.8	99.8
H14-007_27May2015-Spot 76	180	84476	3.0	11.8124	1.0	2.4464	1.5	0.2096	1.2	0.77	1226.6	13.2	1256.4	11.1	1307.7	19.0	1307.7	19.0	93.8
H14-007_27May2015-Spot 77	153	106937	2.9	12.2687	1.1	2.3300	1.5	0.2073	1.0	0.74	1010.7	12.8	1029.1	12.1	1068.6	25.4	1068.6	25.4	94.6
H14-007_27May2015-Spot 78	440	168543	2.3	13.3325	1.3	1.7554	1.9	0.1697	1.4	0.74	1010.7	12.8	1029.1	12.1	1068.6	25.4	1068.6	25.4	94.6
H14-007_27May2015-Spot 79	161	85939	1.1	12.0915	0.8	2.3639	1.8	0.2073	1.6	0.89	1214.5	17.8	1231.8	12.9	1262.2	16.3	1262.2	16.3	96.2
H14-007_27May2015-Spot 80	774	52447	3.7	12.7356	1.1	2.0719	1.5	0.1914	1.1	0.72	1128.8	11.4	1139.6	10.5	1160.0	21.0	1160.0	21.0	97.3
H14-007_27May2015-Spot 81	829	81116	5.7	13.2052	0.8	1.8862	1.6	0.1806	1.4	0.86	1070.5	13.4	1076.2	10.6	1087.9	16.5	1087.9	16.5	98.4
H14-007_27May2015-Spot 82	896	111961	4.8	12.8159	1.0	1.9320	1.8	0.1796	1.4	0.82	1064.7	14.2	1092.2	11.9	1147.6	20.3	1147.6	20.3	92.8
H14-007_27May2015-Spot 83	59	96728	1.2	13.2505	1.8	1.7669	2.2	0.1698	1.3	0.58	1011.0	12.2	1033.4	14.6	1081.0	36.6	1081.0	36.6	93.5
H14-007_27May2015-Spot 84	422	110745	2.6	12.5249	1.0	2.2008	1.8	0.1999	1.5	0.82	1174.9	15.7	1181.3	12.4	1193.1	19.9	1193.1	19.9	98.5
H14-007_27May2015-Spot 85	320	137590	2.9	12.8556	0.9	2.0519	1.6	0.1913	1.3	0.81	1128.5	13.2	1132.9	10.7	1141.4	18.4	1141.4	18.4	97.4
H14-007_27May2015-Spot 86	110	1950714	2.4	12.5031	1.5	2.1839	1.6	0.1980	1.1	0.61	1164.8	12.0	1175.9	12.8	1196.5	28.8	1196.5	28.8	98.9
H14-007_27May2015-Spot 87	90	91119	2.2	12.4260	1.3	2.1705	1.7	0.1956	1.2	0.68	1151.7	12.5	1171.6	12.0	1208.7	24.8	1208.7	24.8	95.3
H14-007_27May2015-Spot 88	155	195062	3.0	13.3046	1.2	1.5813	1.8	0.1526	1.3	0.73	915.4	11.1	962.9	11.1	1072.8	24.5	1072.8	24.5	85.3
H14-007_27May2015-Spot 89	299	226233	4.8	13.1826	1.1	1.9169	1.9	0.1833	1.5	0.79	1084.8	14.5	1087.0	12.4	1091.3	23.0	1091.3	23.0	99.4
H14-007_27May2015-Spot 90	215	194205	2.5	12.5113	1.2	2.1501	1.6	0.1631	1.0	0.63	1149.0	10.3	1165.1	10.8	1195.2	24.0	1195.2	24.0	96.1
H14-007_27May2015-Spot 91	104	253514	2.3	12.8306	1.3	2.2904	2.1	0.2040	1.6	0.78	1197.0	17.9	1209.3	14.8	1231.5	25.5	1231.5	25.5	97.2
H14-007_27May2015-Spot 92	485	182627	2.4	10.8853	1.0	3.0992	1.7	0.2447	1.4	0.82	1411.0	17.5	1432.5	12.9	1464.6	18.4	1464.6	18.4	96.3
H14-007_27May2015-Spot 93	161	229072	3.9	12.8306	1.3	1.9830	1.4	0.1845	1.3	0.73	1091.7	13.5	1109.7	12.5	1145.3	25.2	1145.3	25.2	95.3
H14-007_27May2015-Spot 94	120	71468	1.3	13.0024	1.0	2.0034	1.8	0.1886	1.0	0.70	1114.0	9.8	1115.7	9.3	1118.8	19.7	1118.8	19.7	99.6
H14-007_27May2015-Spot 95	676	205156	2.4	12.7911	1.0	2.0375	1.5	0.1890	1.1	0.75	1116.1	11.4	1128.1	10.1	1151.4	19.6	1151.4	19.6	96.9
H14-007_27May2015-Spot 96	116	84595	1.0	12.6739	1.4	2.1794	1.9	0.2003	1.3	0.67	1177.1	13.5	1174.5	13.0	1169.7	27.3	1169.7	27.3	100.6

Appendix C: LA-ICPMS U-Pb Zircon Geochronology (continued)

Analysis	U (ppm)	206Pb/204Pb	U/Th	206Pb*/207Pb*	± (%)	Isotope ratios				Apparent ages (Ma)				± (Ma)	Best age (Ma)	± (Ma)	Conc (%)		
						207Pb*/235U*	± (%)	206Pb*/238U	± (%)	207Pb*/235U	± (Ma)	206Pb*/207Pb*	± (Ma)						
						error corr.	± (%)	error corr.	± (%)	± (Ma)	± (Ma)	± (Ma)	± (Ma)						
H14-007_27May2015-Spot 101	637	1372086	4.0	12.3432	1.0	2.2445	1.7	0.2009	1.4	0.81	1180.3	14.6	1195.1	11.8	1221.8	19.3	1221.8	19.3	96.6
H14-007_27May2015-Spot 102	497	57880	4.7	12.6763	0.7	2.1402	1.3	0.1968	1.1	0.83	1157.9	11.2	1161.9	8.7	1169.3	13.8	1169.3	13.8	99.0
H14-007_27May2015-Spot 103	38	85381	1.7	12.8456	2.1	2.1468	2.8	0.2000	1.9	0.67	1175.4	20.2	1164.0	19.5	1043.0	41.6	1143.0	41.6	102.8
H14-007_27May2015-Spot 104	601	215979	7.1	13.4611	0.8	1.6656	1.5	0.1626	1.3	0.84	971.3	11.7	995.5	9.8	1049.3	16.9	1049.3	16.9	92.6
H14-007_27May2015-Spot 105	296	56497	1.2	13.4429	1.0	1.8874	1.8	0.1840	1.4	0.81	1088.9	14.5	1076.7	11.8	1052.1	20.9	1052.1	20.9	103.5
H14-007_27May2015-Spot 106	56	49653	2.5	14.2343	2.5	1.4393	2.9	0.1486	1.3	0.47	893.1	11.2	905.4	17.3	935.7	52.2	935.7	52.2	95.4
H14-007_27May2015-Spot 107	89	77437	2.8	12.7157	1.3	2.0965	1.9	0.1933	1.4	0.73	1139.5	14.7	1147.7	13.3	1163.1	26.2	1163.1	26.2	98.0
H14-007_27May2015-Spot 108	258	103957	3.8	12.8338	0.8	2.1799	1.3	0.2029	1.0	0.77	1190.9	10.8	1174.6	8.9	1144.8	16.1	1144.8	16.1	104.0
H14-007_27May2015-Spot 109	133	86586	1.3	13.6933	1.1	1.7420	1.7	0.1730	1.2	0.74	1028.7	11.8	1024.2	10.8	1014.7	22.5	1014.7	22.5	101.4
H14-007_27May2015-Spot 110	220	71868	1.0	12.2437	1.0	2.3395	1.4	0.2077	1.0	0.69	1216.8	10.8	1224.4	10.0	1237.7	19.8	1237.7	19.8	98.3
H14-007_27May2015-Spot 111	336	53646	2.4	13.7276	1.0	1.6116	1.6	0.1605	1.3	0.79	959.3	11.4	974.7	10.1	1009.6	20.1	1009.6	20.1	95.0
H14-007_27May2015-Spot 112	179	57742	3.6	12.1777	1.2	2.3357	1.8	0.2063	1.3	0.75	1209.0	14.7	1233.2	12.7	1248.3	23.1	1248.3	23.1	96.9
H14-007_27May2015-Spot 114	771	474139	1.3	13.1164	0.6	1.8706	1.7	0.1780	1.6	0.93	1055.8	15.5	1070.8	11.3	1101.4	12.4	1101.4	12.4	95.9
H14-007_27May2015-Spot 115	532	187240	5.4	13.5873	1.1	1.7108	2.0	0.1686	1.6	0.81	1004.3	14.8	1012.6	12.6	1030.4	23.2	1030.4	23.2	97.5
H14-007_27May2015-Spot 116	517	57408	1.6	12.8612	1.1	1.9498	1.9	0.1819	1.5	0.79	1077.2	14.7	1098.4	12.5	1140.6	22.7	1140.6	22.7	94.4
H14-007_27May2015-Spot 117	53	43114	1.9	13.3790	2.1	1.7989	2.5	0.1746	1.3	0.54	1037.2	12.8	1045.1	16.1	1061.6	41.7	1061.6	41.7	97.7
H14-007_27May2015-Spot 118	705	144975	5.5	13.1717	1.1	1.7355	1.7	0.1658	1.3	0.77	988.9	11.7	1021.8	10.7	1093.0	21.1	1093.0	21.1	90.5
H14-007_27May2015-Spot 119	292	57466	5.2	12.5513	0.9	2.2737	1.5	0.2070	1.2	0.80	1212.7	13.3	1204.1	10.5	1188.9	17.6	1188.9	17.6	102.0
H14-007_27May2015-Spot 120	537	220775	4.2	13.2371	0.9	1.8905	1.5	0.1815	1.2	0.82	1075.2	11.9	1077.8	9.8	1083.0	17.1	1083.0	17.1	99.3
H14-007_27May2015-Spot 121	304	245623	1.6	11.8334	1.1	2.5221	1.9	0.2165	1.5	0.80	1263.1	17.2	1278.4	13.7	1304.2	22.1	1304.2	22.1	96.8
H14-007_27May2015-Spot 122	368	573030	2.2	12.9726	1.2	2.0099	1.8	0.1891	1.4	0.77	1116.5	14.3	1118.9	12.3	1123.4	23.2	1123.4	23.2	99.4
H14-007_27May2015-Spot 123	235	118909	3.2	13.0922	1.2	1.9389	1.9	0.1841	1.5	0.78	1089.3	14.9	1094.6	12.8	1105.1	23.8	1105.1	23.8	94.6
H14-007_27May2015-Spot 124	115	142195	2.2	13.3894	1.5	1.7248	1.9	0.1675	1.3	0.65	998.3	11.7	1017.8	12.5	1060.1	29.9	1060.1	29.9	94.2
H14-007_27May2015-Spot 125	222	169515	2.3	12.4434	1.0	2.0842	1.7	0.1881	1.4	0.79	1111.1	13.9	1143.6	11.8	1205.9	20.6	1205.9	20.6	92.1
H14-007_27May2015-Spot 126	279	572095	2.2	12.9151	0.9	2.0450	1.4	0.1915	1.1	0.79	1129.8	11.7	1130.6	9.8	1132.3	17.5	1132.3	17.5	99.8
H14-007_27May2015-Spot 127	448	168643	2.7	12.6439	0.8	2.1546	1.4	0.1976	1.2	0.82	1162.3	18.8	1166.5	9.8	1174.4	15.9	1174.4	15.9	99.0
H14-007_27May2015-Spot 128	352	56489	7.3	11.6365	1.4	2.6450	2.1	0.2232	1.6	0.75	1298.9	18.8	1313.2	15.7	1336.7	27.2	1336.7	27.2	97.2
H14-007_27May2015-Spot 129	383	205738	5.7	12.0671	1.1	2.0756	2.3	0.1817	2.0	0.88	1076.0	20.3	1140.8	15.9	1266.1	21.7	1266.1	21.7	85.0
H14-007_27May2015-Spot 130	127	57281	2.4	11.8429	1.4	2.6490	2.1	0.2275	1.6	0.75	1321.5	19.0	1314.4	15.7	1302.7	27.6	1302.7	27.6	101.4
H14-007_27May2015-Spot 131	374	85738	2.1	13.9491	1.2	1.5272	1.7	0.1545	1.3	0.73	926.2	10.8	941.4	10.5	977.1	23.9	977.1	23.9	94.8
H14-007_27May2015-Spot 133	90	58750	1.0	11.0788	1.2	2.5612	1.8	0.2058	1.4	0.78	1206.4	15.8	1289.6	13.5	1431.1	22.2	1431.1	22.2	84.3
H14-007_27May2015-Spot 134	252	160456	2.3	13.4258	0.9	1.7677	1.3	0.1721	1.0	0.76	1023.8	9.5	1033.7	8.5	1054.6	17.2	1054.6	17.2	97.1
H14-007_27May2015-Spot 135	49	30089	1.1	12.5101	1.5	2.1686	3.0	0.1968	2.6	0.86	1157.9	27.7	1171.0	21.0	1195.4	30.2	1195.4	30.2	96.9
H14-007_27May2015-Spot 136	3174	267114	44.9	14.2430	0.7	1.2839	1.3	0.1326	1.1	0.83	802.8	8.3	838.6	7.6	934.5	15.2	802.8	8.3	85.9
H14-007_27May2015-Spot 137	216	62633	1.3	12.0184	1.2	2.2320	1.9	0.1946	1.4	0.76	1146.0	14.8	1191.1	13.1	1274.1	23.8	1274.1	23.8	89.9
H14-007_27May2015-Spot 138	1016	182998	2.5	12.8260	0.9	1.8167	1.3	0.1690	0.9	0.72	1006.6	8.7	1051.5	8.5	1146.0	17.7	1146.0	17.7	87.8
H14-007_27May2015-Spot 139	778	157632	5.2	12.9090	0.7	1.9176	1.3	0.1795	1.0	0.82	1064.4	10.3	1087.2	8.5	1133.2	14.5	1133.2	14.5	93.9
H14-007_27May2015-Spot 140	84	141887	1.0	13.0924	1.2	1.9096	1.9	0.1813	1.4	0.76	1074.2	14.2	1084.5	12.6	1105.0	24.6	1105.0	24.6	97.2
H14-007_27May2015-Spot 141	189	80560	2.8	13.5840	0.9	1.8443	1.5	0.1817	1.1	0.78	1076.3	11.3	1061.4	9.6	1030.9	18.4	1030.9	18.4	104.4
H14-007_27May2015-Spot 142	137	451615	3.4	13.7104	1.4	1.6711	1.9	0.1662	1.4	0.70	991.0	12.5	997.6	12.4	1012.2	28.2	1012.2	28.2	97.9
H14-007_27May2015-Spot 143	493	292062	1.3	12.7244	0.8	2.1159	1.3	0.1953	1.0	0.77	1149.9	10.6	1154.0	9.0	1161.8	16.5	1161.8	16.5	99.0
H14-007_27May2015-Spot 144	367	233562	1.6	9.8381	0.9	3.8835	1.9	0.2771	1.7	0.88	1576.7	24.1	1610.3	15.7	1654.4	16.9	1654.4	16.9	95.3
H14-007_27May2015-Spot 145	333	85683	3.4	12.7253	1.0	2.1139	1.5	0.1951	1.1	0.74	1148.9	11.4	1153.3	10.0	1161.6	19.3	1161.6	19.3	98.9
H14-007_27May2015-Spot 146	80	387731	2.4	12.4425	1.4	2.3048	1.9	0.2080	1.3	0.66	1218.1	13.9	1213.8	13.4	1206.1	28.0	1206.1	28.0	101.0
H14-007_27May2015-Spot 148	203	239384	1.8	10.7159	0.9	3.3503	1.4	0.2604	1.1	0.75	1491.8	14.1	1492.9	11.0	1494.4	17.6	1494.4	17.6	99.8
H14-007_27May2015-Spot 149	638	52677	4.2	13.4294	1.2	1.7787	1.6	0.1732	1.2	0.71	1030.0	11.1	1037.7	10.6	1054.1	23.2	1054.1	23.2	97.7

Appendix C: LA-ICPMS U-Pb Zircon Geochronology (continued)

Analysis	U (ppm)	206Pb/204Pb	U/Th	206Pb*/207Pb*	± (%)	Isotope ratios						Apparent ages (Ma)						Conc (%)	
						207Pb*/235U*	± (%)	206Pb*/238U	± (%)	206Pb*/238U*	error corr.	207Pb*/235U	± (Ma)	206Pb*/207Pb*	± (Ma)	Best age (Ma)	± (Ma)		
						207Pb*/235U*	± (%)	206Pb*/238U	± (%)	206Pb*/238U*	error corr.	207Pb*/235U	± (Ma)	206Pb*/207Pb*	± (Ma)	Best age (Ma)	± (Ma)		
H14-007_27May2015-Spot 150	652	508318	11.4	12.9478	0.7	1.9186	1.4	0.1802	1.2	1067.9	12.2	1087.6	9.5	1127.2	13.8	1127.2	13.8	94.7	
H14-007_27May2015-Spot 151	27	21214	7.0	13.8184	2.6	1.6480	3.1	0.1652	1.6	985.4	15.0	988.8	19.4	996.3	52.7	996.3	52.7	98.9	
H14-007_27May2015-Spot 153	692	215893	25.2	13.3926	0.9	1.6867	1.4	0.1638	1.1	978.0	10.3	1003.5	9.1	1059.6	17.2	1059.6	17.2	92.3	
H14-007_27May2015-Spot 154	287	57515	4.3	12.4479	1.0	2.2259	1.5	0.2010	1.1	0.76	1180.5	12.4	1189.2	10.6	1205.2	19.2	1205.2	19.2	97.9
H14-007_27May2015-Spot 155	415	467233	1.8	9.4533	0.8	4.3768	1.1	0.3001	0.8	0.72	1691.7	12.0	1708.0	9.3	1727.9	14.4	1727.9	14.4	97.9
H14-007_27May2015-Spot 156	96	73255	2.0	12.6418	1.7	2.1591	2.1	0.1980	1.3	0.61	1164.4	13.7	1168.0	14.6	1174.7	33.0	1174.7	33.0	99.1
H14-007_27May2015-Spot 158	578	244555	3.6	13.6208	1.2	1.7509	1.8	0.1730	1.4	0.77	1028.5	13.2	1027.5	11.7	1025.5	23.5	1025.5	23.5	100.3
H14-007_27May2015-Spot 159	131	69333	2.6	12.9942	1.5	1.7762	2.0	0.1674	1.4	0.69	997.7	13.1	1036.8	13.3	1120.1	29.4	1120.1	29.4	89.1
H14-007_27May2015-Spot 160	564	51680	8.2	12.3163	0.9	2.0510	1.4	0.1832	1.1	0.79	1084.5	11.2	1132.6	9.7	1226.1	17.2	1226.1	17.2	88.4
H14-007_27May2015-Spot 161	90	106542	1.6	12.9105	1.5	1.9833	2.0	0.1857	1.4	0.68	1098.1	14.0	1109.9	13.8	1132.9	29.8	1132.9	29.8	96.9
H14-007_27May2015-Spot 163	1299	123458	6.0	12.5195	1.4	2.1281	1.9	0.1932	1.2	0.67	1138.9	12.9	1158.0	12.8	1193.9	27.2	1193.9	27.2	95.4
H14-007_27May2015-Spot 164	207	180576	3.6	13.6500	1.2	1.7429	1.9	0.1725	1.5	0.78	1026.1	14.1	1024.5	12.3	1021.1	24.3	1021.1	24.3	100.5
H14-007_27May2015-Spot 165	467	121307	1.3	12.2778	1.1	2.3707	1.4	0.2111	1.0	0.67	1234.7	10.7	1233.8	10.2	1232.3	20.9	1232.3	20.9	100.2
H14-007_27May2015-Spot 166	1125	256861	27.6	13.3279	0.9	1.6831	1.5	0.1627	1.2	0.80	971.7	10.6	1002.1	9.5	1069.3	18.1	1069.3	18.1	90.9
H14-007_27May2015-Spot 167	143	34281	2.0	13.9695	1.7	1.4023	2.9	0.1421	2.3	0.81	856.4	18.5	889.9	16.9	974.1	34.1	974.1	34.1	87.9
H14-007_27May2015-Spot 168	616	66143	3.2	11.0021	1.1	2.8324	1.4	0.2260	0.9	0.65	1313.6	10.9	1364.2	10.6	1444.3	20.5	1444.3	20.5	90.9
H14-007_27May2015-Spot 169	887	75856	1.7	12.7005	0.8	2.0589	1.4	0.1897	1.2	0.84	1119.5	12.4	1135.3	9.9	1165.5	15.5	1165.5	15.5	96.1
H14-007_27May2015-Spot 171	398	419444	3.2	13.8363	0.8	1.6944	1.4	0.1700	1.1	0.79	1012.3	10.2	1006.4	8.8	993.6	17.2	993.6	17.2	101.9
H14-007_27May2015-Spot 172	902	245466	4.4	14.2636	1.0	1.2216	1.7	0.1264	1.4	0.79	767.1	9.8	810.5	9.6	931.5	21.3	767.1	21.3	82.4
H14-007_27May2015-Spot 173	188	99036	4.9	12.7200	0.8	2.2027	1.6	0.2032	1.3	0.85	1192.5	14.3	1181.9	10.8	1162.5	16.2	1162.5	16.2	102.6
H14-007_27May2015-Spot 174	253	162953	2.6	13.1355	1.3	1.8375	1.7	0.1750	1.1	0.64	1039.9	10.3	1059.0	11.0	1098.5	25.9	1098.5	25.9	94.7
H14-007_27May2015-Spot 175	328	209590	3.0	13.5519	1.2	1.7249	1.8	0.1697	1.4	0.76	1010.3	12.9	1017.9	11.6	1034.2	23.6	1034.2	23.6	97.7
H14-007_27May2015-Spot 176	806	64791	13.6	12.6991	0.9	1.8120	1.5	0.1669	1.2	0.79	994.9	10.9	1049.8	9.7	1165.7	17.9	1165.7	17.9	85.3
H14-007_27May2015-Spot 177	352	114285	7.4	13.6813	1.1	1.7550	1.6	0.1741	1.3	0.76	1034.9	12.0	1029.0	10.6	1016.5	21.5	1016.5	21.5	101.8
H14-007_27May2015-Spot 178	33	31113	1.0	13.6111	2.2	1.7282	2.7	0.1704	1.5	0.56	1014.3	14.2	1018.3	17.3	1026.9	44.9	1026.9	44.9	98.8
H14-007_27May2015-Spot 180	108	63403	2.0	12.7075	1.4	2.1674	1.5	0.2007	1.0	0.71	1178.9	11.1	1170.7	10.1	1155.3	20.2	1155.3	20.2	102.0
H14-007_27May2015-Spot 181	114	76596	1.0	13.5852	1.2	1.7471	1.8	0.1721	1.4	0.76	1023.9	12.8	1026.1	11.5	1030.8	23.5	1030.8	23.5	99.3
H14-007_27May2015-Spot 183	335	146187	1.3	11.6120	1.0	2.6588	1.5	0.2239	1.1	0.76	1302.6	13.5	1317.1	11.1	1340.8	19.1	1340.8	19.1	97.1
H14-007_27May2015-Spot 184	336	164934	6.9	13.7728	1.0	1.5555	1.7	0.1554	1.4	0.80	931.1	12.1	952.7	10.8	1003.0	21.0	1003.0	21.0	92.8
H14-007_27May2015-Spot 185	107	204209	2.1	13.7853	1.6	1.6304	2.0	0.1630	1.2	0.61	973.5	10.8	982.0	12.3	1001.1	31.5	1001.1	31.5	97.2
H14-007_27May2015-Spot 186	127	943345	2.6	12.9221	1.1	2.0032	1.6	0.1877	1.1	0.70	1109.1	11.0	1116.6	10.5	1131.2	22.2	1131.2	22.2	98.0
H14-007_27May2015-Spot 187	282	227854	2.3	13.3671	0.9	1.8528	1.4	0.1796	1.2	0.80	1064.9	11.3	1064.4	9.5	1063.4	17.1	1063.4	17.1	100.1
H14-007_27May2015-Spot 188	197	164162	2.3	12.8744	0.9	2.0329	1.6	0.1898	1.4	0.83	1120.4	13.9	1126.6	11.0	1138.6	17.7	1138.6	17.7	98.4
H14-007_27May2015-Spot 189	97	51448	1.8	11.9765	1.4	2.5462	1.8	0.2212	1.2	0.64	1280.0	13.6	1285.3	13.2	1280.8	27.2	1280.8	27.2	100.6
H14-007_27May2015-Spot 190	121	71599	2.2	11.9673	1.1	2.4444	1.9	0.2122	1.5	0.82	1240.3	17.4	1255.8	13.6	1282.3	21.0	1282.3	21.0	96.7
H14-007_27May2015-Spot 191	627	52363	5.3	10.9999	1.0	1.9665	1.6	0.1816	1.3	0.77	1075.9	12.5	1104.1	11.0	1160.2	20.6	1160.2	20.6	92.7
H14-007_27May2015-Spot 192	490	77208	2.4	10.9999	1.0	3.0421	1.7	0.2427	1.3	0.79	1400.7	16.5	1418.3	12.7	1444.7	19.4	1444.7	19.4	97.0
H14-007_27May2015-Spot 193	111	36814	2.5	13.9202	1.2	1.7076	1.8	0.1724	1.4	0.75	1025.3	13.1	1011.4	11.7	981.4	24.5	981.4	24.5	104.5
H14-007_27May2015-Spot 194	361	83304	3.4	12.4362	0.9	2.3223	1.2	0.2095	0.8	0.68	1225.9	9.4	1219.1	8.8	1207.1	18.0	1207.1	18.0	101.6
H14-007_27May2015-Spot 196	970	63028	13.8	11.9257	0.9	2.1520	1.5	0.1861	1.2	0.80	1100.4	12.4	1165.7	10.6	1289.1	17.7	1289.1	17.7	85.4
H14-007_27May2015-Spot 197	128	249174	2.4	13.4611	1.3	1.8303	2.1	0.1787	1.6	0.79	1059.8	15.8	1056.4	13.5	1049.3	25.5	1049.3	25.5	101.0
H14-007_27May2015-Spot 200	560	151541	9.7	12.4367	0.9	2.3108	1.6	0.2056	1.3	0.81	1205.4	14.6	1215.6	11.6	1233.8	18.5	1233.8	18.5	97.7
H14-007_27May2015-Spot 201	199	217542	4.7	12.4333	1.0	2.2363	1.6	0.2017	1.2	0.78	1184.6	13.4	1192.5	11.1	1206.9	19.6	1206.9	19.6	98.2
H14-007_27May2015-Spot 202	311	145432	5.0	12.7624	0.8	2.0005	1.5	0.1852	1.3	0.83	1095.1	12.6	1115.7	10.2	1155.9	16.5	1155.9	16.5	94.7
H14-007_27May2015-Spot 203	321	240798	2.6	12.2560	1.1	2.2282	1.7	0.1981	1.3	0.76	1164.9	13.4	1190.0	11.6	1235.8	21.3	1235.8	21.3	94.3

Appendix C: LA-ICPMS U-Pb Zircon Geochronology (continued)

Analysis	U (ppm)	206Pb/204Pb	U/Th	206Pb*/207Pb*	± (%)	Isotope ratios						Apparent ages (Ma)						Conc (%)	
						206Pb*/207Pb*	± (%)	207Pb*/235U*	± (%)	206Pb*/238U*	error corr.	± (Ma)	207Pb*/238U	± (Ma)	206Pb*/207Pb*	± (Ma)	Best age (Ma)		± (Ma)
H14-007_27May2015-Spot 204	570	85671	24.8	13.3417	0.7	1.7643	1.3	0.1707	1.2	0.87	1016.1	10.9	1032.4	8.7	1067.3	13.3	1067.3	13.3	95.2
H14-007_27May2015-Spot 205	638	108397	4.7	13.7129	0.8	1.6239	1.4	0.1615	1.1	0.82	965.2	10.3	979.5	8.8	1011.8	16.2	1011.8	16.2	95.4
H14-007_27May2015-Spot 206	327	132189	2.0	13.0353	1.1	1.9316	1.7	0.1826	1.3	0.76	1081.2	13.1	1092.1	11.6	1113.8	22.6	1113.8	22.6	97.1
H14-007_27May2015-Spot 207	152	100426	8.6	15.9799	2.3	0.8448	3.1	0.0979	2.0	0.65	602.2	11.4	621.8	14.2	694.0	49.5	602.2	11.4	86.8
H14-007_27May2015-Spot 208	98	79838	1.3	9.8761	1.0	4.0151	1.6	0.2876	1.2	0.76	1629.5	17.2	1637.3	12.8	1647.2	19.1	1647.2	19.1	98.9
H14-007_27May2015-Spot 209	1240	155502	8.3	13.1771	1.0	1.8099	1.6	0.1730	1.3	0.80	1028.5	12.5	1049.0	10.7	1092.1	19.5	1092.1	19.5	94.2
H14-007_27May2015-Spot 210	534	206501	1.2	9.3567	0.9	4.3884	1.6	0.2978	1.3	0.82	1680.4	19.6	1710.1	13.4	1746.8	16.8	1746.8	16.8	96.2
H14-007_27May2015-Spot 212	213	401096	2.8	12.7774	1.0	2.1421	1.4	0.1985	1.1	0.75	1167.3	11.6	1162.5	10.0	1153.5	19.1	1153.5	19.1	101.2
H14-007_27May2015-Spot 213	132	108937	1.9	13.3653	1.1	1.8319	1.6	0.1776	1.1	0.69	1053.7	10.6	1057.0	10.3	1063.7	22.8	1063.7	22.8	99.1
H14-007_27May2015-Spot 214	760	1306613	5.9	13.4802	0.9	1.7463	1.9	0.1707	1.7	0.87	1016.1	15.5	1025.8	12.2	1046.5	18.7	1046.5	18.7	97.1
H14-007_27May2015-Spot 215	291	101903	3.9	13.4641	1.3	1.7647	2.5	0.1723	2.1	0.84	1024.9	19.7	1032.6	16.1	1048.9	27.2	1048.9	27.2	97.7
H14-007_27May2015-Spot 216	144	108054	2.3	12.4706	1.0	2.1796	1.4	0.1971	1.0	0.71	1159.9	10.2	1174.5	9.5	1201.6	19.0	1201.6	19.0	96.5
H14-007_27May2015-Spot 217	163	149636	1.7	13.4752	1.1	1.7882	1.7	0.1748	1.3	0.76	1038.3	12.6	1041.2	11.3	1047.2	22.8	1047.2	22.8	99.1
H14-007_27May2015-Spot 219	146	102758	1.9	11.7466	1.2	2.6968	1.8	0.2298	1.3	0.73	1333.2	15.4	1327.6	13.0	1318.5	23.2	1318.5	23.2	101.1
H14-007_27May2015-Spot 220	173	79010	2.7	13.7239	1.0	1.6826	1.6	0.1675	1.3	0.80	998.2	11.9	1002.0	10.3	1010.2	19.7	1010.2	19.7	98.8
H14-007_27May2015-Spot 221	168	169525	1.9	12.5697	1.4	2.1193	1.9	0.1932	1.3	0.70	1138.7	14.0	1155.1	13.3	1186.0	27.3	1186.0	27.3	96.0
H14-007_27May2015-Spot 222	838	185731	2.3	12.8249	1.1	1.8015	1.8	0.1676	1.5	0.81	998.7	13.6	1046.0	11.9	1146.2	21.5	1146.2	21.5	87.1
H14-007_27May2015-Spot 223	527	121287	1.8	15.2820	1.1	1.1351	2.0	0.1258	1.7	0.84	763.9	12.1	773.0	10.8	788.4	22.9	763.9	12.1	96.9
H14-007_27May2015-Spot 224	233	108869	2.6	12.5709	1.0	2.1774	1.6	0.1985	1.3	0.79	1167.3	13.4	1173.8	11.1	1185.8	19.2	1185.8	19.2	98.4
H14-007_27May2015-Spot 225	397	70669	2.4	12.0598	1.1	2.4242	1.7	0.2120	1.2	0.74	1239.7	13.9	1249.8	11.9	1267.4	21.7	1267.4	21.7	97.8
H14-007_27May2015-Spot 226	149	168201	2.3	8.8581	0.9	4.9593	1.5	0.3186	1.2	0.81	1782.9	19.3	1812.4	13.0	1846.5	16.4	1846.5	16.4	96.6
H14-007_27May2015-Spot 227	537	90623	4.6	12.3623	0.9	2.2532	1.4	0.2020	1.1	0.79	1186.2	12.2	1197.8	10.1	1218.8	17.5	1218.8	17.5	97.3
H14-007_27May2015-Spot 228	210	97117	1.8	12.7311	1.1	2.1273	1.7	0.1964	1.3	0.78	1156.1	14.2	1157.7	11.9	1160.8	21.4	1160.8	21.4	99.6
H14-007_27May2015-Spot 229	1953	217376	4.1	13.2241	0.9	1.8542	1.4	0.1778	1.1	0.79	1055.2	10.6	1064.9	9.1	1085.0	17.2	1085.0	17.2	97.2
H14-007_27May2015-Spot 230	1104	132695	2.8	11.4337	0.7	2.4657	1.5	0.2045	1.3	0.89	1199.3	14.7	1262.0	10.9	1370.7	13.3	1370.7	13.3	87.5
H14-007_27May2015-Spot 231	224	197052	2.1	12.0454	1.1	2.4190	1.8	0.2113	1.4	0.77	1235.9	15.2	1248.3	12.6	1269.7	21.8	1269.7	21.8	97.3
H14-007_27May2015-Spot 232	234	928373	2.4	13.5902	1.4	1.5129	2.1	0.1491	1.6	0.75	896.0	13.1	935.6	12.8	1030.0	28.1	1030.0	28.1	87.0
H14-007_27May2015-Spot 234	266	119172	2.3	12.3210	0.8	2.3056	1.2	0.2060	0.9	0.74	1207.6	9.6	1214.0	8.3	1225.4	15.5	1225.4	15.5	98.6
H14-007_27May2015-Spot 235	127	1683383	2.6	12.7101	1.1	2.1664	1.8	0.1997	1.4	0.78	1173.7	15.1	1170.3	12.6	1164.0	22.7	1164.0	22.7	100.8
H14-007_27May2015-Spot 236	895	65377	2.4	13.0535	0.9	1.7569	1.6	0.1663	1.3	0.83	991.8	11.9	1029.7	10.1	1111.0	17.4	1111.0	17.4	89.3
H14-007_27May2015-Spot 237	820	72301	6.4	12.3666	1.1	2.1036	1.8	0.1887	1.5	0.81	1114.2	14.8	1150.0	12.4	1218.1	20.9	1218.1	20.9	91.5
H14-007_27May2015-Spot 238	136	91230	2.9	12.3244	1.3	2.2755	1.9	0.2034	1.4	0.73	1193.6	15.3	1204.7	13.7	1224.8	26.2	1224.8	26.2	97.4
H14-007_27May2015-Spot 239	1640	132086	18.4	13.7792	0.8	1.4895	1.3	0.1489	1.0	0.78	894.6	8.3	926.1	7.8	1002.0	16.4	1002.0	16.4	89.3
H14-007_27May2015-Spot 240	621	97952	3.6	13.1287	1.0	1.7282	1.6	0.1646	1.3	0.78	982.1	11.5	1019.1	10.3	1099.5	19.9	1099.5	19.9	89.3
H14-007_27May2015-Spot 241	107	49686	2.2	12.4285	1.5	2.2995	2.0	0.2073	1.3	0.66	1214.3	14.3	1212.1	13.9	1208.3	29.3	1208.3	29.3	100.5
H14-007_27May2015-Spot 242	938	303444	1.6	12.7565	0.8	2.0257	1.3	0.1874	1.1	0.80	1107.4	10.9	1124.2	9.1	1156.8	15.8	1156.8	15.8	95.7
H14-007_27May2015-Spot 243	146	105507	2.0	12.6719	1.1	2.1657	1.6	0.1990	1.2	0.72	1170.1	12.4	1170.1	11.3	1170.0	22.4	1170.0	22.4	100.0
H14-007_27May2015-Spot 244	393	65496	9.2	13.7262	0.8	1.6806	1.4	0.1673	1.1	0.79	997.2	10.0	1001.2	8.7	1009.9	17.0	1009.9	17.0	98.8
H14-007_27May2015-Spot 245	256	84681	3.6	12.4514	1.1	2.0623	1.9	0.1862	1.6	0.83	1101.0	16.1	1136.4	13.1	1204.6	21.1	1204.6	21.1	91.4
H14-007_27May2015-Spot 247	388	78470	2.5	12.7438	1.2	2.1508	1.7	0.1988	1.2	0.69	1168.8	12.7	1165.3	11.9	1158.8	24.5	1158.8	24.5	100.9
H14-007_27May2015-Spot 248	569	78731	5.1	13.7207	0.9	1.6385	1.2	0.1630	0.8	0.67	973.7	7.5	985.1	7.7	1010.7	18.3	1010.7	18.3	96.3
H14-007_27May2015-Spot 249	179	169164	3.4	12.4262	1.0	2.0212	1.7	0.1822	1.4	0.80	1078.8	13.6	1122.7	11.6	1208.7	20.4	1208.7	20.4	89.3
H14-007_27May2015-Spot 250	640	58395	54.0	13.6842	1.1	1.5472	1.8	0.1543	1.4	0.79	925.2	12.3	918.4	11.2	1005.7	22.9	1005.7	22.9	92.0
H14-007_27May2015-Spot 251	1371	54709	3.7	13.6842	1.1	1.4706	1.8	0.1459	1.5	0.82	878.2	12.3	918.4	11.1	1016.1	21.3	1016.1	21.3	86.4
H14-007_27May2015-Spot 252	206	76296	3.9	11.1133	0.9	3.0335	1.6	0.2445	1.3	0.82	1410.1	16.4	1416.1	12.1	1425.1	17.4	1425.1	17.4	98.9
H14-007_27May2015-Spot 253	257	777802	1.4	13.5096	1.2	1.7958	1.6	0.1760	1.0	0.64	1044.8	9.8	1043.9	10.4	1042.0	24.8	1042.0	24.8	100.3

Appendix C: LA-ICPMS U-Pb Zircon Geochronology (continued)

Analysis	U (ppm)	206Pb/204Pb	U/Th	206Pb*/207Pb*	± (%)	Isotope ratios						Apparent ages (Ma)						Conc (%)	
						206Pb*/207Pb*	± (%)	207Pb*/235U*	± (%)	206Pb*/238U*	± (%)	207Pb*/235U*	± (%)	206Pb*/207Pb*	± (%)	Best age	± (Ma)		
						206Pb*/207Pb*	± (%)	207Pb*/235U*	± (%)	206Pb*/238U*	± (%)	207Pb*/235U*	± (%)	206Pb*/207Pb*	± (%)	(Ma)	(Ma)		
H14-007_27May2015-Spot 254	1709	95601	6.7	12.8680	0.7	1.9018	1.4	0.1775	1.2	0.87	1053.2	11.4	1081.7	9.0	1139.5	13.5	1139.5	13.5	92.4
H14-007_27May2015-Spot 255	320	72211	3.7	12.0229	1.0	2.1990	1.9	0.1917	1.6	0.84	1130.8	16.3	1180.7	13.0	1273.3	19.7	1273.3	19.7	88.8
H14-007_27May2015-Spot 256	254	55098	2.6	13.4478	1.5	1.7498	2.1	0.1707	1.5	0.71	1015.7	13.8	1027.1	13.4	1051.3	29.6	1051.3	29.6	96.6
H14-007_27May2015-Spot 257	151	231482	2.6	13.2319	1.0	1.8955	1.8	0.1820	1.5	0.81	1079.9	14.5	1079.9	11.9	1083.8	21.0	1083.8	21.0	99.5
H14-007_27May2015-Spot 258	97	52714	2.2	13.2698	1.4	1.7574	1.8	0.1691	1.2	0.63	1007.3	10.8	1029.9	11.9	1078.1	28.6	1078.1	28.6	93.4
H14-007_27May2015-Spot 259	366	59725	1.8	13.6372	1.1	1.7493	1.7	0.1730	1.3	0.75	1028.7	12.4	1026.9	11.2	1023.0	23.2	1023.0	23.2	100.6
H14-007_27May2015-Spot 260	911	113683	8.5	14.7695	0.7	1.0648	1.4	0.1141	1.2	0.86	696.3	7.9	736.2	7.4	859.6	15.2	696.3	7.9	81.0
H14-007_27May2015-Spot 261	239	161962	4.0	12.6663	0.9	2.0958	1.4	0.1925	1.2	0.80	1135.1	12.1	1147.4	9.9	1170.9	17.0	1170.9	17.0	96.9
H14-007_27May2015-Spot 262	200	206858	2.8	12.6978	1.2	1.8472	2.5	0.1701	2.2	0.88	1012.7	20.4	1062.4	16.3	1165.9	23.3	1165.9	23.3	86.9
H14-007_27May2015-Spot 263	64	74451	2.7	12.1809	1.4	2.3082	1.9	0.2039	1.2	0.66	1196.3	13.6	1214.8	13.4	1247.8	28.0	1247.8	28.0	95.9
H14-007_27May2015-Spot 264	1189	97068	13.3	13.5385	0.9	1.5500	1.5	0.1522	1.3	0.82	913.2	10.8	950.5	9.5	1037.7	17.6	1037.7	17.6	88.0
H14-007_27May2015-Spot 265	422	207195	1.6	12.5622	0.9	1.2182	1.6	0.1939	1.3	0.81	1142.5	13.7	1158.0	11.2	1187.2	18.6	1187.2	18.6	96.2
H14-007_27May2015-Spot 266	109	156282	1.3	12.2966	1.3	2.2892	1.8	0.2042	1.2	0.66	1197.6	12.8	1209.0	12.5	1229.3	26.1	1229.3	26.1	97.4
H14-007_27May2015-Spot 267	415	90771	4.8	12.8750	1.1	1.7669	4.1	0.1650	4.0	0.96	984.4	36.2	1033.4	26.7	1138.5	22.7	1138.5	22.7	86.5
H14-007_27May2015-Spot 268	191	159835	3.4	13.4591	1.1	1.7538	1.5	0.1712	0.9	0.62	1018.7	8.5	1028.6	9.4	1049.6	23.1	1049.6	23.1	97.1
H14-007_27May2015-Spot 269	377	134421	1.0	12.5723	1.2	2.1937	1.8	0.2006	1.4	0.75	1178.4	14.6	1180.9	12.6	1185.6	23.5	1185.6	23.5	99.4
H14-007_27May2015-Spot 270	570	262975	2.1	13.2040	0.9	1.8809	1.5	0.1801	1.2	0.79	1067.7	11.4	1074.4	9.8	1088.1	18.3	1088.1	18.3	98.1
H14-007_27May2015-Spot 271	551	146952	15.4	13.8048	1.0	1.6644	1.7	0.1666	1.4	0.82	993.6	12.7	995.1	10.7	998.3	19.5	998.3	19.5	99.5
H14-007_27May2015-Spot 272	437	112530	0.9	12.6872	1.2	2.2541	1.6	0.2074	1.0	0.64	1215.0	11.5	1198.1	11.4	1167.6	24.6	1167.6	24.6	104.1
H14-007_27May2015-Spot 273	329	90914	1.9	12.4298	1.1	2.2597	1.6	0.2037	1.2	0.74	1195.2	13.0	1199.8	11.3	1208.1	21.2	1208.1	21.2	98.9
H14-007_27May2015-Spot 274	415	230335	2.1	12.0780	0.6	2.4624	1.1	0.2157	0.9	0.82	1259.1	10.6	1261.1	8.2	1264.4	12.6	1264.4	12.6	99.6
H14-007_27May2015-Spot 275	285	179494	3.2	12.5715	1.0	2.1818	1.5	0.1989	1.1	0.75	1169.6	11.7	1175.2	10.1	1185.7	18.9	1185.7	18.9	98.6
H14-007_27May2015-Spot 276	584	74097	2.8	13.0113	0.9	1.9935	1.7	0.1881	1.5	0.86	1111.2	14.9	1113.3	11.5	1117.5	17.4	1117.5	17.4	99.4
H14-007_27May2015-Spot 277	1143	227059	1.8	12.7660	1.1	2.0330	1.5	0.1882	1.0	0.69	1111.8	10.3	1126.6	10.0	1155.3	21.3	1155.3	21.3	96.2
H14-007_27May2015-Spot 278	294	190446	6.6	13.2938	1.1	1.9447	1.7	0.1875	1.4	0.78	1107.8	13.9	1096.6	11.7	1074.5	21.9	1074.5	21.9	103.1
H14-007_27May2015-Spot 279	226	145223	0.6	13.1926	1.1	1.9574	1.5	0.1873	1.0	0.68	1106.6	10.6	1101.0	10.2	1089.8	22.2	1089.8	22.2	101.5
H14-007_27May2015-Spot 280	589	194127	4.3	13.0176	0.9	1.7386	1.5	0.1641	1.2	0.79	979.8	10.7	1022.9	9.6	1116.5	18.3	1116.5	18.3	87.8
H14-007_27May2015-Spot 281	301	102045	2.3	12.7256	1.0	1.7812	1.7	0.1644	1.4	0.81	981.2	12.5	1038.6	11.0	1161.6	19.7	1161.6	19.7	84.5
H14-007_27May2015-Spot 282	83	155875	2.1	11.4444	1.1	3.0095	1.3	0.2433	1.3	0.78	1403.6	16.6	1410.0	12.9	1419.8	20.3	1419.8	20.3	98.9
H14-007_27May2015-Spot 283	87	58020	1.9	13.2348	1.5	1.9454	1.7	0.1867	0.9	0.53	1103.7	9.4	1096.9	11.7	1083.4	29.5	1083.4	29.5	101.9
H14-007_27May2015-Spot 284	692	289171	11.7	16.1731	1.0	0.8115	1.8	0.0952	1.5	0.83	586.1	8.5	603.3	8.4	668.3	22.1	586.1	8.5	87.7
H14-007_27May2015-Spot 285	144	258742	2.9	12.5280	1.0	2.2116	1.7	0.2010	1.4	0.82	1180.4	15.2	1184.7	11.9	1192.6	19.2	1192.6	19.2	99.0
H14-007_27May2015-Spot 286	565	162006	2.0	13.0244	1.1	2.0028	1.8	0.1892	1.4	0.77	1117.0	14.1	1116.5	12.0	1115.4	22.5	1115.4	22.5	100.1
H14-007_27May2015-Spot 287	794	106476	7.1	13.8167	0.9	1.5699	1.3	0.1573	1.0	0.74	941.8	8.7	958.4	8.3	996.5	18.1	996.5	18.1	94.5
H14-007_27May2015-Spot 288	37	51910	1.8	13.2531	2.1	1.9267	2.6	0.1849	1.5	0.58	1094.0	14.8	1090.4	17.1	1083.3	41.9	1083.3	41.9	101.0
H14-007_27May2015-Spot 289	136	79182	3.9	13.3526	1.2	1.8321	1.9	0.1774	1.4	0.76	1052.9	13.9	1057.0	12.3	1065.6	24.3	1065.6	24.3	98.8
H14-007_27May2015-Spot 290	1629	152332	6.4	13.1598	0.8	1.7232	1.5	0.1648	1.3	0.87	983.2	12.1	1018.4	9.9	1094.8	15.4	1094.8	15.4	89.8
H14-007_27May2015-Spot 291	455	77296	1.4	13.4641	1.1	1.7275	1.6	0.1688	1.1	0.73	1004.9	10.7	1018.8	10.1	1048.9	21.7	1048.9	21.7	95.8
H14-007_27May2015-Spot 292	134	49797	1.2	12.4293	0.9	2.2427	1.7	0.2022	1.4	0.85	1187.0	15.3	1194.5	11.7	1208.2	17.4	1208.2	17.4	98.2
H14-007_27May2015-Spot 293	89	56754	5.2	12.8725	1.4	1.9398	2.2	0.1811	1.7	0.77	1073.0	16.4	1094.9	14.5	1138.8	27.6	1138.8	27.6	92.8
H14-007_27May2015-Spot 294	863	286509	3.5	13.1590	1.0	1.7882	1.7	0.1707	1.4	0.82	1015.8	13.0	1041.2	11.0	1094.9	19.5	1094.9	19.5	94.8
H14-007_27May2015-Spot 295	38	27160	3.1	13.8556	2.2	1.7148	2.5	0.1723	1.3	0.50	1024.9	12.1	1014.1	16.2	990.8	44.3	990.8	44.3	103.4
H14-007_27May2015-Spot 296	944	87251	3.0	13.2646	1.3	1.3646	1.9	0.1378	1.4	0.73	832.2	10.9	873.8	11.2	980.9	26.7	980.9	26.7	84.8
H14-007_27May2015-Spot 297	404	180728	6.2	12.9860	1.0	1.8204	1.6	0.1715	1.3	0.79	1020.1	11.9	1052.8	10.4	1121.4	19.5	1121.4	19.5	91.0
H14-007_27May2015-Spot 298	542	109097	3.2	13.2360	0.9	1.8578	1.6	0.1783	1.3	0.82	1057.9	12.6	1066.2	10.4	1083.2	18.0	1083.2	18.0	97.7
H14-007_27May2015-Spot 299	72	48060	2.2	11.7949	1.5	2.5847	2.0	0.2211	1.4	0.68	1287.7	16.0	1296.3	14.7	1310.5	28.5	1310.5	28.5	98.3



Appendix C: LA-ICPMS U-Pb Zircon Geochronology (continued)

Analysis	U (ppm)	206Pb/204Pb	U/Th	206Pb*/207Pb*	± (%)	Isotope ratios					Apparent ages (Ma)					Best age (Ma)	± (Ma)	Conc (%)	
						206Pb*/207Pb*	± (%)	207Pb*/235U*	± (%)	206Pb*/238U	± (%)	206Pb*/238U*	± (Ma)	207Pb*/235U	± (Ma)				206Pb*/207Pb*
H14-007_27May2015-Spot 306	520	314134	2.2	12.6467	1.0	2.1932	1.8	0.2012	1.4	0.82	1181.6	15.6	1178.9	12.3	1174.0	19.8	1174.0	19.8	100.7
H14-007_27May2015-Spot 307	453	90564	2.5	12.3039	1.1	2.3223	1.5	0.2072	1.0	0.65	1214.1	10.7	1219.1	10.5	1228.1	22.0	1228.1	22.0	98.9
H14-007_27May2015-Spot 308	695	72143	2.6	12.5061	1.1	1.8043	1.8	0.1637	1.4	0.79	977.1	12.9	1047.0	11.7	1196.0	21.7	1196.0	21.7	81.7
H14-007_27May2015-Spot 309	38	85443	2.2	10.8437	1.6	3.1069	1.9	0.2443	1.0	0.54	1409.2	12.7	1434.4	14.3	1471.9	29.8	1471.9	29.8	95.7
H14-007_27May2015-Spot 310	226	162371	0.8	13.5689	1.0	1.7476	1.4	0.1720	0.9	0.69	1023.0	8.9	1026.3	8.7	1033.2	19.8	1033.2	19.8	99.0
H14-007_27May2015-Spot 311	853	56409	26.1	11.1760	0.9	2.8699	1.6	0.2326	1.3	0.82	1348.2	16.3	1374.0	12.3	1414.4	17.9	1414.4	17.9	95.3
H14-007_27May2015-Spot 312	511	84420	3.4	12.9091	1.1	2.0247	1.7	0.1896	1.3	0.76	1119.0	13.1	1123.8	11.5	1133.2	22.0	1133.2	22.0	98.8
H14-007_27May2015-Spot 313	45	124269	1.1	14.0758	1.9	1.4901	2.3	0.1521	1.3	0.56	912.8	10.8	926.3	13.7	958.7	38.1	958.7	38.1	95.2
H14-007_27May2015-Spot 314	315	172333	3.3	12.2235	1.2	2.2053	2.0	0.1955	1.6	0.78	1151.1	16.4	1182.7	13.9	1241.0	24.1	1241.0	24.1	92.8
H14-007_27May2015-Spot 315	238	157154	2.7	11.2807	0.8	2.8200	1.3	0.2307	1.0	0.79	1338.3	12.7	1360.9	10.0	1396.5	15.8	1396.5	15.8	95.8

Appendix D: LA-ICPMS U-Pb Zircon Geochronology

Analysis	U (ppm)	206Pb/204Pb	U/Th	206Pb*/207Pb*	Isotope ratios					Apparent ages (Ma)					Best age (Ma)	± (Ma)	Conc (%)		
					± (%)	207Pb*/235U*	± (%)	206Pb*/238U*	± (%)	207Pb*/235U*	± (Ma)	206Pb*/207Pb*	± (Ma)	206Pb*/238U*				± (Ma)	
					206Pb*/207Pb*	± (%)	207Pb*/235U*	± (%)	206Pb*/238U*	± (%)	207Pb*/235U*	± (Ma)	206Pb*/207Pb*	± (Ma)				206Pb*/238U*	± (Ma)
H14-011_Rum1-Spot 1	427	146966	2.1	13.3036	1.1	1.5556	2.6	0.1501	2.4	0.91	901.5	20.1	952.7	16.3	10730	22.4	10730	22.4	84.0
H14-011_Rum1-Spot 10	57	70015	1.5	14.6758	2.8	1.3581	3.1	0.1446	1.4	0.46	870.4	11.7	871.1	18.2	872.8	57.0	870.4	11.7	99.7
H14-011_Rum1-Spot 100	88	290086	3.7	13.1200	1.4	1.8922	2.6	0.1801	2.2	0.84	1067.3	21.4	1078.4	17.2	1100.8	28.2	1100.8	28.2	97.0
H14-011_Rum1-Spot 101	131	60564	6.3	13.6967	2.0	1.5805	2.8	0.1570	2.0	0.71	1047.0	17.7	962.6	17.6	1014.2	40.1	1014.2	40.1	92.7
H14-011_Rum1-Spot 102	44	26184	2.2	13.3826	2.5	1.7965	3.9	0.1744	3.0	0.76	1036.1	28.4	1044.2	25.5	1061.1	51.2	1061.1	51.2	97.6
H14-011_Rum1-Spot 103	376	39775	29.5	17.6453	1.7	0.5874	2.3	0.0752	1.6	0.69	467.3	7.1	469.2	8.6	478.8	37.0	467.3	7.1	97.6
H14-011_Rum1-Spot 104	59	33875	3.9	13.5542	2.1	1.7257	2.8	0.1696	1.9	0.66	1010.1	17.5	1018.1	18.1	1035.4	42.6	1035.4	42.6	97.6
H14-011_Rum1-Spot 105	83	64190	2.5	14.5500	1.6	1.2012	3.4	0.1268	3.0	0.88	769.4	21.4	801.2	18.6	890.6	33.1	769.4	21.4	86.4
H14-011_Rum1-Spot 106	280	32393	10.6	16.8313	1.7	0.6752	2.0	0.0824	1.2	0.57	510.6	5.7	523.9	8.3	582.3	36.2	510.6	5.7	87.7
H14-011_Rum1-Spot 107	100	136665	4.9	16.5168	2.5	0.7001	3.1	0.0839	1.8	0.60	519.1	9.2	538.8	12.8	623.1	53.1	519.1	9.2	83.3
H14-011_Rum1-Spot 108	549	86703	1.8	9.7093	1.0	3.7878	3.0	0.2667	2.9	0.94	1524.2	38.8	1590.2	24.4	1678.8	18.7	1678.8	18.7	90.8
H14-011_Rum1-Spot 109	235	74961	18.8	13.7689	1.3	1.2190	2.4	0.1217	2.0	0.85	740.5	14.1	809.3	13.2	1003.6	25.5	740.5	14.1	73.8
H14-011_Rum1-Spot 110	510	113282	76.2	17.7431	1.9	0.5835	4.4	0.1476	3.5	0.80	887.3	29.2	906.1	26.2	952.3	53.2	952.3	53.2	93.2
H14-011_Rum1-Spot 12	100	53921	2.5	12.6839	2.2	2.2407	2.9	0.2061	1.9	0.66	1208.2	21.1	1193.9	20.3	1168.1	42.8	1168.1	42.8	103.4
H14-011_Rum1-Spot 13	147	63771	2.8	13.6478	1.3	1.7381	2.1	0.1720	1.7	0.79	1023.4	15.8	1022.8	13.7	1021.5	26.6	1021.5	26.6	100.2
H14-011_Rum1-Spot 14	251	141485	3.6	12.6322	1.3	1.5610	2.1	0.1430	1.6	0.78	861.7	12.9	954.9	12.7	1176.2	25.6	1176.2	25.6	73.3
H14-011_Rum1-Spot 15	192	177965	11.0	14.4960	1.8	1.0877	2.6	0.1144	1.8	0.72	698.0	12.1	747.4	13.5	898.3	36.8	698.0	12.1	77.7
H14-011_Rum1-Spot 16	482	56944	13.5	18.0015	1.5	0.5588	2.4	0.0730	1.9	0.79	453.9	8.4	450.7	8.8	434.4	33.3	453.9	8.4	104.5
H14-011_Rum1-Spot 17	221	87271	2.0	9.8200	1.2	3.4769	2.1	0.2736	1.7	0.83	1426.2	21.1	1522.0	16.5	1657.8	21.7	1657.8	21.7	86.0
H14-011_Rum1-Spot 18	547	89747	5.6	13.6719	0.9	1.7576	2.2	0.1743	2.0	0.91	1035.6	18.8	1030.0	14.0	1017.9	18.5	1017.9	18.5	101.7
H14-011_Rum1-Spot 19	273	253239	8.8	13.2238	1.3	1.7844	2.5	0.1711	2.2	0.86	1018.4	20.5	1039.8	16.6	1085.1	26.4	1085.1	26.4	93.9
H14-011_Rum1-Spot 20	363	309435	5.4	13.8073	1.1	1.6260	1.9	0.1628	1.5	0.81	972.5	13.7	980.3	11.8	997.9	22.5	997.9	22.5	97.5
H14-011_Rum1-Spot 21	445	123873	6.1	15.5320	1.3	0.8722	2.4	0.0983	2.0	0.82	604.2	11.3	636.8	11.2	754.2	28.4	604.2	11.3	80.1
H14-011_Rum1-Spot 22	151	50770	1.9	12.2504	1.4	2.3187	2.1	0.2060	1.6	0.77	1207.5	17.9	1218.0	15.1	1236.7	26.7	1236.7	26.7	97.6
H14-011_Rum1-Spot 23	244	86625	5.2	14.0598	1.3	1.2450	2.2	0.1270	1.8	0.80	770.5	12.8	821.1	12.5	961.0	29.0	640.1	9.2	73.3
H14-011_Rum1-Spot 24	374	113067	13.9	14.6743	1.4	0.9809	2.1	0.1044	1.5	0.73	640.1	9.2	694.0	10.4	873.0	29.0	640.1	9.2	73.3
H14-011_Rum1-Spot 25	302	107664	12.8	17.3819	1.5	0.5771	2.3	0.0728	1.7	0.74	452.7	7.4	462.6	8.5	512.0	34.0	452.7	7.4	88.4
H14-011_Rum1-Spot 26	253	97939	4.6	14.6027	1.5	1.3780	2.9	0.1459	2.5	0.85	878.2	20.5	879.6	17.2	883.2	31.5	878.2	20.5	99.4
H14-011_Rum1-Spot 27	235	48760	3.8	13.2325	1.6	1.5699	2.7	0.1507	2.2	0.81	904.7	18.3	958.4	16.7	1083.7	31.8	1083.7	31.8	83.5
H14-011_Rum1-Spot 28	239	62432	2.0	13.8253	1.3	1.6797	2.0	0.1684	1.6	0.78	1003.4	14.8	1000.9	12.9	995.3	25.7	995.3	25.7	100.8
H14-011_Rum1-Spot 29	179	59825	11.0	15.6984	1.4	0.9311	2.2	0.1060	1.7	0.78	649.5	10.8	668.2	11.0	731.7	29.7	649.5	10.8	88.8
H14-011_Rum1-Spot 30	76	24735	4.9	14.2730	1.7	1.3433	2.8	0.1391	2.1	0.78	839.3	16.9	864.6	16.0	930.2	35.5	839.3	16.9	90.2
H14-011_Rum1-Spot 31	669	54797	11.6	15.1486	1.0	1.0377	1.4	0.1140	1.0	0.68	696.0	6.4	722.8	7.3	806.8	21.8	696.0	6.4	86.3
H14-011_Rum1-Spot 32	404	113243	26.9	13.6831	1.6	1.2555	2.7	0.1246	2.2	0.80	756.9	15.4	825.9	15.3	1016.2	32.8	756.9	15.4	74.5
H14-011_Rum1-Spot 33	162	51061	3.1	12.4484	1.6	2.0463	2.6	0.1848	2.0	0.75	1092.9	20.4	1131.1	17.8	1205.1	32.3	1205.1	32.3	90.7
H14-011_Rum1-Spot 34	77	20207	8.9	13.7262	1.7	1.2827	2.6	0.1277	1.9	0.78	774.7	14.1	838.0	14.8	1009.9	34.9	774.7	14.1	76.7
H14-011_Rum1-Spot 35	94	94122	4.2	12.3018	1.3	2.3631	3.1	0.2108	2.8	0.90	1233.3	31.8	1231.5	22.4	1228.4	26.4	1228.4	26.4	100.4
H14-011_Rum1-Spot 36	33	20865	0.9	12.5613	2.5	2.0018	3.4	0.1824	2.3	0.68	1079.9	22.9	1116.1	22.9	1187.4	48.9	1187.4	48.9	91.0
H14-011_Rum1-Spot 37	211	137120	3.4	11.8798	1.5	2.2467	2.1	0.1936	1.4	0.70	1140.7	15.1	1195.8	14.5	1296.6	28.9	1296.6	28.9	88.0
H14-011_Rum1-Spot 38	177	44407	2.2	13.7968	1.6	1.2916	2.4	0.1292	1.8	0.74	783.6	13.0	842.0	13.7	999.5	32.7	783.6	13.0	78.4
H14-011_Rum1-Spot 39	88	65463	1.8	13.3185	2.8	1.7138	3.6	0.1655	2.3	0.64	987.5	21.2	1013.7	23.2	1070.8	55.9	1070.8	55.9	92.2
H14-011_Rum1-Spot 40	599	119106	5.2	12.6035	1.5	1.7689	2.5	0.1617	1.9	0.79	966.2	17.5	1034.1	16.0	1186.7	29.7	1180.7	29.7	81.8
H14-011_Rum1-Spot 41	205	163903	2.0	15.2222	1.3	0.9701	2.2	0.1071	1.8	0.80	655.9	11.2	688.5	11.2	796.6	28.2	655.9	11.2	82.3
H14-011_Rum1-Spot 42	217	132240	7.0	15.3455	1.9	1.0012	2.7	0.1114	2.0	0.73	681.0	12.8	704.4	13.8	779.7	39.1	681.0	12.8	87.4

Appendix D: LA-ICPMS U-Pb Zircon Geochronology (continued)

Analysis	U (ppm)	206Pb/204Pb	U/Th	206Pb*/207Pb*	± (%)	Isotope ratios						Apparent ages (Ma)						Conc (%)	
						207Pb*/235U*	± (%)	206Pb*/238U	± (%)	error corr.	206Pb*/238U*	± (Ma)	207Pb*/235U	± (Ma)	206Pb*/207Pb*	± (Ma)	Best age (Ma)		± (Ma)
						1.4042	2.5	0.1453	2.2	0.87	874.6	18.0	890.7	15.0	930.9	25.4	930.9		25.4
H14-011_Rum1-Spot 41	506	71521	12.6	14.2680	1.2	1.4042	2.5	0.1453	2.2	0.87	874.6	18.0	890.7	15.0	930.9	25.4	930.9	25.4	94.0
H14-011_Rum1-Spot 42	325	29884	8.6	13.8132	2.1	0.9695	2.7	0.0971	1.7	0.62	597.6	9.4	688.2	13.4	997.0	43.1	597.6	9.4	59.9
H14-011_Rum1-Spot 43	323	44897	35.6	17.9109	1.7	0.5727	2.2	0.0744	1.4	0.64	462.6	6.2	459.8	8.1	445.7	37.7	462.6	6.2	103.8
H14-011_Rum1-Spot 44	130	128030	3.0	12.7570	1.6	2.1211	2.2	0.1962	1.5	0.69	1155.1	16.1	1155.7	15.2	1156.7	31.4	1156.7	31.4	99.9
H14-011_Rum1-Spot 45	589	206667	43.6	17.8067	1.3	0.5669	2.4	0.0732	2.0	0.83	455.5	8.8	456.0	8.9	458.6	29.7	455.5	8.8	99.3
H14-011_Rum1-Spot 46	343	72023	3.9	13.6404	1.1	1.6083	1.8	0.1591	1.5	0.80	951.8	12.9	973.4	11.4	1022.6	22.1	1022.6	22.1	93.1
H14-011_Rum1-Spot 47	325	31289	46.5	17.7150	1.9	0.5798	2.4	0.0745	1.5	0.63	463.1	6.8	464.3	9.0	470.1	41.6	463.1	6.8	98.5
H14-011_Rum1-Spot 48	150	48175	3.0	13.5590	1.4	1.7161	2.4	0.1688	1.9	0.81	1005.3	17.7	1014.6	15.1	1034.7	27.9	1034.7	27.9	97.2
H14-011_Rum1-Spot 49	319	122568	1.7	12.5914	1.3	2.1228	2.1	0.1939	1.6	0.78	1142.2	17.2	1156.2	14.5	1182.6	26.0	1182.6	26.0	96.6
H14-011_Rum1-Spot 5	310	139554	7.1	13.2994	1.5	1.7169	3.2	0.1656	2.8	0.88	987.8	25.5	1014.9	20.4	1073.6	30.6	1073.6	30.6	92.0
H14-011_Rum1-Spot 50	480	68299	4.3	13.9384	1.6	1.3560	2.2	0.1371	1.6	0.70	828.1	12.1	870.2	13.1	978.7	32.6	978.7	32.6	84.6
H14-011_Rum1-Spot 51	376	427479	3.8	12.6431	1.5	2.1961	2.2	0.2014	1.6	0.72	1182.7	16.9	1179.8	15.1	1174.5	29.7	1174.5	29.7	100.7
H14-011_Rum1-Spot 52	453	144431	8.9	14.2938	1.2	1.3130	2.5	0.1361	2.3	0.89	822.7	17.5	851.4	14.7	972.2	23.8	822.7	17.5	88.7
H14-011_Rum1-Spot 53	331	51958	1.5	12.5944	1.2	1.9222	2.2	0.1756	1.8	0.82	1042.8	17.0	1088.8	14.4	1182.1	24.6	1182.1	24.6	88.2
H14-011_Rum1-Spot 54	396	118071	9.9	13.5785	1.3	1.4770	2.6	0.1455	2.2	0.86	875.5	18.2	921.0	15.6	1031.8	26.6	1031.8	26.6	84.9
H14-011_Rum1-Spot 55	101	154512	4.2	12.2082	1.7	2.4612	2.9	0.2179	2.3	0.81	1270.9	26.8	1260.7	20.8	1243.4	33.2	1243.4	33.2	102.2
H14-011_Rum1-Spot 56	76	25715	3.2	12.7784	2.1	1.8290	5.7	0.1695	5.3	0.93	1009.4	49.2	1055.9	37.2	1153.4	41.2	1153.4	41.2	87.5
H14-011_Rum1-Spot 57	411	111859	43.9	17.3959	2.0	0.5806	2.5	0.0733	1.5	0.61	455.7	6.6	464.8	9.2	510.2	43.2	455.7	6.6	89.3
H14-011_Rum1-Spot 58	537	95550	17.6	15.1744	1.2	0.9774	2.4	0.1076	2.1	0.87	658.6	13.3	692.3	12.3	803.2	25.5	658.6	13.3	82.0
H14-011_Rum1-Spot 59	143	53764	3.3	12.3154	1.2	2.0338	2.4	0.1817	2.0	0.86	1076.0	20.2	1126.9	16.2	1226.3	24.1	1226.3	24.1	87.7
H14-011_Rum1-Spot 6	417	126489	12.8	16.0053	1.7	0.7526	2.8	0.0874	2.2	0.79	539.9	11.6	569.7	12.3	690.5	36.7	539.9	11.6	78.2
H14-011_Rum1-Spot 60	612	84837	55.6	16.6506	1.9	0.7103	2.6	0.0858	1.8	0.69	530.5	9.1	544.9	10.9	605.6	40.6	530.5	9.1	87.6
H14-011_Rum1-Spot 61	205	97794	2.4	8.9838	0.9	4.3600	2.2	0.2841	2.0	0.91	1611.9	28.6	1704.8	18.2	1820.9	16.3	1820.9	16.3	88.5
H14-011_Rum1-Spot 63	313	158400	34.0	17.8636	1.7	0.5828	2.4	0.0755	1.8	0.72	469.3	8.0	466.3	9.1	451.5	37.5	469.3	8.0	103.9
H14-011_Rum1-Spot 64	215	140014	2.9	12.0611	1.5	2.4201	2.4	0.2117	1.8	0.78	1237.8	20.8	1248.6	17.1	1267.1	29.3	1267.1	29.3	97.7
H14-011_Rum1-Spot 65	492	274601	34.9	17.3727	1.7	0.6373	2.4	0.0803	1.7	0.72	497.9	8.3	500.6	9.5	513.1	36.6	497.9	8.3	97.0
H14-011_Rum1-Spot 66	96	226473	3.4	12.8052	1.7	2.1245	2.4	0.1973	1.7	0.69	1160.8	17.6	1156.8	16.6	1149.2	34.4	1149.2	34.4	101.0
H14-011_Rum1-Spot 67	82	29162	2.5	15.1300	2.5	0.9228	3.5	0.1013	2.5	0.70	621.8	14.6	663.8	17.2	809.3	53.0	621.8	14.6	76.8
H14-011_Rum1-Spot 68	234	99649	4.9	15.3689	1.7	0.9251	3.7	0.1031	3.3	0.89	632.7	19.7	665.1	18.0	776.5	36.1	632.7	19.7	81.5
H14-011_Rum1-Spot 69	375	104487	6.7	11.5188	3.6	1.6586	4.2	0.1386	2.1	0.51	836.5	16.8	992.8	26.4	1356.4	68.9	1356.4	68.9	61.7
H14-011_Rum1-Spot 7	347	534060	28.1	17.7426	1.5	0.5777	2.7	0.0743	2.2	0.84	462.3	10.0	463.0	9.9	466.6	32.2	462.3	10.0	99.1
H14-011_Rum1-Spot 71	841	218556	7.4	12.7941	0.9	2.0169	1.6	0.1872	1.3	0.82	1105.3	13.3	1121.2	10.9	1151.0	18.2	1151.0	18.2	96.1
H14-011_Rum1-Spot 72	247	84545	2.4	9.8305	0.9	3.4290	3.1	0.2445	3.0	0.96	1409.9	37.6	1511.1	24.4	1655.8	16.8	1655.8	16.8	85.2
H14-011_Rum1-Spot 73	582	117788	5.8	13.7515	2.2	1.3226	2.9	0.1319	1.9	0.66	798.8	14.4	855.7	16.7	1006.1	43.7	1006.1	43.7	79.4
H14-011_Rum1-Spot 74	344	249110	29.5	17.4877	1.6	0.5932	2.6	0.0752	2.1	0.78	467.6	9.3	472.9	9.9	498.6	36.2	467.6	9.3	93.8
H14-011_Rum1-Spot 75	377	61735	11.9	14.2618	1.8	1.0974	2.3	0.1135	1.4	0.62	693.1	9.4	752.1	12.2	931.8	36.9	693.1	9.4	74.4
H14-011_Rum1-Spot 76	123	151194	2.4	13.0252	3.3	1.7551	3.8	0.1658	1.7	0.46	988.9	15.9	1029.0	24.3	1115.3	66.5	1115.3	66.5	88.7
H14-011_Rum1-Spot 77	139	165644	1.2	9.4205	1.2	4.2681	2.3	0.2916	1.9	0.84	1649.6	28.2	1687.2	19.0	1734.3	22.9	1734.3	22.9	95.1
H14-011_Rum1-Spot 78	29	17716	7.5	13.1327	2.9	1.7638	3.6	0.1680	2.2	0.62	1001.1	20.7	1032.2	23.5	1098.9	57.1	1098.9	57.1	91.1
H14-011_Rum1-Spot 79	715	67916	4.3	13.2466	1.3	1.9446	2.3	0.1848	2.0	0.84	891.9	16.3	948.3	14.4	1081.6	25.5	1081.6	25.5	82.5
H14-011_Rum1-Spot 8	752	108364	11.9	13.0283	1.2	1.9100	1.9	0.1805	1.5	0.78	1069.6	14.5	1084.6	12.6	1114.8	23.5	1114.8	23.5	95.9
H14-011_Rum1-Spot 80	868	51611	5.3	13.4046	3.2	1.4250	4.8	0.1385	3.5	0.74	836.4	27.8	895.5	28.6	1057.8	64.9	1057.8	64.9	79.1
H14-011_Rum1-Spot 81	298	204365	3.5	12.7766	1.1	2.1759	1.8	0.2016	1.5	0.79	1184.1	15.7	1173.4	12.9	1153.7	22.6	1153.7	22.6	102.6
H14-011_Rum1-Spot 82	298	197643	11.0	17.1302	1.3	0.6182	1.9	0.0768	1.4	0.74	477.1	6.5	488.7	7.5	543.9	28.4	477.1	6.5	87.7
H14-011_Rum1-Spot 83	388	143963	27.6	17.1868	1.4	0.6203	2.4	0.0773	1.9	0.80	480.1	8.7	490.1	9.2	536.7	31.6	480.1	8.7	89.5

Appendix D: LA-ICPMS U-Pb Zircon Geochronology (continued)

H14-011		Isotope ratios										Apparent ages (Ma)									
Analysis	U (ppm)	<sup>206</sup> Pb/ <sup>204</sup> Pb	U/Th	<sup>206</sup> Pb* 207Pb*	± (%)	<sup>207</sup> Pb* 235U*	± (%)	<sup>206</sup> Pb* 238U*	± (%)	error corr.	<sup>206</sup> Pb* 238U*	± (Ma)	<sup>207</sup> Pb* 235U	± (Ma)	<sup>206</sup> Pb* 207Pb*	± (Ma)	Best age (Ma)	± (Ma)	Conc (%)		
H14-011_Run1-Spot 85	217	63786	2.4	12.6669	1.2	2.1593	1.7	0.1984	1.2	0.72	1166.6	13.3	1168.0	12.1	1170.8	24.0	1170.8	24.0	99.6		
H14-011_Run1-Spot 86	118	102934	2.2	13.7939	1.9	1.6241	3.2	0.1625	2.6	0.80	970.6	23.0	979.6	20.1	999.9	39.0	999.9	39.0	97.1		
H14-011_Run1-Spot 87	252	90554	3.4	13.5881	1.4	1.6997	2.3	0.1675	1.7	0.77	998.4	16.1	1008.4	14.4	1030.3	29.0	1030.3	29.0	96.9		
H14-011_Run1-Spot 88	46	47244	3.9	13.9683	1.9	1.5568	2.8	0.1577	2.1	0.76	944.1	18.9	953.2	17.6	974.3	38.0	974.3	38.0	96.9		
H14-011_Run1-Spot 89	245	29932	4.1	14.9045	1.8	1.0513	2.4	0.1136	1.6	0.68	693.9	10.7	729.5	12.5	840.7	36.6	693.9	10.7	82.5		
H14-011_Run1-Spot 9	288	164230	3.4	12.7481	1.8	2.0477	2.7	0.1893	2.0	0.75	1117.7	20.9	1131.5	18.6	1158.1	35.8	1158.1	35.8	96.5		
H14-011_Run1-Spot 91	169	53762	3.5	14.8121	1.0	1.1120	2.1	0.1195	1.8	0.86	727.4	12.2	759.1	11.0	853.6	21.6	727.4	12.2	85.2		
H14-011_Run1-Spot 92	118	57638	2.7	12.9023	2.0	1.7752	3.3	0.1661	2.7	0.81	990.7	24.4	1036.4	21.4	1134.2	38.9	1134.2	38.9	87.3		
H14-011_Run1-Spot 93	148	54054	2.6	12.7930	2.0	1.8497	3.4	0.1716	2.8	0.81	1021.0	26.1	1063.3	22.5	1151.1	40.1	1151.1	40.1	88.7		
H14-011_Run1-Spot 94	309	90491	22.2	15.5984	2.2	0.8031	2.8	0.0909	1.7	0.61	560.6	9.0	598.6	12.4	745.2	46.0	560.6	9.0	75.2		
H14-011_Run1-Spot 95	547	100459	1.7	14.6021	1.7	1.3698	2.6	0.1451	1.9	0.74	873.3	15.7	876.1	15.2	883.2	36.0	873.3	15.7	98.9		
H14-011_Run1-Spot 96	154	164447	2.3	9.7088	1.8	3.3156	2.7	0.2335	2.0	0.74	1352.6	23.8	1484.7	20.7	1678.8	33.2	1678.8	33.2	80.6		
H14-011_Run1-Spot 97	443	56583	6.8	14.9598	2.7	1.0255	4.0	0.1113	3.0	0.75	680.1	19.4	716.7	20.7	833.0	55.9	680.1	19.4	81.6		
H14-011_Run1-Spot 98	473	189462	59.5	17.9115	1.4	0.5728	2.3	0.0744	1.8	0.77	462.7	7.8	459.8	8.4	445.6	31.8	462.7	7.8	103.8		
H14-011_Run1-Spot 99	264	186508	4.2	13.0001	1.5	1.9055	2.4	0.1797	1.9	0.78	1065.1	18.5	1083.0	16.0	1119.2	29.7	1119.2	29.7	95.2		
H14-011_Run2-Spot 112	87	56070	7.6	14.2137	2.0	1.2101	3.1	0.1247	2.4	0.77	757.8	16.9	805.3	17.1	938.7	40.3	757.8	16.9	80.7		
H14-011_Run2-Spot 113	114	44403	1.7	13.8567	2.1	1.5583	3.0	0.1566	2.1	0.72	937.9	18.7	953.8	18.4	990.7	42.0	990.7	42.0	94.7		
H14-011_Run2-Spot 114	383	312567	1.8	12.7759	1.2	1.9328	1.9	0.1791	1.5	0.76	1062.0	14.5	1092.5	12.9	1153.8	24.7	1153.8	24.7	92.0		
H14-011_Run2-Spot 116	762	57770	26.1	13.7088	1.3	1.2991	2.4	0.1292	2.0	0.83	783.1	14.4	845.3	13.5	1012.4	26.6	783.1	14.4	77.3		
H14-011_Run2-Spot 117	405	312618	5.2	14.7387	1.2	1.4435	2.1	0.1222	1.7	0.83	743.4	12.3	774.2	11.4	864.0	24.3	743.4	12.3	86.0		
H14-011_Run2-Spot 118	207	110095	2.2	12.0353	0.9	2.3121	1.5	0.2018	1.2	0.81	1185.1	13.5	1216.0	11.0	1271.3	17.8	1271.3	17.8	93.2		
H14-011_Run2-Spot 119	123	48554	3.1	12.6889	1.8	1.9491	2.5	0.1794	1.7	0.69	1063.5	16.9	1098.1	16.2	1167.3	35.9	1167.3	35.9	91.1		
H14-011_Run2-Spot 120	251	231160	2.4	12.4366	1.4	1.9689	2.4	0.1776	1.9	0.81	1053.8	18.9	1104.9	16.8	1207.0	28.1	1207.0	28.1	87.3		
H14-011_Run2-Spot 121	260	135696	13.0	11.8116	1.8	2.5341	2.7	0.2055	2.1	0.75	1204.8	22.7	1281.9	20.0	1413.4	34.5	1413.4	34.5	85.2		
H14-011_Run2-Spot 122	295	45834	20.1	15.6726	2.0	0.8052	3.6	0.0915	3.0	0.83	564.5	16.2	599.7	16.3	735.2	42.2	564.5	16.2	76.8		
H14-011_Run2-Spot 123	179	28692	4.5	14.9389	1.4	0.9354	2.1	0.1013	1.6	0.75	622.3	9.3	670.5	10.2	835.9	28.6	622.3	9.3	74.4		
H14-011_Run2-Spot 124	129	137108	3.5	12.5944	1.9	1.9133	3.8	0.1748	3.3	0.87	1038.3	32.1	1085.7	25.6	1182.1	37.3	1182.1	37.3	87.8		
H14-011_Run2-Spot 126	377	85632	8.0	10.0157	1.1	3.9924	2.5	0.2900	2.2	0.90	1641.6	32.3	1632.6	20.1	1621.1	19.9	1621.1	19.9	101.3		
H14-011_Run2-Spot 127	442	81014	15.9	17.5741	1.5	0.5855	2.5	0.0746	2.0	0.80	464.0	8.8	468.0	9.3	487.7	33.0	464.0	8.8	95.1		
H14-011_Run2-Spot 128	91	79063	2.1	13.6651	2.4	1.3317	3.0	0.1320	1.8	0.60	799.2	13.6	859.6	17.5	1018.9	48.9	1018.9	48.9	78.4		
H14-011_Run2-Spot 129	148	31184	5.4	17.5996	2.8	0.5943	3.4	0.0759	1.9	0.56	471.4	8.7	473.6	12.8	484.5	61.8	471.4	8.7	97.3		
H14-011_Run2-Spot 130	288	87437	14.8	15.2793	2.0	0.9111	3.2	0.1010	2.5	0.78	620.0	14.6	657.6	15.4	788.7	41.8	620.0	14.6	78.6		
H14-011_Run2-Spot 131	68	35546	3.0	13.9953	2.4	1.6589	2.9	0.1684	1.6	0.57	1003.2	15.2	992.9	18.1	970.4	48.0	970.4	48.0	103.4		
H14-011_Run2-Spot 132	287	232602	6.7	15.4146	1.9	0.9181	2.7	0.1026	1.9	0.71	629.9	11.5	661.4	13.0	770.2	39.7	629.9	11.5	81.8		
H14-011_Run2-Spot 133	260	79867	51.3	16.2191	1.9	0.7838	2.4	0.0922	1.5	0.61	568.5	10.8	587.7	10.8	662.2	40.8	568.5	10.8	85.9		
H14-011_Run2-Spot 134	231	27795	13.1	13.9978	2.1	1.0571	2.8	0.1073	1.8	0.65	657.2	11.3	732.4	14.5	970.0	43.2	657.2	11.3	67.7		
H14-011_Run2-Spot 135	206	139144	3.9	12.2553	0.9	2.1809	2.0	0.1938	1.8	0.88	1142.2	18.5	1175.0	13.9	1235.9	18.3	1235.9	18.3	92.4		
H14-011_Run2-Spot 136	384	59803	39.1	17.3623	2.0	0.6055	2.9	0.0763	2.1	0.74	473.7	9.8	480.7	11.1	514.4	43.2	473.7	9.8	92.1		
H14-011_Run2-Spot 137	207	61185	4.2	12.7446	1.6	1.9556	2.3	0.1808	1.6	0.70	1071.1	15.7	1100.4	15.3	1158.6	32.2	1158.6	32.2	92.4		
H14-011_Run2-Spot 138	388	65759	4.8	13.8806	1.6	1.4877	2.9	0.1498	2.4	0.83	899.7	20.0	925.4	17.4	987.2	32.4	987.2	32.4	91.1		
H14-011_Run2-Spot 139	274	33164	3.1	13.1080	1.5	1.7022	2.7	0.1618	2.3	0.85	966.9	20.9	1009.4	17.6	1102.7	29.1	1102.7	29.1	87.7		
H14-011_Run2-Spot 140	65	83804	4.8	12.9912	3.1	2.0269	4.8	0.1910	3.7	0.77	1126.7	37.8	1124.6	32.5	1120.6	61.4	1120.6	61.4	100.5		
H14-011_Run2-Spot 141	487	87566	73.4	17.7935	1.7	0.5704	2.7	0.0736	2.1	0.77	457.9	9.3	458.3	10.1	460.3	38.3	457.9	9.3	99.5		
H14-011_Run2-Spot 142	321	114396	5.1	14.9384	2.0	0.9880	2.7	0.1065	1.7	0.64	652.4	10.4	695.2	13.2	836.0	41.7	652.4	10.4	78.0		
H14-011_Run2-Spot 143	557	217239	6.6	15.1668	0.9	0.9982	2.6	0.1098	2.6	0.95	671.6	16.4	702.9	13.8	804.2	18.6	671.6	16.4	83.5		
H14-011_Run2-Spot 144	386	75199	6.1	13.5805	1.5	1.6553	2.8	0.1630	2.4	0.84	973.7	21.4	991.6	17.8	1031.5	30.9	1031.5	30.9	94.4		

Appendix D: LA-ICPMS U-Pb Zircon Geochronology (continued)

H14-011		Isotope ratios										Apparent ages (Ma)									
Analysis	U (ppm)	<sup>206</sup> Pb/ <sup>204</sup> Pb	U/Th	<sup>206</sup> Pb*/ <sup>207</sup> Pb*	± (%)	<sup>207</sup> Pb*/ <sup>235</sup> U*	± (%)	<sup>206</sup> Pb*/ <sup>238</sup> U*	± (%)	error corr.	<sup>206</sup> Pb*/ <sup>238</sup> U*	± (Ma)	<sup>207</sup> Pb*/ <sup>235</sup> U*	± (Ma)	<sup>206</sup> Pb*/ <sup>207</sup> Pb*	± (Ma)	Best age (Ma)	± (Ma)	Conc (%)		
H14-011_Rum2-Spot 145	99	72988	2.1	12.5736	1.9	2.0131	2.5	0.1836	1.7	0.67	1086.5	16.9	1119.9	17.2	1185.4	37.2	1185.4	37.2	91.7		
H14-011_Rum2-Spot 146	101	42264	4.1	12.4129	1.9	2.1870	2.9	0.1969	2.1	0.73	1158.6	22.2	1176.9	19.9	1210.8	38.2	1210.8	38.2	95.7		
H14-011_Rum2-Spot 147	120	141814	3.7	13.5207	1.7	1.7162	3.1	0.1683	2.6	0.84	1002.7	24.0	1014.6	19.8	1040.4	33.9	1040.4	33.9	96.4		
H14-011_Rum2-Spot 148	330	65216	5.4	14.9589	1.8	1.0137	4.1	0.1100	3.6	0.89	672.6	23.0	710.7	20.8	833.1	67.2	833.1	67.2	80.7		
H14-011_Rum2-Spot 149	286	1820490	7.7	14.8179	1.2	1.0994	2.1	0.1182	1.8	0.84	719.9	12.1	753.1	11.3	852.8	24.3	719.9	12.1	84.4		
H14-011_Rum2-Spot 150	288	249671	4.7	14.4057	2.1	1.2130	3.3	0.1267	2.5	0.78	769.2	18.4	806.6	18.1	911.1	42.3	769.2	18.4	84.4		
H14-011_Rum2-Spot 151	135	104025	4.3	12.4110	1.4	2.2018	2.8	0.1982	2.5	0.87	1165.6	26.2	1181.6	19.7	1211.1	26.9	1211.1	26.9	96.2		
H14-011_Rum2-Spot 152	435	80755	50.7	17.6399	1.6	0.5979	2.7	0.0765	2.2	0.81	475.2	9.9	475.9	10.2	479.5	35.1	475.2	9.9	99.1		
H14-011_Rum2-Spot 153	204	54906	6.2	17.4252	1.7	0.6442	2.6	0.0814	1.9	0.76	504.5	9.4	504.9	10.2	506.5	37.0	504.5	9.4	99.6		
H14-011_Rum2-Spot 154	397	122229	4.8	12.6349	1.1	1.8123	2.2	0.1661	1.9	0.88	990.4	17.9	1049.9	14.5	1175.8	21.1	1175.8	21.1	84.2		
H14-011_Rum2-Spot 156	332	177674	16.6	17.2937	1.6	0.6469	2.2	0.0811	1.4	0.66	502.9	6.9	506.6	8.6	523.1	35.5	502.9	6.9	96.1		
H14-011_Rum2-Spot 157	686	50472	21.4	15.4207	1.0	0.9301	2.1	0.1040	1.9	0.88	638.0	11.4	667.7	10.5	769.4	21.6	638.0	11.4	82.9		
H14-011_Rum2-Spot 158	124	63989	2.5	10.0974	1.0	2.7537	3.5	0.2017	3.4	0.96	1184.3	36.5	1343.1	26.2	1606.0	18.0	1606.0	18.0	73.7		
H14-011_Rum2-Spot 159	1680	78752	28.2	15.4510	1.2	0.8589	2.0	0.0962	1.6	0.81	592.4	9.1	629.5	9.4	765.3	24.8	592.4	9.1	77.4		
H14-011_Rum2-Spot 160	461	75378	2.7	9.6103	1.3	3.6436	2.2	0.2540	1.8	0.81	1458.9	23.0	1559.1	17.3	1697.7	23.4	1697.7	23.4	85.9		
H14-011_Rum2-Spot 161	334	124587	21.4	16.8182	1.8	0.6781	3.0	0.0827	2.4	0.80	512.3	11.9	525.6	12.4	583.9	39.5	512.3	11.9	87.7		
H14-011_Rum2-Spot 162	29	38861	1.1	12.6116	3.2	1.8692	4.2	0.1710	2.7	0.65	1017.5	25.3	1070.2	27.6	1179.4	63.0	1179.4	63.0	86.3		
H14-011_Rum2-Spot 163	559	127859	6.1	9.6637	1.1	3.0746	2.7	0.2155	2.5	0.92	1258.0	28.8	1426.4	21.0	1687.4	19.8	1687.4	19.8	74.6		
H14-011_Rum2-Spot 164	279	91957	14.9	16.3452	2.0	0.7884	2.6	0.0923	1.7	0.65	569.0	9.2	584.6	11.6	645.6	42.7	569.0	9.2	88.1		
H14-011_Rum2-Spot 165	61	36652	4.1	12.5239	1.8	2.2805	2.9	0.2071	2.3	0.78	1213.6	25.2	1206.3	20.6	1193.2	36.1	1193.2	36.1	101.7		
H14-011_Rum2-Spot 166	306	71930	6.8	14.5807	1.7	1.2584	2.6	0.1331	2.0	0.75	805.4	14.8	827.2	14.8	886.3	35.7	805.4	14.8	90.9		
H14-011_Rum2-Spot 167	323	34885	9.6	16.1992	1.6	0.7770	2.2	0.0913	1.6	0.71	563.2	8.5	583.8	9.9	664.8	33.7	563.2	8.5	84.7		
H14-011_Rum2-Spot 168	474	95672	4.7	12.8253	1.7	1.6012	3.0	0.1489	2.4	0.82	895.0	20.2	970.7	18.5	1146.2	34.0	1146.2	34.0	78.1		
H14-011_Rum2-Spot 169	146	34444	10.6	13.5374	2.1	1.0292	2.9	0.1010	2.0	0.69	620.5	11.8	718.5	14.9	1037.9	42.3	620.5	11.8	59.8		
H14-011_Rum2-Spot 170	181	207915	6.6	14.0817	1.9	1.2808	2.8	0.1308	2.1	0.73	792.4	15.4	837.2	16.2	957.8	39.7	792.4	15.4	82.7		
H14-011_Rum2-Spot 171	425	200303	8.1	12.6850	1.3	1.6576	3.5	0.1525	3.2	0.92	914.9	27.6	992.4	22.2	1167.9	26.6	1167.9	26.6	78.3		
H14-011_Rum2-Spot 172	187	234567	3.3	13.2475	1.9	1.6304	3.3	0.1566	2.7	0.82	938.1	23.7	982.0	20.9	1081.5	38.1	1081.5	38.1	86.7		
H14-011_Rum2-Spot 173	528	192637	72.2	17.6392	1.2	0.5883	2.1	0.0753	1.7	0.81	467.8	7.7	469.8	7.9	479.6	27.1	467.8	7.7	97.5		
H14-011_Rum2-Spot 176	469	88186	14.0	17.4345	1.5	0.5835	2.4	0.0738	1.8	0.76	458.9	7.9	466.7	8.8	505.3	33.8	458.9	7.9	90.8		
H14-011_Rum2-Spot 175	360	179357	76.1	17.7847	1.6	0.5895	2.2	0.0760	1.4	0.65	472.4	6.4	470.5	8.1	461.4	36.4	472.4	6.4	102.4		
H14-011_Rum2-Spot 176	406	104605	8.1	13.5070	1.3	1.6711	2.1	0.1637	1.7	0.80	977.3	15.3	997.6	13.4	1042.4	25.5	1042.4	25.5	93.8		
H14-011_Rum2-Spot 177	159	43839	8.3	15.9235	2.7	0.7492	4.8	0.0865	3.9	0.82	534.9	20.2	567.8	20.8	701.5	57.6	534.9	20.2	76.3		
H14-011_Rum2-Spot 178	179	100360	3.6	13.9871	1.6	1.4271	2.0	0.1448	1.2	0.62	871.6	10.1	900.3	11.9	971.6	31.7	971.6	31.7	89.7		
H14-011_Rum2-Spot 179	483	144964	3.1	12.5463	1.5	1.9565	2.2	0.1780	1.6	0.75	1056.2	16.0	1100.7	14.8	1189.7	28.7	1189.7	28.7	88.8		
H14-011_Rum2-Spot 180	624	276289	1.4	9.4960	1.0	4.1341	1.6	0.2847	1.3	0.80	1615.1	18.0	1661.1	12.9	1719.7	17.6	1719.7	17.6	93.9		
H14-011_Rum2-Spot 181	308	176136	12.9	17.9240	2.0	0.5601	2.7	0.0728	1.7	0.65	453.0	7.6	451.6	9.7	444.0	44.9	453.0	7.6	102.0		
H14-011_Rum2-Spot 182	305	120900	6.5	13.8662	2.0	1.2734	3.3	0.1281	1.8	0.78	776.8	18.5	833.9	18.5	989.2	41.7	776.8	18.5	78.5		
H14-011_Rum2-Spot 183	138	49115	5.8	10.9808	1.6	3.1023	2.3	0.2471	1.6	0.71	1423.3	20.3	1433.3	17.3	1448.0	30.4	1448.0	30.4	98.3		
H14-011_Rum2-Spot 184	329	97612	20.0	17.4906	2.1	0.5878	2.7	0.0746	1.7	0.62	463.6	7.4	469.4	10.2	498.2	47.0	463.6	7.4	93.0		
H14-011_Rum2-Spot 185	113	57903	3.4	13.5632	1.1	1.6966	2.2	0.1669	1.9	0.86	995.0	17.6	1007.3	14.1	1034.0	22.4	1034.0	22.4	96.2		
H14-011_Rum2-Spot 186	308	219462	8.1	12.8411	1.2	1.9379	1.6	0.1805	1.1	0.65	1069.6	10.5	1094.3	11.0	1143.7	24.6	1143.7	24.6	93.5		
H14-011_Rum2-Spot 187	185	56940	1.2	12.6639	1.7	2.1835	2.4	0.2006	1.7	0.70	1178.3	18.1	1175.8	16.8	1171.3	34.3	1171.3	34.3	100.6		
H14-011_Rum2-Spot 188	337	109670	3.5	12.8044	1.3	2.0220	2.2	0.1878	1.8	0.82	1109.3	18.5	1122.9	15.0	1149.4	25.2	1149.4	25.2	96.5		
H14-011_Rum2-Spot 189	508	59658	9.2	12.4700	1.9	1.6505	2.6	0.1493	1.8	0.69	896.9	15.1	989.8	16.6	1201.7	37.5	1201.7	37.5	74.6		
H14-011_Rum2-Spot 190	282	92027	1.6	12.5403	1.1	2.2602	1.8	0.2056	1.4	0.78	1205.2	15.5	1200.0	12.7	1190.6	22.2	1190.6	22.2	101.2		
H14-011_Rum2-Spot 191	336	59591	13.4	17.9865	1.8	0.5609	2.8	0.0732	2.2	0.76	455.2	9.5	452.1	10.3	436.3	40.4	455.2	9.5	104.3		

Appendix D: LA-ICPMS U-Pb Zircon Geochronology (continued)

H14-011		Isotope ratios												Apparent ages (Ma)					
		U (ppm)	<sup>206</sup> Pb/ <sup>204</sup> Pb	U/Th	<sup>206</sup> Pb* <sup>207</sup> Pb*	± (%)	<sup>207</sup> Pb* <sup>235</sup> U*	± (%)	error corr.	<sup>206</sup> Pb* <sup>238</sup> U*	± (Ma)	<sup>207</sup> Pb* <sup>235</sup> U	± (Ma)	<sup>206</sup> Pb* <sup>207</sup> Pb*	± (Ma)	Best age (Ma)	± (Ma)	Conc (%)	
H14-011_Rum2-Spot 192	114	37985	6.3	14.2209	2.2	1.0812	2.7	0.1115	1.6	0.61	681.5	10.6	744.2	14.3	937.7	44.1	681.5	10.6	72.7
H14-011_Rum2-Spot 193	46	23528	3.4	12.4237	3.0	2.0769	3.7	0.1871	2.2	0.59	1105.9	22.2	1141.2	25.4	1209.1	59.1	1209.1	59.1	91.5
H14-011_Rum2-Spot 194	83	137056	2.9	13.6884	1.9	1.7743	2.5	0.1762	1.7	0.68	1045.9	16.6	1036.1	16.5	1015.5	37.9	1015.5	37.9	103.0
H14-011_Rum2-Spot 195	340	6741	24.5	16.9975	2.5	0.6686	3.3	0.0824	2.2	0.67	510.6	11.0	519.9	13.6	560.9	54.0	510.6	11.0	91.0
H14-011_Rum2-Spot 196	142	164925	7.0	13.1391	1.4	1.7293	2.3	0.1648	1.8	0.80	983.3	16.6	1019.5	14.7	1097.9	27.4	1097.9	27.4	89.6
H14-011_Rum2-Spot 197	360	105221	32.3	14.9644	2.0	0.8373	3.7	0.0909	3.1	0.84	560.7	16.8	617.7	17.2	832.4	41.6	560.7	16.8	67.4
H14-011_Rum2-Spot 198	148	272916	1.9	12.5797	1.5	1.7993	2.3	0.1642	1.8	0.77	979.9	16.4	1045.2	15.3	1184.5	29.7	1184.5	29.7	82.7
H14-011_Rum2-Spot 199	435	112205	25.4	17.7465	1.7	0.5732	2.5	0.0738	1.9	0.73	458.8	8.2	460.1	9.4	466.2	38.3	458.8	8.2	98.4
H14-011_Rum2-Spot 200	386	90924	3.1	14.9504	1.3	1.2703	1.8	0.1377	1.3	0.71	831.9	10.0	832.5	10.2	834.3	26.5	831.9	10.0	99.7
H14-011_Rum2-Spot 201	282	147332	4.8	10.5051	1.4	3.0081	2.0	0.2292	1.5	0.74	1330.2	17.9	1409.7	15.4	1531.9	25.8	1531.9	25.8	86.8
H14-011_Rum2-Spot 202	322	38985	13.4	17.5542	1.9	0.6005	2.4	0.0765	1.5	0.62	474.9	6.8	477.6	9.2	490.3	41.9	474.9	6.8	96.9
H14-011_Rum2-Spot 203	86	15874	3.2	15.8890	2.5	0.8659	3.1	0.0998	1.8	0.57	613.1	10.2	633.3	14.5	706.1	53.8	613.1	10.2	86.8
H14-011_Rum2-Spot 204	513	57718	20.1	15.0017	1.5	0.9936	2.6	0.1081	2.1	0.82	661.7	13.3	700.6	13.0	827.1	30.7	661.7	13.3	80.0
H14-011_Rum2-Spot 205	389	73265	62.1	17.7299	1.5	0.5745	2.7	0.0739	2.2	0.82	459.5	9.6	460.9	9.8	468.2	33.7	459.5	9.6	98.1
H14-011_Rum2-Spot 206	94	54962	2.2	12.3331	1.7	2.2121	3.1	0.1979	2.6	0.85	1163.8	28.2	1184.9	21.9	1223.4	32.8	1223.4	32.8	95.1
H14-011_Rum2-Spot 207	596	158661	9.5	14.1743	1.0	1.3586	1.8	0.1397	1.5	0.82	842.8	11.7	871.3	10.6	944.4	21.4	842.8	11.7	89.2
H14-011_Rum2-Spot 208	250	132132	3.7	12.4347	1.7	1.8220	3.0	0.1643	2.4	0.82	980.7	22.2	1053.4	19.7	1207.3	34.2	1207.3	34.2	81.2
H14-011_Rum2-Spot 209	33	15115	1.2	12.7041	3.8	1.7964	4.2	0.1655	1.7	0.41	987.4	15.8	1044.2	27.3	1164.9	75.6	1164.9	75.6	84.8
H14-011_Rum2-Spot 210	220	37934	2.5	13.1874	1.6	1.6444	3.0	0.1573	2.5	0.83	941.6	21.7	987.4	18.7	1090.6	32.8	1090.6	32.8	86.3
H14-011_Rum2-Spot 211	371	234810	1.9	9.8144	1.1	3.7919	2.1	0.2699	1.8	0.84	1540.3	24.1	1591.0	16.8	1658.8	20.9	1658.8	20.9	92.9
H14-011_Rum2-Spot 212	423	226588	62.3	17.4426	1.8	0.5848	3.5	0.0740	3.0	0.86	460.1	13.3	467.5	13.0	504.3	38.9	460.1	13.3	91.2
H14-011_Rum2-Spot 213	369	71605	43.3	17.8402	1.8	0.5808	3.8	0.0751	3.3	0.88	467.1	15.1	465.0	14.2	454.5	41.0	467.1	15.1	102.8
H14-011_Rum2-Spot 214	247	28040	57.3	17.3445	2.3	0.5901	2.7	0.0742	1.4	0.51	461.6	6.3	470.9	10.3	516.7	51.6	461.6	6.3	89.3
H14-011_Rum2-Spot 215	349	35947	2.0	15.6745	1.2	1.0549	2.2	0.1199	1.9	0.84	730.1	13.0	731.3	11.7	735.0	26.2	730.1	13.0	99.3
H14-011_Rum2-Spot 216	32	17017	1.6	12.6437	2.1	1.9541	3.0	0.1792	2.1	0.71	1062.6	20.6	1099.9	20.0	1174.4	41.8	1174.4	41.8	90.5
H14-011_Rum2-Spot 217	285	210381	4.9	12.6314	1.4	1.7873	2.2	0.1637	1.7	0.79	977.5	15.8	1040.8	14.4	1176.4	27.1	1176.4	27.1	83.1
H14-011_Rum2-Spot 218	170	128403	2.3	13.5508	1.6	1.8035	2.1	0.1772	1.4	0.67	1051.9	13.6	1046.7	13.6	1035.9	31.4	1035.9	31.4	101.5
H14-011_Rum2-Spot 219	441	232296	2.0	9.9081	1.1	3.3420	1.9	0.2402	1.5	0.82	1387.5	19.2	1490.9	14.7	1641.2	20.2	1641.2	20.2	84.5
H14-011_Rum3-Spot 220	253	80722	3.2	13.4208	1.7	1.6970	2.1	0.1652	1.2	0.59	985.5	11.3	1007.4	13.3	1055.4	33.8	1055.4	33.8	93.4
H14-011_Rum3-Spot 221	325	29028	6.9	17.3832	1.5	0.6217	2.0	0.0784	1.3	0.67	486.5	6.3	490.9	7.7	511.8	32.4	486.5	6.3	95.1
H14-011_Rum3-Spot 224	822	186134	44.7	17.7583	1.4	0.5770	2.5	0.0743	2.1	0.84	462.1	9.4	462.5	9.4	464.7	30.8	462.1	9.4	99.4
H14-011_Rum3-Spot 225	128	42189	1.5	12.8152	1.7	1.9030	4.2	0.1769	3.9	0.92	1049.9	37.5	1082.1	28.1	1147.7	33.6	1147.7	33.6	91.5
H14-011_Rum3-Spot 226	1189	106559	8.3	13.6903	1.1	1.4402	3.0	0.1430	2.8	0.92	861.6	22.5	905.8	18.1	1015.2	23.2	1015.2	23.2	84.9
H14-011_Rum3-Spot 227	172	154643	2.5	13.4568	1.3	1.7597	1.8	0.1717	1.2	0.70	1021.7	11.8	1030.7	11.6	1050.0	25.8	1050.0	25.8	97.3
H14-011_Rum3-Spot 228	578	71544	8.4	14.8396	1.0	1.1927	2.1	0.1284	1.9	0.89	778.6	13.9	797.2	11.7	849.8	20.1	778.6	13.9	91.6
H14-011_Rum3-Spot 229	95	90761	2.8	12.4430	1.5	2.2145	3.5	0.1998	3.1	0.90	1174.5	33.8	1185.6	24.4	1206.0	29.6	1206.0	29.6	97.4
H14-011_Rum3-Spot 230	1536	2448467	30.5	17.9063	1.1	0.5638	2.4	0.0732	2.1	0.89	455.5	9.3	454.0	8.7	446.2	24.0	455.5	9.3	102.1
H14-011_Rum3-Spot 231	476	61840	2.0	13.1213	1.2	1.8498	3.6	0.1760	3.4	0.94	1045.3	33.1	1063.3	24.0	1100.6	24.2	1100.6	24.2	95.0
H14-011_Rum3-Spot 232	128	69574	0.9	14.0849	2.5	1.6334	2.9	0.1669	1.5	0.51	994.7	13.6	983.2	18.1	957.3	50.4	957.3	50.4	103.9
H14-011_Rum3-Spot 233	82	257030	2.3	11.8592	1.7	2.7874	2.5	0.2276	1.9	0.73	1321.8	22.2	1352.2	19.0	1400.6	33.3	1400.6	33.3	94.4
H14-011_Rum3-Spot 234	559	605109	3.4	11.8932	0.8	2.6311	1.6	0.2269	1.4	0.87	1318.5	16.5	1309.4	11.6	1294.4	15.0	1294.4	15.0	101.9
H14-011_Rum3-Spot 235	421	80082	3.8	14.0804	1.8	1.9039	2.5	0.1536	1.8	0.70	921.0	15.1	932.0	15.2	958.0	36.1	958.0	36.1	96.1
H14-011_Rum3-Spot 236	522	97833	2.2	12.5446	1.0	2.1205	1.6	0.1929	1.3	0.78	1137.2	13.4	1155.5	11.4	1190.0	20.3	1190.0	20.3	95.6
H14-011_Rum3-Spot 237	217	66200	4.5	11.6896	1.6	2.4399	2.3	0.2069	1.6	0.72	1212.1	18.1	1254.5	16.4	1327.9	30.5	1327.9	30.5	91.3
H14-011_Rum3-Spot 238	136	25742	1.3	13.8520	1.9	1.4653	2.7	0.1472	1.9	0.69	885.3	15.5	916.2	16.3	991.3	39.4	991.3	39.4	89.3
H14-011_Rum3-Spot 239	71	55368	3.2	14.1570	3.1	1.5628	3.9	0.1605	2.4	0.62	959.3	21.5	955.6	24.1	946.9	62.5	946.9	62.5	101.3

Appendix D: LA-ICPMS U-Pb Zircon Geochronology (continued)

Analysis	Isotope ratios										Apparent ages (Ma)									
	U (ppm)	206Pb/204Pb	U/Th	206Pb*/207Pb*	± (%)	207Pb*/235U*	± (%)	206Pb*/238U*	± (%)	206Pb*/238U*	± (Ma)	207Pb*/235U*	± (Ma)	206Pb*/207Pb*	± (Ma)	Best age (Ma)	± (Ma)	Conc (%)		
H14-011_Rum3-Spot 240	302	120977	2.6	12.1454	0.8	2.4180	1.9	0.2130	1.7	0.90	1244.8	19.6	1248.0	13.8	1253.5	16.0	1253.5	16.0	99.3	
H14-011_Rum3-Spot 241	378	118855	1.4	12.5107	1.1	2.2019	2.3	0.1998	2.0	0.87	1174.2	21.4	1181.6	16.0	1195.3	22.3	1195.3	22.3	98.2	
H14-011_Rum3-Spot 242	895	58064	1.6	12.7184	0.9	2.2534	1.8	0.2079	1.5	0.85	1217.4	17.0	1197.9	12.7	1162.7	18.7	1162.7	18.7	104.7	
H14-011_Rum3-Spot 243	69	22958	2.8	13.7754	2.6	1.6890	4.1	0.1680	3.2	0.77	1005.2	29.6	1004.4	26.2	1002.6	53.1	1002.6	53.1	100.3	
H14-011_Rum3-Spot 244	615	94112	4.1	13.2731	1.5	1.8843	2.1	0.1814	1.5	0.72	1074.6	15.3	1075.6	14.2	1077.6	29.7	1077.6	29.7	99.7	
H14-011_Rum3-Spot 245	602	132266	5.1	17.9055	1.4	0.5637	1.9	0.0732	1.2	0.65	455.4	5.4	453.9	6.9	446.3	31.9	455.4	5.4	102.0	
H14-011_Rum3-Spot 246	627	78855	12.0	17.8334	1.7	0.5850	2.4	0.0757	1.7	0.71	470.2	7.8	467.7	9.0	455.3	37.4	470.2	7.8	103.3	
H14-011_Rum3-Spot 247	1280	316457	2.9	12.8296	0.9	2.0353	1.9	0.1894	1.7	0.89	1118.0	17.4	1127.4	12.9	1145.5	17.0	1145.5	17.0	97.6	
H14-011_Rum3-Spot 248	172	101689	1.2	13.8146	1.8	1.5463	2.4	0.1549	1.6	0.67	928.5	13.9	949.0	14.9	996.8	36.7	996.8	36.7	93.1	
H14-011_Rum3-Spot 249	1055	57480	92.3	17.5578	1.6	0.5827	2.6	0.0742	2.0	0.77	461.4	8.8	466.2	9.6	489.8	36.4	461.4	8.8	94.2	
H14-011_Rum3-Spot 250	176	35111	7.1	13.1732	1.6	1.6548	2.4	0.1581	1.7	0.74	946.2	15.3	991.4	14.9	1092.7	31.8	1092.7	31.8	86.6	
H14-011_Rum3-Spot 251	46	18328	1.3	12.7775	2.7	2.0588	3.2	0.1908	1.6	0.52	1125.7	16.9	1135.2	21.6	1153.5	53.5	1153.5	53.5	97.6	
H14-011_Rum3-Spot 252	142	161444	1.8	13.7220	2.5	1.5154	3.3	0.1508	2.2	0.62	905.5	19.0	936.6	20.4	1010.5	50.0	1010.5	50.0	89.6	
H14-011_Rum3-Spot 253	304	50721	1.8	14.2221	1.3	1.3229	2.6	0.1365	2.3	0.87	824.6	17.5	855.8	15.0	937.5	25.9	824.6	17.5	88.0	
H14-011_Rum3-Spot 254	666	139663	33.1	17.5958	1.3	0.6097	2.5	0.0778	2.1	0.85	483.0	9.7	483.4	9.5	485.0	28.9	483.0	9.7	99.6	
H14-011_Rum3-Spot 255	700	68294	29.7	17.3079	2.0	0.6161	2.5	0.0773	1.4	0.58	480.2	6.7	487.4	9.7	521.3	44.6	480.2	6.7	92.1	
H14-011_Rum3-Spot 256	1021	125160	11.5	14.5384	1.3	1.1251	2.1	0.1186	1.7	0.80	722.7	11.4	765.4	11.2	892.2	26.0	722.7	11.4	81.0	
H14-011_Rum3-Spot 257	592	158432	4.3	13.2454	2.1	1.4627	2.9	0.1405	2.0	0.70	847.6	16.2	915.1	17.5	1081.8	41.4	1081.8	41.4	78.3	
H14-011_Rum3-Spot 258	785	80606	7.0	14.0698	1.6	1.3657	3.2	0.1394	2.7	0.86	841.0	21.6	874.3	18.5	959.5	32.5	959.5	32.5	87.7	
H14-011_Rum3-Spot 259	436	201198	2.0	12.7830	1.5	1.9121	2.7	0.1773	2.2	0.83	1052.1	21.5	1085.3	17.8	1152.7	29.6	1152.7	29.6	91.3	
H14-011_Rum3-Spot 260	608	120522	19.4	17.6683	1.4	0.5935	2.3	0.0761	1.7	0.77	472.5	7.9	473.1	8.5	475.9	31.7	472.5	7.9	99.3	
H14-011_Rum3-Spot 261	2315	71659	33.3	14.2956	1.0	1.2590	2.0	0.1305	1.7	0.86	790.9	12.6	827.5	11.2	926.9	20.9	790.9	12.6	85.3	
H14-011_Rum3-Spot 262	174	28757	1.8	12.3150	1.9	2.2625	2.7	0.2021	2.0	0.73	1186.5	21.8	1200.7	19.4	1226.3	36.8	1226.3	36.8	96.8	
H14-011_Rum3-Spot 263	895	320413	12.3	13.7971	1.3	1.2507	3.2	0.1252	3.0	0.92	760.1	21.2	823.7	18.3	999.4	26.4	760.1	21.2	76.1	
H14-011_Rum3-Spot 264	487	122183	8.2	15.5187	1.2	0.8935	2.8	0.0967	2.6	0.91	595.3	14.6	629.9	13.3	756.0	25.4	595.3	14.6	78.7	
H14-011_Rum3-Spot 265	480	806076	1.5	12.8461	1.1	1.9321	1.8	0.1800	1.4	0.77	1067.0	13.3	1092.2	11.7	1142.9	22.1	1142.9	22.1	93.4	
H14-011_Rum3-Spot 266	596	230619	25.5	17.6777	1.6	0.5989	2.7	0.0768	2.1	0.78	476.9	9.6	476.5	10.1	474.7	36.5	476.9	9.6	100.5	
H14-011_Rum3-Spot 268	736	68348	48.3	17.4610	1.6	0.5868	2.6	0.0743	2.0	0.79	462.1	9.0	468.8	9.6	502.0	34.6	462.1	9.0	92.1	
H14-011_Rum3-Spot 269	560	166549	3.7	13.6819	1.3	1.5480	2.1	0.1536	1.6	0.77	921.1	13.9	949.7	12.9	1016.4	26.9	1016.4	26.9	90.6	
H14-011_Rum3-Spot 270	98	23788	3.5	13.1280	2.0	1.6337	2.9	0.1556	2.1	0.73	932.0	18.3	983.3	18.2	1099.6	39.7	1099.6	39.7	84.8	
H14-011_Rum3-Spot 271	539	133255	29.6	17.4634	1.3	0.5905	2.0	0.0748	1.6	0.78	465.0	7.1	471.2	7.6	501.7	27.8	465.0	7.1	92.7	
H14-011_Rum3-Spot 272	141	68914	1.1	13.1213	1.6	1.7441	2.3	0.1660	1.6	0.71	989.9	15.1	1025.0	15.0	1100.6	32.9	1100.6	32.9	89.9	
H14-011_Rum3-Spot 273	93	108960	1.2	12.6262	2.1	2.1640	3.4	0.1982	2.6	0.78	1165.5	27.9	1169.6	23.4	1177.2	42.0	1177.2	42.0	99.0	
H14-011_Rum3-Spot 274	601	47047	36.1	17.8302	2.0	0.5736	2.8	0.0742	2.1	0.72	461.3	9.2	460.4	10.5	455.7	43.7	461.3	9.2	101.2	
H14-011_Rum3-Spot 275	455	151627	35.5	17.6488	1.3	0.5872	2.5	0.0752	2.2	0.86	467.2	9.8	469.1	9.5	478.3	28.7	467.2	9.8	97.7	
H14-011_Rum3-Spot 276	199	69907	3.0	11.1631	2.3	2.3819	3.0	0.1928	1.9	0.62	1136.8	19.4	1237.2	21.3	1416.6	44.5	1416.6	44.5	80.2	
H14-011_Rum3-Spot 277	626	247960	26.5	14.9555	1.3	0.9521	2.5	0.1033	2.1	0.85	633.6	17.7	679.2	12.4	833.6	27.7	633.6	17.7	76.0	
H14-011_Rum3-Spot 278	204	48649	1.3	13.3558	1.8	1.6757	3.0	0.1623	2.4	0.80	969.7	21.7	999.4	19.1	1065.1	36.0	1065.1	36.0	91.0	
H14-011_Rum3-Spot 279	784	76743	52.3	17.7453	1.8	0.5518	3.1	0.0710	2.5	0.80	442.3	10.6	446.2	11.2	466.3	40.7	442.3	10.6	94.8	
H14-011_Rum3-Spot 280	55	26759	1.1	13.7278	3.5	1.6107	4.5	0.1604	2.8	0.63	958.8	25.2	974.4	28.1	1009.6	70.6	1009.6	70.6	95.0	
H14-011_Rum3-Spot 281	688	158935	1.2	13.2863	0.9	1.5049	2.3	0.1450	2.1	0.92	873.0	17.6	932.4	14.2	1075.6	18.1	1075.6	18.1	81.2	
H14-011_Rum3-Spot 282	825	62089	39.3	17.6971	2.1	0.5699	2.7	0.0732	1.6	0.59	455.1	7.0	458.0	9.8	472.3	47.5	455.1	7.0	96.4	
H14-011_Rum3-Spot 283	613	487796	2.6	12.7480	1.9	1.6948	2.5	0.1567	1.7	0.65	938.4	14.5	1006.6	16.3	1158.1	38.2	1158.1	38.2	81.0	
H14-011_Rum3-Spot 284	40	18376	0.8	13.7497	3.3	1.6623	4.1	0.1658	2.4	0.59	988.8	22.0	994.3	25.9	1006.4	67.2	1006.4	67.2	98.2	
H14-011_Rum3-Spot 285	183	102359	0.9	13.6247	2.1	1.6042	2.6	0.1589	1.4	0.55	948.6	12.5	971.9	16.0	1024.9	43.3	1024.9	43.3	92.6	
H14-011_Rum3-Spot 286	359	89218	3.9	15.3425	1.7	0.9074	2.1	0.1010	1.3	0.63	620.1	8.0	655.7	10.4	780.1	35.2	620.1	8.0	79.5	

Appendix D: LA-ICPMS U-Pb Zircon Geochronology (continued)

Analysis	U (ppm)	206Pb/204Pb	U/Th	206Pb*/207Pb*	± (%)	Isotope ratios						Apparent ages (Ma)						Conc (%)	
						207Pb*/235U*	± (%)	206Pb*/238U	± (%)	206Pb*/238U*	± (Ma)	207Pb*/235U	± (Ma)	206Pb*/207Pb*	± (Ma)	Best age (Ma)	± (Ma)		
						error corr.	± (%)	error corr.	± (Ma)	error corr.	± (Ma)	error corr.	± (Ma)	error corr.	± (Ma)	error corr.	± (Ma)		
H14-011_Rum3-Spot 287	650	82285	47.4	17.6065	1.8	0.5949	2.5	0.0760	1.7	0.67	472.0	7.6	474.0	9.5	483.7	40.8	472.0	7.6	97.6
H14-011_Rum3-Spot 290	253	2310773	2.7	12.4440	1.5	2.1514	2.8	0.1942	2.4	0.84	1143.9	24.7	1165.5	19.5	1205.8	30.2	1205.8	30.2	94.9
H14-011_Rum3-Spot 291	1069	12274718	20.0	12.6155	1.5	1.6632	2.2	0.1522	1.7	0.75	913.2	14.4	994.6	14.2	1178.8	29.1	1178.8	29.1	77.5
H14-011_Rum3-Spot 292	557	112974	14.3	17.6335	1.2	0.5771	1.8	0.0738	1.3	0.75	459.1	5.9	462.6	6.6	480.3	25.8	459.1	5.9	95.6
H14-011_Rum3-Spot 293	204	66926	0.9	12.7839	1.8	1.9222	2.6	0.1782	1.8	0.70	1057.3	17.6	1088.8	17.2	1152.5	36.5	1152.5	36.5	91.7
H14-011_Rum3-Spot 294	297	112169	3.3	13.7997	1.9	1.4083	2.8	0.1409	2.0	0.73	850.0	16.3	892.4	16.6	999.0	38.6	999.0	38.6	85.1
H14-011_Rum3-Spot 295	1547	112312	8.6	14.5560	1.2	1.1096	1.7	0.1171	1.2	0.70	714.1	7.9	758.0	8.9	889.7	24.7	714.1	7.9	80.3
H14-011_Rum3-Spot 297	519	87661	11.7	12.4233	1.3	2.1017	2.6	0.1894	2.2	0.86	1117.9	22.8	1149.3	17.9	1209.1	26.4	1209.1	26.4	92.5
H14-011_Rum3-Spot 298	166	194202	4.5	12.1213	1.9	2.2473	2.8	0.1976	2.1	0.76	1162.2	22.8	1195.9	20.0	1257.4	36.4	1257.4	36.4	92.4
H14-011_Rum3-Spot 299	590	144437	27.9	17.8044	1.6	0.5767	2.4	0.0745	1.7	0.72	463.0	7.7	462.4	8.8	458.9	36.2	463.0	36.2	100.9
H14-011_Rum3-Spot 300	497	79201	4.0	14.4611	1.7	1.1115	2.7	0.1166	2.0	0.77	710.8	13.8	758.9	14.3	903.2	35.3	710.8	13.8	78.7
H14-011_Rum3-Spot 301	854	93667	39.3	14.7635	1.3	1.1332	2.6	0.1213	2.3	0.88	738.2	16.3	769.3	14.3	860.4	26.2	738.2	16.3	85.8
H14-011_Rum3-Spot 302	438	80895	4.7	12.6999	1.2	2.0271	2.1	0.1867	1.7	0.80	1103.5	17.1	1124.6	14.3	1165.6	24.7	1165.6	24.7	94.7
H14-011_Rum3-Spot 303	400	41548	6.1	15.8036	2.0	0.8813	2.9	0.1010	2.2	0.75	620.3	12.9	641.7	14.0	717.5	41.5	620.3	12.9	86.5
H14-011_Rum3-Spot 304	493	60190	4.4	11.5385	1.5	2.4946	2.5	0.2088	2.0	0.79	1222.2	22.0	1270.5	18.0	1353.1	29.1	1353.1	29.1	90.3
H14-011_Rum3-Spot 305	761	77507	44.1	17.8544	1.6	0.5762	2.3	0.0746	1.6	0.70	463.9	7.1	462.0	8.4	452.7	35.9	463.9	7.1	102.5
H14-011_Rum3-Spot 306	601	192254	16.8	14.4703	1.5	1.1155	2.2	0.1171	1.6	0.74	713.7	10.7	760.8	11.5	901.9	30.0	713.7	10.7	79.1
H14-011_Rum3-Spot 307	330	100469	12.6	12.5082	1.4	2.0738	2.3	0.1881	1.9	0.81	1111.2	18.9	1140.2	15.7	1195.7	26.7	1195.7	26.7	92.9
H14-011_Rum3-Spot 308	646	51003	2.0	14.4927	1.4	1.2521	2.0	0.1316	1.4	0.71	797.0	10.5	824.3	11.1	898.7	28.4	797.0	28.4	88.7
H14-011_Rum3-Spot 309	628	158555	2.8	13.4620	1.3	1.4524	3.1	0.1418	2.8	0.91	854.9	22.8	910.9	18.8	1049.2	26.1	1049.2	26.1	81.5
H14-011_Rum3-Spot 310	318	189484	3.5	14.0309	1.6	1.2330	3.0	0.1255	2.6	0.85	762.0	18.6	815.7	17.0	965.2	32.1	762.0	18.6	78.9
H14-011_Rum3-Spot 311	219	1001765	1.1	12.3832	1.8	2.2661	3.0	0.2035	2.4	0.81	1194.2	26.0	1201.8	20.9	1215.5	34.5	1215.5	34.5	98.2
H14-011_Rum3-Spot 312	460	249075	4.9	10.7635	1.2	2.6889	2.1	0.2099	1.7	0.82	1228.3	18.9	1325.4	15.4	1486.0	22.7	1486.0	22.7	82.7
H14-011_Rum3-Spot 313	571	90871	16.3	16.3543	1.7	0.7409	2.3	0.0879	1.6	0.68	543.0	8.2	562.9	10.1	644.4	36.8	543.0	36.8	84.3
H14-011_Rum3-Spot 315	774	53963	37.2	17.5718	1.6	0.5953	2.7	0.0759	2.1	0.80	471.4	9.8	474.2	10.2	488.0	35.6	471.4	9.8	96.6
H14-011_Rum3-Spot 316	554	136089	24.2	17.4762	1.6	0.5828	2.6	0.0739	2.1	0.78	459.5	9.2	466.3	9.9	500.1	36.2	459.5	9.2	91.9
H14-011_Rum3-Spot 317	384	63017	2.1	13.7212	1.3	1.5781	2.3	0.1570	1.8	0.80	940.3	15.8	961.6	14.0	1010.6	27.2	1010.6	27.2	93.0
H14-011_Rum3-Spot 319	736	59773	34.2	17.9721	1.5	0.5647	2.1	0.0736	1.5	0.71	457.9	6.6	454.6	7.7	438.1	32.8	457.9	6.6	104.5
H14-011_Rum3-Spot 320	603	98301	47.4	17.8794	1.7	0.5823	2.3	0.0755	1.6	0.70	469.2	7.4	465.9	8.7	449.6	36.8	469.2	7.4	104.4
H14-011_Rum3-Spot 321	817	203602	44.2	17.5426	1.5	0.5604	2.4	0.0713	1.8	0.76	444.0	7.7	451.8	8.6	491.7	33.6	444.0	7.7	90.3
H14-011_Rum3-Spot 322	81	26465	1.3	13.9271	2.4	1.6126	3.0	0.1629	1.8	0.61	972.8	16.4	975.1	18.7	980.3	48.3	980.3	48.3	99.2
H14-011_Rum3-Spot 323	98	152459	0.9	13.6391	2.0	1.6326	2.6	0.1615	1.6	0.63	965.1	14.7	982.8	16.5	1022.8	41.2	1022.8	41.2	94.4
H14-011_Rum3-Spot 324	406	298013	15.2	16.3157	1.7	0.7394	2.4	0.0875	1.7	0.70	540.7	8.6	562.0	10.3	649.4	36.7	540.7	36.7	83.3
H14-011_Rum3-Spot 325	165	193457	0.6	12.7557	1.8	2.0031	2.2	0.1853	1.3	0.59	1095.9	13.1	1116.6	14.9	1156.9	35.3	1156.9	35.3	94.7
H14-011_Rum3-Spot 326	457	101668	6.7	17.4008	1.8	0.5671	2.5	0.0716	1.6	0.67	445.6	7.1	456.2	9.0	509.6	40.2	445.6	40.2	87.4
H14-011_Rum3-Spot 327	137	105785	3.2	12.5425	1.5	1.9807	2.1	0.1802	1.5	0.71	1067.9	14.5	1109.0	14.0	1190.3	28.8	1190.3	28.8	89.7
H14-011_Rum3-Spot 328	800	244919	28.0	17.6491	1.2	0.5824	2.6	0.0746	2.3	0.89	463.5	10.4	466.0	9.8	478.3	26.5	463.5	26.5	96.9
H14-011_Rum3-Spot 330	1414	208524	9.7	13.2863	1.0	1.5686	2.1	0.1511	1.9	0.88	907.4	15.8	957.9	13.1	1075.6	19.9	1075.6	19.9	84.4



Appendix E: LA-ICPMS U-Pb Zircon Geochronology

Analysis	U (ppm)	206Pb/204Pb	U/Th	206Pb*/207Pb*	Isotope ratios				Apparent ages (Ma)							Conc (%)			
					±	207Pb*/235U*	±	206Pb*/238U*	error corr.	±	206Pb*/238U*	±	207Pb*/235U*	±	206Pb*/207Pb*		±	Best age	±
					(%)	(%)	(%)	(%)	(%)	(Ma)	(Ma)	(Ma)	(Ma)	(Ma)	(Ma)		(Ma)	(Ma)	(Ma)
H15-003-Spot 1	124	121287	1.1	12.6466	1.3	2.1376	2.1	0.1961	1.7	0.81	1154.2	18.1	1161.1	14.7	1174.0	24.8	1174.0	24.8	98.3
H15-003-Spot 3	78	132559	1.8	12.4594	1.0	2.1902	1.7	0.1979	1.3	0.79	1164.1	14.3	1177.9	11.9	1203.4	20.5	1203.4	20.5	96.7
H15-003-Spot 4	101	137732	1.1	12.7665	0.9	2.0592	1.3	0.1907	1.0	0.73	1125.0	10.1	1135.4	9.2	1155.2	18.4	1155.2	18.4	97.4
H15-003-Spot 5	67	65918	1.5	12.7598	1.1	2.0307	1.6	0.1879	1.1	0.74	1110.1	11.7	1125.8	10.6	1156.3	20.9	1156.3	20.9	96.0
H15-003-Spot 6	78	65256	3.0	12.7094	1.0	2.1863	1.8	0.2015	1.6	0.85	1183.5	16.8	1176.7	12.7	1164.1	19.0	1164.1	19.0	101.7
H15-003-Spot 7	86	56060	1.5	12.4291	1.0	2.2498	1.6	0.2028	1.2	0.79	1190.4	13.5	1196.7	11.0	1208.2	18.8	1208.2	18.8	98.5
H15-003-Spot 8	61	185046	1.1	12.2337	1.0	2.3915	1.5	0.2122	1.1	0.73	1240.5	12.3	1240.1	10.7	1239.3	20.0	1239.3	20.0	100.1
H15-003-Spot 9	70	186682	1.4	12.6050	0.8	2.1793	1.8	0.1992	1.6	0.88	1171.2	16.7	1174.5	12.4	1180.5	16.8	1180.5	16.8	99.2
H15-003-Spot 10	122	82673	0.9	13.1822	1.1	1.8301	1.4	0.1750	0.9	0.63	1039.4	8.7	1056.3	9.5	1091.4	22.4	1091.4	22.4	95.2
H15-003-Spot 11	95	110463	3.2	12.4771	1.0	2.2327	1.4	0.2020	1.0	0.69	1186.3	10.6	1191.4	10.0	1200.6	20.5	1200.6	20.5	98.8
H15-003-Spot 13	60	913872	1.3	12.6207	1.2	2.1561	1.7	0.1974	1.2	0.72	1161.1	12.8	1167.0	11.6	1178.0	23.0	1178.0	23.0	98.6
H15-003-Spot 14	60	48553	1.6	12.9219	1.2	2.0777	1.7	0.1947	1.2	0.71	1146.9	12.7	1141.5	11.7	1131.2	24.1	1131.2	24.1	101.4
H15-003-Spot 15	153	124682	6.1	13.3909	0.8	1.8675	1.4	0.1814	1.1	0.83	1074.5	11.3	1069.6	9.1	1059.9	15.5	1059.9	15.5	101.4
H15-003-Spot 16	131	279551	1.1	14.1086	0.9	1.3832	1.3	0.1415	1.0	0.77	853.4	8.1	881.8	7.8	933.9	17.4	933.9	17.4	89.5
H15-003-Spot 17	292	112621	4.1	12.5759	1.1	2.0006	1.6	0.1825	1.1	0.70	1080.5	10.9	1115.7	10.6	1185.1	22.1	1185.1	22.1	91.2
H15-003-Spot 18	50	140615	1.3	12.2640	1.2	2.4123	1.6	0.2146	1.2	0.71	1253.1	13.3	1246.3	11.8	1234.5	22.6	1234.5	22.6	101.5
H15-003-Spot 19	245	79062	2.7	13.0267	0.9	1.9206	2.5	0.1815	2.3	0.93	1074.9	23.2	1088.3	16.8	1115.1	18.2	1115.1	18.2	96.4
H15-003-Spot 20	133	142484	1.4	14.2044	1.0	1.2551	1.7	0.1293	1.4	0.79	783.9	10.1	825.7	9.7	940.0	21.4	783.9	21.4	83.4
H15-003-Spot 21	45	33765	16.4	17.7108	1.9	0.5702	2.3	0.0732	1.2	0.54	455.6	5.4	458.1	8.4	470.6	42.4	455.6	42.4	96.8
H15-003-Spot 22	134	166550	2.5	12.9870	1.1	1.8929	1.6	0.1783	1.1	0.71	1057.7	11.0	1078.6	10.6	1121.2	22.5	1121.2	22.5	94.3
H15-003-Spot 23	90	98961	2.7	14.2797	1.3	1.3119	2.1	0.1359	1.6	0.77	821.2	12.6	851.0	12.2	929.2	27.5	821.2	27.5	88.4
H15-003-Spot 24	72	147619	1.2	12.6004	0.9	2.2293	1.6	0.2037	1.3	0.80	1195.3	13.8	1190.3	11.1	1181.2	18.8	1181.2	18.8	101.2
H15-003-Spot 25	58	106218	1.5	12.4070	1.2	2.2996	1.6	0.2069	1.0	0.63	1212.4	11.1	1212.2	11.2	1211.7	24.2	1211.7	24.2	100.1
H15-003-Spot 27	76	130508	1.9	13.2974	1.1	1.6403	2.2	0.1582	1.9	0.87	946.7	16.6	985.8	13.6	1073.9	21.1	1073.9	21.1	88.2
H15-003-Spot 28	121	1287489	1.7	12.4310	0.8	2.3209	1.4	0.2092	1.2	0.83	1224.8	13.1	1218.7	10.1	1207.9	15.7	1207.9	15.7	101.4
H15-003-Spot 29	54	61585	21.4	14.0321	1.6	1.3686	2.0	0.1393	1.2	0.61	840.6	9.5	875.6	11.7	965.0	32.4	965.0	32.4	87.1
H15-003-Spot 30	70	119591	1.3	12.6569	1.2	2.2641	2.3	0.2078	1.9	0.84	1217.3	21.2	1201.2	16.0	1172.4	24.1	1172.4	24.1	103.8
H15-003-Spot 31	211	65219	2.7	12.4923	1.0	2.2055	1.4	0.1998	1.0	0.69	1174.4	10.6	1182.8	10.0	1198.2	20.3	1198.2	20.3	98.0
H15-003-Spot 32	212	2006884	1.2	12.9763	1.3	1.9318	1.7	0.1818	1.1	0.63	1076.9	10.5	1092.2	11.2	1122.9	26.0	1122.9	26.0	95.9
H15-003-Spot 33	58	96645	1.6	13.2416	1.1	1.6531	1.4	0.1588	0.9	0.66	949.9	8.4	990.7	9.1	1082.3	21.7	1082.3	21.7	87.8
H15-003-Spot 34	115	159720	0.9	12.6041	0.9	2.1474	1.3	0.1963	0.9	0.73	1155.4	9.9	1164.2	8.9	1180.6	17.3	1180.6	17.3	97.9
H15-003-Spot 35	63	120774	1.0	12.3877	1.1	2.3224	1.6	0.2087	1.1	0.71	1221.6	12.7	1219.2	11.3	1214.8	22.0	1214.8	22.0	100.6
H15-003-Spot 36	54	184368	0.7	12.4120	1.3	2.2491	1.6	0.2025	1.0	0.62	1188.6	10.9	1196.5	11.3	1210.9	24.9	1210.9	24.9	98.2
H15-003-Spot 37	79	67089	1.8	12.8590	1.4	1.9920	2.4	0.1858	1.9	0.81	1098.5	19.5	1112.8	16.0	1140.9	27.5	1140.9	27.5	96.3
H15-003-Spot 38	211	78618	2.4	12.4431	1.0	2.2658	1.4	0.2045	1.1	0.73	1199.3	11.6	1201.7	10.2	1206.0	19.4	1206.0	19.4	99.5
H15-003-Spot 39	52	94601	1.1	12.5408	1.2	2.1769	1.8	0.1980	1.3	0.74	1164.6	14.0	1173.7	12.4	1190.5	23.6	1190.5	23.6	97.8
H15-003-Spot 40	27	47196	1.6	13.8975	1.8	1.4119	2.7	0.1423	2.0	0.75	857.7	16.4	894.0	16.1	984.7	36.1	984.7	36.1	87.1
H15-003-Spot 41	19	43129	0.9	14.0368	1.7	1.4911	2.3	0.1518	1.5	0.66	911.1	13.0	926.8	14.1	964.4	35.7	964.4	35.7	94.5
H15-003-Spot 42	89	106429	1.1	12.1789	1.0	2.5438	1.7	0.2247	1.3	0.81	1306.6	15.9	1284.7	12.0	1248.1	18.9	1248.1	18.9	104.7
H15-003-Spot 43	65	218843	1.4	13.5357	1.5	1.4982	2.6	0.1471	2.1	0.81	884.6	17.4	929.7	15.8	1038.1	30.8	1038.1	30.8	85.2
H15-003-Spot 44	100	184438	1.1	12.7518	0.9	2.0742	1.6	0.1918	1.4	0.84	1131.3	14.1	1140.3	11.0	1157.5	17.2	1157.5	17.2	97.7
H15-003-Spot 45	111	129435	1.5	12.4383	0.9	2.0803	1.3	0.1877	0.9	0.71	1108.7	9.4	1142.3	8.9	1206.8	17.9	1206.8	17.9	91.9
H15-003-Spot 46	50	50777	1.3	13.2312	1.6	1.6661	2.1	0.1599	1.4	0.65	956.1	12.1	995.7	13.4	1083.9	32.3	1083.9	32.3	88.2
H15-003-Spot 47	87	72055	1.2	12.8322	1.5	2.0092	2.1	0.1865	1.5	0.70	1102.5	15.1	1116.9	14.5	1145.1	30.3	1145.1	30.3	96.3
H15-003-Spot 48	75	122176	1.6	12.4349	1.0	2.1279	1.5	0.1919	1.1	0.74	1131.7	11.5	1157.9	10.3	1207.3	19.6	1207.3	19.6	93.7
H15-003-Spot 49	234	115087	9.7	13.5989	1.0	1.6818	1.5	0.1659	1.2	0.77	989.3	10.7	1001.7	9.7	1028.7	19.7	1028.7	19.7	96.2

Appendix E: LA-ICPMS U-Pb Zircon Geochronology (continued)

Analysis	Isotope ratios										Apparent ages (Ma)									
	U (ppm)	<sup>206</sup> Pb/ <sup>204</sup> Pb	U/Th	<sup>206</sup> Pb* <sup>207</sup> Pb*	± (%)	<sup>207</sup> Pb* <sup>235</sup> U*	± (%)	<sup>206</sup> Pb* <sup>238</sup> U*	error corr.	<sup>206</sup> Pb* <sup>238</sup> U*	± (Ma)	<sup>207</sup> Pb* <sup>235</sup> U	± (Ma)	<sup>206</sup> Pb* <sup>207</sup> Pb*	± (Ma)	Best age (Ma)	± (Ma)	Conc (%)		
H15-003-Spot 50	138	154346	3.6	12.4252	0.7	2.2530	1.3	0.2030	1.1	0.83	1191.6	11.6	1197.7	9.0	1208.8	14.1	1208.8	14.1	98.6	
H15-003-Spot 51	105	220593	1.2	13.3460	1.0	1.7420	1.6	0.1686	1.3	0.78	1004.5	11.9	1024.2	10.5	1066.6	20.4	1066.6	20.4	94.2	
H15-003-Spot 52	38	57993	1.1	12.4309	1.7	1.9197	2.1	0.1731	1.2	0.58	1029.0	11.8	1088.0	14.1	1207.9	33.9	1207.9	33.9	85.2	
H15-003-Spot 53	115	209601	1.0	12.8083	1.1	2.0494	1.7	0.1904	1.3	0.75	1123.4	12.9	1132.1	11.4	1148.8	22.0	1148.8	22.0	97.8	
H15-003-Spot 54	68	85769	1.3	12.5428	1.3	2.2649	1.8	0.2060	1.3	0.71	1207.7	14.3	1201.4	13.0	1190.2	25.8	1190.2	25.8	101.5	
H15-003-Spot 55	43	98277	1.7	13.6825	1.2	1.6567	1.6	0.1644	1.0	0.65	981.2	9.4	992.1	10.1	1016.3	24.6	1016.3	24.6	96.5	
H15-003-Spot 56	82	54242	1.6	13.2316	1.1	1.8057	1.6	0.1733	1.2	0.75	1030.2	11.6	1047.5	10.6	1083.9	21.4	1083.9	21.4	95.0	
H15-003-Spot 57	175	60636	1.1	12.6886	0.9	2.0287	1.5	0.1867	1.1	0.77	1103.4	11.5	1125.2	10.0	1167.4	18.6	1167.4	18.6	94.5	
H15-003-Spot 58	102	52319	1.0	12.6474	0.9	2.0890	1.4	0.1916	1.1	0.77	1130.1	11.3	1145.2	9.7	1173.8	18.1	1173.8	18.1	96.3	
H15-003-Spot 59	66	54578	1.3	12.2728	0.8	2.4118	1.3	0.2147	1.0	0.77	1253.7	11.6	1246.1	9.5	1233.1	16.5	1233.1	16.5	101.7	
H15-003-Spot 60	94	69361	2.4	12.6227	1.0	2.1450	1.5	0.1964	1.1	0.75	1155.8	11.8	1163.4	10.3	1177.7	19.3	1177.7	19.3	98.1	
H15-003-Spot 61	225	58496	1.3	12.5861	0.8	2.1691	1.4	0.1980	1.1	0.81	1164.6	11.9	1171.2	9.6	1183.5	16.2	1183.5	16.2	98.4	
H15-003-Spot 63	14	40815	43.0	17.0255	3.7	0.6745	5.8	0.0833	4.4	0.77	515.7	22.0	523.5	23.6	557.3	80.1	515.7	22.0	92.5	
H15-003-Spot 64	31	90481	1.1	12.5678	1.8	2.1326	2.3	0.1944	1.3	0.57	1145.1	13.5	1159.4	15.6	1186.3	36.5	1186.3	36.5	96.5	
H15-003-Spot 65	133	137897	0.9	12.4275	1.1	2.1318	1.6	0.1921	1.1	0.72	1133.0	11.9	1159.2	10.9	1208.5	21.6	1208.5	21.6	93.8	
H15-003-Spot 66	144	81645	1.0	13.4059	1.2	1.5238	1.7	0.1482	1.2	0.69	890.6	9.6	940.0	10.3	1057.6	24.6	1057.6	24.6	84.2	
H15-003-Spot 67	56	159943	28.9	17.7535	2.2	0.5622	2.5	0.0724	1.2	0.47	450.6	5.1	453.0	9.1	465.3	48.8	450.6	5.1	96.8	
H15-003-Spot 68	48	115767	1.5	13.6626	1.5	1.6771	1.8	0.1662	0.9	0.53	991.0	8.6	999.9	11.2	1019.3	30.2	1019.3	30.2	97.2	
H15-003-Spot 69	190	54416	8.7	13.6788	0.8	1.6798	1.4	0.1667	1.1	0.83	993.6	10.4	1000.9	8.7	1016.9	15.4	1016.9	15.4	97.7	
H15-003-Spot 70	24	27268	1.3	14.4076	2.1	1.1697	2.6	0.1222	1.4	0.56	743.4	10.1	786.5	14.1	910.9	43.9	743.4	10.1	81.6	
H15-003-Spot 72	136	222150	1.9	12.5768	1.1	2.2302	1.9	0.2034	1.6	0.84	1193.7	17.6	1190.6	13.6	1184.9	21.0	1184.9	21.0	100.7	
H15-003-Spot 73	123	120508	1.0	12.9865	1.0	1.9039	1.6	0.1793	1.3	0.81	1063.3	12.9	1082.5	10.9	1121.3	19.3	1121.3	19.3	94.8	
H15-003-Spot 74	309	523324	1.3	13.2682	0.9	1.7582	1.3	0.1692	1.0	0.62	1007.7	9.2	1030.2	8.4	1078.3	17.2	1078.3	17.2	93.4	
H15-003-Spot 75	143	107291	1.0	12.5153	0.8	2.2181	1.3	0.2013	1.1	0.80	1182.5	11.7	1186.8	9.4	1194.6	15.9	1194.6	15.9	99.0	
H15-003-Spot 76	48	89882	1.2	12.4820	1.2	2.3402	1.8	0.2118	1.3	0.74	1238.7	15.1	1224.6	12.9	1199.8	24.2	1199.8	24.2	103.2	
H15-003-Spot 77	52	119610	1.3	12.4788	1.5	2.2099	1.9	0.2048	1.2	0.62	1175.3	12.5	1184.2	13.2	1200.4	29.4	1200.4	29.4	97.9	
H15-003-Spot 78	58	81352	2.4	13.0209	1.6	1.9186	2.0	0.1812	1.3	0.64	1073.5	13.1	1087.6	13.7	1116.0	31.3	1116.0	31.3	96.2	
H15-003-Spot 79	64	79463	1.4	12.9092	1.0	2.0040	1.6	0.1876	1.2	0.78	1108.5	12.5	1116.9	10.6	1133.2	19.2	1133.2	19.2	97.8	
H15-003-Spot 80	178	173367	2.9	12.5927	1.0	2.2421	1.3	0.2048	0.8	0.61	1200.9	8.8	1194.3	9.2	1182.4	20.4	1182.4	20.4	101.6	
H15-003-Spot 81	80	159537	2.3	12.6284	1.1	2.2045	1.6	0.2019	1.2	0.74	1185.6	13.2	1182.5	11.5	1176.8	21.8	1176.8	21.8	100.7	
H15-003-Spot 82	108	124652	3.4	12.4315	0.8	2.2597	1.3	0.2037	1.0	0.80	1195.4	11.2	1199.8	9.1	1207.8	15.4	1207.8	15.4	99.0	
H15-003-Spot 83	98	137878	4.3	13.6055	0.9	1.6815	1.4	0.1659	1.1	0.80	989.6	10.5	1001.6	9.1	1027.7	17.4	1027.7	17.4	96.3	
H15-003-Spot 85	88	116505	1.0	12.7048	1.3	1.8637	1.8	0.1717	1.2	0.68	1021.6	11.5	1068.3	11.9	1164.8	26.3	1164.8	26.3	87.7	
H15-003-Spot 86	247	70410	18.2	12.6282	0.8	2.2748	1.3	0.2083	1.1	0.81	1220.0	11.8	1204.5	9.2	1176.9	15.2	1176.9	15.2	103.7	
H15-003-Spot 87	75	241987	0.8	12.2291	1.0	2.3117	1.6	0.2050	1.3	0.78	1202.3	14.0	1215.9	11.6	1240.1	19.9	1240.1	19.9	97.0	
H15-003-Spot 88	132	124980	0.7	14.2330	0.9	1.3470	1.5	0.1390	1.2	0.80	839.3	9.3	866.3	8.6	935.9	18.4	839.3	9.3	89.7	
H15-003-Spot 89	61	83600	1.6	13.5828	1.0	1.6014	1.6	0.1695	1.3	0.77	944.3	11.0	970.7	10.2	1031.1	21.2	1031.1	21.2	91.6	
H15-003-Spot 90	102	78559	0.9	13.1252	1.2	1.7802	1.6	0.1695	1.0	0.65	1009.2	9.7	1038.3	10.4	1100.1	24.2	1100.1	24.2	91.7	
H15-003-Spot 91	69	85505	1.4	12.6607	1.0	2.2648	3.1	0.2080	2.9	0.95	1218.0	32.5	1201.4	21.8	1171.8	19.6	1171.8	19.6	103.9	
H15-003-Spot 92	107	205270	1.5	13.2521	1.1	1.7805	1.7	0.1711	1.3	0.77	1018.3	12.4	1038.4	11.1	1080.7	22.0	1080.7	22.0	94.2	
H15-003-Spot 93	240	463658	10.0	13.4429	1.2	1.6052	2.5	0.1565	2.2	0.87	937.3	18.9	972.3	15.5	1052.0	24.2	1052.0	24.2	89.1	
H15-003-Spot 94	229	89053	1.8	12.4933	0.8	2.1825	1.6	0.1978	1.4	0.85	1163.3	14.5	1175.5	11.2	1198.0	16.5	1198.0	16.5	97.1	
H15-003-Spot 95	103	61951	1.3	13.0318	0.9	1.8547	1.6	0.1753	1.3	0.83	1041.2	12.5	1065.1	10.3	1114.3	17.5	1114.3	17.5	93.4	
H15-003-Spot 96	56	81041	1.2	12.9565	1.4	1.8032	2.1	0.1694	1.5	0.75	1009.1	14.4	1046.6	13.4	1125.9	27.0	1125.9	27.0	89.6	
H15-003-Spot 97	128	107048	1.3	12.8310	0.8	1.9246	1.4	0.1791	1.2	0.83	1062.1	11.6	1089.7	9.5	1145.3	15.5	1145.3	15.5	92.7	
H15-003-Spot 98	38	75482	1.8	13.5725	3.6	1.4023	3.9	0.1380	1.4	0.36	833.6	10.7	889.9	22.9	1032.7	73.1	1032.7	73.1	80.7	

Appendix E: LA-ICPMS U-Pb Zircon Geochronology (continued)

Analysis	U (ppm)	206Pb/204Pb	U/Th	206Pb*/207Pb*	± (%)	Isotope ratios						Apparent ages (Ma)						Conc (%)	
						207Pb*/207Pb*	± (%)	206Pb*/238U	± (%)	206Pb*/238U*	error corr.	207Pb*/235U	± (Ma)	206Pb*/207Pb*	± (Ma)	Best age (Ma)	± (Ma)		
						207Pb*/235U*	± (%)	206Pb*/238U	± (%)	206Pb*/238U*	± (%)	207Pb*/235U	± (Ma)	206Pb*/207Pb*	± (Ma)	Best age (Ma)	± (Ma)		
H15-003-Spot 99	154	456631	2.5	12.8028	1.2	2.1188	1.5	0.1967	0.9	0.62	1157.8	9.7	1155.0	10.1	1149.6	22.9	1149.6	22.9	100.7
H15-003-Spot 100	69	69378	1.9	12.4148	1.1	2.2854	1.5	0.2058	1.0	0.66	1206.3	11.0	1207.8	10.7	1210.5	22.3	1210.5	22.3	99.7
H15-003-Spot 101	123	72967	3.3	14.3500	1.0	1.2470	1.5	0.1298	1.2	0.76	786.7	8.7	822.1	8.7	919.1	20.5	786.7	8.7	85.6
H15-003-Spot 102	181	208868	2.2	12.4245	0.9	2.2361	1.6	0.2015	1.3	0.81	1183.3	13.9	1192.4	11.1	1208.9	18.1	1208.9	18.1	97.9
H15-003-Spot 103	142	59977	2.3	14.1834	1.1	1.4198	1.6	0.1460	1.2	0.74	878.8	9.9	897.3	9.6	943.1	22.1	943.1	22.1	93.2
H15-003-Spot 104	110	81338	2.5	12.3728	1.1	2.2374	1.9	0.2008	1.6	0.83	1179.5	17.1	1192.9	13.5	1217.1	21.4	1217.1	21.4	96.9
H15-003-Spot 105	83	235564	1.2	13.9858	1.3	1.4660	1.7	0.1487	1.0	0.61	893.7	8.6	916.5	10.1	971.7	26.9	971.7	26.9	92.0
H15-003-Spot 106	98	185319	1.8	12.5637	1.3	2.1602	1.9	0.1968	1.4	0.74	1158.3	15.2	1168.3	13.4	1187.0	25.5	1187.0	25.5	97.6
H15-003-Spot 107	58	38897	3.6	15.2741	1.4	0.9618	1.8	0.1065	1.2	0.66	652.7	7.3	684.2	8.9	789.5	28.4	652.7	7.3	82.7
H15-003-Spot 108	222	80336	1.9	12.5152	0.9	2.2740	1.5	0.2064	1.2	0.82	1209.7	13.5	1204.3	10.6	1194.6	17.2	1194.6	17.2	101.3
H15-003-Spot 109	86	61194	1.6	12.9960	1.0	1.9896	2.0	0.1875	1.7	0.85	1108.0	17.1	1112.0	13.3	1119.8	20.5	1119.8	20.5	98.9
H15-003-Spot 110	98	185140	1.5	12.2326	1.2	2.2269	1.6	0.1976	1.1	0.69	1162.2	12.0	1189.5	11.5	1239.5	23.3	1239.5	23.3	93.8
H15-003-Spot 111	71	145729	1.5	12.7509	1.1	2.0469	1.4	0.1893	1.0	0.69	1117.5	10.2	1131.2	9.9	1157.7	20.9	1157.7	20.9	96.5
H15-003-Spot 112	92	130150	8.3	13.2830	0.8	1.8008	1.3	0.1735	1.1	0.80	1031.3	10.3	1045.7	8.8	1076.1	16.0	1076.1	16.0	95.8
H15-003-Spot 113	142	55568	4.9	12.9390	1.4	1.8652	2.5	0.1750	2.1	0.83	1039.8	19.9	1068.8	16.4	1128.6	27.2	1128.6	27.2	92.1
H15-003-Spot 114	26	70596	6.4	13.8419	1.9	1.6259	2.6	0.1632	1.7	0.67	974.7	15.6	980.3	16.3	992.8	39.2	992.8	39.2	98.2
H15-003-Spot 115	176	110640	1.4	12.5070	0.8	2.2879	1.5	0.2075	1.2	0.84	1215.7	13.7	1208.6	10.4	1195.9	15.8	1195.9	15.8	101.7
H15-003-Spot 116	485	101058	5.6	12.9599	0.8	1.8745	1.3	0.1762	1.1	0.82	1046.2	10.6	1072.1	8.9	1125.4	15.3	1125.4	15.3	93.0
H15-003-Spot 117	105	2110645	2.0	12.5058	1.2	2.3449	2.1	0.2127	1.7	0.82	1243.1	19.6	1226.0	15.0	1196.1	23.9	1196.1	23.9	103.9
H15-003-Spot 118	103	94468	1.4	12.7830	0.9	2.0160	1.9	0.1869	1.7	0.89	1104.6	17.5	1120.9	13.1	1152.7	17.5	1152.7	17.5	95.8
H15-003-Spot 119	55	52708	2.5	13.6283	1.3	1.5603	1.9	0.1542	1.4	0.74	924.6	12.3	954.6	12.0	1024.4	26.5	1024.4	26.5	90.3
H15-003-Spot 120	28	167047	1.5	13.4058	1.4	1.7774	2.2	0.1728	1.8	0.79	1027.6	16.6	1037.2	14.4	1057.6	27.5	1057.6	27.5	97.2
H15-003-Spot 121	70	88541	1.5	12.5172	1.2	2.3024	1.6	0.2090	1.1	0.69	1223.6	12.2	1213.0	11.3	1194.3	22.9	1194.3	22.9	102.5
H15-003-Spot 122	67	113285	1.1	12.5400	1.0	2.2648	1.9	0.2060	1.7	0.86	1207.4	18.3	1201.4	13.6	1190.7	19.6	1190.7	19.6	101.4
H15-003-Spot 123	145	106084	3.0	13.9964	1.0	1.3321	1.5	0.1352	1.2	0.77	817.6	9.0	859.8	8.8	970.2	19.6	817.6	19.6	84.3
H15-003-Spot 124	22	241394	0.7	13.5697	1.9	1.8601	2.6	0.1831	1.7	0.68	1083.7	17.4	1067.0	17.0	1033.1	38.2	1033.1	38.2	104.9
H15-003-Spot 125	57	56802	0.9	13.9601	1.2	1.4075	1.7	0.1425	1.2	0.69	858.8	9.3	892.1	9.9	975.5	24.8	975.5	24.8	88.0
H15-003-Spot 126	132	49200	13.3	17.8635	1.5	0.5700	1.9	0.0738	1.1	0.59	459.3	4.9	458.0	6.9	451.6	33.8	459.3	4.9	101.7
H15-003-Spot 129	63	111101	1.1	13.3738	1.3	1.7487	1.8	0.1696	1.3	0.72	1010.0	12.1	1026.7	11.7	1062.4	25.3	1062.4	25.3	95.1
H15-003-Spot 130	173	175658	2.3	12.8859	0.9	2.0157	1.7	0.1884	1.4	0.83	1112.6	14.7	1120.8	11.7	1136.8	18.9	1136.8	18.9	97.9
H15-003-Spot 131	93	111072	1.1	12.4846	1.2	2.3000	1.8	0.2083	1.3	0.75	1219.5	15.0	1212.3	12.7	1199.4	23.3	1199.4	23.3	101.7
H15-003-Spot 132	166	165380	2.5	12.6689	1.1	2.1308	2.0	0.1958	1.7	0.84	1152.7	17.5	1158.9	13.6	1170.5	21.0	1170.5	21.0	98.5
H15-003-Spot 133	183	172159	4.7	13.2523	0.8	1.8125	1.5	0.1742	1.2	0.83	1035.3	11.9	1050.0	9.8	1080.7	16.9	1080.7	16.9	95.8
H15-003-Spot 134	77	203305	13.8	17.5122	1.7	0.6160	2.2	0.0782	1.4	0.63	485.6	6.5	487.3	8.5	495.5	37.9	485.6	37.9	98.0
H15-003-Spot 135	87	197936	5.2	13.7770	1.4	1.5880	2.0	0.1587	1.4	0.73	949.4	12.8	965.5	12.4	1002.4	27.7	1002.4	27.7	94.7
H15-003-Spot 136	117	151046	3.5	12.5504	1.0	2.1419	1.5	0.1950	1.0	0.71	1148.2	10.9	1162.5	10.2	1189.1	20.5	1189.1	20.5	96.6
H15-003-Spot 137	67	45060	1.2	12.8593	1.3	1.9832	1.8	0.1850	1.3	0.71	1094.0	12.8	1109.8	12.2	1140.8	25.3	1140.8	25.3	95.9
H15-003-Spot 138	83	179621	1.3	12.8683	1.0	1.9336	1.6	0.1935	1.2	0.75	1069.5	11.7	1092.8	10.6	1139.5	20.8	1139.5	20.8	93.9
H15-003-Spot 139	86	56007	1.4	12.9210	1.5	2.0022	1.9	0.1876	1.2	0.61	1108.5	11.7	1116.2	12.8	1131.4	29.6	1131.4	29.6	98.0
H15-003-Spot 140	185	78295	2.0	12.6224	0.9	2.1885	1.6	0.2003	1.3	0.83	1177.2	14.4	1177.4	11.2	1177.8	17.5	1177.8	17.5	100.0
H15-003-Spot 141	86	162262	1.6	12.4944	0.9	2.1334	1.4	0.1933	1.1	0.77	1139.3	11.2	1159.7	9.6	1197.9	17.4	1197.9	17.4	95.1
H15-003-Spot 142	101	144765	1.3	13.7490	0.9	1.6053	1.3	0.1601	0.9	0.71	957.2	8.4	972.3	8.3	1006.5	19.0	1006.5	19.0	95.1
H15-003-Spot 143	117	454436	1.8	12.5934	0.9	2.2708	1.3	0.2074	1.0	0.74	1215.0	10.9	1203.3	9.4	1182.3	17.9	1182.3	17.9	102.8
H15-003-Spot 144	21	203865	1.1	13.9257	1.7	1.5398	2.1	0.1555	1.2	0.59	931.8	10.7	946.4	12.8	980.5	34.1	980.5	34.1	95.0

Appendix E: LA-ICPMS U-Pb Zircon Geochronology (continued)

Analysis		Isotope ratios										Apparent ages (Ma)										Conc (%)
		U (ppm)	206Pb/204Pb	U/Th	206Pb*/207Pb*	± (%)	207Pb*/235U*	± (%)	206Pb*/238U*	± (%)	error corr.	206Pb*/238U*	± (Ma)	207Pb*/235U*	± (Ma)	206Pb*/207Pb*	± (Ma)	Best age (Ma)	± (Ma)			
H15-003-Spot 145	141	306598	0.9	12.4616	0.7	2.2494	1.6	0.2033	1.4	0.88	1193.0	15.1	1196.6	11.1	1203.0	14.6	1203.0	14.6	1203.0	14.6	99.2	
H15-003-Spot 146	51	164792	1.2	12.6243	0.8	2.0769	1.7	0.1902	1.4	0.87	1122.3	14.9	1141.2	11.4	1177.5	16.3	1177.5	16.3	1177.5	16.3	95.3	
H15-003-Spot 147	44	204089	3.0	13.9324	1.3	1.6524	1.9	0.1670	1.4	0.75	995.4	13.2	990.5	12.1	979.5	26.0	979.5	26.0	979.5	26.0	101.6	
H15-003-Spot 148	66	48568	1.6	14.6309	1.4	1.1624	2.3	0.1233	1.8	0.78	749.8	12.8	783.1	12.6	879.1	29.5	749.8	29.5	749.8	29.5	85.3	
H15-003-Spot 149	144	221925	12.7	13.5822	0.9	1.7387	1.2	0.1713	0.8	0.69	1019.1	7.9	1023.0	7.8	1031.2	17.6	1031.2	17.6	1031.2	17.6	98.8	
H15-003-Spot 150	287	193229	12.5	13.6198	0.9	1.6924	1.2	0.1672	0.9	0.70	996.5	7.9	1005.7	7.8	1025.6	17.7	1025.6	17.7	1025.6	17.7	97.2	
H15-003-Spot 151	279	210452	9.5	13.2703	1.0	1.8140	1.8	0.1746	1.5	0.84	1037.3	14.1	1050.5	11.5	1078.0	19.4	1078.0	19.4	1078.0	19.4	96.2	
H15-003-Spot 152	65	51789	1.5	13.1384	1.4	1.8186	2.1	0.1733	1.6	0.74	1030.2	14.9	1052.2	13.9	1098.0	28.6	1098.0	28.6	1098.0	28.6	93.8	
H15-003-Spot 153	118	156086	3.2	12.6967	1.2	2.0882	3.2	0.1923	3.0	0.93	1133.8	30.8	1144.9	22.0	1166.1	24.1	1166.1	24.1	1166.1	24.1	97.2	
H15-003-Spot 154	23	67778	0.6	13.7098	1.5	1.6832	2.0	0.1674	1.4	0.68	997.6	12.7	1002.2	12.9	1012.3	30.1	1012.3	30.1	1012.3	30.1	98.5	
H15-003-Spot 155	198	4146234	2.5	12.8002	1.0	2.1279	1.4	0.1975	1.0	0.72	1162.1	10.9	1157.9	9.8	1150.0	19.5	1150.0	19.5	1150.0	19.5	101.1	
H15-003-Spot 156	57	102986	1.3	12.6609	1.3	2.1858	1.5	0.2007	1.1	0.76	1179.2	12.0	1176.5	10.2	1171.7	19.0	1171.7	19.0	1171.7	19.0	100.6	
H15-003-Spot 157	268	220132	8.8	13.4481	0.6	1.7758	1.3	0.1730	1.2	0.88	1028.6	10.9	1035.9	8.5	1051.3	12.5	1051.3	12.5	1051.3	12.5	97.8	
H15-003-Spot 158	230	202171	2.6	12.6660	0.9	2.0164	1.4	0.1852	1.1	0.80	1095.5	11.4	1121.0	9.6	1170.9	16.9	1170.9	16.9	1170.9	16.9	93.6	
H15-003-Spot 159	42	36283	60.9	17.6273	1.8	0.5774	2.2	0.0738	1.3	0.58	459.1	5.7	462.8	8.4	481.0	40.6	459.1	40.6	459.1	40.6	95.4	
H15-003-Spot 160	756	407947	5.2	12.4491	0.9	2.2815	1.7	0.2060	1.4	0.84	1207.4	15.6	1206.6	11.9	1205.0	17.9	1205.0	17.9	1205.0	17.9	100.2	
H15-003-Spot 161	55	56237	1.2	12.7559	1.1	2.0409	1.7	0.1888	1.3	0.75	1114.9	12.9	1129.3	11.4	1156.9	21.7	1156.9	21.7	1156.9	21.7	96.4	
H15-003-Spot 162	158	79608	1.7	12.4914	0.9	2.1337	1.4	0.1933	1.1	0.80	1139.2	11.8	1159.8	9.8	1198.3	16.8	1198.3	16.8	1198.3	16.8	95.1	
H15-003-Spot 163	52	85024	1.7	13.9967	1.5	1.4389	2.2	0.1461	1.6	0.75	878.9	13.5	905.3	13.2	970.2	29.9	970.2	29.9	970.2	29.9	90.6	
H15-003-Spot 164	93	134113	1.0	12.1491	1.0	2.3546	1.7	0.2075	1.4	0.80	1215.4	15.3	1229.0	12.2	1252.9	19.9	1252.9	19.9	1252.9	19.9	97.0	
H15-003-Spot 165	71	218748	1.2	12.7895	1.3	2.0461	2.0	0.1898	1.5	0.75	1120.3	15.3	1131.0	13.6	1151.7	26.2	1151.7	26.2	1151.7	26.2	97.3	
H15-003-Spot 166	126	117035	3.7	12.7814	0.9	2.0606	1.4	0.1910	1.0	0.75	1126.9	10.7	1135.8	9.4	1152.9	18.0	1152.9	18.0	1152.9	18.0	97.7	
H15-003-Spot 167	62	45405	1.2	13.0743	1.3	1.8979	1.8	0.1800	1.2	0.70	1066.8	12.3	1080.4	11.9	1107.8	25.5	1107.8	25.5	1107.8	25.5	96.3	
H15-003-Spot 168	59	179642	1.5	13.4350	1.1	1.7071	1.8	0.1663	1.5	0.79	991.9	13.3	1011.2	11.8	1053.2	22.6	1053.2	22.6	1053.2	22.6	94.2	
H15-003-Spot 169	115	85118	1.0	13.0519	1.3	1.9189	1.8	0.1816	1.2	0.66	1076.0	11.8	1087.7	12.0	1111.2	26.8	1111.2	26.8	1111.2	26.8	96.8	
H15-003-Spot 170	30	56041	1.3	13.8204	1.7	1.6209	3.7	0.1625	3.2	0.88	970.5	29.3	978.3	23.2	996.0	35.4	996.0	35.4	996.0	35.4	97.4	
H15-003-Spot 171	85	59549	1.5	12.6729	1.3	2.1193	1.7	0.1948	1.1	0.65	1147.3	11.7	1155.1	10.7	1169.8	26.0	1169.8	26.0	1169.8	26.0	98.1	
H15-003-Spot 172	254	60160	2.0	12.5432	0.7	2.2363	1.5	0.2034	1.3	0.88	1193.8	14.7	1192.5	10.7	1190.2	14.0	1190.2	14.0	1190.2	14.0	100.3	
H15-003-Spot 173	117	50501	1.0	12.4849	1.1	2.1949	1.8	0.1987	1.5	0.81	1168.6	15.6	1179.4	12.6	1199.4	21.1	1199.4	21.1	1199.4	21.1	97.4	
H15-003-Spot 174	57	170890	1.0	12.2654	1.1	2.3685	1.9	0.2107	1.5	0.80	1232.5	17.0	1233.1	13.4	1234.3	21.9	1234.3	21.9	1234.3	21.9	99.9	
H15-003-Spot 175	26	33104	0.4	13.8829	1.7	1.6002	2.3	0.1611	1.6	0.69	963.0	14.3	970.3	14.6	986.8	34.5	986.8	34.5	986.8	34.5	97.6	
H15-003-Spot 176	15	19170	0.5	13.8670	2.0	1.5231	2.5	0.1532	1.6	0.63	918.8	13.6	939.7	15.5	989.1	39.9	989.1	39.9	989.1	39.9	92.9	
H15-003-Spot 177	85	126679	1.4	13.4897	1.1	1.7657	1.7	0.1728	1.3	0.76	1027.3	12.1	1033.0	10.9	1045.0	22.2	1045.0	22.2	1045.0	22.2	98.3	
H15-003-Spot 178	71	63861	1.5	12.4556	1.2	2.2746	1.8	0.2055	1.4	0.74	1204.7	13.8	1204.5	12.0	1204.0	22.6	1204.0	22.6	1204.0	22.6	100.1	
H15-003-Spot 179	99	67926	1.5	12.4060	1.1	2.2379	1.8	0.2014	1.4	0.80	1182.6	15.7	1193.0	12.7	1211.9	21.5	1211.9	21.5	1211.9	21.5	97.6	
H15-003-Spot 180	136	209538	2.3	12.6085	0.9	2.2019	1.3	0.2014	1.0	0.74	1182.6	10.7	1181.7	9.3	1179.9	17.8	1179.9	17.8	1179.9	17.8	100.2	
H15-003-Spot 181	78	121469	1.1	13.0126	1.2	1.7481	1.9	0.1650	1.5	0.80	984.4	13.9	1026.5	12.3	1117.3	23.0	1117.3	23.0	1117.3	23.0	88.1	
H15-003-Spot 182	136	80078	1.1	12.3770	0.8	2.2806	1.3	0.2047	1.0	0.80	1200.7	11.5	1206.3	9.2	1216.5	15.4	1216.5	15.4	1216.5	15.4	98.7	
H15-003-Spot 183	31	78064	2.1	13.6772	1.6	1.7503	2.0	0.1736	1.2	0.61	1032.1	11.7	1027.3	13.0	1017.1	32.4	1017.1	32.4	1017.1	32.4	101.5	
H15-003-Spot 184	136	261897	3.7	13.7881	1.0	1.5131	1.5	0.1513	1.2	0.75	908.3	9.8	935.7	9.5	1000.7	20.8	1000.7	20.8	1000.7	20.8	90.8	
H15-003-Spot 185	126	257448	0.9	12.4681	0.9	2.2804	1.5	0.2062	1.2	0.80	1208.6	13.3	1206.2	10.7	1202.0	18.0	1202.0	18.0	1202.0	18.0	100.5	
H15-003-Spot 186	310	499942	2.6	12.6365	1.0	2.0871	1.3	0.1913	0.9	0.68	1128.3	9.3	1144.6	9.0	1175.6	19.0	1175.6	19.0	1175.6	19.0	96.0	
H15-003-Spot 187	265	337815	2.1	12.6408	0.5	2.0508	1.5	0.1880	1.4	0.95	1110.6	14.6	1132.6	10.3	1174.9	9.5	1174.9	9.5	1174.9	9.5	94.5	
H15-003-Spot 188	71	230748	0.9	12.4025	1.2	2.3142	1.5	0.2082	1.0	0.63	1219.0	10.9	1216.6	10.9	1212.4	23.5	1212.4	23.5	1212.4	23.5	100.5	
H15-003-Spot 189	25	39300	47.3	13.9611	1.9	1.5524	2.3	0.1572	1.3	0.57	941.1	11.2	951.5	13.9	975.4	37.9	975.4	37.9	975.4	37.9	96.5	
H15-003-Spot 190	122	74064	1.0	12.4843	0.8	2.2416	1.8	0.2030	1.6	0.88	1191.2	16.9	1194.2	12.3	1199.5	16.2	1199.5	16.2	1199.5	16.2	99.3	

Appendix E: LA-ICPMS U-Pb Zircon Geochronology (continued)

Analysis	U (ppm)	206Pb/204Pb	U/Th	206Pb*/207Pb*	± (%)	Isotope ratios					Apparent ages (Ma)					Best age (Ma)	± (Ma)	Conc (%)		
						206Pb*/207Pb*	± (%)	206Pb*/238U*	± (%)	207Pb*/235U*	± (%)	206Pb*/238U*	± (Ma)	207Pb*/235U*	± (Ma)				206Pb*/207Pb*	± (Ma)
						error corr.	± (%)	error corr.	± (%)	error corr.	± (%)	error corr.	± (Ma)	error corr.	± (Ma)				error corr.	± (Ma)
H15-003-Spot 191	127	535818	0.8	12.7232	0.8	2.0680	1.3	0.1908	1.0	0.78	1125.9	10.7	1138.3	9.1	1162.0	16.4	1162.0	16.4	96.9	
H15-003-Spot 192	91	144560	1.6	13.1019	1.4	1.8801	1.8	0.1787	1.2	0.64	1059.6	11.3	1074.1	12.0	1103.6	27.6	1103.6	27.6	96.0	
H15-003-Spot 193	122	60498	15.9	13.7002	0.9	1.6811	1.6	0.1670	1.1	0.82	995.8	12.4	1001.4	10.4	1013.7	18.7	1013.7	18.7	98.2	
H15-003-Spot 194	356	78481	8.6	13.5243	0.6	1.7277	1.3	0.1697	1.3	0.88	1009.1	10.4	1018.9	8.2	1039.8	12.3	1039.8	12.3	97.0	
H15-003-Spot 195	52	108996	1.4	13.1230	1.2	1.8668	1.7	0.1777	1.2	0.68	1054.3	11.3	1069.4	11.2	1100.4	24.7	1100.4	24.7	95.8	
H15-003-Spot 196	24	28648	0.7	13.3709	1.9	1.6791	2.3	0.1628	1.3	0.57	972.5	11.7	1000.7	14.5	1062.9	37.8	1062.9	37.8	91.5	
H15-003-Spot 197	71	76711	4.4	13.8809	1.2	1.6476	1.8	0.1659	1.4	0.75	989.3	12.5	988.6	11.5	987.1	24.4	987.1	24.4	100.2	
H15-003-Spot 198	61	136302	1.5	13.0813	1.0	1.9112	1.8	0.1813	1.5	0.84	1074.2	14.8	1085.0	11.8	1106.8	19.0	1106.8	19.0	97.1	
H15-003-Spot 199	184	290305	2.3	13.8567	0.9	1.5256	1.5	0.1533	1.2	0.81	919.5	10.6	940.7	9.4	990.7	18.3	990.7	18.3	92.8	
H15-003-Spot 200	16	34590	0.5	13.7705	2.3	1.6955	2.7	0.1694	1.5	0.55	1009.0	14.1	1007.2	17.4	1003.3	46.1	1003.3	46.1	100.6	
H15-003-Spot 201	69	99938	1.5	12.5914	1.3	2.1424	1.8	0.1956	1.2	0.68	1151.9	13.0	1162.6	12.5	1182.6	26.3	1182.6	26.3	97.4	
H15-003-Spot 202	117	180549	1.9	12.4306	0.9	2.2973	1.7	0.2071	1.5	0.84	1213.4	16.3	1211.5	12.4	1208.0	18.4	1208.0	18.4	100.5	
H15-003-Spot 203	54	104035	0.9	12.8779	1.2	2.0602	2.4	0.1924	2.1	0.86	1134.5	22.0	1135.7	16.7	1138.0	24.5	1138.0	24.5	99.7	
H15-003-Spot 204	141	52319	2.1	12.7046	1.0	2.0918	1.5	0.1927	1.0	0.70	1136.2	10.7	1146.1	10.1	1164.9	20.7	1164.9	20.7	97.5	
H15-003-Spot 205	50	73779	1.4	13.2385	1.1	1.6901	1.5	0.1623	1.0	0.67	969.4	9.1	1004.8	9.6	1082.8	22.4	1082.8	22.4	89.5	
H15-003-Spot 206	89	143963	1.1	12.8685	1.0	2.0071	1.6	0.1873	1.2	0.79	1106.9	12.7	1117.9	10.7	1139.5	19.1	1139.5	19.1	97.1	
H15-003-Spot 208	110	290845	1.1	13.0895	1.5	1.7990	1.5	0.1708	1.0	0.92	1016.4	34.5	1045.1	26.0	1105.5	30.5	1105.5	30.5	91.9	
H15-003-Spot 209	18	14444	55.4	17.2855	3.6	0.5885	4.0	0.0738	1.6	0.41	458.9	7.2	469.9	14.9	524.1	79.0	458.9	7.2	87.5	
H15-003-Spot 210	76	1172422	2.0	12.9051	1.1	2.0246	1.4	0.1895	0.9	0.63	1118.7	9.4	1123.8	9.8	1133.8	22.4	1133.8	22.4	98.7	
H15-003-Spot 211	73	64018	0.8	13.2708	1.4	1.7554	1.8	0.1690	1.1	0.61	1006.4	10.0	1029.2	11.4	1077.9	28.2	1077.9	28.2	93.4	
H15-003-Spot 212	224	244919	1.7	12.7353	0.9	2.1006	1.5	0.1940	1.3	0.83	1143.1	13.4	1149.0	10.6	1160.1	17.3	1160.1	17.3	98.5	
H15-003-Spot 214	167	118360	2.1	12.9157	0.8	1.8369	1.3	0.1721	1.0	0.79	1023.5	9.7	1058.7	8.6	1132.2	16.0	1132.2	16.0	90.4	
H15-003-Spot 215	71	94260	1.5	12.3846	1.2	2.3398	2.2	0.2297	1.8	0.82	1229.7	20.0	1224.5	15.5	1215.3	24.6	1215.3	24.6	101.2	
H15-003-Spot 216	68	94630	1.3	12.6532	1.7	2.1588	2.4	0.1981	1.8	0.73	1165.2	19.0	1167.9	16.9	1172.9	32.7	1172.9	32.7	99.3	
H15-003-Spot 217	68	57817	1.4	12.2755	1.2	2.4399	2.4	0.2172	2.1	0.86	1267.2	23.7	1254.5	17.4	1232.7	24.5	1232.7	24.5	102.8	
H15-003-Spot 218	176	124118	6.6	12.6551	0.9	2.1217	1.5	0.1947	1.2	0.79	1147.0	12.5	1155.9	10.4	1172.6	18.2	1172.6	18.2	97.8	
H15-003-Spot 219	111	72437	22.5	14.2841	1.3	1.5361	1.8	0.1591	1.3	0.73	952.0	11.9	944.9	11.4	928.6	26.1	928.6	26.1	102.5	
H15-003-Spot 220	179	125734	6.9	13.3767	1.0	1.7996	1.8	0.1746	1.5	0.83	1037.4	14.6	1045.3	12.0	1062.0	20.5	1062.0	20.5	97.7	
H15-003-Spot 221	79	120297	1.4	12.6377	1.0	2.1818	1.3	0.2000	0.8	0.64	1175.2	9.1	1175.2	9.1	1175.4	19.9	1175.4	19.9	100.0	
H15-003-Spot 223	59	107018	1.4	12.4832	1.2	2.2309	1.7	0.2020	1.3	0.73	1185.9	13.7	1190.8	12.2	1199.6	23.5	1199.6	23.5	98.9	
H15-003-Spot 224	46	53206	1.4	14.3449	1.7	1.2145	2.0	0.1264	1.2	0.56	767.0	8.3	807.3	11.4	919.9	34.7	767.0	8.3	83.4	
H15-003-Spot 225	96	164294	1.0	13.0394	1.1	1.7221	1.5	0.1629	1.0	0.68	972.6	9.2	1016.8	9.6	1113.1	21.8	1113.1	21.8	87.4	
H15-003-Spot 226	379	200545	0.7	12.7960	0.9	1.8729	1.4	0.1738	1.1	0.77	1033.1	10.1	1071.6	9.1	1150.7	17.2	1150.7	17.2	89.8	
H15-003-Spot 227	168	233001	2.9	12.6241	0.9	2.1892	1.4	0.2004	1.0	0.76	1177.7	11.1	1177.6	9.4	1177.5	17.4	1177.5	17.4	100.0	
H15-003-Spot 228	92	57114	1.2	12.7626	1.1	2.0910	1.5	0.1936	1.1	0.76	1140.6	11.4	1145.9	10.6	1155.9	21.8	1155.9	21.8	98.7	
H15-003-Spot 229	79	158277	1.2	12.5317	1.1	2.2563	1.6	0.2051	1.1	0.72	1202.5	12.3	1198.7	11.0	1192.0	21.4	1192.0	21.4	100.9	
H15-003-Spot 230	18	121444	1.3	14.2565	2.6	1.2473	3.2	0.1290	1.8	0.57	782.0	8.22	822.2	17.9	932.6	53.5	782.0	13.4	83.9	
H15-003-Spot 231	72	167664	1.6	13.3031	1.2	1.7859	1.8	0.1721	1.3	0.72	1023.8	12.3	1039.6	11.7	1073.1	24.9	1073.1	24.9	95.4	
H15-003-Spot 232	26	36056	0.7	13.5139	1.3	1.7314	1.7	0.1697	1.1	0.64	1010.4	10.3	1020.3	11.0	1041.4	26.4	1041.4	26.4	97.0	
H15-003-Spot 234	85	59647	1.7	12.5405	1.1	2.2774	1.6	0.2071	1.2	0.73	1213.5	13.0	1205.3	11.4	1190.6	21.8	1190.6	21.8	101.9	
H15-003-Spot 235	18	38562	0.7	12.9931	1.8	1.7383	2.3	0.1638	1.5	0.64	977.9	13.5	1022.8	14.9	1120.3	35.3	1120.3	35.3	87.3	
H15-003-Spot 236	84	157723	1.4	12.9462	1.0	1.9914	1.5	0.1870	1.1	0.72	1105.0	10.9	1112.6	10.1	1127.5	20.6	1127.5	20.6	98.0	
H15-003-Spot 237	143	88244	2.9	13.3106	1.1	1.7563	1.5	0.1696	1.0	0.69	1009.6	9.6	1029.5	9.5	1072.0	21.4	1072.0	21.4	94.2	
H15-003-Spot 238	57	109776	0.5	12.7178	1.3	1.9604	1.8	0.1808	1.2	0.69	1071.5	11.9	1102.0	11.8	1162.8	25.3	1162.8	25.3	92.1	
H15-003-Spot 239	199	386860	5.3	12.9598	1.0	1.8220	3.1	0.1713	2.9	0.95	1019.0	27.2	1053.4	20.0	1125.4	19.9	1125.4	19.9	90.5	
H15-003-Spot 240	228	219266	7.1	13.3715	0.9	1.7851	1.6	0.1731	1.3	0.84	1029.3	12.6	1040.1	10.2	1062.8	17.1	1062.8	17.1	96.8	

Appendix E: LA-ICPMS U-Pb Zircon Geochronology (continued)

Analysis	U (ppm)	206Pb/204Pb	U/Th	206Pb*/207Pb*	± (%)	Isotope ratios						Apparent ages (Ma)						Conc (%)	
						206Pb*/207Pb*	± (%)	206Pb*/238U	± (%)	206Pb*/238U* error corr.	206Pb*/238U* ± (Ma)	207Pb*/235U	± (Ma)	206Pb*/207Pb*	± (Ma)	Best age (Ma)	± (Ma)		
																			206Pb*/238U
H15-003-Spot 241	137	153035	4.8	13.5694	1.4	1.5140	1.8	0.1490	1.1	0.61	895.4	9.2	936.1	11.1	1033.1	29.3	1033.1	29.3	86.7
H15-003-Spot 242	102	98626	1.2	12.8933	0.9	1.9154	1.5	0.1791	1.2	0.81	1062.1	12.0	1086.5	10.1	1135.6	17.8	1135.6	17.8	93.5
H15-003-Spot 243	62	324712	1.9	12.8109	1.3	1.9191	2.3	0.1783	2.0	0.83	1057.7	19.1	1087.7	15.7	1148.3	25.7	1148.3	25.7	92.1
H15-003-Spot 244	257	474496	2.2	12.5223	0.9	2.2886	1.5	0.2079	1.3	0.83	1217.4	14.2	1208.8	10.9	1193.4	16.8	1193.4	16.8	102.0
H15-003-Spot 245	90	60596	0.9	13.1121	1.0	1.8248	1.6	0.1735	1.2	0.80	1031.6	11.9	1054.4	10.3	1102.1	19.0	1102.1	19.0	93.6
H15-003-Spot 246	508	74127	4.8	12.9074	0.7	1.8755	1.6	0.1756	1.4	0.88	1042.7	13.2	1072.5	10.3	1133.4	14.7	1133.4	14.7	92.0
H15-003-Spot 247	40	117803	2.5	14.6276	3.1	1.3411	3.5	0.1423	1.6	0.46	857.5	12.9	863.7	20.1	879.6	63.4	857.5	12.9	97.5
H15-003-Spot 248	78	207179	1.3	12.5796	1.3	2.0719	2.0	0.1890	1.5	0.77	1116.1	15.6	1139.6	13.5	1184.5	24.8	1184.5	24.8	94.2
H15-003-Spot 249	74	57845	1.0	12.6338	1.1	2.2084	1.6	0.2024	1.2	0.74	1188.0	12.9	1183.7	11.3	1176.0	21.6	1176.0	21.6	101.0
H15-003-Spot 250	171	141260	2.2	12.5987	1.0	2.0918	1.6	0.1911	1.2	0.78	1127.5	12.8	1146.1	10.9	1181.5	19.8	1181.5	19.8	95.4
H15-003-Spot 251	55	64330	2.8	13.7079	1.5	1.5234	2.2	0.1515	1.5	0.71	909.1	13.1	939.9	13.4	1012.6	31.4	1012.6	31.4	89.8
H15-003-Spot 252	102	65115	1.2	12.7478	0.9	2.0054	1.3	0.1854	0.9	0.73	1096.5	9.4	1117.3	8.6	1158.1	17.0	1158.1	17.0	94.7
H15-003-Spot 253	48	76541	1.3	12.8700	1.1	1.9936	1.4	0.1861	0.9	0.63	1100.1	9.1	1113.3	9.7	1139.2	22.3	1139.2	22.3	96.6
H15-003-Spot 255	114	74827	1.0	12.7528	1.1	1.7206	1.6	0.1591	1.2	0.72	952.0	10.6	1016.2	10.6	1157.4	22.6	1157.4	22.6	82.3
H15-003-Spot 256	74	105639	1.7	13.1417	1.2	1.6527	1.9	0.1575	1.5	0.77	943.0	12.8	990.6	12.1	1097.5	24.6	1097.5	24.6	85.9
H15-003-Spot 257	222	236478	2.2	12.6437	0.9	2.2020	2.2	0.2019	2.0	0.92	1185.7	21.9	1181.7	15.4	1174.4	17.2	1174.4	17.2	101.0
H15-003-Spot 258	35	56227	1.0	13.9065	1.6	1.6136	2.3	0.1627	1.6	0.71	972.0	14.9	975.5	14.6	983.4	33.3	983.4	33.3	98.8
H15-003-Spot 259	58	127711	1.6	13.1586	1.4	1.7652	1.8	0.1685	1.0	0.58	1003.6	9.7	1032.7	11.5	1095.0	28.8	1095.0	28.8	91.7
H15-003-Spot 261	55	63772	245.0	14.0498	1.3	1.5452	1.7	0.1575	1.1	0.66	942.6	10.1	948.6	10.8	962.5	26.8	962.5	26.8	97.9
H15-003-Spot 262	53	249097	1.9	12.9983	1.3	2.0342	2.0	0.1918	1.5	0.75	1131.0	15.3	1127.0	13.4	1119.5	26.1	1119.5	26.1	101.0
H15-003-Spot 264	70	44865	3.0	13.3203	1.3	1.5198	2.5	0.1468	2.1	0.86	883.1	17.7	938.4	15.2	1070.5	25.4	1070.5	25.4	82.5
H15-003-Spot 265	147	91483	3.0	12.3397	1.0	2.2223	1.6	0.1989	1.3	0.79	1169.3	13.7	1188.1	11.4	1222.4	19.7	1222.4	19.7	95.7
H15-003-Spot 266	130	110005	6.2	14.0414	1.1	1.4748	1.8	0.1502	1.3	0.76	902.0	11.2	920.1	10.6	963.7	23.5	963.7	23.5	93.6
H15-003-Spot 267	26	21087	3.1	14.1186	1.7	1.3597	2.2	0.1392	1.3	0.61	840.3	10.4	871.7	12.7	952.5	35.3	840.3	10.4	88.2
H15-003-Spot 268	15	30305	0.5	13.4115	2.0	1.7212	2.6	0.1674	1.6	0.63	997.9	15.2	1016.5	16.6	1056.8	40.3	1056.8	40.3	94.4
H15-003-Spot 269	43	173478	89.1	14.6081	1.7	1.2033	2.1	0.1275	1.2	0.58	773.5	9.0	802.1	11.9	882.4	36.1	773.5	9.0	87.7
H15-003-Spot 270	76	108513	2.3	13.0278	1.1	1.9544	1.9	0.1847	1.5	0.81	1092.4	15.3	1100.0	12.6	1114.9	22.0	1114.9	22.0	98.0
H15-003-Spot 271	198	75178	3.4	12.5901	0.8	2.1693	1.6	0.1981	1.4	0.85	1165.0	14.5	1171.2	11.1	1182.8	16.6	1182.8	16.6	98.5
H15-003-Spot 272	65	51301	2.7	12.5930	1.1	2.1862	1.7	0.1997	1.2	0.75	1173.5	13.3	1176.6	11.5	1182.4	21.5	1182.4	21.5	99.3
H15-003-Spot 273	76	82428	1.4	12.8002	1.2	2.0089	2.0	0.1865	1.7	0.82	1102.4	16.9	1118.5	13.8	1150.0	23.2	1150.0	23.2	95.9
H15-003-Spot 274	187	53039	10.2	13.7265	1.1	1.6658	1.8	0.1658	1.5	0.81	989.1	13.3	995.6	11.4	1009.8	21.3	1009.8	21.3	100.5
H15-003-Spot 276	58	95709	1.3	12.3933	1.1	2.3173	1.5	0.2083	1.0	0.67	1219.7	10.9	1217.6	10.4	1213.9	21.3	1213.9	21.3	100.5
H15-003-Spot 277	49	75984	1.3	13.4017	1.2	1.6880	1.6	0.1641	1.1	0.66	979.4	9.6	1004.0	10.3	1058.2	24.5	1058.2	24.5	92.5
H15-003-Spot 278	138	50053	1.0	12.6173	0.8	2.1409	1.3	0.1959	1.0	0.76	1153.3	10.6	1162.1	9.1	1178.6	16.8	1178.6	16.8	97.9
H15-003-Spot 279	75	250119	1.6	13.7284	1.4	1.5095	2.1	0.1503	1.6	0.75	902.6	13.5	934.2	13.0	1009.5	28.6	1009.5	28.6	89.4
H15-003-Spot 280	56	90245	1.1	12.5223	1.4	2.0713	1.8	0.1881	1.1	0.61	1111.2	11.1	1139.4	12.2	1193.5	28.0	1193.5	28.0	93.1
H15-003-Spot 281	73	214032	1.6	12.9455	1.2	1.8897	2.0	0.1774	1.6	0.81	1052.9	15.5	1077.5	13.1	1127.6	23.3	1127.6	23.3	93.4
H15-003-Spot 282	89	166288	2.0	12.8042	1.1	1.9456	1.5	0.1807	1.0	0.69	1070.7	10.1	1096.9	10.0	1149.4	21.6	1149.4	21.6	93.2
H15-003-Spot 283	59	118098	1.4	12.7138	1.3	2.1576	1.9	0.1989	1.4	0.73	1169.7	14.6	1167.5	13.0	1163.4	25.5	1163.4	25.5	100.5
H15-003-Spot 284	116	213746	6.8	12.9137	1.0	1.1084	2.5	0.1975	2.2	0.90	1161.7	23.6	1151.5	17.0	1132.5	21.5	1132.5	21.5	102.6
H15-003-Spot 285	112	79488	9.3	13.7593	1.0	1.6549	1.4	0.1651	1.0	0.71	985.3	8.8	991.4	8.6	1005.0	19.3	1005.0	19.3	98.0
H15-003-Spot 287	148	964482	3.0	12.4322	0.9	2.2099	1.6	0.1993	1.3	0.81	1171.3	13.5	1184.2	10.9	1207.7	18.0	1207.7	18.0	97.0
H15-003-Spot 288	65	63283	1.2	12.8587	0.9	2.0246	1.2	0.1888	0.8	0.64	1115.0	8.1	1123.8	8.3	1141.0	18.7	1141.0	18.7	97.7
H15-003-Spot 289	59	141202	1.3	12.6990	1.2	2.0114	1.6	0.1853	1.0	0.62	1095.6	9.8	1119.4	10.7	1165.7	24.4	1165.7	24.4	94.0
H15-003-Spot 290	63	86856	1.3	12.8721	1.0	1.9729	1.5	0.1842	1.1	0.76	1089.8	11.3	1106.3	10.0	1138.9	19.3	1138.9	19.3	95.7
H15-003-Spot 291	97	284432	1.6	13.5364	1.1	1.6708	1.5	0.1640	1.0	0.68	979.1	9.2	997.5	9.4	1038.0	21.9	1038.0	21.9	94.3

Appendix E: LA-ICPMS U-Pb Zircon Geochronology (continued)

Analysis	U (ppm)	206Pb/204Pb	U/Th	206Pb*/207Pb*	± (%)	Isotope ratios						Apparent ages (Ma)						Conc (%)
						207Pb*/235U*	± (%)	206Pb*/238U	± (%)	206Pb*/238U*	error corr.	207Pb*/235U	± (Ma)	206Pb*/207Pb*	± (Ma)	Best age (Ma)	± (Ma)	
						207Pb*/235U*	± (%)	206Pb*/238U	± (%)	206Pb*/238U*	error corr.	207Pb*/235U	± (Ma)	206Pb*/207Pb*	± (Ma)	Best age (Ma)	± (Ma)	
H15-003-Spot 292	75	145874	1.4	12.6319	1.0	2.1331	1.4	0.1954	0.9	1150.7	9.9	1159.6	9.3	1176.3	19.3	1176.3	19.3	97.8
H15-003-Spot 293	73	53068	1.8	12.7317	1.1	2.1567	1.8	0.1991	1.4	1170.7	14.9	1167.2	12.3	1160.7	21.6	1160.7	21.6	100.9
H15-003-Spot 294	55	59164	1.0	12.5509	1.4	2.1256	1.8	0.1935	1.1	1140.3	12.0	1157.2	12.3	1189.0	27.0	1189.0	27.0	95.9
H15-003-Spot 295	65	8034901	1.3	12.4746	1.3	2.1339	1.7	0.1931	1.1	1137.9	11.8	1159.8	11.8	1201.0	25.3	1201.0	25.3	94.7
H15-003-Spot 296	98	73170	1.5	12.4261	1.2	2.4085	1.7	0.2171	1.1	1266.3	12.9	1245.1	12.0	1208.7	24.3	1208.7	24.3	104.8
H15-003-Spot 297	66	186037	1.7	13.3508	1.0	1.7476	1.9	0.1692	1.6	1007.8	15.3	1026.3	12.4	1065.9	20.0	1065.9	20.0	94.6
H15-003-Spot 298	127	93418	6.7	13.8541	0.9	1.3979	2.0	0.1405	1.8	847.3	14.2	888.1	12.0	991.1	19.3	991.1	19.3	85.5
H15-003-Spot 299	506	276516	5.8	12.9222	0.9	1.8971	1.5	0.1778	1.2	1054.9	12.0	1080.1	10.0	1131.2	17.3	1131.2	17.3	93.3
H15-003-Spot 300	95	98901	1.0	12.5227	0.9	2.1003	1.2	0.1908	0.9	1125.5	9.2	1148.9	8.6	1193.4	17.2	1193.4	17.2	94.3
H15-003-Spot 301	94	150212	2.7	12.6288	0.8	2.0970	1.3	0.1921	1.0	1132.6	10.3	1147.8	8.8	1176.8	16.0	1176.8	16.0	96.2
H15-003-Spot 302	19	108022	0.6	13.9955	2.2	3.3923	3.0	0.1413	2.1	852.2	16.8	885.7	17.8	970.3	43.9	970.3	43.9	87.8
H15-003-Spot 303	50	35723	1.3	13.2417	1.3	1.7538	1.8	0.1684	1.3	1003.5	11.8	1028.6	11.9	1082.3	26.8	1082.3	26.8	92.7
H15-003-Spot 304	238	78508	9.0	13.3480	0.7	1.8056	1.4	0.1748	1.2	1038.5	11.4	1047.5	9.1	1066.3	15.0	1066.3	15.0	97.4
H15-003-Spot 305	85	88108	0.7	12.8714	1.2	1.9441	1.6	0.1815	1.1	1075.1	10.4	1096.4	10.5	1139.0	23.0	1139.0	23.0	94.4
H15-003-Spot 306	135	223699	1.4	12.8991	1.0	1.9647	1.3	0.1838	0.9	1087.7	9.1	1103.5	8.9	1134.7	19.2	1134.7	19.2	95.9
H15-003-Spot 307	20	87355	0.5	14.5147	2.6	1.2200	3.2	0.1284	1.9	778.9	13.8	809.8	17.7	895.6	52.8	778.9	13.8	87.0
H15-003-Spot 308	58	66919	1.3	12.8219	1.1	2.0428	1.7	0.1900	1.3	1121.2	13.1	1129.9	11.5	1146.6	22.2	1146.6	22.2	97.8
H15-003-Spot 309	57	81948	1.7	13.6889	2.6	1.4048	2.8	0.1395	1.2	841.6	9.2	890.9	16.8	1015.4	52.3	1015.4	52.3	82.9
H15-003-Spot 310	55	56578	1.3	12.4656	1.1	2.2034	1.5	0.1992	1.1	1171.0	11.3	1182.1	10.7	1202.4	21.8	1202.4	21.8	97.4
H15-003-Spot 311	86	96781	2.4	13.7761	1.1	1.9961	1.7	0.1595	1.3	953.8	11.7	968.7	10.7	1002.5	22.3	1002.5	22.3	95.1
H15-003-Spot 312	72	131876	1.3	12.9574	1.3	1.9799	1.6	0.1861	0.9	1100.0	9.4	1108.7	10.7	1125.7	25.7	1125.7	25.7	97.7
H15-003-Spot 313	86	107905	1.9	12.8428	1.0	2.1656	1.5	0.2017	1.1	1184.5	11.8	1170.1	10.2	1143.4	19.4	1143.4	19.4	103.6
H15-003-Spot 314	210	369044	2.6	12.6953	0.8	2.0597	1.4	0.1896	1.1	1119.4	11.2	1135.5	9.3	1166.3	16.2	1166.3	16.2	96.0
H15-003-Spot 315	96	80922	1.7	12.6600	1.0	1.9848	1.4	0.1822	1.0	1079.2	10.4	1110.4	9.6	1171.9	19.1	1171.9	19.1	92.1

Appendix F: LA-ICPMS U-Pb Zircon Geochronology

Analysis	U (ppm)	206Pb/204Pb	U/Th	206Pb*/207Pb*	Isotope ratios			Apparent ages (Ma)							Conc (%)				
					± (%)	207Pb* 235U*	± (%)	206Pb* 238U*	± (%)	206Pb* 238U*	± (Ma)	207Pb* 235U*	± (Ma)	206Pb* 207Pb*		± (Ma)	Best age (Ma)	± (Ma)	
H15-004 26May2014-Spot1	352	56460	18.2	15.4579	1.6	0.9542	2.4	0.1070	1.8	0.76	655.1	11.4	680.3	12.0	764.3	33.2	655.1	11.4	85.7
H15-004 26May2014-Spot2	191	112646	4.6	12.3714	1.3	2.1112	1.6	0.1894	1.1	0.64	1118.3	10.8	1152.5	11.4	1217.3	24.9	1217.3	24.9	91.9
H15-004 26May2014-Spot3	117	56920	4.5	13.3448	1.2	1.4906	1.7	0.1443	1.2	0.69	868.8	9.5	926.6	10.2	1066.8	24.3	1066.8	24.3	81.4
H15-004 26May2014-Spot4	95	72980	6.7	13.8860	1.1	1.6929	1.7	0.1705	1.4	0.78	1014.8	12.7	1005.8	11.0	986.4	21.8	986.4	21.8	102.9
H15-004 26May2014-Spot5	572	79057	4.5	13.9418	1.1	1.4637	2.0	0.1480	1.7	0.82	889.8	13.9	915.5	12.2	978.2	23.3	978.2	23.3	91.0
H15-004 26May2014-Spot6	65	78528	2.9	13.3135	1.4	1.8698	2.2	0.1805	1.7	0.76	1070.0	16.4	1070.5	14.6	1071.5	29.0	1071.5	29.0	99.9
H15-004 26May2014-Spot7	170	68175	2.2	13.1189	1.0	1.9138	1.8	0.1821	1.5	0.82	1078.4	14.5	1085.9	11.9	1101.0	20.4	1101.0	20.4	97.9
H15-004 26May2014-Spot8	53	35965	1.6	12.5907	1.2	2.1288	2.2	0.1944	1.8	0.83	1145.1	19.4	1158.2	15.4	1182.7	24.6	1182.7	24.6	96.8
H15-004 26May2014-Spot9	139	71477	1.2	13.8060	1.2	1.6445	2.0	0.1647	1.5	0.78	982.7	13.9	987.5	12.4	998.1	25.1	998.1	25.1	98.5
H15-004 26May2014-Spot10	149	84457	1.8	13.8851	1.2	1.5896	1.7	0.1601	1.2	0.71	957.2	10.6	966.1	10.4	986.5	23.7	986.5	23.7	97.0
H15-004 26May2014-Spot11	144	242050	5.2	12.8879	1.4	2.0182	2.0	0.1886	1.5	0.72	1114.0	15.0	1121.7	13.8	1136.5	28.2	1136.5	28.2	98.0
H15-004 26May2014-Spot12	97	198693	1.0	11.7096	1.2	2.6546	1.7	0.2254	1.3	0.75	1310.6	15.5	1315.9	12.9	1324.6	22.5	1324.6	22.5	98.9
H15-004 26May2014-Spot13	656	62805	5.2	13.8651	0.7	1.4593	1.6	0.1467	1.4	0.89	882.7	11.7	913.7	9.7	989.4	15.2	989.4	15.2	89.2
H15-004 26May2014-Spot14	75	53549	3.0	12.2079	1.1	2.3279	1.7	0.2061	1.2	0.73	1208.1	13.2	1220.8	11.7	1243.4	22.2	1243.4	22.2	97.2
H15-004 26May2014-Spot15	396	248171	3.7	12.7282	1.1	2.0939	1.8	0.1933	1.4	0.78	1139.2	14.9	1146.8	12.5	1161.2	22.5	1161.2	22.5	98.1
H15-004 26May2014-Spot16	407	1705410	1.9	11.8392	1.2	2.5296	2.0	0.2172	1.5	0.79	1267.1	17.7	1280.6	14.3	1303.3	23.5	1303.3	23.5	97.2
H15-004 26May2014-Spot17	1511	116123	3.2	13.4875	1.0	1.6835	1.6	0.1647	1.2	0.78	982.8	11.1	1002.3	10.0	1045.4	19.9	1045.4	19.9	94.0
H15-004 26May2014-Spot18	530	60833	46.8	13.5833	1.1	1.6219	1.7	0.1598	1.3	0.77	955.6	12.0	978.7	11.0	1031.0	22.5	1031.0	22.5	92.7
H15-004 26May2014-Spot19	395	178775	7.5	13.1105	1.4	1.6425	2.1	0.1562	1.6	0.76	935.8	14.0	986.7	13.4	1101.7	27.6	1101.7	27.6	84.9
H15-004 26May2014-Spot20	201	165594	3.1	13.9562	1.2	1.6159	1.7	0.1636	1.2	0.70	976.6	10.6	976.4	10.5	976.1	24.5	976.1	24.5	100.0
H15-004 26May2014-Spot21	813	99567	4.9	12.3154	1.1	2.2467	1.8	0.2007	1.4	0.80	1179.0	15.2	1195.8	12.4	1226.2	20.7	1226.2	20.7	96.1
H15-004 26May2014-Spot22	357	124235	3.6	15.6443	1.2	0.9783	1.9	0.1110	1.5	0.77	678.6	9.4	692.7	9.4	739.0	25.1	678.6	9.4	91.8
H15-004 26May2014-Spot23	375	207102	11.6	12.9950	1.0	2.0007	1.8	0.1886	1.6	0.86	1113.6	16.2	1115.7	12.5	1120.0	19.1	1120.0	19.1	99.4
H15-004 26May2014-Spot24	134	87950	2.1	12.7912	0.9	1.8570	1.9	0.1723	1.7	0.89	1024.6	16.2	1065.9	12.7	1151.4	17.2	1151.4	17.2	89.0
H15-004 26May2014-Spot25	163	154249	3.5	12.7676	1.3	2.1420	1.9	0.1983	1.3	0.72	1166.4	14.2	1162.5	12.8	1155.1	25.6	1155.1	25.6	101.0
H15-004 26May2014-Spot26	121	196424	2.4	13.4489	1.7	1.7828	2.0	0.1739	1.2	0.57	1033.6	11.0	1039.2	13.1	1051.2	33.4	1051.2	33.4	98.3
H15-004 26May2014-Spot27	142	133511	3.0	13.8512	1.2	1.5187	1.8	0.1526	1.3	0.75	915.3	11.3	937.9	10.8	991.5	23.6	991.5	23.6	92.3
H15-004 26May2014-Spot28	265	47516	30.3	16.4487	1.6	0.7341	2.0	0.0876	1.2	0.60	541.2	6.4	558.9	8.7	632.0	34.8	541.2	6.4	85.6
H15-004 26May2014-Spot29	272	53039	27.7	17.0394	1.3	0.6387	2.1	0.0789	1.7	0.78	489.7	7.8	501.5	8.4	555.5	28.7	489.7	7.8	88.2
H15-004 26May2014-Spot30	795	195141	5.0	13.0498	1.1	1.7147	1.6	0.1623	1.2	0.75	969.5	11.0	1041.1	10.5	1111.5	21.6	1111.5	21.6	87.2
H15-004 26May2014-Spot31	187	117622	1.5	12.9156	0.9	1.8755	1.6	0.1757	1.3	0.80	1043.4	12.2	1072.5	10.4	1132.2	18.8	1132.2	18.8	92.2
H15-004 26May2014-Spot32	114	72909	3.8	12.7650	1.2	2.0739	1.9	0.1920	1.5	0.79	1132.2	15.4	1140.2	12.9	1155.5	23.1	1155.5	23.1	98.0
H15-004 26May2014-Spot33	160	162128	3.2	12.7266	1.1	2.1189	1.9	0.1955	1.6	0.82	1151.4	16.8	1155.0	13.3	1161.8	21.7	1161.8	21.7	99.1
H15-004 26May2014-Spot34	129	34210	4.7	13.7768	1.1	1.7195	1.8	0.1718	1.4	0.79	1022.1	13.2	1015.8	11.4	1002.4	22.1	1002.4	22.1	102.0
H15-004 26May2014-Spot35	242	259959	3.3	12.7686	0.8	1.9963	2.2	0.1849	2.0	0.93	1093.5	20.5	1144.3	14.8	1154.9	16.0	1154.9	16.0	94.7
H15-004 26May2014-Spot36	115	32038	2.6	12.7253	1.0	2.0971	1.8	0.1935	1.5	0.82	1140.6	15.2	1147.9	12.2	1161.6	20.3	1161.6	20.3	98.2
H15-004 26May2014-Spot37	58	74453	2.7	12.8358	1.7	1.9988	2.3	0.1861	1.6	0.69	1100.1	15.8	1115.1	15.4	1144.5	33.0	1144.5	33.0	96.1
H15-004 26May2014-Spot38	281	131116	18.1	16.1279	1.9	2.1529	1.8	0.0906	1.3	0.74	558.9	7.2	582.2	8.1	674.2	26.6	558.9	7.2	82.9
H15-004 26May2014-Spot39	403	199538	2.4	12.3829	0.2	1.7543	1.8	0.1933	1.5	0.87	1139.5	16.1	1166.0	12.3	1215.5	17.5	1215.5	17.5	93.7
H15-004 26May2014-Spot40	90	43514	3.1	13.4324	1.6	1.7725	2.0	0.1727	1.2	0.59	1026.9	11.1	1035.4	12.9	1053.6	32.3	1053.6	32.3	97.5
H15-004 26May2014-Spot41	259	69097	5.3	13.6081	1.1	1.7018	1.8	0.1680	1.5	0.80	1000.9	13.5	1009.2	11.6	1027.4	21.8	1027.4	21.8	97.4
H15-004 26May2014-Spot42	963	1204731	2.2	12.5339	1.3	2.1010	2.0	0.1910	1.5	0.74	1126.7	15.2	1149.1	13.7	1191.6	26.5	1191.6	26.5	94.6
H15-004 26May2014-Spot43	529	73925	1.7	12.7469	0.9	2.1153	1.4	0.1956	1.0	0.73	1151.4	10.5	1153.8	9.4	1158.3	18.3	1158.3	18.3	99.4
H15-004 26May2014-Spot44	189	206610	1.9	12.9338	1.0	2.0999	2.3	0.1970	2.1	0.90	1159.1	22.1	1148.8	15.8	1129.4	19.7	1129.4	19.7	102.6
H15-004 26May2014-Spot45	785	469196	3.4	12.1860	0.9	2.1157	1.8	0.1870	1.6	0.88	1105.0	16.4	1143.9	12.6	1247.0	17.0	1247.0	17.0	88.6
H15-004 26May2014-Spot46	264	64855	13.5	13.1045	1.3	1.9554	2.1	0.1858	1.6	0.77	1098.8	16.0	1100.3	13.8	1103.2	26.3	1103.2	26.3	99.6



Appendix F. LA-ICPMS U-Pb Zircon Geochronology (continued)

Analysis	U (ppm)	206Pb/204Pb	U/Th	206Pb*/207Pb*	± (%)	Isotope ratios			Apparent ages (Ma)			Best age (Ma)	± (Ma)	Conc (%)					
						207Pb*/235U*	± (%)	206Pb*/238U*	± (%)	207Pb*/235U*	± (Ma)				206Pb*/207Pb*	± (Ma)			
H15-004 26May2014-Spot 48	55	88926	2.9	12.8017	1.3	2.0596	2.0	0.1912	1.5	0.76	1128.0	15.8	1135.5	13.8	1149.8	26.2	1149.8	26.2	98.1
H15-004 26May2014-Spot 49	483	127774	0.5	13.3087	1.1	1.8368	1.8	0.1773	1.5	0.82	1052.2	14.4	1058.7	12.0	1072.2	21.1	1072.2	21.1	98.1
H15-004 26May2014-Spot 50	215	280402	3.3	11.8599	1.2	2.6368	2.0	0.2268	1.6	0.80	1317.7	19.5	1311.0	15.1	1299.9	24.1	1299.9	24.1	101.4
H15-004 26May2014-Spot 51	821	389754	6.9	13.5938	1.3	1.7203	2.2	0.1696	1.8	0.82	1009.9	16.8	1016.1	14.1	1029.5	25.7	1029.5	25.7	98.1
H15-004 26May2014-Spot 52	166	208652	2.9	13.7579	1.4	1.5373	2.1	0.1534	1.5	0.73	919.9	13.0	945.4	12.7	1005.2	28.7	1005.2	28.7	91.5
H15-004 26May2014-Spot 54	70	90590	7.2	11.9288	1.2	2.4975	2.1	0.2160	1.7	0.82	1260.9	19.7	1271.3	15.3	1288.9	23.8	1288.9	23.8	97.8
H15-004 26May2014-Spot 55	423	77444	1.4	11.9072	1.1	2.4248	2.1	0.2094	1.8	0.85	1225.6	19.7	1250.0	15.0	1292.1	21.5	1292.1	21.5	94.9
H15-004 26May2014-Spot 56	85	98389	2.2	13.2914	1.3	1.8327	1.8	0.1767	1.2	0.67	1048.8	11.4	1057.3	11.5	1074.8	26.1	1074.8	26.1	97.6
H15-004 26May2014-Spot 57	183	136652	1.2	12.1302	1.0	2.2762	1.6	0.2003	1.2	0.79	1176.7	13.3	1204.9	11.0	1256.0	18.6	1256.0	18.6	93.7
H15-004 26May2014-Spot 58	324	75864	3.2	13.6273	1.0	1.7762	1.6	0.1756	1.2	0.78	1042.6	11.8	1036.8	10.2	1024.5	20.0	1024.5	20.0	101.8
H15-004 26May2014-Spot 59	128	143579	2.6	12.8575	1.1	2.0105	1.8	0.1875	1.4	0.78	1107.7	14.0	1119.1	12.0	1141.1	22.2	1141.1	22.2	97.1
H15-004 26May2014-Spot 60	325	215503	1.6	13.9789	1.2	1.4499	1.7	0.1470	1.2	0.70	884.1	10.0	909.8	10.4	972.8	25.2	972.8	25.2	90.9
H15-004 26May2014-Spot 61	488	157114	3.6	12.7709	0.9	2.1687	1.7	0.2009	1.4	0.83	1180.0	15.1	1171.1	11.7	1154.5	18.5	1154.5	18.5	102.2
H15-004 26May2014-Spot 62	210	167102	2.6	13.4862	1.2	1.8657	2.0	0.1825	1.5	0.78	1080.5	15.4	1069.0	13.1	1045.6	25.1	1045.6	25.1	103.3
H15-004 26May2014-Spot 63	201	74367	3.4	13.8052	1.2	1.7182	1.8	0.1720	1.2	0.71	1023.3	11.8	1015.4	11.3	998.2	25.1	998.2	25.1	102.5
H15-004 26May2014-Spot 64	42	144953	2.2	13.2237	1.5	1.7687	1.9	0.1696	1.2	0.61	1010.1	10.9	1034.0	12.4	1085.1	30.2	1085.1	30.2	93.1
H15-004 26May2014-Spot 65	188	154900	2.4	13.2808	1.1	1.7754	1.9	0.1710	1.5	0.80	1017.7	14.2	1036.5	12.3	1076.4	23.0	1076.4	23.0	94.5
H15-004 26May2014-Spot 66	146	120991	2.6	14.2838	2.3	1.3432	3.8	0.1391	3.1	0.81	839.8	24.3	864.6	22.3	925.6	36.1	1257.6	36.1	90.4
H15-004 26May2014-Spot 67	51	41796	5.3	12.1201	1.2	2.3195	2.2	0.2039	1.3	0.56	1196.2	13.7	1218.3	15.9	1257.6	36.1	1257.6	36.1	95.1
H15-004 26May2014-Spot 68	366	173204	5.7	9.8942	1.1	3.6366	1.8	0.2610	1.5	0.82	1494.8	20.2	1557.6	14.7	1643.8	19.7	1643.8	19.7	90.9
H15-004 26May2014-Spot 69	487	55172	2.6	13.6765	0.9	1.7165	1.5	0.1703	1.3	0.83	1013.5	11.9	1014.7	9.9	1017.2	17.5	1017.2	17.5	99.6
H15-004 26May2014-Spot 70	116	106517	2.4	13.0880	1.2	1.8834	1.9	0.1788	1.5	0.80	1060.3	15.0	1075.3	12.8	1105.7	23.3	1105.7	23.3	95.9
H15-004 26May2014-Spot 71	413	83499	13.7	13.1618	1.1	1.9682	1.8	0.1879	1.5	0.81	1109.9	15.1	1104.7	12.4	1094.5	21.9	1094.5	21.9	101.4
H15-004 26May2014-Spot 72	397	64637	2.3	12.3686	1.0	2.3878	1.6	0.2142	1.2	0.79	1251.2	14.1	1239.0	11.3	1217.8	19.3	1217.8	19.3	102.7
H15-004 26May2014-Spot 73	98	90397	5.3	14.4829	1.7	1.1685	2.3	0.1227	1.6	0.68	746.3	11.1	786.0	12.6	900.1	34.9	746.3	34.9	82.9
H15-004 26May2014-Spot 75	297	187580	67.8	17.1873	2.0	0.6327	2.5	0.0789	1.5	0.60	489.3	7.0	497.8	9.7	536.7	42.9	489.3	42.9	91.2
H15-004 26May2014-Spot 76	149	56274	2.7	7.7886	0.8	6.3917	1.8	0.3611	1.6	0.89	1987.2	27.3	2031.1	15.8	2076.1	14.4	2076.1	14.4	95.7
H15-004 26May2014-Spot 77	421	661066	2.3	12.9556	1.1	1.9470	1.9	0.1829	1.6	0.81	1083.0	15.5	1097.4	12.9	1126.0	22.7	1126.0	22.7	96.2
H15-004 26May2014-Spot 78	317	77011	1.6	13.8853	1.0	1.4961	1.7	0.1507	1.4	0.81	904.7	11.6	928.8	10.4	986.5	20.5	986.5	20.5	91.7
H15-004 26May2014-Spot 79	48	28654	1.8	12.4431	1.8	2.1716	2.7	0.1960	2.0	0.75	1153.7	21.1	1172.0	18.6	1206.0	35.1	1206.0	35.1	95.7
H15-004 26May2014-Spot 80	432	57474	5.3	13.7799	1.0	1.5796	1.8	0.1579	1.5	0.84	944.9	13.2	962.2	11.2	1001.9	19.9	1001.9	19.9	94.3
H15-004 26May2014-Spot 81	85	110568	2.9	12.7539	1.4	2.1418	2.2	0.1981	1.6	0.76	1165.2	17.5	1162.4	14.9	1157.2	27.6	1157.2	27.6	100.7
H15-004 26May2014-Spot 82	103	50079	2.9	12.5133	1.4	2.1726	2.0	0.1972	1.4	0.68	1160.1	14.4	1172.3	13.8	1194.9	28.6	1194.9	28.6	97.1
H15-004 26May2014-Spot 83	97	72819	5.5	13.7095	1.2	1.7061	2.0	0.1696	1.6	0.79	1010.1	14.5	1010.8	12.6	1012.3	24.5	1012.3	24.5	98.8
H15-004 26May2014-Spot 84	952	2451909	25.7	13.4571	0.9	1.6189	1.6	0.1580	1.4	0.85	945.7	12.3	977.6	10.3	1049.9	17.4	1049.9	17.4	90.1
H15-004 26May2014-Spot 85	104	99436	2.6	12.8914	1.5	2.0743	2.4	0.1939	1.9	0.77	1147.7	19.4	1140.3	16.5	1135.9	30.5	1135.9	30.5	100.6
H15-004 26May2014-Spot 87	161	172245	3.5	11.8882	1.1	2.0316	1.9	0.1752	1.6	0.81	1040.5	15.2	1126.1	13.2	1295.2	22.2	1295.2	22.2	80.3
H15-004 26May2014-Spot 88	205	79054	2.7	12.8882	1.1	1.9570	1.6	0.1829	1.1	0.70	1083.0	11.1	1100.9	10.6	1136.4	22.4	1136.4	22.4	95.3
H15-004 26May2014-Spot 89	468	105270	3.3	13.5960	0.9	1.7392	1.4	0.1715	1.1	0.78	1020.4	10.3	1023.2	9.1	1029.2	17.9	1029.2	17.9	99.1
H15-004 26May2014-Spot 90	188	132860	2.7	12.5629	1.3	2.0275	1.7	0.1660	1.1	0.66	1092.8	11.6	1124.8	11.1	1187.1	24.8	1187.1	24.8	92.1
H15-004 26May2014-Spot 91	543	231677	2.2	13.3610	1.1	1.8044	1.8	0.1749	1.4	0.78	1038.8	13.6	1047.0	11.9	1064.3	23.0	1064.3	23.0	97.6
H15-004 26May2014-Spot 92	582	235047	6.1	13.4730	1.1	1.7250	2.1	0.1686	1.8	0.84	1004.2	16.7	1017.9	13.7	1047.5	23.2	1047.5	23.2	95.9
H15-004 26May2014-Spot 93	195	240709	2.3	12.4353	1.2	1.4521	1.6	0.2094	1.2	0.75	1225.8	13.2	1219.1	11.3	1206.2	20.8	1207.2	20.8	101.5
H15-004 26May2014-Spot 94	248	57323	5.8	14.1598	1.1	1.4592	1.8	0.1499	1.4	0.78	900.1	12.0	913.7	11.0	946.5	23.2	946.5	23.2	95.1
H15-004 26May2014-Spot 95	1152	63439	5.0	13.3067	0.9	1.5708	1.7	0.1516	1.4	0.84	909.9	12.0	958.7	10.5	1072.5	18.5	1072.5	18.5	84.8
H15-004 26May2014-Spot 96	93	396334	3.0	12.4676	1.2	2.2739	1.8	0.2056	1.4	0.77	1205.4	15.5	1204.2	12.9	1202.1	22.9	1202.1	22.9	100.3

Appendix F: LA-ICPMS U-Pb Zircon Geochronology (Continued)

Analysis	U (ppm)	206Pb/204Pb	U/Th	206Pb*/207Pb*	± (%)	Isotope ratios			Apparent ages (Ma)			Best age (Ma)	± (Ma)	Conc (%)			
						207Pb*/235U*	± (%)	206Pb*/238U	± (%)	207Pb*/235U	± (Ma)				206Pb*/207Pb*	± (Ma)	
H15-004_26May2014-Spot 97	371	457994	1.8	13.0936	1.8	0.1911	1.6	0.85	1127.4	16.7	1119.7	12.9	1104.9	20.1	1104.9	20.1	102.0
H15-004_26May2014-Spot 98	244	66503	8.9	13.6246	1.0	1.6628	1.5	0.83	980.7	13.4	994.5	11.3	1024.9	20.3	1024.9	20.3	95.7
H15-004_26May2014-Spot 100	140	47586	3.1	12.9031	1.3	1.9264	1.2	0.67	1068.5	11.9	1090.3	12.1	1134.1	26.7	1134.1	26.7	94.2
H15-004_26May2014-Spot 101	106	193738	2.2	13.4494	1.5	1.6904	1.3	0.65	983.9	12.1	1004.9	13.0	1051.1	31.1	1051.1	31.1	93.6
H15-004_26May2014-Spot 102	359	112339	8.8	12.2405	1.0	2.3127	1.8	0.84	1203.8	16.6	1216.2	12.8	1238.3	19.3	1238.3	19.3	97.2
H15-004_26May2014-Spot 103	171	113877	0.7	12.7832	1.0	2.1020	1.4	0.81	1147.8	14.8	1149.5	11.9	1152.6	19.9	1152.6	19.9	98.6
H15-004_26May2014-Spot 104	608	219078	13.6	12.3464	0.8	2.2911	2.0	0.92	1203.0	20.2	1209.5	14.2	1221.3	15.9	1221.3	15.9	98.5
H15-004_26May2014-Spot 105	308	167807	3.7	13.1917	1.1	1.8437	2.2	0.87	1047.2	18.6	1061.2	14.6	1089.9	22.2	1089.9	22.2	96.1
H15-004_26May2014-Spot 106	311	2103620	3.3	12.8273	0.9	2.1434	1.5	0.83	1172.1	13.6	1162.9	10.6	1145.8	17.2	1145.8	17.2	102.3
H15-004_26May2014-Spot 107	78	98448	2.6	13.1093	1.3	1.8119	1.8	0.66	1024.6	11.1	1049.7	11.6	1102.5	26.8	1102.5	26.8	92.9
H15-004_26May2014-Spot 108	286	138408	6.0	13.6047	0.8	1.7379	1.6	0.87	1020.2	13.6	1022.7	10.6	1027.9	16.1	1027.9	16.1	99.3
H15-004_26May2014-Spot 109	234	209316	5.1	13.2163	1.3	1.5997	1.8	0.67	919.6	10.2	970.1	11.0	1086.2	26.0	1086.2	26.0	84.7
H15-004_26May2014-Spot 110	84	158813	1.9	13.3872	1.6	1.8333	2.1	0.65	1056.0	13.4	1057.5	13.9	1060.4	32.6	1060.4	32.6	99.6
H15-004_26May2014-Spot 125	449	169318	4.7	12.6383	1.0	2.1253	1.8	0.83	1147.4	16.1	1157.1	12.7	1175.3	20.3	1175.3	20.3	97.6
H15-004_Run2-Spot 146	1612	76696	2.9	12.5532	1.4	2.1071	2.7	0.85	1131.3	23.6	1151.1	18.3	1188.6	27.5	1188.6	27.5	95.2
H15-004_Run2-Spot 147	847	204879	4.9	12.7295	1.2	2.1015	2.8	0.90	1143.1	26.7	1149.3	19.4	1161.0	24.0	1161.0	24.0	98.5
H15-004_Run2-Spot 148	425	70887	3.7	13.6944	2.0	1.4857	3.1	0.77	887.3	19.8	924.6	18.9	1014.6	40.4	1014.6	40.4	87.5
H15-004_Run2-Spot 149	448	154830	2.8	11.4120	1.5	2.6308	2.6	0.80	1269.9	23.7	1309.3	18.9	1374.3	29.5	1374.3	29.5	92.4
H15-004_Run2-Spot 150	607	188948	2.9	12.5507	1.9	1.9430	4.1	0.89	1049.8	35.4	1096.0	27.6	1189.0	37.2	1189.0	37.2	88.3
H15-004_Run2-Spot 151	254	43175	1.9	13.4624	1.9	1.8390	2.9	0.76	1061.3	21.4	1057.3	18.9	1049.1	37.7	1049.1	37.7	101.2
H15-004_Run2-Spot 152	1346	97725	3.4	13.2380	1.2	1.5873	2.5	0.1524	180	965.2	15.3	1082.9	25.0	1082.9	25.0	84.4	
H15-004_Run2-Spot 153	280	41712	6.0	12.5342	2.0	2.1514	4.0	0.86	914.4	18.0	965.2	15.3	1082.9	25.0	1082.9	25.0	84.4
H15-004_Run2-Spot 154	969	484021	8.1	12.8786	1.3	1.8612	4.5	0.96	1033.2	41.4	1067.4	29.9	1137.9	26.1	1137.9	26.1	90.8
H15-004_Run2-Spot 155	780	97456	11.0	13.5331	1.5	1.6075	2.7	0.83	944.4	19.6	973.1	16.8	1038.5	30.1	1038.5	30.1	90.9
H15-004_Run2-Spot 156	442	50301	1.8	13.3071	1.4	1.6059	2.6	0.84	928.9	19.0	972.5	16.4	1072.5	28.9	1072.5	28.9	86.6
H15-004_Run2-Spot 157	288	143686	3.9	12.2471	1.8	2.2963	2.3	0.63	1196.6	15.6	1211.2	16.1	1237.2	34.9	1237.2	34.9	96.7
H15-004_Run2-Spot 158	1887	151631	39.4	17.7776	1.4	0.5703	2.0	0.74	457.4	6.7	458.2	7.5	462.3	30.4	457.4	6.7	99.0
H15-004_Run2-Spot 159	1038	108897	3.5	12.8740	1.5	1.9268	2.5	0.80	1066.4	19.3	1090.4	16.5	1138.6	29.6	1138.6	29.6	93.7
H15-004_Run2-Spot 160	1680	221342	23.7	13.6232	1.2	1.4972	1.9	0.77	889.4	12.1	929.3	11.4	1025.1	24.1	1025.1	24.1	86.8
H15-004_Run2-Spot 161	265	43336	1.6	12.3521	1.8	2.2603	2.9	0.80	1188.7	25.3	1200.0	20.5	1220.4	34.6	1220.4	34.6	97.4
H15-004_Run2-Spot 162	1384	209727	5.2	14.3682	2.3	1.1285	3.9	0.80	716.7	21.1	767.0	20.9	916.5	48.2	716.7	21.1	78.2
H15-004_Run2-Spot 163	108	58439	1.5	13.0677	1.7	1.8017	2.5	0.76	1016.3	18.1	1046.1	16.6	1108.8	33.2	1108.8	33.2	91.7
H15-004_Run2-Spot 164	395	42453	5.7	12.2804	1.5	2.0978	2.0	0.65	1104.2	13.0	1148.1	13.5	1231.9	29.1	1231.9	29.1	89.6
H15-004_Run2-Spot 165	1181	139190	2.2	13.1066	1.3	1.8428	2.7	0.88	1040.6	23.2	1060.9	18.0	1102.9	25.9	1102.9	25.9	94.3
H15-004_Run2-Spot 166	119	34559	2.1	12.8812	2.5	1.7649	3.7	0.74	983.8	24.8	1032.6	23.9	1137.5	49.3	1137.5	49.3	86.5
H15-004_Run2-Spot 167	340	37577	1.4	13.2620	1.6	1.7874	2.4	0.60	655.2	15.2	708.6	20.9	881.6	67.8	655.2	15.2	74.3
H15-004_Run2-Spot 168	81	22001	3.3	14.6130	3.3	1.0095	4.1	0.1070	20.4	0.60	655.2	15.2	708.6	67.8	655.2	15.2	74.3
H15-004_Run2-Spot 169	191	35665	1.3	13.0326	2.2	1.8565	3.0	0.68	1042.3	20.3	1065.8	19.6	1114.2	43.5	1114.2	43.5	93.5
H15-004_Run2-Spot 170	779	221920	12.6	12.2446	2.3	2.2981	3.4	0.73	1197.2	27.3	1211.7	24.2	1237.6	45.8	1237.6	45.8	96.7
H15-004_Run2-Spot 171	244	191622	2.7	12.5191	1.8	2.2939	3.3	0.83	1219.7	30.4	1210.4	23.4	1194.0	36.5	1194.0	36.5	102.2
H15-004_Run2-Spot 172	1547	137280	36.8	12.9671	1.3	1.8648	2.4	0.80	1041.7	19.1	1068.7	15.8	1124.2	26.3	1124.2	26.3	92.7
H15-004_Run2-Spot 173	776	92353	1.8	13.6134	1.4	1.7459	2.3	0.80	1025.2	17.8	1025.6	15.1	1026.6	28.2	1026.6	28.2	99.9
H15-004_Run2-Spot 174	1064	162274	3.2	12.7497	1.3	1.9628	3.0	0.81	1075.2	26.7	1102.8	20.0	1157.8	25.0	1157.8	25.0	92.9
H15-004_Run2-Spot 175	81	44972	3.2	13.9372	3.3	1.5143	3.9	0.54	918.2	17.9	936.2	23.7	978.8	66.6	978.8	66.6	93.8
H15-004_Run2-Spot 176	227	81583	3.5	12.2920	1.6	2.1447	2.4	0.73	1127.9	18.1	1163.3	16.5	1230.0	31.7	1230.0	31.7	91.7
H15-004_Run2-Spot 177	163	50362	4.8	12.3142	2.1	2.2794	2.8	0.66	1194.5	20.3	1205.9	19.8	1226.4	41.3	1226.4	41.3	97.4

Appendix F. LA-ICPMS U-Pb Zircon Geochronology (continued)

Analysis	U (ppm)	206Pb/204Pb	U/Th	206Pb*/207Pb*	± (%)	Isotope ratios			Apparent ages (Ma)			Best age (Ma)	± (Ma)	Conc (%)					
						207Pb*/235U*	± (%)	206Pb*/238U*	± (%)	207Pb*/235U*	± (Ma)				206Pb*/207Pb*	± (Ma)			
H15-004_Run2_Spot 178	248	115833	3.4	12.5354	1.5	2.0081	2.9	0.86	1081.0	24.7	1182.2	19.5	1191.4	28.8	1191.4	28.8	1191.4	28.8	90.7
H15-004_Run2_Spot 179	179	50149	1.9	13.2159	2.1	1.7478	2.6	0.62	998.5	15.1	1026.4	17.0	1086.3	41.5	1086.3	41.5	1086.3	41.5	91.9
H15-004_Run2_Spot 180	486	85409	3.7	13.3214	1.3	1.8174	2.4	0.83	1042.8	19.0	1051.7	15.6	1070.3	26.7	1070.3	26.7	1070.3	26.7	97.4
H15-004_Run2_Spot 181	479	68106	2.0	13.1203	1.8	1.7209	3.2	0.82	977.6	23.7	1016.3	20.5	1100.8	36.6	1100.8	36.6	1100.8	36.6	88.8
H15-004_Run2_Spot 182	226	38776	2.0	13.4102	2.2	1.5887	3.6	0.80	926.2	2.9	965.8	22.7	1057.0	44.0	1057.0	44.0	1057.0	44.0	87.6
H15-004_Run2_Spot 183	311	49505	2.3	12.7348	1.9	2.1046	2.9	0.74	1145.1	22.3	1150.3	19.7	1160.2	38.2	1160.2	38.2	1160.2	38.2	98.7
H15-004_Run2_Spot 184	295	58780	3.4	11.6660	1.7	2.3089	3.5	0.88	1150.3	32.3	1215.0	24.8	1331.8	32.4	1331.8	32.4	1331.8	32.4	86.4
H15-004_Run2_Spot 185	720	70019	1.2	14.2513	1.7	1.4164	1.7	0.70	880.8	9.8	895.9	10.1	933.3	24.7	933.3	24.7	933.3	24.7	94.4
H15-004_Run2_Spot 186	294	122640	2.3	14.0075	1.6	1.6159	2.5	0.76	979.9	17.5	976.4	15.8	968.6	33.3	968.6	33.3	968.6	33.3	101.2
H15-004_Run2_Spot 187	980	252050	3.4	12.6872	1.3	1.9797	3.0	0.82	1078.8	26.4	1108.6	19.9	1167.6	25.5	1167.6	25.5	1167.6	25.5	92.4
H15-004_Run2_Spot 188	741	111067	12.5	16.0739	1.9	0.7526	3.8	0.87	542.1	17.1	569.7	16.6	681.4	41.2	542.1	17.1	542.1	17.1	79.6
H15-004_Run2_Spot 189	496	74269	2.5	12.5294	1.4	2.2102	2.4	0.81	1179.8	21.0	1184.3	16.9	1192.3	28.3	1192.3	28.3	1192.3	28.3	99.0
H15-004_Run2_Spot 190	652	62669	6.0	13.2083	1.7	1.4736	2.5	0.75	851.2	15.1	919.6	15.3	1087.4	33.8	1087.4	33.8	1087.4	33.8	78.3
H15-004_Run2_Spot 191	214	30341	2.9	12.7025	1.9	2.0234	3.2	0.80	1101.9	26.3	1123.4	22.0	1165.2	38.3	1165.2	38.3	1165.2	38.3	94.6
H15-004_Run2_Spot 192	116	26106	2.4	12.4226	2.7	1.9973	3.8	0.69	1066.7	25.7	1114.6	25.5	1209.2	53.6	1209.2	53.6	1209.2	53.6	88.2
H15-004_Run2_Spot 193	222	67924	3.0	12.7207	1.9	2.0933	3.2	0.80	1138.3	26.5	1146.6	21.7	1162.4	37.5	1162.4	37.5	1162.4	37.5	97.9
H15-004_Run2_Spot 194	133	50362	3.2	13.9829	2.9	1.5356	3.7	0.62	933.0	19.7	944.8	22.5	972.2	58.3	972.2	58.3	972.2	58.3	96.0
H15-004_Run2_Spot 195	629	84544	3.9	13.3099	1.5	1.6667	2.3	0.74	961.7	14.9	995.9	14.3	1072.1	30.5	1072.1	30.5	1072.1	30.5	89.7
H15-004_Run2_Spot 196	688	81693	210.4	17.6001	2.0	0.5785	3.0	0.73	459.2	2.2	484.5	11.2	484.5	45.2	459.2	9.8	484.5	9.8	94.8
H15-004_Run2_Spot 197	267	39605	4.2	12.7185	2.5	1.7537	3.9	0.77	966.6	27.3	1028.5	25.4	1162.7	49.5	1162.7	49.5	1162.7	49.5	83.1
H15-004_Run2_Spot 198	277	121524	2.9	12.5750	2.0	1.9020	3.1	0.76	1031.2	22.4	1081.8	20.4	1185.2	39.1	1185.2	39.1	1185.2	39.1	87.0
H15-004_Run2_Spot 199	107	157154	2.0	12.7982	1.9	2.0261	2.7	0.71	1110.9	19.7	1124.3	18.3	1150.3	37.5	1150.3	37.5	1150.3	37.5	96.6
H15-004_Run2_Spot 200	2871	3657751	4.3	12.4968	1.3	1.9805	2.2	0.81	1064.3	17.1	1108.9	14.5	1197.5	24.9	1197.5	24.9	1197.5	24.9	88.9
H15-004_Run2_Spot 201	847	136623	3.0	12.1414	1.5	2.3823	2.9	0.2098	1227.6	28.1	1237.3	21.1	1254.1	29.8	1254.1	29.8	1254.1	29.8	97.9
H15-004_Run2_Spot 202	288	78970	1.0	13.2957	1.3	1.8682	2.8	0.88	1067.8	24.5	1069.9	18.7	1074.2	26.6	1074.2	26.6	1074.2	26.6	99.4
H15-004_Run2_Spot 203	387	74077	2.2	13.7011	2.6	1.3545	3.5	0.68	814.0	18.4	869.5	20.6	1013.6	52.4	1013.6	52.4	1013.6	52.4	80.3
H15-004_Run2_Spot 204	385	73750	1.1	13.1316	2.0	1.8447	2.8	0.70	1043.4	18.9	1061.5	18.4	1099.1	39.8	1099.1	39.8	1099.1	39.8	94.9
H15-004_Run2_Spot 205	348	159118	5.9	12.9314	1.9	1.6999	3.3	0.82	963.6	24.1	1008.5	20.9	1107.4	37.1	1107.4	37.1	1107.4	37.1	87.0
H15-004_Run2_Spot 206	907	155043	5.5	12.9647	1.9	1.8886	2.7	0.72	1053.8	18.9	1077.1	17.9	1124.6	37.1	1124.6	37.1	1124.6	37.1	93.7
H15-004_Run2_Spot 207	113	119327	2.6	14.4994	2.9	1.5195	3.1	0.40	955.6	11.1	938.3	19.1	897.8	58.9	897.8	58.9	897.8	58.9	106.4
H15-004_Run2_Spot 208	708	279117	5.9	12.8017	1.4	2.0456	2.8	0.87	1121.0	25.1	1130.8	19.1	1149.8	27.5	1149.8	27.5	1149.8	27.5	97.5
H15-004_Run2_Spot 209	1137	143575	5.9	12.9314	1.1	1.9365	3.7	0.96	1075.8	35.1	1093.8	24.8	1129.8	21.7	1129.8	21.7	1129.8	21.7	95.2
H15-004_Run2_Spot 210	648	41568	6.1	15.8022	2.1	0.8416	3.1	0.73	593.6	12.8	620.0	14.4	717.7	45.1	593.6	12.8	593.6	12.8	82.7
H15-004_Run2_Spot 211	95	84652	3.6	13.0593	2.7	2.0861	3.5	0.66	1162.3	24.7	1144.2	24.3	1110.1	53.4	1110.1	53.4	1110.1	53.4	104.7
H15-004_Run2_Spot 212	454	126121	3.5	13.1435	1.4	1.8221	3.0	0.73	1032.4	24.9	1053.4	19.5	1097.3	28.5	1097.3	28.5	1097.3	28.5	94.1
H15-004_Run2_Spot 213	321	94308	4.7	13.2534	2.2	1.7678	3.4	0.66	1032.4	24.9	1053.4	19.5	1097.3	28.5	1097.3	28.5	1097.3	28.5	94.1
H15-004_Run2_Spot 214	293	128351	5.6	13.4903	2.5	1.6954	3.1	0.59	989.4	16.8	1006.8	19.8	1045.0	50.5	1045.0	50.5	1045.0	50.5	94.7
H15-004_Run2_Spot 215	520	106300	2.7	13.7487	1.5	1.6183	2.8	0.85	964.4	21.1	977.3	17.5	1006.5	29.9	1006.5	29.9	1006.5	29.9	95.8
H15-004_Run2_Spot 216	369	73334	2.6	12.8478	1.8	2.1103	3.5	0.85	1160.6	31.2	1154.4	23.9	1142.7	36.4	1142.7	36.4	1142.7	36.4	101.6
H15-004_Run2_Spot 217	2123	72446	7.2	13.0105	1.4	1.8323	3.1	0.90	1028.1	26.8	1057.1	20.6	1117.6	27.5	1117.6	27.5	1117.6	27.5	92.0
H15-004_Run2_Spot 218	1092	90574	2.6	12.8705	1.2	1.7916	4.4	0.96	996.9	38.8	1042.4	28.5	1139.1	24.7	1139.1	24.7	1139.1	24.7	87.5
H15-004_Run2_Spot 219	419	163047	3.9	13.2497	2.0	1.7597	2.5	0.58	1007.1	13.5	1030.7	16.1	1081.2	40.4	1081.2	40.4	1081.2	40.4	93.2
H15-004_Run2_Spot 220	204	129010	2.0	13.2589	2.4	1.8859	4.3	0.84	1074.3	35.7	1076.1	28.6	1079.9	47.3	1079.9	47.3	1079.9	47.3	99.5
H15-004_Run3_Spot 221	408	114777	2.9	13.7899	2.0	1.7277	2.9	0.74	1027.5	20.5	1018.9	18.8	1000.5	40.3	1000.5	40.3	1000.5	40.3	102.7
H15-004_Run3_Spot 222	304	69001	2.4	12.4416	1.3	2.1844	2.4	0.84	1159.8	21.3	1176.1	16.7	1206.2	25.8	1206.2	25.8	1206.2	25.8	96.1
H15-004_Run3_Spot 223	171	28013	2.1	13.5280	1.8	1.7395	2.7	0.73	1015.8	18.5	1023.3	17.4	1099.3	37.2	1099.3	37.2	1099.3	37.2	97.7

Appendix F. LA-ICPMS U-Pb Zircon Geochronology (continued)

Analysis	U (ppm)	206Pb/204Pb	U/Th	206Pb*/207Pb*	± (%)	Isotope ratios			Apparent ages (Ma)							Conc (%)			
						207Pb*/235U*	± (%)	206Pb*/238U*	± (%)	206Pb*/238U*	± (Ma)	207Pb*/235U*	± (Ma)	206Pb*/207Pb*	± (Ma)		Best age (Ma)	± (Ma)	
H15-004_Run3-Spot 224	48	36321	2.0	13.5431	3.4	1.7521	4.0	0.1721	2.0	0.49	1023.6	18.6	1027.9	25.6	1037.0	69.5	1037.0	69.5	98.7
H15-004_Run3-Spot 225	567	192254	6.7	13.5851	1.6	1.6290	2.5	0.1605	2.0	0.79	959.6	18.0	981.5	16.0	1030.8	31.4	1030.8	31.4	93.1
H15-004_Run3-Spot 226	89	33486	2.0	13.2759	2.8	1.7444	3.6	0.1680	2.3	0.63	1000.8	21.4	1025.1	23.5	1077.2	56.5	1077.2	56.5	92.9
H15-004_Run3-Spot 227	218	5315362	3.5	10.2191	1.6	3.1206	4.0	0.1312	3.7	0.81	1341.2	44.4	1437.8	30.8	1583.6	30.3	1583.6	30.3	84.7
H15-004_Run3-Spot 228	194	173817	2.1	13.2090	1.5	1.8326	2.6	0.1755	2.1	0.81	1042.3	20.2	1057.2	20.2	1088.2	29.9	1088.2	29.9	95.8
H15-004_Run3-Spot 229	685	85397	3.4	12.8403	1.8	2.0474	2.7	0.1907	1.9	0.73	1125.0	20.1	1131.4	18.2	1143.8	36.2	1143.8	36.2	98.4
H15-004_Run3-Spot 230	170	35381	2.7	13.7694	2.0	1.5032	2.8	0.1501	2.0	0.71	901.6	16.7	931.7	17.1	1003.5	40.0	1003.5	40.0	89.8
H15-004_Run3-Spot 231	1852	70708	7.3	13.9960	1.3	1.3439	3.9	0.1364	3.6	0.94	824.4	28.1	864.9	22.5	970.3	26.4	970.3	26.4	85.0
H15-004_Run3-Spot 232	583	267588	5.3	12.6160	2.1	2.2393	3.5	0.2049	2.8	0.80	1201.5	30.3	1193.4	24.2	1178.8	40.9	1178.8	40.9	101.9
H15-004_Run3-Spot 233	125	42875	2.3	13.6266	1.7	1.8072	2.8	0.1786	2.2	0.80	1059.4	21.8	1048.1	18.3	1024.6	34.1	1024.6	34.1	103.4
H15-004_Run3-Spot 234	217	43438	2.4	13.3920	2.1	1.7247	2.8	0.1675	2.2	0.64	998.4	16.4	1017.8	17.9	1059.7	43.2	1059.7	43.2	94.2
H15-004_Run3-Spot 235	420	56511	15.6	16.1701	1.8	0.7018	2.8	0.0823	2.1	0.76	509.9	10.3	539.9	11.7	668.7	39.0	509.9	10.3	76.3
H15-004_Run3-Spot 236	200	69226	5.8	14.1994	2.4	1.1790	3.3	0.1208	2.2	0.69	735.2	15.6	788.0	17.9	940.8	48.3	735.2	15.6	78.1
H15-004_Run3-Spot 237	140	48504	3.2	11.6067	2.1	1.6962	3.3	0.2270	2.6	0.77	1318.6	30.4	1327.4	24.5	1341.7	40.8	1341.7	40.8	98.3
H15-004_Run3-Spot 241	207	81867	1.5	10.3369	1.8	3.7915	2.6	0.2843	1.9	0.73	1612.7	27.7	1590.9	21.3	1562.2	33.8	1562.2	33.8	103.2
H15-004_Run3-Spot 242	62	17379	2.2	13.9296	2.7	1.5599	3.2	0.1576	1.8	0.55	943.4	15.5	954.4	19.9	980.0	54.7	980.0	54.7	96.3
H15-004_Run3-Spot 243	546	231754	4.0	13.5477	1.6	1.8367	2.3	0.1805	1.7	0.72	1069.5	16.3	1058.7	15.1	1036.3	32.4	1036.3	32.4	103.2
H15-004_Run3-Spot 244	340	44243	7.3	14.8055	1.1	1.1202	3.5	0.1203	2.8	0.80	732.2	19.5	763.1	18.9	854.6	43.6	732.2	19.5	85.7
H15-004_Run3-Spot 245	297	1565767	1.8	13.9235	1.4	1.5366	2.7	0.1552	2.3	0.85	929.9	19.6	945.1	16.3	980.9	28.2	980.9	28.2	94.8
H15-004_Run3-Spot 246	147	64910	3.6	13.7794	2.2	1.7013	3.0	0.1700	2.0	0.67	1012.3	18.8	1009.0	19.3	1002.0	45.5	1002.0	45.5	101.0
H15-004_Run3-Spot 247	483	61158	4.4	12.6482	1.9	2.1099	2.3	0.1936	1.4	0.59	1140.6	14.3	1152.0	16.0	1173.6	37.0	1173.6	37.0	97.2
H15-004_Run3-Spot 248	191	35633	1.7	13.3271	2.0	1.8835	3.2	0.1821	2.5	0.78	1078.2	25.2	1075.3	21.5	1069.5	40.6	1069.5	40.6	100.8
H15-004_Run3-Spot 249	292	142233	4.8	12.7211	1.2	2.1276	2.3	0.1963	2.0	0.86	1155.4	21.0	1157.8	15.9	1162.3	23.3	1162.3	23.3	99.4
H15-004_Run3-Spot 250	978	248313	5.6	13.3407	1.1	1.8304	2.5	0.1771	2.2	0.89	1051.1	21.5	1056.4	16.3	1067.4	22.6	1067.4	22.6	98.5
H15-004_Run3-Spot 251	603	174756	5.6	12.4223	1.4	2.2179	2.5	0.1998	2.1	0.84	1174.4	22.8	1186.7	17.7	1209.3	27.0	1209.3	27.0	97.1
H15-004_Run3-Spot 252	922	166070	2.2	13.0973	1.2	1.9343	3.1	0.1837	2.8	0.92	1087.4	28.2	1093.0	20.5	1104.3	23.5	1104.3	23.5	98.5
H15-004_Run3-Spot 253	624	73341	2.0	13.0365	1.4	1.9434	2.6	0.1838	2.2	0.85	1087.4	22.3	1096.2	17.5	1113.6	27.1	1113.6	27.1	97.7
H15-004_Run3-Spot 254	286	242626	3.8	13.2670	1.8	1.6507	2.9	0.1588	2.3	0.79	950.3	20.1	989.8	18.3	1078.5	36.0	1078.5	36.0	88.1
H15-004_Run3-Spot 255	387	1155086	3.0	13.1104	1.8	2.0072	2.8	0.1909	2.1	0.76	1126.0	22.1	1117.9	19.0	1102.3	36.0	1102.3	36.0	102.1
H15-004_Run3-Spot 256	88	101757	2.8	13.1795	2.2	1.9094	4.1	0.1825	3.5	0.84	1080.7	34.5	1084.4	27.4	1091.8	44.0	1091.8	44.0	99.0
H15-004_Run3-Spot 257	189	103213	1.5	13.3120	2.3	1.8661	3.3	0.1802	2.4	0.72	1067.9	23.3	1069.1	21.6	1071.7	45.4	1071.7	45.4	99.6
H15-004_Run3-Spot 258	260	54425	5.0	12.0477	1.7	1.9329	2.8	0.1689	2.2	0.80	1006.0	20.8	1092.5	18.8	1269.3	33.0	1269.3	33.0	79.3
H15-004_Run3-Spot 259	235	137145	1.8	11.7305	1.8	2.5653	2.5	0.2183	1.8	0.72	1272.6	21.0	1290.8	18.5	1321.2	33.9	1321.2	33.9	96.3
H15-004_Run3-Spot 260	208	36929	1.6	11.4536	1.8	2.6973	4.2	0.2241	3.8	0.90	1303.3	44.6	1327.7	31.0	1367.3	34.4	1367.3	34.4	95.3
H15-004_Run3-Spot 261	446	61941	2.1	12.8684	1.8	2.0572	2.5	0.1920	1.7	0.69	1132.2	17.8	1134.7	16.9	1139.5	35.6	1139.5	35.6	99.4
H15-004_Run3-Spot 262	446	82701	3.5	12.9500	1.4	1.9588	2.5	0.1840	2.0	0.82	1088.6	20.2	1101.5	16.6	1126.9	28.2	1126.9	28.2	96.6
H15-004_Run3-Spot 263	83	69082	2.5	10.9641	2.8	2.2718	3.6	0.2218	2.3	0.63	1291.4	26.5	1352.7	26.7	1450.9	52.7	1450.9	52.7	89.0
H15-004_Run3-Spot 264	91	29413	3.4	13.3304	2.6	1.8395	3.5	0.1778	2.4	0.68	1055.2	23.2	1059.7	23.1	1069.0	52.1	1069.0	52.1	98.7
H15-004_Run3-Spot 265	215	69111	2.8	11.7690	1.8	2.9853	3.1	0.2548	2.5	0.80	1463.3	32.2	1403.9	23.3	1314.8	35.5	1314.8	35.5	111.3
H15-004_Run3-Spot 266	131	25688	1.1	11.6426	1.7	1.6655	2.7	0.2251	2.2	0.79	1308.6	25.6	1318.9	20.1	1069.0	52.1	1069.0	52.1	98.7
H15-004_Run3-Spot 267	197	49819	3.3	13.6731	1.7	1.7115	2.2	0.1697	1.4	0.65	1010.6	13.5	1012.8	14.3	1017.7	34.3	1017.7	34.3	99.3
H15-004_Run3-Spot 268	260	178096	2.3	12.8729	1.9	1.9880	3.0	0.1856	2.3	0.78	1097.5	23.2	1111.4	20.0	1138.8	36.9	1138.8	36.9	96.4
H15-004_Run3-Spot 269	403	185766	2.1	12.9368	1.6	1.8609	2.6	0.1746	2.1	0.79	1037.4	19.9	1067.3	17.5	1128.9	32.6	1128.9	32.6	91.9

Appendix F. LA-ICPMS U-Pb Zircon Geochronology (continued)

Analysis	U (ppm)	206Pb/204Pb	U/Th	206Pb*/207Pb*	± (%)	Isotope ratios			Apparent ages (Ma)			Best age (Ma)	± (Ma)	Conc (%)							
						207Pb*/235U*	± (%)	206Pb*/238U*	± (%)	207Pb*/235U*	± (Ma)				206Pb*/207Pb*	± (Ma)					
H15-004_R.un3-Spot 270	328	44361	66.9	17.5084	2.5	0.6138	2.9	0.0779	1.5	0.51	483.8	7.0	483.8	7.0	97.5						
H15-004_R.un3-Spot 271	112	29121	4.2	13.2791	1.8	1.7872	2.9	0.1721	2.2	0.80	1040.8	20.8	1040.8	36.6	95.1						
H15-004_R.un3-Spot 272	864	236202	12.6	13.4021	1.3	1.7342	2.3	0.1686	1.8	0.80	1004.2	16.8	1021.3	14.5	1058.2	27.0	1058.2	27.0	1058.2	27.0	94.9
H15-004_R.un3-Spot 273	209	25886	2.2	13.8269	2.0	1.5334	2.7	0.1537	1.8	0.66	921.5	15.3	943.4	16.7	995.1	41.5	995.1	41.5	995.1	41.5	92.6
H15-004_R.un3-Spot 274	76	16281	1.2	13.8719	2.7	1.5882	3.6	0.1598	2.3	0.64	955.6	20.4	965.6	22.2	988.4	55.6	988.4	55.6	988.4	55.6	96.7
H15-004_R.un3-Spot 275	828	147954	2.6	11.7457	1.2	2.5823	2.7	0.2200	2.5	0.91	1281.8	28.9	1295.6	20.1	1318.7	22.4	1318.7	22.4	1318.7	22.4	97.2
H15-004_R.un3-Spot 276	162	57468	5.7	14.8630	2.8	0.9367	3.7	0.1010	2.5	0.67	620.1	14.9	671.1	18.3	846.5	57.4	620.1	14.9	73.3	14.9	73.3
H15-004_R.un3-Spot 277	190	34108	6.7	13.6698	2.3	1.7230	3.0	0.1708	2.0	0.65	1016.7	18.6	1017.2	19.5	1018.2	46.7	1018.2	46.7	1018.2	46.7	99.8
H15-004_R.un3-Spot 278	265	80519	3.7	13.7185	1.4	1.6443	2.3	0.1636	1.9	0.80	976.8	16.8	987.4	14.7	1011.0	28.3	1011.0	28.3	1011.0	28.3	96.6
H15-004_R.un3-Spot 279	1212	104858	3.0	13.9709	1.6	1.6465	2.6	0.1668	2.0	0.79	994.6	18.7	988.2	16.2	973.9	32.2	973.9	32.2	973.9	32.2	102.1
H15-004_R.un3-Spot 280	188	70151	3.8	12.6936	1.9	2.1550	2.5	0.1984	1.7	0.67	1166.7	18.1	1166.7	17.4	1166.6	36.7	1166.6	36.7	1166.6	36.7	100.0
H15-004_R.un3-Spot 281	288	170914	3.7	13.6303	1.8	1.6499	3.3	0.1631	2.8	0.83	974.0	25.0	989.5	21.0	1024.1	37.4	1024.1	37.4	1024.1	37.4	95.1
H15-004_R.un3-Spot 282	171	114172	2.1	11.6545	2.0	2.5668	2.6	0.2170	1.8	0.66	1265.8	20.1	1291.2	19.3	1333.7	38.1	1333.7	38.1	1333.7	38.1	94.9
H15-004_R.un3-Spot 283	198	71154	2.2	13.7318	1.9	1.6030	2.7	0.1596	1.9	0.71	954.8	16.9	971.4	16.7	1009.0	37.9	1009.0	37.9	1009.0	37.9	94.6
H15-004_R.un3-Spot 284	141	38312	1.8	13.2135	1.8	1.7954	3.8	0.1721	3.3	0.88	1023.5	31.6	1043.8	24.8	1086.6	36.6	1086.6	36.6	1086.6	36.6	94.2
H15-004_R.un3-Spot 285	354	46655	2.0	12.6451	1.1	2.1152	2.0	0.1940	1.7	0.84	1142.9	18.0	1153.8	14.1	1174.2	22.0	1174.2	22.0	1174.2	22.0	97.3
H15-004_R.un3-Spot 286	1683	167662	30.2	13.6614	1.7	1.2222	2.5	0.1211	1.9	0.76	736.9	13.4	810.8	14.2	1019.4	33.5	736.9	13.4	73.3	13.4	73.3
H15-004_R.un3-Spot 287	538	142337	6.5	13.5104	1.5	1.4501	2.1	0.1421	1.4	0.70	856.5	11.6	909.9	12.4	1041.9	29.7	1041.9	29.7	1041.9	29.7	82.2
H15-004_R.un3-Spot 288	251	57888	3.8	13.0872	2.0	1.9254	2.9	0.1828	2.1	0.73	1082.0	21.1	1090.0	19.4	1105.8	39.5	1105.8	39.5	1105.8	39.5	97.8
H15-004_R.un3-Spot 289	617	125651	22.6	16.7724	2.0	0.7118	3.1	0.0866	2.3	0.75	535.3	11.9	545.8	13.0	589.9	43.8	535.3	11.9	90.8	11.9	90.8
H15-004_R.un3-Spot 290	1757	208368	6.2	14.0177	1.0	1.5371	1.6	0.1563	1.3	0.81	936.0	11.6	945.4	10.1	967.1	19.6	967.1	19.6	967.1	19.6	96.8
H15-004_R.un3-Spot 291	633	87445	6.7	12.6421	1.6	2.0353	2.5	0.1866	2.1	0.84	1103.0	21.2	1127.4	17.0	1174.7	26.8	1174.7	26.8	1174.7	26.8	93.9
H15-004_R.un3-Spot 292	2283	231047	7.8	13.4341	1.2	1.7835	2.0	0.1738	1.6	0.79	1032.9	14.9	1039.5	12.9	1063.4	24.7	1063.4	24.7	1063.4	24.7	98.1
H15-004_R.un3-Spot 293	423	130239	13.0	13.4034	1.7	1.4203	2.5	0.1381	1.8	0.73	833.7	14.3	897.5	14.9	1058.0	34.6	1058.0	34.6	1058.0	34.6	78.8
H15-004_R.un3-Spot 294	701	215477	3.6	12.7641	1.1	2.2090	2.4	0.2045	2.1	0.89	1199.4	23.1	1183.9	16.5	1155.6	21.3	1155.6	21.3	1155.6	21.3	103.8
H15-004_R.un3-Spot 295	633	87445	6.7	12.6421	1.6	2.0353	2.5	0.1866	2.1	0.84	1103.0	21.2	1127.4	17.0	1174.7	26.8	1174.7	26.8	1174.7	26.8	93.9
H15-004_R.un3-Spot 296	95	72125	4.2	12.6601	2.8	2.1865	3.9	0.2008	2.7	0.69	1179.4	29.2	1176.8	27.3	1171.9	56.1	1171.9	56.1	1171.9	56.1	100.6
H15-004_R.un3-Spot 297	857	58667	4.0	13.5272	1.1	1.7402	2.2	0.1707	1.9	0.87	1016.1	17.8	1023.5	14.0	1039.4	21.6	1039.4	21.6	1039.4	21.6	97.8
H15-004_R.un3-Spot 298	325	45872	3.4	13.5769	1.6	1.7343	2.7	0.1708	2.2	0.81	1016.4	20.4	1021.3	17.3	1032.0	32.2	1032.0	32.2	1032.0	32.2	98.5
H15-004_R.un3-Spot 299	196	64828	1.0	13.3208	1.5	1.8218	3.4	0.1760	3.1	0.90	1045.1	29.5	1053.3	22.2	1070.4	29.2	1070.4	29.2	1070.4	29.2	97.6
H15-004_R.un3-Spot 300	1821	80556	6.6	13.5394	1.1	1.6912	2.4	0.1661	2.2	0.89	990.4	19.9	1005.2	15.5	1037.6	22.4	1037.6	22.4	1037.6	22.4	95.5
H15-004_R.un3-Spot 301	504	166671	92.2	17.8489	1.8	0.5829	2.7	0.0755	2.0	0.73	468.9	8.9	466.3	10.0	453.4	40.6	468.9	8.9	103.4	8.9	103.4
H15-004_R.un3-Spot 302	1975	61947	4.3	13.9999	0.9	1.6788	1.9	0.1705	1.7	0.89	1014.6	16.2	1000.5	12.4	969.7	18.5	969.7	18.5	969.7	18.5	104.6
H15-004_R.un3-Spot 303	396	66704	2.3	12.7708	1.8	2.0720	2.5	0.1919	1.9	0.75	1131.8	19.2	1139.6	17.0	1154.6	32.9	1154.6	32.9	1154.6	32.9	98.0
H15-004_R.un3-Spot 304	103	195063	3.2	13.8859	1.7	1.6447	4.1	0.1656	3.7	0.91	988.0	34.0	987.5	25.8	986.4	34.6	986.4	34.6	986.4	34.6	100.2
H15-004_R.un3-Spot 305	719	127509	1.5	12.8125	1.3	2.1085	2.0	0.1959	1.5	0.76	1153.4	16.3	1151.6	14.1	1148.1	26.5	1148.1	26.5	1148.1	26.5	100.5
H15-004_R.un3-Spot 306	657	242917	3.7	13.4039	1.1	1.8292	2.1	0.1778	1.8	0.85	1055.1	17.6	1056.0	14.0	1057.9	22.8	1057.9	22.8	1057.9	22.8	99.7
H15-004_R.un3-Spot 307	439	60706	5.3	12.8714	1.2	2.0281	2.2	0.1893	1.9	0.85	1117.7	19.1	1125.0	14.9	1139.0	23.1	1139.0	23.1	1139.0	23.1	98.1
H15-004_R.un3-Spot 308	252	76089	2.9	12.7297	1.6	2.0797	2.4	0.1920	1.7	0.72	1132.2	17.6	1142.1	16.2	1161.0	32.6	1161.0	32.6	1161.0	32.6	97.5
H15-004_R.un3-Spot 309	1538	82246	2.8	13.1453	1.3	1.9100	2.5	0.1821	2.1	0.85	1078.4	20.9	1084.6	16.5	1097.0	26.1	1097.0	26.1	1097.0	26.1	98.3
H15-004_R.un3-Spot 310	247	50939	11.4	11.1200	1.6	2.9544	3.0	0.2383	2.5	0.84	1377.7	31.0	1396.0	22.5	1424.0	30.8	1424.0	30.8	1424.0	30.8	96.7
H15-004_R.un3-Spot 311	528	78891	3.2	12.6028	1.5	1.9901	2.2	0.1819	1.5	0.70	1077.4	14.9	1112.1	14.6	1180.8	30.4	1180.8	30.4	1180.8	30.4	91.2
H15-004_R.un3-Spot 312	374	101102	2.1	7.7826	1.1	6.3924	3.2	0.3608	3.1	0.94	1986.0	52.2	2031.2	28.5	2077.4	19.5	2077.4	19.5	2077.4	19.5	95.6
H15-004_R.un3-Spot 313	343	346321	2.8	13.8181	1.4	1.6252	2.8	0.1820	2.4	0.86	972.7	21.5	980.0	17.5	996.3	29.0	996.3	29.0	996.3	29.0	97.6
H15-004_R.un3-Spot 314	365	46127	4.3	13.1965	1.8	1.9611	3.1	0.1877	2.5	0.81	1108.9	25.8	1102.2	21.1	1089.2	37.0	1089.2	37.0	1089.2	37.0	101.8
H15-004_R.un3-Spot 315	188	46894	4.6	13.7399	2.4	1.5306	3.2	0.1525	2.1	0.66	915.1	18.2	942.7	19.8	1007.8	49.1	1007.8	49.1	1007.8	49.1	90.8

Appendix F: LA-ICPMS U-Pb Zircon Geochronology (continued)

Analysis	U (ppm)	206Pb/204Pb	U/Th	206Pb*/207Pb*		206Pb*/238U*		207Pb*/235U*		206Pb*/238U*		207Pb*/235U*		206Pb*/207Pb*		Best age (Ma)	± (Ma)	Conc (%)	
				206Pb*/207Pb*	U/Th	± (%)	206Pb*/238U*	± (%)	207Pb*/235U*	± (%)	206Pb*/207Pb*	± (Ma)	206Pb*/238U*	± (%)	207Pb*/235U*				± (Ma)
H15-004_Run3-Spot 316	413	215250	6.2	12.7544	1.5	2.0877	2.6	0.1931	2.1	0.81	1138.2	22.0	1144.8	18.0	1157.1	30.7	1157.1	30.7	98.4
H15-004_Run3-Spot 317	863	141093	2.9	13.0355	1.3	1.9848	2.8	0.1876	2.4	0.88	1108.6	24.8	1110.3	18.8	1113.7	26.7	1113.7	26.7	99.5
H15-004_Run3-Spot 318	931	81290	2.2	12.4192	1.2	2.2780	2.5	0.2052	2.3	0.89	1203.1	24.8	1205.5	17.9	1209.8	22.9	1209.8	22.9	99.5
H15-004_Run3-Spot 319	263	32592	3.9	13.4435	1.9	1.7007	2.9	0.1658	2.1	0.74	989.0	19.4	1008.8	18.2	1052.0	38.6	1052.0	38.6	94.0
H15-004_Run3-Spot 320	140	224594	2.4	12.3366	2.3	2.2480	3.0	0.2011	1.9	0.64	1181.4	20.5	1196.2	20.8	1222.9	44.5	1222.9	44.5	96.6
H15-004_Run3-Spot 321	667	177269	153.3	17.2541	2.3	0.5738	6.9	0.0718	6.5	0.94	447.0	28.0	460.5	25.5	528.2	50.2	447.0	28.0	84.6
H15-004_Run3-Spot 322	332	40102	202.1	17.6786	1.6	0.5851	2.4	0.0750	1.8	0.74	466.4	7.9	467.8	8.9	474.6	35.1	466.4	7.9	98.3
H15-004_Run3-Spot 323	1127	746538	25.2	13.9829	1.5	1.3469	3.0	0.1366	2.6	0.87	825.4	20.2	866.2	17.4	972.2	29.8	825.4	20.2	84.9
H15-004_Run3-Spot 324	161	30334	5.4	14.4707	3.6	1.1736	4.9	0.1232	3.3	0.68	748.8	23.3	788.3	26.7	901.9	73.9	748.8	23.3	83.0
H15-004_Run3-Spot 325	1375	124455010	4.7	13.3505	1.4	1.6585	2.7	0.1606	2.4	0.86	960.0	21.0	992.8	17.3	1065.9	27.8	1065.9	27.8	90.1
H15-004_Run3-Spot 326	183	25896	2.0	12.7003	2.0	1.7318	2.6	0.1595	1.7	0.65	954.1	15.0	1020.4	16.9	1165.5	39.7	1165.5	39.7	81.9
H15-004_Run3-Spot 327	738	52340	3.1	11.0260	1.1	3.0920	2.0	0.2473	1.6	0.81	1424.3	20.4	1430.7	15.1	1440.2	21.8	1440.2	21.8	98.9
H15-004_Run3-Spot 328	655	107745	4.1	13.8024	1.4	1.6044	2.3	0.1606	1.8	0.78	960.1	16.1	971.9	14.4	998.6	29.1	998.6	29.1	96.1
H15-004_Run3-Spot 329	281	70108	1.9	12.1018	1.4	2.2876	4.3	0.2008	4.0	0.95	1179.5	43.5	1208.5	30.1	1260.5	26.6	1260.5	26.6	93.6
H15-004_Run3-Spot 330	684	212021	4.5	12.5251	1.2	2.0716	2.4	0.1882	2.1	0.85	1111.5	20.9	1139.5	16.4	1193.1	24.7	1193.1	24.7	93.2













Appendix G: LA-ICPMS U-Pb Zircon Geochronology (continued)

Analysis	U (ppm)	206Pb/204Pb	U/Th	206Pb*/207Pb*	Isotope ratios			Apparent ages (Ma)					Conc (%)						
					± (%)	207Pb*/235U*	± (%)	206Pb*/238U	± (%)	206Pb*/238U*	error corr.	207Pb*/235U		± (Ma)	206Pb*/207Pb*	± (Ma)	Best age (Ma)	± (Ma)	
DEL14-1 26May2015-Spot 185	136	289848	3.1	11.6833	0.9	2.7300	1.7	0.2316	1.4	0.83	1342.8	17.0	1337.5	12.6	1329.0	18.3	1329.0	18.3	101.0
DEL14-1 26May2015-Spot 186	924	69634	8.7	13.1620	1.0	1.8651	1.7	0.1780	1.4	0.80	1056.3	13.4	1068.8	11.1	1094.5	19.3	1094.5	19.3	96.5
DEL14-1 26May2015-Spot 187	385	226615	6.0	13.3255	1.0	1.7712	1.7	0.1712	1.4	0.82	1018.6	13.0	1035.0	11.2	1069.7	20.9	1069.7	20.9	95.2
DEL14-1 26May2015-Spot 188	93	28647	1.3	13.8406	2.4	1.7183	3.3	0.1725	2.2	0.67	1025.8	20.7	1015.4	21.0	993.0	49.4	993.0	49.4	103.3
DEL14-1 26May2015-Spot 190	901	123071	3.4	13.5070	1.0	1.8787	2.4	0.1840	2.2	0.90	1089.0	21.9	1073.6	16.1	1042.4	21.0	1042.4	21.0	104.5
DEL14-1 26May2015-Spot 193	76	29587	2.5	12.7855	1.6	2.1453	2.1	0.1989	1.4	0.67	1169.6	15.3	1163.5	14.9	1152.3	31.7	1152.3	31.7	101.5
DEL14-1 26May2015-Spot 194	202	187830	3.1	12.3645	1.1	2.2973	2.3	0.2060	2.0	0.88	1207.6	22.0	1211.5	16.2	1218.4	21.7	1218.4	21.7	99.1
DEL14-1 26May2015-Spot 195	286	81749	3.8	12.4797	1.1	2.1240	1.7	0.1922	1.3	0.75	1133.5	13.5	1156.6	11.9	1200.2	22.4	1200.2	22.4	94.4
DEL14-1 26May2015-Spot 196	130	2500202	4.2	12.5356	1.0	2.0126	1.9	0.1830	1.7	0.85	1083.2	16.6	1119.8	13.2	1191.4	20.1	1191.4	20.1	90.9
DEL14-1 26May2015-Spot 197	210	31140	2.3	12.7501	1.6	2.1104	2.8	0.1951	2.3	0.82	1149.2	23.8	1152.2	19.0	1157.8	31.2	1157.8	31.2	99.3
DEL14-1 26May2015-Spot 198	169	72316	4.1	11.2523	1.3	2.9591	2.1	0.2415	1.7	0.79	1394.5	20.9	1397.2	16.1	1401.4	25.1	1401.4	25.1	99.5
DEL14-1 26May2015-Spot 199	78	150849	3.0	13.4826	1.2	1.7751	2.0	0.1736	1.6	0.80	1031.8	14.9	1036.4	12.7	1046.1	23.9	1046.1	23.9	98.6
DEL14-1 26May2015-Spot 200	353	1803187	0.5	12.3047	0.9	2.3242	1.4	0.2074	1.1	0.76	1215.0	12.2	1219.7	10.3	1228.0	18.3	1228.0	18.3	98.9
DEL14-1 26May2015-Spot 201	337	318224	2.4	12.2397	1.5	2.3598	2.2	0.2095	1.7	0.75	1226.0	18.7	1230.5	15.9	1238.4	28.7	1238.4	28.7	99.0
DEL14-1 26May2015-Spot 202	895	134762	4.5	11.7439	1.1	2.3378	2.4	0.1991	2.1	0.88	1170.6	22.2	1223.9	16.8	1319.0	21.6	1319.0	21.6	88.8
DEL14-1 26May2015-Spot 203	40	66903	2.9	11.0995	1.3	3.0119	1.9	0.2425	1.4	0.75	1399.5	18.1	1410.6	14.7	1427.5	24.5	1427.5	24.5	98.0
DEL14-1 26May2015-Spot 204	146	217973	3.6	12.3295	1.0	2.3316	1.5	0.2085	1.1	0.77	1220.8	12.7	1222.0	10.6	1224.0	18.9	1224.0	18.9	99.7
DEL14-1 26May2015-Spot 205	379	745810	1.6	13.3665	0.9	1.7841	1.6	0.1730	1.3	0.81	1028.4	12.4	1039.7	10.4	1063.5	18.8	1063.5	18.8	96.7
DEL14-1 26May2015-Spot 206	341	175789	15.6	15.4358	1.4	0.9201	1.9	0.1030	1.2	0.65	632.0	7.4	662.4	9.2	767.3	30.4	632.0	7.4	82.4
DEL14-1 26May2015-Spot 207	647	202555	7.6	13.4354	1.0	1.7837	1.8	0.1738	1.5	0.84	1033.1	14.5	1039.5	11.8	1053.2	19.6	1053.2	19.6	98.2
DEL14-1 26May2015-Spot 208	430	155587	6.1	13.7819	1.0	1.5955	1.9	0.1595	1.6	0.86	953.9	14.3	968.4	11.7	1001.6	19.6	1001.6	19.6	95.2
DEL14-1 26May2015-Spot 209	332	68483	3.2	12.3829	0.9	2.3198	1.6	0.2083	1.4	0.83	1219.9	15.2	1218.3	11.7	1215.5	17.9	1215.5	17.9	100.4
DEL14-1 26May2015-Spot 210	420	50906	14.4	12.9954	1.1	1.9672	1.6	0.1854	1.1	0.71	1096.5	11.1	1104.3	10.6	1119.9	22.2	1119.9	22.2	97.9
DEL14-1 26May2015-Spot 211	276	66801	1.2	13.8009	1.7	1.6531	2.3	0.1655	1.6	0.69	987.1	14.3	990.7	14.4	998.8	33.5	998.8	33.5	98.8
DEL14-1 26May2015-Spot 212	281	38617	2.4	12.3378	1.5	2.1942	2.2	0.1963	1.6	0.73	1155.7	17.3	1179.2	15.7	1222.7	30.2	1222.7	30.2	94.5
DEL14-1 26May2015-Spot 213	109	90806	6.7	14.6570	1.7	1.1064	2.1	0.1176	1.3	0.61	716.8	8.7	756.5	11.2	875.5	34.3	716.8	8.7	81.9
DEL14-1 26May2015-Spot 214	1409	23952839	29.6	13.7021	1.2	1.5581	1.9	0.1548	1.4	0.75	928.0	12.0	953.7	11.5	1013.4	24.9	1013.4	24.9	104.4
DEL14-1 26May2015-Spot 215	94	231493	1.6	13.6141	1.3	1.8314	1.9	0.1808	1.4	0.73	1071.5	14.0	1056.8	12.8	1026.5	26.8	1026.5	26.8	104.6
DEL14-1 26May2015-Spot 216	167	78215	1.3	13.1603	2.1	1.8113	3.2	0.1729	2.4	0.75	1028.0	22.8	1049.6	20.8	1094.7	41.8	1094.7	41.8	93.9
DEL14-1 26May2015-Spot 217	189	163564	1.8	12.5201	1.9	2.1909	3.0	0.1969	2.3	0.77	1169.7	24.4	1178.2	20.6	1193.8	37.1	1193.8	37.1	98.0
DEL14-1 26May2015-Spot 218	305	53196	3.7	12.9536	1.6	1.8344	2.4	0.1723	1.8	0.75	1025.0	16.8	1057.8	15.5	1126.3	31.0	1126.3	31.0	91.0
DEL14-1 26May2015-Spot 219	302	54405	2.4	12.3342	0.9	2.3336	2.0	0.2088	1.8	0.89	1222.2	20.3	1222.6	14.5	1223.2	18.2	1223.2	18.2	99.9
DEL14-1 26May2015-Spot 220	172	143795	2.0	15.9595	1.1	1.0271	1.8	0.1189	1.4	0.77	724.2	9.3	717.5	9.1	696.6	24.2	724.2	24.2	104.0

Appendix H: SIMS U-Pb Zircon Geochronology

Analysis		Apparent ages (Ma)						Isotope ratios							
		206Pb/ 238U	206Pb/ 235U	207Pb/ 235U	207Pb/ 206Pb	207Pb/ 206Pb	207Pb/ 206Pb	206Pb*/ 238U	206Pb*/ 235U	207Pb*/ 235U	207Pb*/ 235U	206Pb*/ 238U	206Pb*/ 238U	Correlation of Concordia Ellipses	207Pb*/ 206Pb*
2014_10_29Oct\	H14-020_Gr1_zone_3.ais	1136	1147	25	1167	12	99.95	2.0940	0.0759	0.1928	0.0070	0.0788	0.0005	0.9856	
2014_10_29Oct\	H14-020_Gr10_zone3.ais	1087	1101	26	1127	21	99.89	1.9560	0.0761	0.1837	0.0067	0.0772	0.0008	0.9638	
2014_10_29Oct\	H14-020_Gr17_zone3.ais	1167	1154	29	1130	26	99.94	2.1170	0.0899	0.1985	0.0080	0.0773	0.0010	0.9519	
2014_10_29Oct\	H14-020_Gr29_zone3.ais	1153	1145	27	1130	23	99.94	2.0900	0.0820	0.1959	0.0076	0.0774	0.0009	0.9568	
2014_10_29Oct\	H14-020_Gr20_zone3.ais	1153	1154	33	1155	27	99.91	2.1150	0.1000	0.1958	0.0083	0.0783	0.0011	0.9596	
2014_10_29Oct\	H14-020_Gr15_core.ais	1135	1128	28	1114	22	99.87	2.0370	0.0823	0.1926	0.0072	0.0767	0.0008	0.9636	
2014_10_29Oct\	H14-020_Gr5_core.ais	1181	1169	30	1148	32	99.8	2.1630	0.0937	0.2010	0.0084	0.0781	0.0013	0.9274	
2014_10_29Oct\	H14-020_Gr4_core.ais	1232	1207	34	1161	63	99.58	2.2810	0.1100	0.2106	0.0076	0.0786	0.0025	0.7561	
2014_10_29Oct\	H14-020_Gr13_core.ais	1144	1100	66	1014	150	99.14	1.9540	0.1930	0.1942	0.0123	0.0730	0.0054	0.6613	

## REFERENCES

- Aleinikoff, J.N., Southworth, S., and Merschat, A.J., 2013, Implications for late Grenvillian (Rigolet phase) construction of Rodinia using new U-Pb data from the Mars Hill terrane, Tennessee and North Carolina, United States: *Geology*, v. 41, no. 10, p. 1087–1090, doi: 10.1130/G34779.1.
- Anderson, A.D., 2011, Petrologic, geochemical, and geochronologic constraints on the tectonic evolution of the southern Appalachian orogen, Blue Ridge Province of western North Carolina [Ph.D. dissertation]: University of Kentucky, Lexington, Kentucky, 280 p.
- Ashwal, L.D., Tucker, R.D. and Zinner, E.K., 1999, Slow cooling of deep crustal granulites and Pb-loss in zircon. *Geochimica et Cosmochimica Acta*, v. 63, no. 18, p.2839-2851.
- Bream, B. R., 2003, Tectonic implications of geochronology and geochemistry of para- and orthogneisses from the southern Appalachian crystalline core [Ph.D. dissertation]: Knoxville, University of Tennessee, 296 p.
- Bream, B.R. and Hatcher Jr, R.D., 2002, October. Southern Appalachian terranes amended: timing of accretion and delimiting provenance from new detrital zircon and Nd isotopic data, In *Geological Society of America Abstracts with Programs*, v. 34, no. 6.
- Bream, B.R., Hatcher, R.D., Miller, C.F., and Fullagar, P.D., 2004, Detrital zircon ages and Nd isotopic data from the southern Appalachian crystalline core, Georgia, South Carolina, North Carolina, and Tennessee: New provenance constraints for part of the Laurentian margin: *Geological Society of America Memoirs*, v. 197, p. 459–475, doi: 10.1130/0-8137-1197-5.
- Cawood, P.A., McCausland, P.J. and Dunning, G.R., 2001, Opening Iapetus: constraints from the Laurentian margin in Newfoundland, *Geological Society of America Bulletin*, v. 113 no. 4, p.443-453.
- Chakraborty, S., 2010, Provenance of the Neoproterozoic Ocoee Supergroup, eastern Great Smoky Mountains [Ph.D. dissertation]: University of Kentucky, 307 p.
- Cherniak, D.J., and Watson, E.B., 2001, Pb diffusion in zircon: *Chemical Geology*, v. 172, p. 5-24.
- Clemons, K.M. and Moecher, D.P., 2009, Reinterpretation of the Greenbrier fault, Great Smoky Mountains: New petrofabric constraints and implications for southern Appalachian tectonics. *Geological Society of America Bulletin*, v. 121, no. 7-8, p.1108-1122.
- Corrie, S.L. and Kohn, M.J., 2007, Resolving the timing of orogenesis in the Western Blue Ridge, southern Appalachians, via in situ ID-TIMS monazite geochronology, *Geology*, v. 35, no. 7, p.627-630.
- Fedo, C.M., Nesbitt, H.W. and Young, G.M., 1995, Unraveling the effects of potassium metasomatism in sedimentary rocks and paleosols, with implications for paleoweathering conditions and provenance, *Geology*, v.23, n.10, p.921-924.

- Fisher, C.M., Loewy, S.L., Miller, C.F., Berquist, P., Van Schmus, W.R., Hatcher, R.D., Wooden, J.L., and Fullagar, P.D., 2010, Whole-rock Pb and Sm-Nd isotopic constraints on the growth of southeastern Laurentia during Grenvillian orogenesis: *Geological Society of America Bulletin*, v. 122, no. 9-10, p. 1646–1659, doi: 10.1130/B30116.1.
- Gehrels, G.E., Valencia, V. a., and Ruiz, J., 2008, Enhanced precision, accuracy, efficiency, and spatial resolution of U-Pb ages by laser ablation-multicollector-inductively coupled plasma-mass spectrometry: *Geochemistry, Geophysics, Geosystems*, v. 9, no. 1, p. n/a–n/a, doi: 10.1029/2007GC001805.
- Gehrels, G., 2014, Detrital zircon U-Pb geochronology applied to tectonics, *Annual Review of Earth and Planetary Sciences*, v.42, p.127-149.
- Hadley, J.B., and Goldsmith, R., 1963, *Geology of the Eastern Great Smoky Mountains, North Carolina and Tennessee*: , p. 118.
- Hadley, J.B., and Nelson, A.E., 1971, *Geologic map of the Knoxville quadrangle, North Carolina, Tennessee and South Carolina*: US Geological Survey, p. 1–654.
- Hatcher Jr, R.D., 1979, The Coweeta Group and Coweeta syncline: major features of the North Carolina–Georgia Blue Ridge, *Southeastern Geology*, v. 21, no.1, p.17-29.
- Hatcher Jr, R.D., 2005, Southern and central Appalachians, *Encyclopedia of Geology*, p.72-81.
- Hatcher Jr, R.D., Bream, B.R. and Eckert, J.O., 2003, March. Southern Blue Ridge terranes and problems with rock units, ages, and timing of events: read the detailed geologic maps. In *Geological Society of America Abstracts with Programs*, v. 35, no. 1.
- Hatcher Jr, R.D., Mersch, A.J., and Thigpen, J.R., 2005, Blue ridge primer, in Hatcher Jr., and Mersch, A.J., R.D. ed., *Blue Ridge Geology Geotraverse East of the Great Smoky Mountains National Park, Western North Carolina*: Carolina Geological Society Annual Field Trip Guidebook, November 5–6, p. 1–24.
- Hatcher Jr, R.D., Thomas, W.A. and Viele, G.W. eds., 1989, *The Appalachian-Ouachita Orogen in the United States*, Geological Society of America.
- Hatcher, R.D., Bream, B.R., Miller, C.F., Eckert, J.O., Fullagar, P.D. and Carrigan, C.W., 2004, Paleozoic structure of internal basement massifs, southern Appalachian Blue Ridge, incorporating new geochronologic, Nd and Sr isotopic, and geochemical data, *Geological Society of America Memoirs*, v.197, p.525-547.
- Hietpas, J., Samson, S., Moecher, D. and Chakraborty, S., 2011., Enhancing tectonic and provenance information from detrital zircon studies: assessing terrane-scale sampling and grain-scale characterization, *Journal of the Geological Society*, v. 168, no. 2, p.309-318.
- Hoffman, P.F., 1999, The break-up of Rodinia, birth of Gondwana, true polar wander and the snowball Earth, *Journal of African Earth Sciences*, v. 28, no. 1, p. 17-33.

- Hynes, A. and Rivers, T., 2010, Protracted continental collision—evidence from the Grenville Orogen. *Canadian Journal of Earth Sciences*, v. 47, no. 5, p.591-620.
- King, P.B., Hadley, J.B., Neuman, R.B., and Hamilton, W., 1958, Stratigraphy of Ocoee Series, Great Smoky Mountains, Tennessee and North Carolina: *Geological Society of America Bulletin*, v. 69, no. 8, p. 947–966, doi: 10.1130.
- Kunk, M.J., Southworth, S., Aleinikoff, J.N., Naeser, N.D., Naeser, C.W., Merschat, C.E., and Cattanach, B.L., 2006, Preliminary U-Pb, 40 Ar-39 Ar and fission-track ages support a long and complex tectonic history in the Western Blue Ridge in North Carolina and Tennessee, in *Geological Society of America Abstracts with Programs*, p. 66.
- Loewy, S.L., Connelly, J.N., Dalziel, I.W.D., and Gower, C.F., 2003, Eastern Laurentia in Rodinia: constraints from whole-rock Pb and U/Pb geochronology: *Tectonophysics*, v. 375, no. 1, p. 169–197.
- Loughry, D.F., 2010, Origin of Blue Ridge basement rocks, Dellwood Quad, Western NC: New evidence from U-Pb zircon geochronology and whole rock geochemistry [M.S. thesis]:University of Kentucky, 136p.
- Ludwig, K., 1999, Isoplot/Ex v. 2.10b.
- Massey, M.A., and Moecher, D.P., 2005, Deformation and metamorphic history of the Western Blue Ridge–Eastern Blue Ridge terrane boundary, southern Appalachian Orogen: *Tectonics*,
- McDowell, S., Miller, C.F., Fullagar, P.D., Bream, B.R. and Mapes, R.W., 2002, The Persimmon Creek Gneiss, eastern Blue Ridge, North Carolina–Georgia: evidence for the missing Taconic arc, *Southeastern Geology*, v.41, p.103-117.
- McLelland, J., Daly, J.S. and McLelland, J.M., 1996, The Grenville orogenic cycle (ca. 1350-1000 Ma): an Adirondack perspective, *Tectonophysics*, v. 265, no.1, p.1-28.
- McLennan, S.M., Hemming, S., McDaniel, D.K. and Hanson, G.N., 1993, Geochemical approaches to sedimentation, provenance, and tectonics.*Geological Society of America Special Papers*, v. 284, p.21-40.
- Merschat, A.J., 2009, Assembling the Blue Ridge and Inner Piedmont: Insights Into the Nature and Timing of Terrane Accretion in the Southern Appalachian Orogen from Geologic Mapping, Stratigraphy, Kinematic Analysis, Petrology, Geochemistry, and Modern Geochronology [Ph.D. dissertation]: University of Tennessee Knoxville, 455p.
- Merschat, A.J., Jr, R.D.H., Bream, B.R., Miller, C.F., Byars, H.E., Gatewood, M.P., and Wooden, J.L., 2010, Detrital zircon geochronology and provenance of southern Appalachian Blue Ridge and Inner Piedmont crystalline terranes: *The Geological Society of America Memoir*, v. 206, no. 26, p. 661–699, doi: 10.1130/2010.1206(26).For.
- Miller, B.V., Fetter, A.H. and Stewart, K.G., 2006, Plutonism in three orogenic pulses, eastern Blue Ridge Province, southern Appalachians.*Geological Society of America Bulletin*, vo. 118, no. 1-2, p.171-184.



- Miller, C.F., Hatcher, R.D., Ayers, J.C., Coath, C.D., Harrison, T.M., 2000, Age and zircon inheritance of eastern Blue Ridge plutons, southwestern North Carolina and northeastern Georgia, with implications for magma history and evolution of the southern Appalachian orogen, *American Journal of Science*, v. 300, p.142-172.
- Moecher, D., Hietpas, J., Samson, S., and Chakraborty, S., 2011, Insights into southern Appalachian tectonics from ages of detrital monazite and zircon in modern alluvium: *Geosphere*, v. 7, no. 2, p. 494–512, doi: 10.1130/GES00615.1.
- Moecher, D.P., Samson, S.D., and Miller, C.F., 2004, Precise Time and Conditions of Peak Taconian Granulite Facies Metamorphism in the Southern Appalachian Orogen, U.S.A., with Implications for Zircon Behavior during Crustal Melting Events: *The Journal of Geology*, v. 112, no. 3, p. 289–304, doi: 10.1086/382760.
- Montes C., 1997, The Greenbrier and Hayesville faults in central-western North Carolina [M.S. thesis]: Knoxville University of Tennessee, 145 p.
- Nesbitt, I.I.W. and Young, G.M., 1982, Early Proterozoic climates and plate, *Nature*, v.299, p.21.
- Paces, J.B. and Miller, J.D., 1993, Precise U- Pb ages of Duluth complex and related mafic intrusions, northeastern Minnesota: Geochronological insights to physical, petrogenetic, paleomagnetic, and tectonomagmatic processes associated with the 1.1 Ga midcontinent rift system, *Journal of Geophysical Research: Solid Earth*, v. 98, no. B8, p.13997-14013.
- Parker, A., 1970, An index of weathering for silicate rocks, *Geological Magazine*, v.107, no.06, p.501-504.
- Price, J.R. and Velbel, M.A., 2003, Chemical weathering indices applied to weathering profiles developed on heterogeneous felsic metamorphic parent rocks, *Chemical Geology*, v.202, no.3, p.397-416.
- Pullen, A., Ibanez-Mejia, M., Gehrels, G., Ibanez-Mejia, J., and Pecha, M., 2014, What happens when n= 1000? Creating large-n geochronological datasets with LA-ICP-MS for geologic investigations: *Journal of Analytical Atomic Spectrometry*, v. 29, p. 971-980.
- Quinn, R.J., 2012, The evolution of Grenville basement in the eastern Great Smoky Mountains; Constraints from U-Pb zircon, whole rock Sm-Nd, and feldspar Pb geochemistry [M.S. thesis]: University of Kentucky, 115p.
- Rainbird, R., Cawood, P. and Gehrels, G., 2012, The great Grenvillian sedimentation episode: Record of supercontinent Rodinia's assembly, *Tectonics of Sedimentary Basins: Recent Advances: Blackwell Publishing Ltd*, p.583-601.
- Rankin, D.W., 1975, The continental margin of eastern North America in the southern Appalachians: The opening and closing of the Proto-Atlantic ocean: *American Journal of Science*, v. 279A, p. 298–336.

- Rankin, D.W., Tollo, R.P., Aleinikoff, J.A. and Ayuso, R.A., 1997, Manhattan Prong A-type metagranites with feldspar Pb isotope affinities to Laurentia and zircon ages of 563 Ma: support for late Neoproterozoic Iapetian rifting, In *Geol. Soc. Am. Abstr. Program*, v. 33, p. 74.
- Rivers, T., 2008, Assembly and preservation of lower, mid, and upper orogenic crust in the Grenville Province—Implications for the evolution of large hot long-duration orogens: *Precambrian Research*, v. 167, p. 237–259, doi: 10.1016/j.precamres.2008.08.005.
- Sinha, A.K., Hogan, J.P. and Parks, J., 1996, Lead isotope mapping of crustal reservoirs within the Grenville Superterrane: I. Central and Southern Appalachians. *Earth Processes: Reading the Isotopic Code*, p.293-305.
- Southworth, S., Schultz, A.P., Aleinikoff, J.N., and Mersch, A.J., 2012, Geologic Map of the Great Smoky Mountains National Park Region, Tennessee and North Carolina, US Geological Survey.
- Southworth, S., Schultz, A.P., Denenny, D., 2005, Geologic Map of the Great Smoky Mountains National Park Region, Tennessee and North Carolina, US Geological Survey Open-File Report 2005-1225.
- Thigpen, J.R., 2005, Stratigraphic and structural relationships of the Ocoee Supergroup, southern Appalachians: Implications for Neoproterozoic rift basin architecture and Paleozoic collisional orogenesis [M.S. thesis]: Knoxville, University of Tennessee.
- Tohver, E., Bettencourt, J.S., Tosdal, R., Mezger, K., Leite, W.B., and Payolla, B.L., 2004, Terrane transfer during the Grenville orogeny: tracing the Amazonian ancestry of southern Appalachian basement through Pb and Nd isotopes: *Earth and Planetary Science Letters*, v. 228, no. 1, p. 161–176.
- Tohver, E., D’Agrella-Filho, M.S. and Trindade, R.I., 2006, Paleomagnetic record of Africa and South America for the 1200–500Ma interval, and evaluation of Rodinia and Gondwana assemblies, *Precambrian Research*, v. 147, no. 3, p.193-222.
- Tohver, E., Trindade, R.I.F., Solum, J.G., Hall, C.M., Riccomini, C. and Nogueira, A.C., 2010, Closing the Clymene ocean and bending a Brasiliano belt: Evidence for the Cambrian formation of Gondwana, southeast Amazon craton. *Geology*, v. 38, no.3, p.267-270.
- Tollo, R.P., Aleinikoff, J.N., Bartholomew, M.J., and Rankin, D.W., 2004, Neoproterozoic A-type granitoids of the central and southern Appalachians: intraplate magmatism associated with episodic rifting of the Rodinian supercontinent: *Precambrian Research*, v. 128, p. 3–38, doi: 10.1016/j.precamres.2003.08.007.
- Whitmeyer, S.J. and Karlstrom, K.E., 2007, Tectonic model for the Proterozoic growth of North America, *Geosphere*, v. 3, no. 4, p. 220-259.

## VITA

Emma Anne Larkin

### Education:

Bachelor of Science, Geologic Sciences, Salem State University, Salem, Massachusetts, 2013

### Professional Positions:

- Research Assistant, University of Kentucky, Department of Earth and Environmental Sciences, 2014 – 2016
- Teaching Assistant, University of Kentucky, Department of Earth and Environmental Sciences, 2013 – 2014

### Scholastic Honors:

- Sigma Gamma Epsilon National Honor Society for the Earth Sciences; Jan 2015 – Present
- Outstanding Teaching Assistant, Hydrogeology, University of Kentucky, 2014

### Professional Publications

- Larkin, E.A., Moecher, D.P., 2015, Geologic Map of the North Half of the Hazelwood 7.5" Quadrangle: Extent of the Oldest Basement Component in the Southern Appalachians, Abstracts with Programs, SEGSA, Chattanooga, TN, 19-20 Mar.
- McFadden, R.R., Rice, A.K., Sutcliffe, R., Killam, S.L., Larkin, E.A., 2015, Neocadian Northward Extrusion of the Croydon Dome within the Bronson Hill Anticline in Southwestern New Hampshire, Abstracts with Programs, NEGSA, Bretton Woods, NH, 23-25 Mar.
- McFadden, R.R., Larkin, E.A., Rice, A.K., Sutcliffe, R., Jercinovic, Michael J., 2014, Neo-Acadian Deformation in the New England Appalachians Documented by Northward Extrusion of the Croydon Dome in Southwestern New Hampshire, Abstracts with Programs, Rocky Mountain and Cordilleran Joint GSA, Bozeman, MT, 19-21 May.
- Larkin, E.A., McFadden, R.R., Valley, P.M., 2013, Deformation History and Emplacement of the Croydon Dome, Southwestern New Hampshire, Abstracts with Programs, NEGSA, Bretton Woods, NH, 18-20 Mar.
- Larkin, E.A., and McFadden, R.R., 2013, Metamorphism and deformation within the Croydon dome, southwestern New Hampshire, Sigma Xi Research Conference